1-1-1993

Surface chemical transformations of poly(ether ether ketone) ; Adsorption/migration of selectively-functionalized polystyrenes from a polystyrene matrix/

Nicole L. Franchina
University of Massachusetts Amherst

I. SURFACE CHEMICAL TRANSFORMATIONS OF POLY(ETHER ETHER KETONE)

II. ADSORPTION/MIGRATION OF SELECTIVELY-FUNCTIONALIZED POLYSTYRENES FROM A POLYSTYRENE MATRIX

A Dissertation Presented

by

NICOLE L. FRANCHINA

Submitted to the Graduate School of the
University of Massachusetts in partial fulfillment
of the degree requirements for the degree of

DOCTOR OF PHILOSOPHY

February 1993

Polymer Science and Engineering

I. SURFACE CHEMICAL TRANSFORMATIONS OF POLY(ETHER ETHER KETONE)

II. ADSORPTION/MIGRATION OF SELECTIVELY-FUNCTIONALIZED POLYSTYRENES FROM A POLYSTYRENE MATRIX

A Dissertation Presented

by

NICOLE L. FRANCHINA

Approved as to style and content by:

Thomas J. McCarthy, Chair

David A. Tirrell, Member

Paul M. Lahti, Member

William J. MacKnight, Department Head
Polymer Science and Engineering

To my parents Maureen and Joseph Franchina

ACKNOWLEDGMENTS

Several people have had an impact on my life in graduate school and many of them deserve special mention. In particular, I want to express gratitude to my advisor Dr. Tom McCarthy for his help and guidance. Somehow Tom always has had faith in me, even from the beginning when I hardly trusted myself; this has helped immensely to build my self-confidence. Drs. Lahti and Tirrell deserve my gratitude, as well, for the help and time they have given me in the last year. Special thanks to Tom and DT for helping me get a job.

I would like to thank the current members of the McCarthy group (Tim, Molly, Katrina Anthony, Bob, Eric, Damo and Juha-Matti) for their friendship and especially for their tolerance of my "nic"- pickiness. It is hard to believe that those guys still like me after all the jumping up and down I have done in the last five years. Many thanks to Jack Hirsch for his friendship and diligence in keeping the XPS (rather, *my xps*) working well.

Most of all, I would like to express deep gratitude to my husband, Dr. Brant Kolb. Brant is undoubtedly one of the best scientists I will ever meet, capable of extraordinary things. I greatly appreciate the countless hours he has spent helping me to understand and develop my own science, as well as the immeasurable joy and happiness he has brought to my life.

I also want to thank my parents for their love and total support throughout my tenure in grad school. (What other parents would have trouble sleeping the night before a cume??) Thanks to Justine and Greg for their support, as well, and of course to Casta, Angus, Sammy and Charlie, my favorites.

ABSTRACT

I. SURFACE CHEMICAL TRANSFORMATIONS OF POLY(ETHER ETHER KETONE)

II. ADSORPTION/MIGRATION OF SELECTIVELY-FUNCTIONALIZED POLYSTYRENES FROM A POLYSTYRENE MATRIX

FEBRUARY 1993

NICOLE L. FRANCHINA, A.B., PRINCETON UNIVERSITY

Ph.D., UNIVERSITY OF MASSACHUSETTS

Directed by: Professor Thomas J. McCarthy

Several carbonyl-selective reactions were carried out with semicrystalline poly(ether ether ketone) (PEEK) film to assess the reactivity of the diaryl ketones at the film-solution interface. Surface analyses with X-ray photoelectron spectroscopy (XPS), attenuated total reflectance infrared spectroscopy (ATR IR) and contact angle measurement indicate that a thin layer of reagent-induced functionality results from these derivatizations in roughly 50% reaction yield. Data obtained indicate that derivatized surfaces can be functionalized further. Several PEEK-alcohol surfaces were prepared containing primary, secondary and tertiary alcohols, and the secondary and tertiary species were chain extended by reaction with lithium diisopropylamide and ethylene oxide. Primary alcohol groups were introduced by reacting PEEK with acetaldehyde

lithiopropyl ethyl acetal and subsequent deprotection. Secondary alcohols were produced by reducing PEEK with Red-Al® reagent, and tertiary hydroxyls result from reaction with methyllithium. In general, the alcohol surfaces were reactive toward electrophiles.

XPS and contact angle measurement were used to follow surface reconstruction in heat-treated samples containing specific concentrations of surface-active polystyrenes (SAP) in a polystyrene matrix (Mn = 10 K). The objective was to determine how certain molecular and environmental parameters influence surface reconstruction. The SAPs were prepared with three different architectures: the first (SAP:E-1) (Mn = 1, 5, 10, 40 and 100 K) contained a single perfluoroalkyl endgroup, the second (SAP:E-2) (Mn = 10 K) contained two fluorinated endgroups and the third contained a single perfluoroalkyl group in the middle of the chain (SAP:M-1) (Mn = 10 K). SAP:E-1 samples were annealed at different temperatures (180, 150, 110 °C and room temperature) for varied lengths of time (24, 48, 72, 96, 120 h and two weeks) to determine optimum annealing conditions to maximize surface fluorine enrichment (as detected by XPS). Comparison of these data indicate the effect of increasing polystyrene tail length on surface-activity of perfluoroalkyl groups. Optimum annealing conditions were used for heat treatment of SAP:E-2 and SAP:M-1 samples and comparisons were made on the basis of differences in architecture.

TABLE OF CONTENTS

LIST OF TABLES

LIST OF FIGURES

LIST OF SCHEMES

CHAPTER I

SURFACE CHEMICAL TRANSFORMATIONS OF POLY(ETHER ETHER KETONE): INTRODUCTION

Research in the McCarthy group has been directed toward the preparation of specifically functionalized and well-characterized polymer substrates with the objective of correlating macroscopic surface properties with microscopic chemical structure.[1] Surface chemical structure and composition determine critical surface tension. This surface energy controls surface properties which dictate the suitability of a material for a given application. Some of the macroscopic properties that are influenced by the (microscopic) characteristics of a surface are adhesion, wettability, biocompatibility, dyeability, gas permeability and frictional behavior. Knowledge of the association between desirable surface properties and the appropriate surface composition and structure allows "tailoring" of a surface. The strategy developed in the McCarthy group has been to control polymer surface properties by manipulating surface chemical structure using organic chemistry. In this approach, standard organic reactions are carried out to effect changes in the surface region of the film. Changes in atomic composition are monitored with X-ray photoelectron spectroscopy (XPS), and changes in surface properties, namely wettability, are monitored with contact angle measurements.

Polymer Surface Modification

Among the main approaches to polymer surface modification are plasma and corona discharge techniques, surface graft polymerizations using ultra-violet (UV) radiation, and chemical modification. Less commonly used methods include entrapment-functionalization,[2,3] surface reconstruction,[4-6] flame treatment[7] and UV-induced crosslinking.[8] Most often polymer surface treatments are carried out with the objective of increasing the surface energy to promote adhesion and wettability;[7,9] sometimes the objective is to change frictional properties.[10] Gas plasma treatments can induce changes in the morphology, roughness, chemical composition and molecular weight of a polymer surface.[11] Some plasma treatments have been used to implant fluorine-containing moieties on surfaces[12-15] as a means of reducing wettability. Experiments using oxygen-containing plasmas for surface treatments indicate that short exposure times effect changes in the chemical composition of the surface whereas longer times tend to cause more physical changes, namely etching of the surface.[16] Surface graft polymerizations using acrylic monomers have been carried out on polyethylene[8,17] and poly(ethylene terepthalate) (PET)[18] films by photoinitiation methods (sometimes using benzophenone as a photosensitizer[8]) to increase the wettability of these surfaces. In some cases, grafted polymer chains could be functionalized[17] for further surface property control.

Chemical polymer surface modifications encompass a wide variety of reaction types. In general these reactions (can) cause less physical damage than other surface treatments. These modifications include oxidations,[19,20] reductions,[21] halogenations,[22,23] dehydrohalogenations,[24] sulfonations,[25,26]

ozonations,[27] and aromatic electrophilic substitutions.[28] Chemical derivatizations[29,30] of surface-confined functional groups are sometimes carried out for XPS identification purposes (labelling reactions).

Structure-Property Relationships

Polymer surface modification studies by the McCarthy research group have been directed toward preparing and characterizing specifically functionalized substrates with the objective of correlating surface chemical structure with macroscopic surface properties. The virtue of controlled surface modification is that with the introduction to and manipulation of functional groups on a surface, new (surface) properties can be developed without changing the properties of the bulk material. From a practical standpoint, this is important for polymer materials that require different properties at the surface than in the bulk; surface modification can increase the versatility of any given polymeric material. From a scientific standpoint, this presents an ideal arrangement for studying the reactivity of surface-confined functional groups as well as for the examination of structure-property relationships at the molecular level. With this design, functional groups are covalently attached to an inert substrate. Reactions carried out on the surface can be compared with those from solution chemistry and any new properties that develop upon manipulation of the surface structure (or composition) must be attributed to differences in the functional groups.

Surface-confined functional groups would be expected to have different reactivities than similar molecules in solution for several reasons.

The two-dimensional nature of the environment at the surface may limit access to reactive sites. For example, S_N2 displacements (requiring attack from the back[31]) may be restricted. Solvation of the functional groups may be modified by the solid surface, and the close proximity of (many) other functional groups may affect the reactivity or even the nature of the reaction.

The polymer films chosen for surface modification are by necessity chemically inert substrates. Chemical inertness of the bulk material allows use of a range of reaction conditions to introduce new properties to the surface (prepare a reactive exterior) without affecting the underlying material (maintain an inert interior). Substrates that have been used by the McCarthy group for modification include several fluoropolymer films which are known for high chemical resistance, low wettability and poor adhesion characteristics. Among them are poly(vinylidene fluoride) (PVF_2),[32-35] poly(tetrafluoroethylene) (PTFE),[36,37] poly(tetrafluoro-ethylene-*co*-hexafluoropropylene) (FEP)[35,38] and poly(chlorotrifluoro-ethylene) (PCTFE).[35,39-43] Nonfluorinated chemically resistant polymers, including polyethylene (PE)[44] and polypropylene (PP),[45,46] which also have poor wetting properties, have been used for surface modification, as well. Initial modification of all of these polymer films entails brutal reaction conditions to introduce functional groups (reactive handles) to the surface; these reactive handles provide a means of further functionalizing the surface. The wetting properties of these substrates can be changed dramatically with chemical surface modification by the introduction of various polar functional groups,[32-47] and the adhesion properties can be manipulated, as well.[43]

Introduction of alcohol functionality is the surface modification utilized most frequently by the group. Hydroxyl groups in general are technologically important because of their impact on adhesion technology and in coupling agent chemistry.[48] Reactions with polymers containing hydroxyl groups (e.g. poly(vinyl alcohol)) have been carried out and reported in the literature.[49,50] Surface-confined alcohol species are interesting in terms of the increased surface wettability they cause and because they can lead to a wide variety of new surface transformations. For example, primary alcohol groups[41] have been introduced to the surface of PCTFE (termed PCTFE-OH) and subsequently reacted with a number of electrophiles in very high yield.[40] Adhesive joint studies were carried out on PCTFE-OH[43] to examine the facility of silane coupling and adhesion of the film to glass. Examination of the adhesion of PCTFE-OH to epoxy has been undertaken recently.[51] Contact angle measurements made on the PCTFE-OH surface indicate increased wettability relative to the original material.[40,41]

Oxidized FEP,[35] PP[45] and PCTFE[39] samples have been reduced to yield alcohol-containing surfaces and reduced PTFE[36] and FEP[38] films were oxidized to yield PTFE-OH and FEP-OH, respectively. Reactions of the hydroxylated surfaces with acid chlorides have produced surface-confined esters.[36,38,39,45] Friction studies have been initiated to examine the effect of different ester surface functionality on frictional behavior.[52] Other derivatizations of these functionalized surfaces include conversion of secondary hydroxyl groups to primary species (a concommitant increase in reactivity toward electrophiles was observed),[38] and reaction with isocyanates.[40,45] The alcohol-containing surfaces are more wettable than

the virgin polymer films, and this wettability can be manipulated by subsequent reaction with various electrophiles.

Surface Modification of Poly(ether ether ketone)

Surface modification studies were carried out with poly(ether ether ketone) (PEEK) films.[53-55] PEEK differs from substrates traditionally used by the McCarthy group for surface modification because it contains a potentially versatile functional group, the diaryl ketone, which is present in known concentration. PEEK qualifies as a chemically resistant substrate, although the ketones are present throughout the bulk. The goal in these surface studies was to use the carbonyl group as a reactive handle for modifying the surface and to monitor changes in wettability that occur with surface chemical differences. Because the diaryl ketone is structurally similar to benzophenone, many of the reactions attempted with PEEK were chosen from the literature of benzophenone chemistry; all successfully completed reactions transformed the carbonyl group. Initial studies focussed on the reactivity of the diaryl ketone as a surface functional group, and PEEK-alcohol surfaces were prepared and examined, as well.

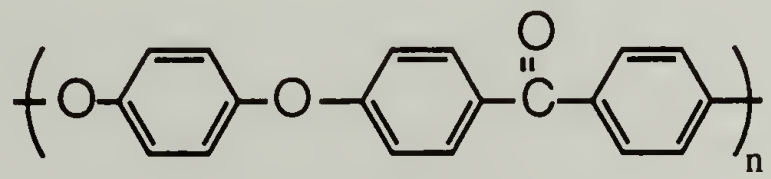

PEEK

Properties of PEEK

PEEK has received considerable attention recently as a high performance thermoplastic and its mechanical properties have been studied

extensively.[56] PEEK is known for its high temperature, chemical and radiation resistance and easy processing.[56,57] These characteristics make PEEK a suitable material for high performance applications, such as in aerospace and automotive industries. Studies carried out on PEEK include thermooxidation[58] experiments, physical[56,59] and thermal[56] aging analyses, as well as investigation of the effect of carbon fiber reinforcement on the mechanical properties[60] and biocompatibility[61] of composites. Solid PEEK can exist as an amorphous polymer or a semicrystalline material because the crystallinity can be developed with heat treatment.[57,62] The morphology has been studied using permanganate etching,[63] X-ray diffraction experiments,[64,65] and multiple reflection spectroscopy.[66] PEEK is prepared by the aromatic nucleophilic substitution reaction between hydroquinone and 4,4'-difluorobenzophenone in diphenyl sulphone at temperatures approaching the melting point of the polymer, 334 °C.[67-69] PEEK is insoluble in common organic solvents, but can be dissolved in strong acids, such as sulfuric acid.[70] (Solution crystallization studies have been carried out in benzophenone and α-chloronapthalene at temperatures around 200 °C.[71]) Studies examining sorption properties indicate that PEEK does not have utmost solvent resistance: PEEK absorbs a fair amount of methylene chloride[72] and moderate amounts of molten caprolactam,[73] and the mechanical properties of the polymer are dramatically diminished by this uptake.

The few surface modification studies that have been reported in the literature were designed to improve the wettability and adhesion properties of PEEK. Contact angle measurements indicate critical surface tension of virgin PEEK is about 36-39 dyn/cm.[74] Oxygen plasma treatments (and

sanding treatments) have been carried out on molded films to increase the surface energy and improve the bond strength with certain adhesives.[74] Photo-oxidation experiments using UV radiation in a flowing oxygen atmosphere also have been carried out to monitor structural changes in the polymer upon oxidation.[75]

Objective

Standard ketone transformations were carried out on PEEK films to assess the reactivity of the surface-confined diaryl ketone. The objective of these studies was to use the diaryl ketone as a reactive handle for modifying the surface and to monitor changes in wettability that occur with surface chemical differences. X-ray photoelectron spectroscopy (XPS) was used to assess the atomic composition of derivatized surfaces and contact angle measurements were used to assess changes in wettability. Appropriate solvent and temperature ranges were sought to determine optimum reaction conditions for these substrates. Several reactions attempted on PEEK came from the literature of benzophenone chemistry, although reaction conditions had to be adapted for use with PEEK film. Comparison of yields obtained for reactions with benzophenone and those with PEEK sheds some light on the reduced reactivity of surface-confined functional groups.

Several PEEK-alcohol surfaces were prepared with the objectives of first characterizing them using XPS, contact angle analyses and labelling reactions, and then comparing the reactivities of the surface-confined hydroxyl groups based on differences in structure. Surfaces containing

primary, secondary and tertiary hydroxyl groups were prepared, and the secondary and tertiary alcohol surfaces were "chain extended" to produce more reactive species. Because XPS survey spectra for PEEK-alcohol surfaces look identical to that for the unreacted material, reactions using "XPS-visible" reagents were carried out to confirm the presence of hydroxyl species. Labelling reactions were used to differentiate the reactivity of surface alcohol groups of different structure. The goals in this work included drawing correlations between the structure of surface-confined alcohols and the reactivity and wettability of each surface.

Polymer Surface Analytical Techniques

Analysis of polymer surfaces requires special analytical techniques which probe at very shallow depths. The surface of a material is loosely defined as the region which can be influenced by its environment and, relative to the bulk, this region contains little material. Various surface analytical techniques probe the surface at varied depths and reveal different types of information. For this reason, these techniques are most informative when used in combination. The derivatized PEEK samples were analyzed by XPS and contact angle measurements, and attenuated total reflectance infrared (ATR IR) spectra were recorded, although these spectra did not reveal any changes in the films. This information indicates that reactions on PEEK did not exceed depths of a couple hundred angstroms; ATR IR is considerably less surface-sensitive than the other two techniques and probes depths on the order of microns. A brief discussion of XPS and contact angle measurements as characterization techniques

follows, and, because of the lack of utility of ATR IR in our experiments, we chose to omit discussion of this technique.

X-Ray Photoelectron Spectroscopy. X-ray photoelectron spectroscopy (XPS) utilizes the photoelectric effect to reveal the atomic composition of the outer surface region of a material, ranging from depths of 10 - 100 Å[76,77] or 200 Å.[78] In this technique, the sample is exposed to (nearly) monoenergetic soft x-rays under ultra high vacuum and electrons are ejected. The detector analyzes the kinetic energy of the core electrons (E_k) and determines the binding energy of an electron in an atomic orbital of the source element (E_b) with

$$E_k = h\nu - E_b - \phi \qquad (1.1)$$

where $h\nu$ is the energy of the x-ray photons and ϕ is the work function of the spectrometer. Each atomic orbital of every element has a distinct binding energy, and XPS reveals the number of emitted electrons per element present. Other factors are important in quantitative determination of surface atomic composition including sensitivity factor corrections. The photoelectric cross-sections of the atoms comprising the surface vary and this means that peak sizes between elements cannot be compared directly. Atomic sensitivity factors compensate for differences in electron mean free paths and efficiencies of photoelectron generation and detection between elements.[77]

The surface sensitivity of XPS can be ascribed to the finite escape depth of the ejected photoelectrons. Electrons travel only short distances through matter due to inelastic scattering, and as a result, XPS sensitivity

decreases exponentially with depth. The number of electrons (N) detected relates to the number ejected (No) as

$$N = N_o e^{-\left(\frac{z}{\lambda \sin\theta}\right)} \qquad (1.2)$$

where z is the thickness of the material traversed (in the z direction), λ is the mean free path of an electron in a given material and θ is the angle to the detector (from the plane of the sample surface).[78] This exponential decrease in sensitivity indicates that XPS data can be biased high by functionality concentrated in the outermost surface layers. The mean free path of an electron in a material depends on its kinetic energy,[78] and using Mg K_α excitation, the mean free path for C_{1s} electrons has been determined to be 14 Å.[76] For XPS analysis of all film samples carried out for this dissertation, both of the Mg K_α and Al K_α anodes were used and 14 Å was used as mean free path length for depth determinations.

Variable angle XPS analysis utilizes the dependence of the escape depth of ejected electrons on the angle between sample and detector, and this allows assessment of the vertical homogeneity of the sample. At shallow angles, electrons have to travel through more of the solid sample to reach the detector so only those emitted from the outermost layers are analyzed. At steeper angles, electrons ejected from deeper within the sample still reach the detector and this allows analysis of material at greater depths. All samples in this work were analyzed at 15° and 75° takeoff angles (between the plane of the sample surface and detector). The scheme below describes the sample/detector geometry. From integration of

equation 1.2 within the limits of 0 to thickness t, we can determine the intensity (or number (N) of electrons detected) as

$$N = k\lambda\sin\theta\left(1 - e^{-\left(\frac{t}{\lambda\sin\theta}\right)}\right) \qquad (1.3)$$

where k is a constant. Data from the 15° takeoff angle geometry represent the atomic concentration of the top 11 Å of the film sample and equation 1.3 indicates that 94% of the electrons detected originate from this region. Spectra recorded at the 75° takeoff angle represent the composition of the outer 40 Å of the surface and 95% of the electrons detected are emitted from this region. Roughly 54% of the photoelectrons measured at 75° actually originate in the top 11 Å of the material. For this reason, large

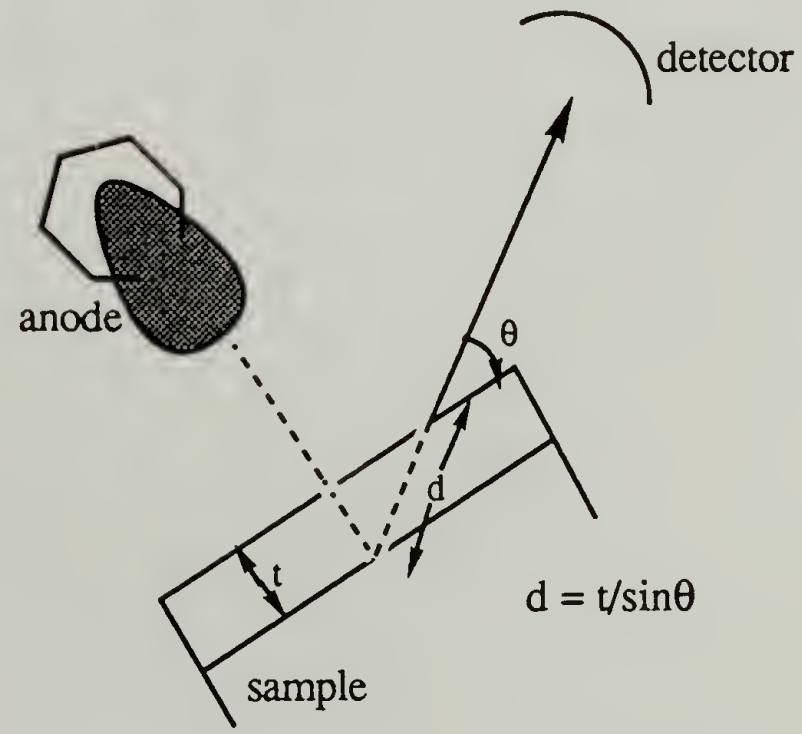

Scheme 1.1. Sample/Detector Geometry in Variable Angle XPS.

discrepancies between data recorded at 15 and 75° can reveal information about the distribution of functionality in a sample.

Contact Angle. Contact angle measurements provide the most surface-selective analysis of all the surface analytical techniques employed because only the outermost layers of the surface are sampled. Contact angle measurements are used to describe the surface tension of a material as well as give an indication of surface wettability. Young's equation[79]

$$\gamma_{SV} - \gamma_{SL} = \gamma_{LV} \cos \theta \qquad (1.4)$$

treats the angle (θ) formed by a liquid resting on a solid plane as the result of the mechanical equilibrium established as the balance of the three surface tensions involved, namely γ_{SL} of the solid-liquid interface, γ_{LV} of the liquid-vapor interface and γ_{SV} of the solid-vapor interface.

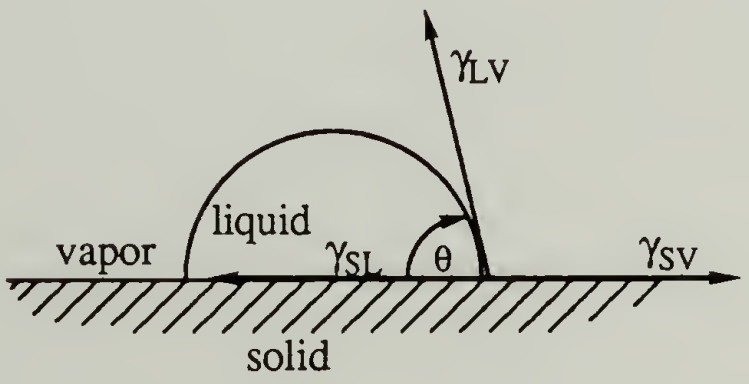

For the dynamic measurements made on PEEK, water was used as the probe fluid, and advancing (θ_A) and receding (θ_R) angles were recorded as water was added to and withdrawn from the drop. In this technique, it is

assumed that the surface is completely smooth, immobile, nondeforming, chemically homogeneous and does not interact with the probe fluid.[80] Within these requirements, a surface should have equal advancing and receding contact angles, but in reality surfaces do not meet all of these requirements and the advancing and receding angles differ; this is termed contact angle hysteresis. Hysteresis can stem from a variety (or combination) of causes, namely chemical heterogeneity,[81] surface roughness,[82] or low mechanical properties of the surface.[80] Swelling of the surface layers with the probe fluid also can cause hysteresis.[80]

References

1. For a review, see Ward, W.J; McCarthy, T.J. In *Encyclopedia of Polymer Science and Engineering*, 2nd ed.; Mark, H.F.; Bikales, N.M.; Overberger, C.G.; Menges, G.; Kroschwitz, J.I., eds.; John Wiley and Sons: New York, 1989; suppl. vol., p. 674.
2. Bergbreiter, D.E.; Hu, H.-P.; Hein, M.D. *Macromolecules* **1989**, *22*, 654.
3. Bergbreiter, D.E.; Chen, Z.; Hu, H.-P.; *Macromolecules* **1984**, *17*, 2111.
4. Gagnon, D.R.; McCarthy, T.J. *J. Appl. Polym. Sci.* **1984**, *29*, 4335.
5. Cross, E.M.; McCarthy, T.J. *Macromolecules* **1990**, *23*, 3921.
6. Ruckenstein, E.; Gourisankar, S.V. *J. Coll. and Interf. Sci.* **1985**, *107*, 488.
7. Brewis, D.M.; Briggs, D. *Polymer* **1981**, *22*, 7 and references therein.
8. Oster G.; Oster, G.K.; Moroson, H. *J. Polym. Sci.* **1959**, *34*, 671.
9. Hsieh, Y.-L.; Timm, D.A.; Wu, M. *J. Appl. Polym. Sci.* **1989**, *38*, 1719.
10. Triolo, P.M.; Andrade, J.D. *J. Biomed. Mater. Res.* **1983**, *17*, 129.
11. Coopes, I.H.; Gifkins, K.J. J. *Macromol. Sci.-Chem.* **1982**, *A17*, 217.
12. Yasuda, T.; Okuno, T.; Yoshida, K.; Yasuda, H. *J. Polym. Sci., Polym. Phys.* **1988**, *26*, 1781.
13. Corbin, G.A.; Cohen, R.E.; Baddour, R.F. *Macromolecules* **1985**, *18*, 98.
14. Clark, D.T.; Feast, E.J.; Musgrave, W.K.R.; Ritchie, I. *J. Polym. Sci. Polym. Chem.* **1975**, *13*, 857.
15. Kogoma, M.; Kasai, H.; Takahashi, K.; Moriwaki, T.; Okazaki, S. *J. Phys. D: Appl. Phys.* **1987**, *20*, 147.
16. Morra, M.; Occhiello, E.; Garbassi, F. *Langmuir* **1989**, *5*, 872.
17. Allmér, K.; Hult, A.; Rånby, B. *J. Polym. Sci. Polym. Chem.* **1989**, *27*, 1641.

18. Uchida, E.; Uyama, Y.; Ikada, Y. *J. Polym. Sci. Polym. Chem.* **1989**, *27*, 527.

19. Rasmussen, J.R.; Stredonsky, E.R.; Whitesides, G.M. *J. Am. Chem. Soc.* **1977**, *99*, 4736.

20. Rasmussen, J.R.; Bergbreiter, D.E.; Whitesides, G.M. *J. Am. Chem. Soc.* **1977**, *99*, 4746.

21. Barker, D.J.; Brewis, D.M.; Dahm, R.H. *Polymer* **1978**, *19*, 856.

22. Nambu, K. *J. Appl. Polym. Sci.* **1960**, *4*, 69.

23. Campbell, T.W.; Lyman, D.J. *J. Polym. Sci.* **1961**, *55*, 169.

24. Urban, M.W.; Salazar-Rojas, E.M. *Macromolecules* **1988**, *21*, 372.

25. Gibson, H.W.; Bailey, F.C. *Macromolecules* **1980**, *13*, 34.

26. Matsuda, T.; Litt, M.H. *J. Polym. Sci. Polym. Chem.* **1974**, *12*, 489.

27. Peeling, J.; Clark, D.T. *J. Polym. Sci. Polym. Chem.* **1983**, *21*, 2047.

28. Trott, G.F. *J. Appl. Polym. Sci.* **1974**, *18*, 1411.

29. Batich, C.D.; Wendt, R.C. In *Photon, Electron, and Ion Probes of Polymer Structure and Properties,* Dwight, D.W.; Fabishi, T.J.; Thomas, H.R., eds. *ACS Symp. Ser.*, 1981, *162*, Ch. 15.

30. Everhart, D.S.; Reilley, C.N. *Anal. Chem.* **1981**, *53*, 665.

31. Kemp, D.S.; Vellacio, F. *Organic Chemistry,* Worth Publishers, New York, 1980, Ch. 6.

32. Dias, A.J.; McCarthy, T.J. *Macromolecules* **1984**, *17*, 2529.

33. Brennan, J.V.; McCarthy, T.J. *Polym. Prepr. (Am. Chem. Soc., Div. Polym. Chem.)* **1988**, *29(2)*, 338.

34. Brennan, J.V.; McCarthy, T.J. *Polym. Prepr. (Am. Chem. Soc., Div. Polym. Chem.)* **1989**, *30(2)*, 152.

35. Shoichet, M.S.; McCarthy, T.J. *Macromolecules* **1991**, *24*, 982.

36. Costello, C.A.; McCarthy, T.J. *Macromolecules* **1987**, *20*, 2819.

37. Costello, C.A.; McCarthy, T.J. *Macromolecules* **1984**, *17*, 2940.

38. Bening, R.C.; McCarthy, T.J. *Macromolecules* **1990**, *23*, 2648.

39. Bee, T.G..; McCarthy, T.J. *Macromolecules* **1992**, *25*, 2093.

40. Lee, K.-W.; McCarthy, T.J. *Macromolecules* **1988**, *21*, 2318.

41. Dias, A.J.; McCarthy, T.J. *Macromolecules* **1987**, *20*, 2068.

42. Dias, A.J.; McCarthy, T.J. *Macromolecules* **1985**, *18*, 1826.

43. Lee, K.-W.; McCarthy, T.J. *Macromolecules* **1988**, *21*, 3353.

44. Cross, E.M.; McCarthy, T.J. *Polym. Prepr. (Am. Chem. Soc., Div. Polym. Chem.)* **1989**, *30(1)*, 422.

45. Lee, K.-W.; McCarthy, T.J. *Polym. Prepr. (Am. Chem. Soc., Div. Polym. Chem.)* **1987**, *28*, 250.

46. Lee, K.-W.; McCarthy, T.J. *Macromolecules* **1988**, *21*, 309.

47. Baskin, A.; Ter-Minassian-Saraga, L. *J. Polym. Sci. Part C* **1971**, *34*, 243.

48. Plueddemann, E.P. *Silane Coupling Agents*; Plenum: New York, 1982.

49. Varma, D.S.; Nedungadi, C. *J. Appl. Polym. Sci.* **1976**, *20*, 681.

50. Bonafini, J. Master of Science Thesis, Univ. of Mass., 1985.

51. Fleming, R.J. dissertation research, descriptions in progress reports.

52. Bee, T.G. dissertation research, descriptions in progress reports.

53. Franchina, N.L.; McCarthy, T.J. *Macromolecules* **1991**, *24*, 3045.

54. Franchina, N.L.; McCarthy, T.J. In *Chemically Modified Surfaces*; Mottola, H.A.; Steinmetz, J.R. eds., Elsevier Science Publishers: New York, 1991, 173.

55. Franchina, unpublished work on PEEK-alcohol surfaces.

56. For a review, see Nguyen, H.X; Ishida, H. In *Polymer Composites* **1987**, *8*, 57.

57. May, R. In *Encyclopedia of Polymer Science and Engineering*, 2nd ed.; Mark, H.F.; Bikales, N.M.; Overberger, C.G.; Menges, G.; Kroschwitz, J.I., eds., John Wiley and Sons: New York, **1989**; Vol. 12 , p. 313.

58. Brauman, S.K.; Pronko, J.G. *J. Polym. Sci. Part B* **1988**, *26*, 1205.

59. Kemmish, D.J.; Hay, J.N. *Polymer* **1985**, *26*, 905.

60. Bozarth, M.J.; Gillespie, J.W., Jr.; McCullough, R.L. *Polymer Composites* **1987**, *8*, 74.

61. Williams, D.F.; McNamara, A.; Turner, R.M. *J. Mater. Sci. Let.* **1987**, *6*, 188.

62. Technical data sheet from ICI, Americas.

63. Olley, R.H.; Bassett, D.C.; Blundell, D.J. *Polymer* **1986**, *27*, 343.

64. Blundell, D.J.; Osborn, B.N. *Polymer* **1983**, *24*, 953.

65. Dawson, P.C.; Blundell, D.J. *Polymer* **1980**, *21*, 577.

66. Chalmers, J.M.; Gaskin, W.F.; Mackenzie, M.W. *Polymer Bulletin* **1984**, *11*, 433.

67. Attwood, T.E.; Dawson, P.C.; Freeman, J.L.; Hoy, L.R.J.; Rose, J.B.; Staniland, P.A. *Polymer* **1981**, *22*, 1006.

68. Clendinning, R.A.; Farnham, A.G.; Johnson, R.N. *Polym. Prepr. (Am. Chem. Soc., Div. Polym. Chem.)* **1986**, *27(1)*, 478.

69. Rose, J.B. *Polym. Prepr. (Am. Chem. Soc., Div. Polym. Chem.)* **1986**, *27(1)*, 480.

70. Bishop, M.T.; Karasz, F.E.; Russo, P.S.; Langley, K.H. *Macromolecules* **1985**, *18*, 86.

71. Lovinger, A.J.; Davis, D.D. *Macromolecules* **1986**, *19*, 1861.

72. Pao, P.S.; Grayson, M.A.; Wolf, C.J. *J. Polym. Sci.* **1988**, *35*, 727.

73. Wilfong, D.L. *Polym. Prepr. (Am. Chem. Soc., Div. Polym. Chem.)* **1987**, *28(1)*, 61.

74. Whitaker, R.B.; Attalla, A.; Sullenger, D.B.; Wang, P.S.; Dichiaro, J.V.; Kenyon, A.S. *16th National SAMPE Tech. Conference* **1984**, 361.

75. Munro, H.S.; Clark, D.T.; Recca, A. *Polymer Degradation and Stability* **1987**, *19*, 353.

76. Clark, D.T.; Thomas, H.R. *J. Polym. Sci., Polym. Chem. Ed.* **1977**, *15*, 2843.

77. Muilenberg, G.E. *Handbook of X-Ray Photoelectron Spectroscopy,* Perkin-Elmer Corp., 1979.

78. Andrade, J.D.; Gregonis, D.E.; Smith, L.M. In *Surface and Interfacial Aspects of Biomedical Polymers*; Andrade, J.D. ed. Plenum: New York, 1986, Vol. 1, Ch. 5.

79. Zisman, W.A. *Adv. Chem. Ser.* **1964**, *43*, 1, and references therein.

80. Reference 76, Ch. 7.

81. Johnson, R.E.; Dettre, R.H. *J. Phys. Chem.* **1964**, *68*, 1744.

82. Huh, C.; Mason, S.G. *J. Coll. and Interf. Sci.* **1977**, *60*, 11.

CHAPTER II

EXPERIMENTAL

Materials

3-Bromo-1-propanol (Aldrich) was distilled from potassium carbonate (64 °C, 5 mm) and stored over potassium carbonate.

Carbon tetrachloride (Fisher) was degassed using three freeze-pump-thaw cycles.

Chloroform (Fisher) was distilled from phosphorous pentoxide.

Dimethylsulfoxide (Aldrich) was distilled from calcium hydride (73 - 75 °C, 10 mm).

Ethanol was distilled from magnesium.

Ethylene oxide (Kodak) was purified by freeze-pump-thaw cycles and trap-to-trap distillation from calcium hydride.

Hexane (Fisher) was distilled from calcium hydride.

Heptane (Fisher) was distilled from calcium hydride.

Methanol (Fisher) was distilled from magnesium.

Poly(ether ether ketone) was obtained from ICI: amorphous as 1-, 2- and 5-mil Stabar K200, 40% crystalline as 4-mil Stabar XK300. Amorphous film samples were cleaned by immersion in methanol for 30 min followed by immersion in heptane for 30 min. Semicrystalline films were extracted (Soxhlet) with THF for 12-24 h. All film samples were subsequently dried (room temperature, 0.05 mm, >48 h).

Pyridine (Aldrich) was distilled from calcium hydride.

Tetrahydrofuran (Aldrich) was distilled from sodium benzophenone dianion.

Water (house distilled) was redistilled using a Gilmont still.

Benzenesulfonyl isocyanate, phenyl isocyanate, *n*-propyl isocyanate, thionyl chloride, trichloroacetyl chloride, trichloroacetyl isocyanate and trimethylsilyl cyanide were obtained from Aldrich and purified by freeze-pump-thaw cycles and trap-to-trap distillation from calcium hydride.

tert-Butyllithium, dibutyltin dilaurate, 2,4-dinitrophenylhydrazine, lithium diisopropylamide, methyllithium and methyltriphenylphosphonium bromide (all from Aldrich) were used as received. Wash solvents that were not distilled were sparged with nitrogen immediately prior to use.

Materials Handling

All solvents and distilled reagents were either used immediately or stored under nitrogen for short periods of time in Schlenk flasks. All transfers of reagents and solvents were done by cannula or syringe.

Methods

All distillations and reactions were carried out under nitrogen unless otherwise indicated, and reaction solutions were not stirred. Experiments were carried out on commercially available PEEK film samples that had been extracted with THF and dried to constant mass. X-ray photoelectron spectra (XPS) were recorded using a Perkin Elmer-Physical Electronics 5100 spectrometer with Mg K_α or Al K_α excitation (400 W or 300 W, respectively). Spectra were analyzed at two takeoff angles, 15° and 75°, from the plane of the sample surface. Contact angle measurements were made with a Ramé-Hart telescopic goniometer using a Gilmont syringe with a 24-gauge flat-tipped needle. Water purified as described above was used as the probe fluid. Dynamic advancing and receding angles were measured while adding or withdrawing water to or from the drop. The values reported are averages of five measurements made at random points on the surface. Attenuated total reflectance infrared (ATR IR) spectra were recorded with an IBM 38 FTIR spectrometer using a germanium internal reflection element (45°). Data obtained from all reactions with PEEK have been tabulated and included in Chapter III.

Ketone Derivatizations

A variety of reactions were carried out on PEEK to derivatize the diaryl ketones on the surface. These reactions are shown in Scheme 2.1.

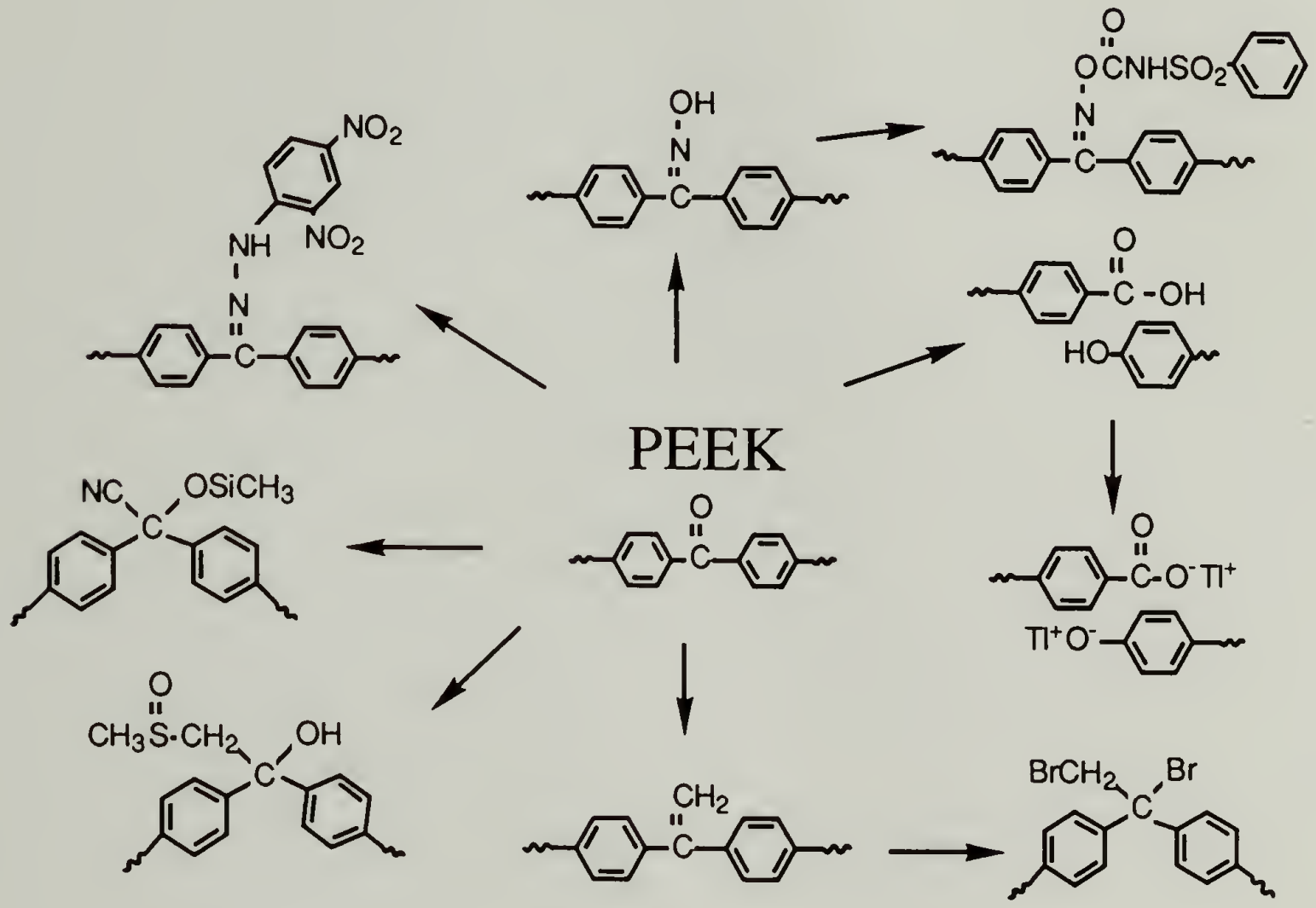

Scheme 2.1. Reactions with PEEK Film.

Reaction of PEEK with 2,4-Dinitrophenylhydrazine (PEEK~C=NNHØ(NO_2)$_2$). (1:5, 33, 47, 83, 139, 141)[1] A solution of 2,4-dinitrophenylhydrazine and a few drops of conc. HCl in 25 mL THF was introduced via cannula to a Schlenk tube containing a PEEK film sample. After sparging with nitrogen, the tube was heated at 45 °C for 48

h. After this time, the solution was removed and the film was washed with THF (5 x 20 mL) and then methanol (5 x 20 mL). The film sample was extracted overnight with methanol (Soxhlet) and dried (room temperature, 0.05 mm, 48 h). Representative contact angle and XPS data for this reaction are given in Tables 5 and 6, respectively.

Reaction of PEEK with Hydroxylamine (PEEK~C=N-OH).[2] (1:95, 97, 103, 109, 113-118, 129; 2:5, 27, 41, 55, 61, 65; 3:34, 53, 71) A PEEK sample, 3.0 g hydroxylamine hydrochloride, 10 mL ethanol and 2 mL water were introduced to a water-jacketed (for reflux) Schlenk tube. Sodium hydroxide (5.5 g) was added in five portions, with shaking after each addition. The tube was sparged with nitrogen, heated at 40 °C for 24 h, and then heated at reflux for 24 h. The flask was cooled, the solution was removed and the film was rinsed with 10% aqueous HCl (5 x 30 mL), water (3 x 30 mL), methanol (2 x 30 mL) and hexane[3] (3 x 30 mL), and dried (room temperature, 0.05 mm, 48 h). XPS and contact angle data for different reactions times are in Table 2. Representative XPS and contact angle data for optimum reaction conditions are in Tables 5 - 6.

Reaction of PEEK-Oxime with Benzenesulfonyl Isocyanate (PEEK~C=N-OC(O)NHSO$_2$Ø).[4] (1:138; 3:47, 67, 89, 105) THF (10 mL) containing four drops of dibutyltin dilaurate was introduced via cannula to a Schlenk tube containing PEEK~C=N-OH film. Benzene-sulfonyl isocyanate (1.2 mL) was added; the tube was shaken and allowed to sit at room temperature for 24 h. The solution was removed and the film sample was washed with THF (5 x 20 mL) and dried (room temperature,

0.05 mm, 48 h). Representative contact angle and XPS data for this reaction are in Tables 5 and 6, respectively.

Oxidation of PEEK with $KClO_3/H_2SO_4/H_2O$ (PEEK(OH)CO_2H).[5] (2:18, 37, 45, 63, 98, 117, 134; 3:39) Potassium chlorate was dissolved in 100 mL of 50:50 (v/v) sulfuric acid/water in a flask open to the air. After the solution cooled to ~40 °C, a PEEK film sample was introduced and the solution was stirred for 30 min. The solution was removed and the film was rinsed with water (5 x 30 mL), methanol (5 x 30 mL) and hexane (3 x 30 mL) and then dried (room temperature, 0.05 mm, 24 h). Contact angle data for different sulfuric acid/water ratios are in Table 3, and contact angle data for different reaction times are in Table 4. Representative XPS and contact angle data for optimum reaction conditions are in Tables 5 - 6.

Reaction of PEEK-(OH)CO_2H with Thallous Ethoxide (PEEK(OTl)CO_2Tl).[6] (2:135a, 136) Thallous ethoxide (~20 mL) was introduced via cannula to a Schlenk tube containing an oxidized PEEK sample. After 30 s, the thallous ethoxide was removed and the film was washed with ethanol (5 x 20 mL) and dried (room temperature, 0.05 mm, 24 h). Representative XPS and contact angle data are in Tables 5 and 6.

Reaction of PEEK with Methylenetriphenylphosphorane (PEEK~C=CH_2).[7] (3:32, 49a,c, 69, 95, 101) Me_2SO (10 mL) was added to a flask containing 0.48 g sodium hydride. The flask was heated to 75-80 °C for 45 min, after which time the evolution of hydrogen had ceased. The salt solution was introduced via cannula into a Schlenk tube containing warm (~40 °C) Me_2SO (10 mL), methyltriphenylphosphonium bromide

(7.0 g), and PEEK film. The tube was heated to 60 °C for 24 h and the solution was then removed. The film sample was rinsed with Me_2SO (3 x 20 mL), methanol (5 x 20 mL), hexane (3 x 20 mL), and then dried (room temperature, 0.05 mm, 48 h). Representative XPS and contact angle data are in Tables 5 and 6.

Bromination of PEEK~C=CH_2 (PEEK~CBr-CH_2Br). (3:52, 74, 75, 103) A 0.2 M solution of bromine in carbon tetrachloride (15 mL) was prepared and introduced via cannula to a Schlenk tube containing a PEEK~C=CH_2 sample. The tube was maintained at 0 °C in darkness for 24 h, after which time the solution was removed and the film was washed with carbon tetrachloride (2 x 20 mL), THF (5 x 20 mL), extracted (Soxhlet) with THF for 24 h and then dried (room temperature, 0.05 mm, 48 h). Representative contact angle and XPS data are in Tables 5 and 6.

Reaction of PEEK with Dimsyl Sodium (PEEK~C(OH)-$CH_2S(O)CH_3$).[7] (3:33, 49a,b, 70) A dimsylsodium solution was prepared (as described above for the PEEK~C=CH_2 preparation) and introduced to a Schlenk tube containing a PEEK film sample and 10 mL Me_2SO. After 24 h at 60 °C, the solution was removed and the film was washed with Me_2SO (3 x 20 mL), 10 % aqueous HCl (3 x 30 mL), water (2 x 30 mL), methanol (3 x 20 mL) and hexane (2 x 20 mL), and then dried (room temperature, 0.05 mm, 48 h). XPS and contact angle data are in Tables 5 - 6.

Reaction of PEEK with Trimethylsilyl Cyanide (PEEK~C(CN)OSiMe_3).[8] (3:23, 25, 43, 55, 73, 97) Chloroform (10 mL) was introduced via cannula to a Schlenk tube containing zinc iodide (15-20

mg) and a PEEK film sample. Trimethyl-silyl cyanide (1.5 mL) was added and the solution was shaken until it became bright orange-red. The tube was heated to 40 °C for 24 h. The solution was removed and the film sample was rinsed with chloroform (2 x 20 mL), methanol (5 x 20 mL), and hexane (3 x 20 mL) and then dried (room temperature, 0.05 mm, 24 h). Representative contact angle and XPS data are in Tables 5 and 6.

PEEK-Alcohol Surfaces

Primary, secondary and tertiary hydroxyl groups were introduced to the surface of PEEK film. The secondary and tertiary alcohol surfaces were chain extended to produced different primary hydroxyl species. The different PEEK-alcohol structures are shown in Scheme 2.2.

Reduction of PEEK with Sodium Bis(2-methoxyethoxy)aluminum Hydride (PEEK~$OH^{2°}$).[9] (2:107, 113, 131, 139; 3:5, 45, 57, 79, 127, 143; 4:21a, 44a, 66a) THF (10 mL) and sodium bis(2-methoxyethoxy)-aluminum hydride (3.4 mmol) were introduced via cannula to a Schlenk tube containing PEEK film. The flask was heated to 40 °C for 3 h and then the solution was removed. The film sample was washed with THF (2 x 20 mL), 15 % aqueous NaOH (5 x 30 mL), water (3 x 30 mL), 10 % aqueous sulfuric acid (3 x 30 mL), water (3 x 30 mL), methanol (3 x 30 mL) and hexane (2 x 30 mL), and then dried (room temperature, 0.05 mm, 24 h). Contact angle data for manipulation of reaction conditions are in Table 7.

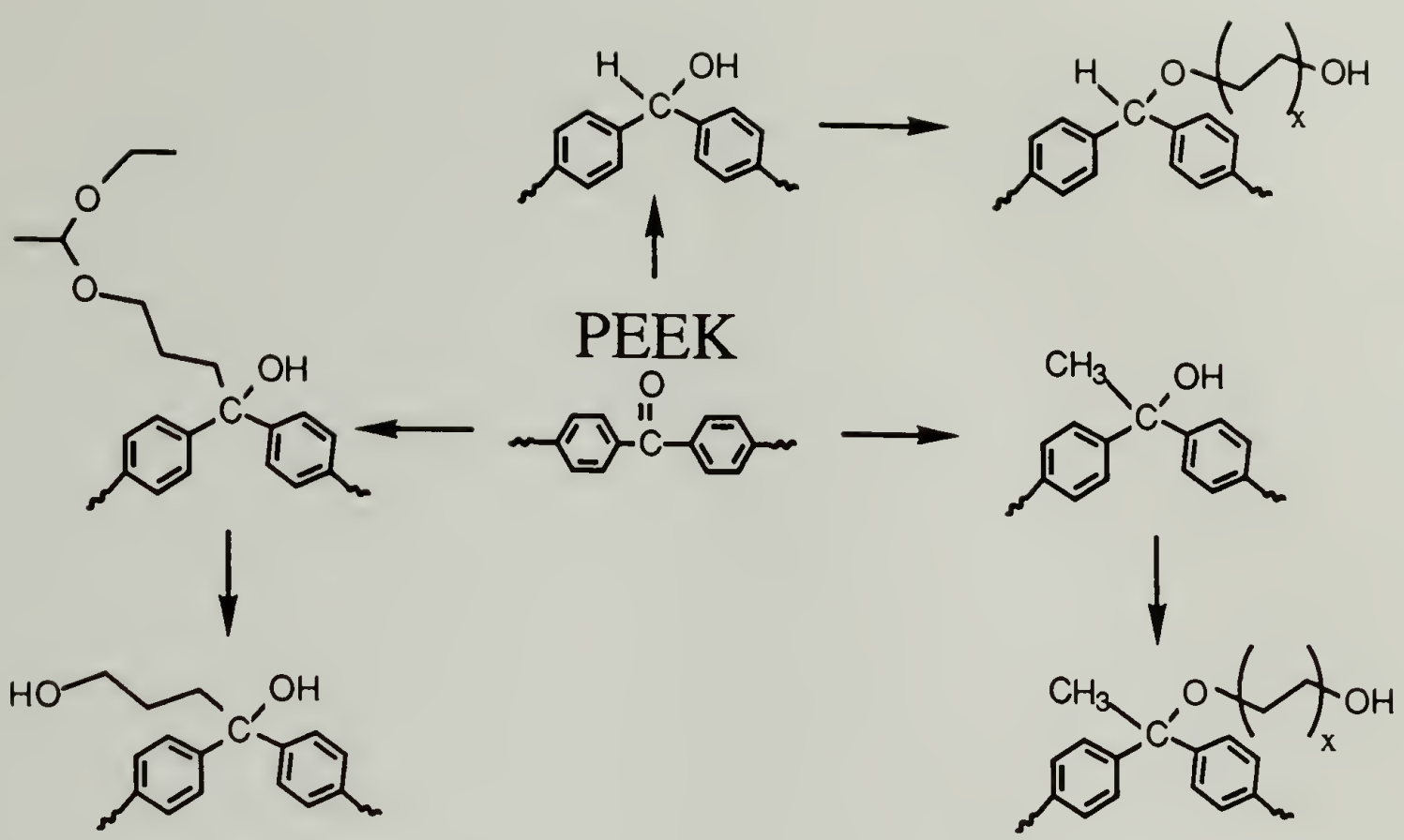

Scheme 2.2. Preparation of PEEK-Alcohol Surfaces.

Reaction of PEEK with Methyllithium (PEEK~$OH^{3°}$). (1:105; 2:39, 43, 85, 109, 115, 144; 3:109, 115, 125, 143; 4:21b, 44b, 66b) A 0.36 M solution of methyllithium in THF was introduced to a Schlenk tube containing PEEK film. The tube was maintained at 40 °C for 3 h, and after this time, the solution was removed and the films were washed with THF (2 x 30 mL), 10 % aqueous HCl (5 x 30 mL), water (3 x 30 mL), methanol (3 x 30 mL) and hexane (2 x 30 mL), and then dried (room temperature, 0.05 mm, 24 h). XPS and contact angle data for this surface can be found in Tables 11 and 12, respectively.

Reaction of PEEK~OH$^{2°}$ and PEEK~OH$^{3°}$ with Ethylene Oxide (PEEK~ce-OH$^{2°}$ and PEEK~ce-OH$^{3°}$). (4:18a,b, 23a,b, 47a,b, 67a,b) Ethylene oxide (0.1 mol) was introduced via cannula into a Schlenk tube containing LDA (2.8 g) and a PEEK~OH film sample in THF (45 mL) at 0 °C. After 24 h, the reaction solution was removed and the films were washed with THF (3 x 50 mL), 10 % aqueous HCl (3 x 50 mL), a methanol/water solution (25 mL/25 mL) that was heated to 70 °C overnight, methanol (3 x 50 mL) and hexane (2 x 50 mL), and then dried (room temperature, 0.05 mm, 48 h). XPS and contact angle data for the chain extended 2° and 3° surfaces are in Tables 15 and 16, and Tables 17 and 18, respectively.

Preparation of Acetaldehyde Lithiopropyl Ethyl Acetal (LiPrOP).[10] (3:129a,b; 4:5, 25, 65, 80) Two (well-dried and purged) 100 mL Schlenk flasks (A and B) containing 10 mL and 5 mL of heptane, respectively, were equilibrated at -78 °C using a dry ice/acetone bath. Acetaldehyde bromopropyl ethyl acetal (5.5 mmol) was added to flask A and *tert*-butyllithium (3.0 mL of 1.7 M solution in heptane, 5.1 mmol) was added to flask B, and both solutions were stirred at -78 °C for 15 min. The solution from flask B was cannulated into flask A and the resulting clear solution was stirred vigorously at -78 °C for 15 min. The solution was warmed to -20 °C, at which temperature it became a white suspension, and was stirred for 15 min. After this time, the suspension was cooled to -78 °C, and THF (25 mL that had been equilibrated to -78 °C) was added and the resulting solution of LiPrOP in THF/heptane was stirred for 15 min.

Preparation of PEEK~C(OH)PrOP. (3:129a,b; 4:5, 25, 65, 80) The solution of LiPrOP in THF/heptane was introduced via cannula into

two Schlenk tubes containing PEEK film. The tubes were maintained at 0 °C for 5 h and then the solution was removed. The films were washed with THF (3 x 40 mL), water (5 x 40 mL) and methanol (3 x 40 mL) and were dried (room temperature, 0.05 mm, 48 h). Contact angle data for different reaction times and temperatures are in Table 8.

Hydrolysis of PEEK~C(OH)PrOP (PEEK~OH$^{1°}$). (3:137a,b; 4:8, 25, 65, 80) PEEK~C(OH)PrOP film samples were placed into a solution containing concentrated HCl (6 mL), water (16 mL), and methanol (18 mL) in a water-jacketed (for reflux) Schlenk tube. The solution was refluxed for 5 hours and then the samples were removed. The film samples were washed with water (3 x 40 mL), methanol (3 x40 mL), and hexane (2 x 40 mL), and then dried (room temperature, 0.05 mm, 48 h). XPS and contact angle data for this surface are in Tables 13 and 14.

Reactions with PEEK-Alcohol Surfaces

All of the different PEEK~OH^{11} surfaces were reacted with a variety of reagents in an effort to estimate relative hydroxylation reaction yields and to shed some light on differences in reactivity among the surfaces. Generic resulting surface structures for reactions carried out on PEEK~OH substrates are shown in Scheme 2.3.

Reaction of PEEK~OH with Trichloroacetyl Chloride (PEEK~OC(O)CCl_3). (2:121, 133a,b; 3:139a,b,c; 4:3a,b, 20a,b, 54, 57, 61a,b, 68a,b,c,) Trichloroacetyl chloride (9.8 mmol) was added to a Schlenk tube containing a PEEK~OH film sample in a solution of THF (13

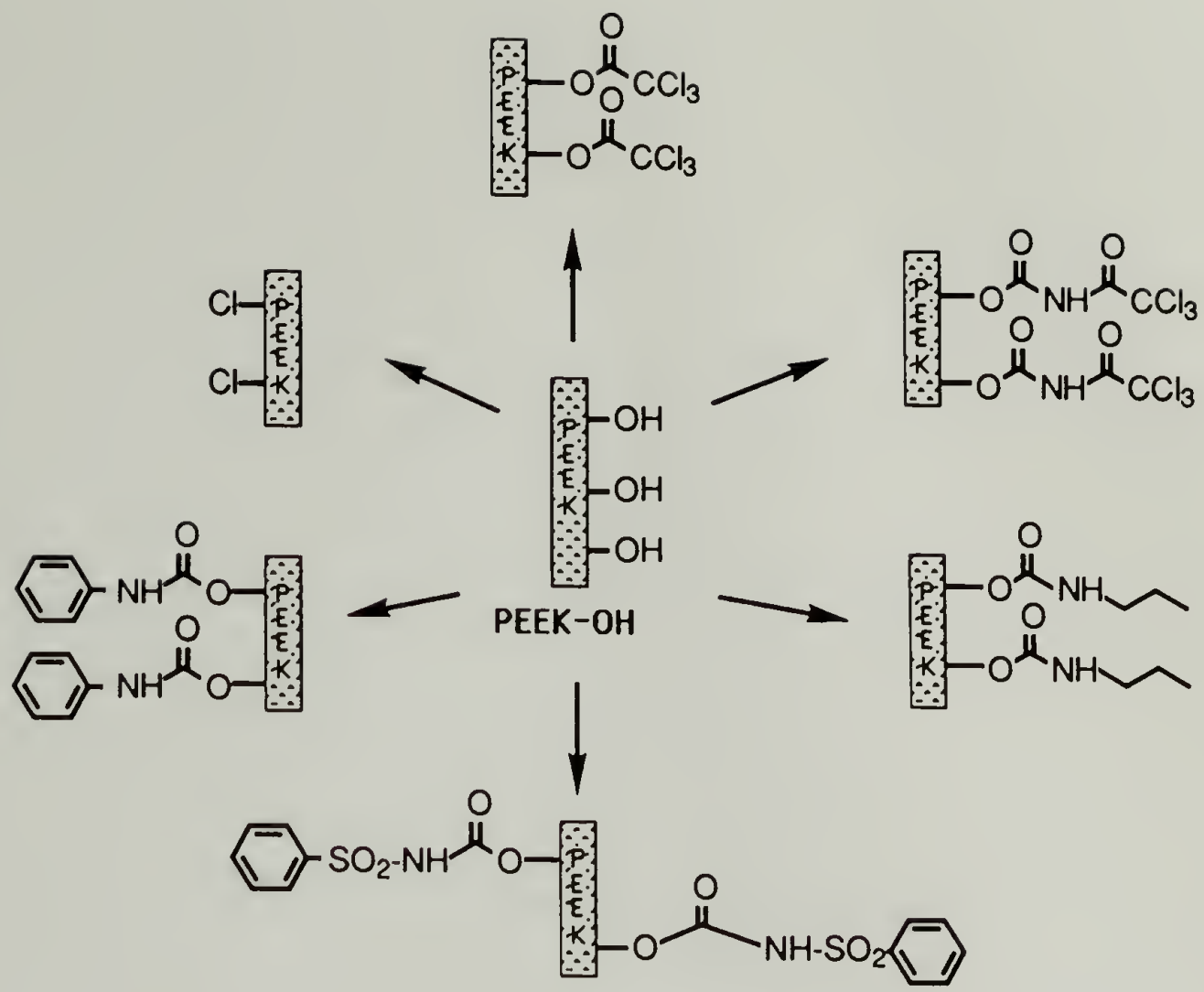

Scheme 2.3. Reactions with PEEK~OH.

mL) and pyridine (2 mL). The reaction solution (initially clear) was maintained at room temperature for 24 h during which time it became bright yellow. The reaction solution was removed and the films were washed with methanol (5 x 20 mL), THF (3 x 20 mL), methanol (3 x 20 mL) and hexane (2 x 20 mL), and then dried (room temperature, 0.05 mm, 24 h). Representative XPS and contact angle data for reactions with PEEK~OH$^{2°}$ are in Tables 9 and 10, data for PEEK~OH$^{3°}$ are in Tables 11 and 12, data for reactions with PEEK~OH$^{1°}$ are in Tables 13 and 14, data for PEEK~ce-OH$^{2°}$ are in Tables 15 and 16, and data for PEEK~ce-OH$^{3°}$ are in Tables 17 and 18.

Reaction of PEEK~OH with Isocyanates (Trichloroacetyl Isocyanate, Benzenesulfonyl Isocyanate, n-Propyl Isocyanate, Phenyl Isocyanate) (PEEK~OC(O)NHC(O)R). (2: {121, 133a,b}, {89a,b,c} {0} {0}; 3:{0}, {29, 47, 89a,b, 105a,b}, {0}, {0}; 4:{17a,b, 28a,b, 32, 43a,b, 59a,b,c, 70a,b,c, 73a,b,c}, {11a,b,c, 15a,b, 34a,b, 42, 62a,b}, {12a,b,c, 35a,b, 55a,b,c, 63a,b, 72a,b,c}, {22a,b, 33, 71a,b,c})[12] Each isocyanate (4-9 mmol) was added to a Schlenk tube containing a PEEK~OH film sample in a solution of THF (10-15 mL) and a catalytic amount of dibutyltin dilaurate. Each reaction was carried out at room temperature for 24 h, after which time the reaction solution was removed and the films were washed with THF (5 x 20 mL), methanol (3 x 20 mL), THF (3 x 20 mL) and hexane (2 x 20 mL), and dried (room temperature, 0.05 mm, 24 h). Representative XPS and contact angle data for reactions with PEEK~OH$^{2°}$ are in Tables 9 and 10, data for PEEK~OH$^{3°}$ are in Tables 11 and 12, data for reactions with PEEK~OH$^{1°}$ are in Tables 13 and 14, data for PEEK~ce-OH$^{2°}$ are in Tables 15 and 16 , and data for PEEK~ce-OH$^{3°}$ are in Tables 17 and 18.

Reaction of PEEK~OH with Thionyl Chloride (PEEK~Cl). (3:41, 134a,b, 147a,b; 4:10a,b,c, 40,a,b,c, 41, 51a,b,c,d, 52a,b,c, 74a,b,c,d) THF (15 mL) and thionyl chloride 1.5 mL) were introduced via cannula to a Schlenk tube containing a PEEK~OH film sample. After 24 h at room temperature, the solution was removed and the film was washed with THF (3 x 20 mL), methanol (3 x 20 mL), THF (2 x 20 mL) and hexane (2 x 20 mL), and then dried (room temperature, 0.05 mm, 24 h). Representative XPS and contact angle data for reactions with PEEK~OH$^{2°}$ are in Tables 9 and 10, data for PEEK~OH$^{3°}$ are in Tables 11 and 12, data for PEEK~ce-

$OH^{2°}$ are in Tables 15 and 16 and data for PEEK~ce-$OH^{3°}$ are in Tables 17 and 18.

Failed Reactions with PEEK

A few reactions attempted with PEEK film were unsuccessful. Four of such attempts are described here. Three of the reactions transform the carbonyl group and the fourth involves Friedel Crafts acylation.

Attempted Synthesis of PEEK~$C(NH_2)CN$.[13,14] (2:47, 50, 52, 57) A solution of sodium cyanide (10 mmol) in water (5 mL) was added to a solution of ammonium chloride (11 mmol) in water (7 mL). Ammonium hydroxide (1.3 mL) and ethanol (15 mL) were added and the resulting solution was introduced to a Schlenk tube containing a PEEK film sample. After 48 h at 60 °C, the solution was removed and the film sample was washed with methanol (5 x 50 mL), water (10 x 50 mL), methanol (2 x 20 mL) and hexane (2 x 20 mL), and then dried (room temperature, 0.05 mm, 48 h).

Attempted Synthesis of PEEK~$COCH_2$.[15] (3:93, 99, 107, 113; 4:48, 64, 67, 75, 76-78) Trimethyloxosulfonium iodide (10 mmol), sodium hydride (10 mmol) and DMSO (10 mL) were stirred at toom temperature for 45 min to produce dimethyloxosulfonium methylide. The ylide solution was introduced to a Schlenk tube containing a PEEK film sample. After 24 h at 50 °C, the solution was removed and the film sample was washed with DMSO (3 x 20 mL), water (3 x 20 mL), THF (2 x 20 mL) and hexane (2 x 20 mL), and dried (room temperature, 0.05 mm, 48 h).

Attempted Synthesis of PEEK~CCl_2.[13] (2:127; 3:11, 12) Chloroform (10 mL) was introduced to a Schlenk tube containing phosphorous pentachloride (4.0 mmol) and a PEEK film sample. The tube was maintained at room temperature for 48 h during which time most of the phosphorous pentachloride had dissolved. The reaction mixture was removed and the film sample was washed with chloroform (3 x 20 mL), methanol (5 x 20 mL), and hexane (2 x 20 mL), and then dried (room temperature, 0.05 mm, 48 h).

Attempted Friedel Crafts Acylations. (2:65, 69, 72, 77, 79, 105, 111, 129) A solution of nitrobenzene (20 mL), aluminum chloride (20 mmol) and either trichloroacetyl chloride (TCAC) or heptafluorobutyryl chloride (HFBC) (10 mmol) was cannulated into a Schlenk tube containing PEEK film. After 48 h at 65 °C, 30 °C or room temperature, the solution was removed and the film sample was washed with nitrobenzene (3 x 20 mL), warm methanol (5 x 20 mL), 10 % aqueous HCl (5 x 20 mL) and water (5 x 20 mL), and then dried (room temperature, 0.05 mm, 48 h).

References

1. The numbers in parentheses refer to notebook numbers and pages.
2. Lachman, A. In *Organic Syntheses;* Blatt, A. H., ed., John Wiley & Sons: New York, 1943, Collect. Vol. II, p. 70.
3. Washing procedures are usually finished with a hexane wash to minimize contamination of the surface with silicon-containing impurities.
4. McFarland, J.W.; Howard, J.B. *J. Org. Chem.* **1965**, *30*, 957.
5. Baszkin, A.; Ter-Minassian-Saraga, L. *J. Polym. Sci., Part C.* **1971**, *34*, 243.
6. Reilley, C.N.; Everhart, D.S.; Ho, F.F.L. In *Applied Electron Spectroscopy for Chemical Analysis*; Windawi, H., Ho, F.F.L., eds.; John Wiley & Sons: New York, 1982, Chapter 6.
7. Corey, E.J.; Chaykovsky, M. *J. Am. Chem. Soc.* **1962**, *84*, 866.
8. Evans, D.A.; Truesdale, L.K.; Carroll, G.L. *Chem. Commun.* **1973**, 55.
9. Capka, M.; Chvalovsky, V.; Kochloefl, K.; Kraus, M. *Coll. Czech. Chem. Comm.* **1969**, *34*, 118.
10. Dias, A.J.; McCarthy, T.J. *Macromolecules* **1987**, *20*, 2068.
11. The term PEEK~OH refers to PEEK-alcohol surfaces in general or as a group.
12. Parentheses are ordered according to listing of isocyanates.
13. March, J. *Advanced Organic Chemistry*, 3rd ed. Wiley-Interscience: New York, 1985.
14. Steiger, R.E. In *Organic Syntheses*; Blatt, A.H., John Wiley and Sons: New York, 1965, Coll. Vol. III, p. 66.
15. Corey, E.J.; Chaykovsky, M. *J. Am. Chem. Soc.* **1965**, *87*, 1353.

CHAPTER III

RESULTS AND DISCUSSION

Several carbonyl-selective reactions were carried out on poly(ether ether ketone) (PEEK) films and the modified surfaces were analyzed with X-ray photoelectron spectroscopy (XPS), attenuated total reflectance infrared spectroscopy (ATR IR) and contact angle measurements. The first section of this work included assessment of the solvent and temperature stability of amorphous and semicrystalline PEEK films (under conditions appropriate for reactions). Once suitable solvent and temperature conditions had been established, a series of experiments was carried out to determine the extent to which the surface-confined ketone reacts as a functional group at PEEK-solvent interfaces. In the second section of this work on PEEK, several surfaces containing alcohol groups of different structure were prepared to determine differences in reactivity between such surface-confined hydroxyl groups relative to each other and relative to alcohol groups in solution. Surface analyses were carried out to assess changes in surface properties that occurred with surface chemical differences.

Solvent Resistance

The ability of amorphous and semicrystalline PEEK films to function as surface modification substrates was assessed by examining their resistance to solvents that would likely be used for surface chemical reactions. Amorphous PEEK is (visibly) stable to methanol, ethanol and

heptane at reflux temperatures and acetone at room temperature. However, solvent-induced crystallization and/or plasticization occur within 30 min of exposure at room temperature to benzene, pyridine, toluene or methylene chloride; the films become opaque and roll into scrolls. Because of this limited solvent resistance, amorphous PEEK was eliminated as a surface modification substrate. Semicrystalline PEEK is considerably more solvent resistant. Exposure for 24 h to THF, methanol, ethanol, benzene, toluene, water, hexane and heptane at reflux temperatures causes no visible changes in the films. No changes are observed upon exposure to dimethyl sulfoxide at temperatures below 65 °C or nitrobenzene at room temperature. Methylene chloride and carbon tetrachloride plasticize semicrystalline PEEK at room temperature as do pyridine and chloroform above 45 °C. These solvent resistance data are summarized in Table 1.

Characterization of PEEK

Semicrystalline PEEK films (4-mil thick Stabar XK300 obtained from ICI)[1] were characterized fully before any surface modification reactions were carried out. These films are produced by a process (rolled) that causes the two sides of the material to differ visibly but not spectroscopically. One side (called side a) is reflective while the other side (side b) is nonreflective and dull. Water contact angles of the two sides are slightly different: side b exhibits a receding contact angle ~5° lower than side a. (For side a: $\theta_A/\theta_R = 85°/55°$ and side b: $\theta_A/\theta_R = 85°/50°$.) This difference is fairly consistent for the derivatized PEEK surfaces, so dynamic advancing and receding contact angle data are reported for both sides of the film. XPS and ATR IR spectra of the two sides are

Table 1. Solvent Resistance of Amorphous and Semicrystalline PEEK Films.

Solvent	Temperature	Amorph. PEEK	Semicryst. PEEK
MeOH	refluxing	no change	no change
EtOH	refluxing	no change	no change
H_2O	refluxing	no change	no change
heptane	refluxing	no change	no change
THF	RT	film scrolls up	no change
	refluxing	film scrolls up	no change
benzene	RT	film scrolls up	no change
	refluxing	film scrolls up	no change
toluene	refluxing	film scrolls up	no change
pyridine	<45 °C	film scrolls up	no change
	>45 °C	film scrolls up	film grows splotchy
DMSO	<65 °C	film scrolls up	no change
nitrobenzene	RT		no change
CH_2Cl_2	all	film scrolls up	film peels
$CHCl_3$	<45 °C		no change
	>45 °C		film curls
CCl_4	RT		no change

indistinguishable, but side a was used consistently for XPS analysis. Figure 3.1 shows survey and O_{1s} region XPS spectra for PEEK and Figure 3.2 shows the ATR IR spectrum. Quantitation of the XPS data indicates a C/O ratio of 6.4 although the empirical formula is $C_{19}O_3$ which corresponds to a C/O ratio of 6.3. The O_{1s} spectrum is comprised of two partially resolved photoelectron lines due to the ether oxygen (at higher binding

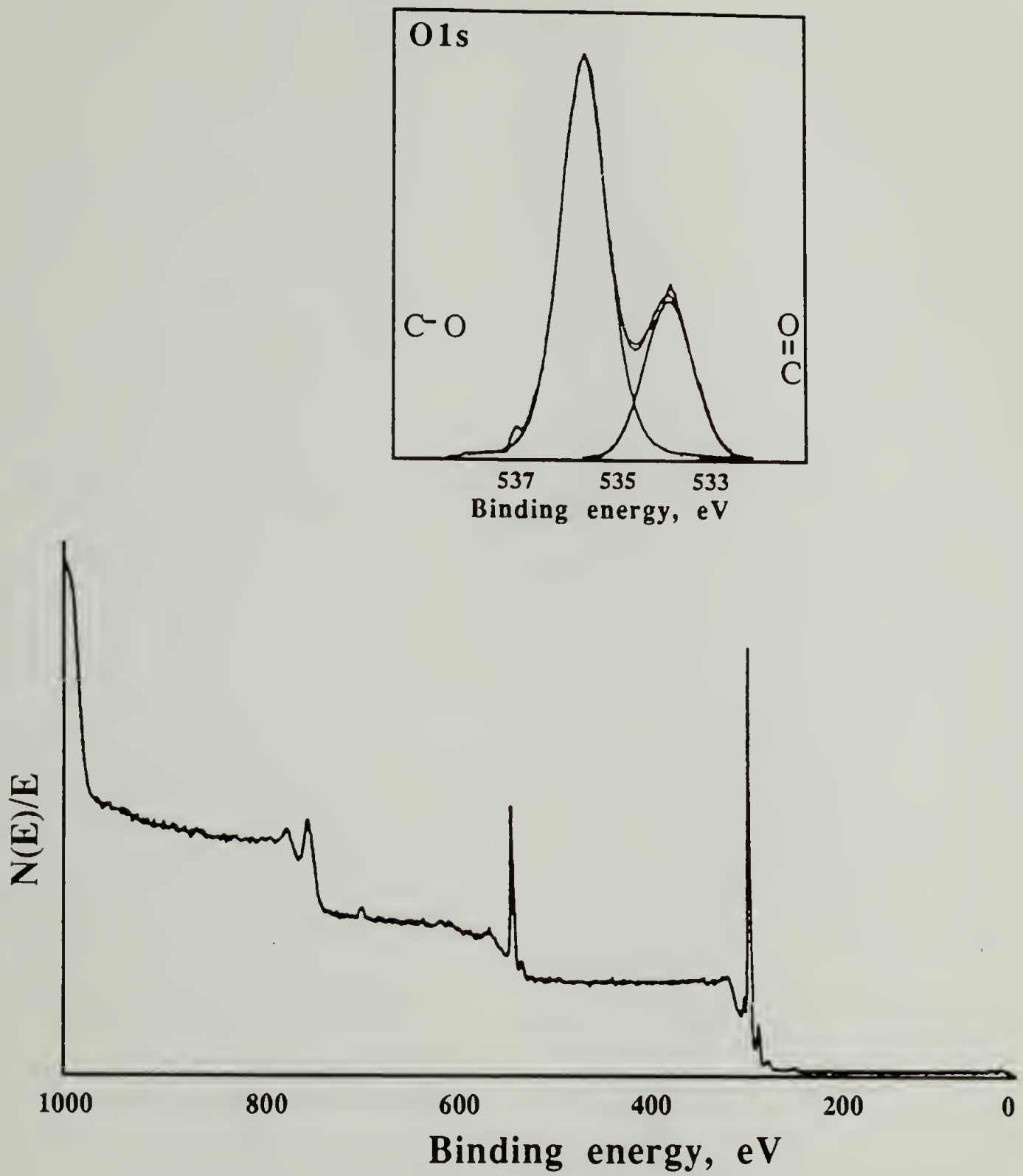

Figure 3.1. XPS Survey Spectrum and O_{1s} Region of Semicrystalline PEEK.

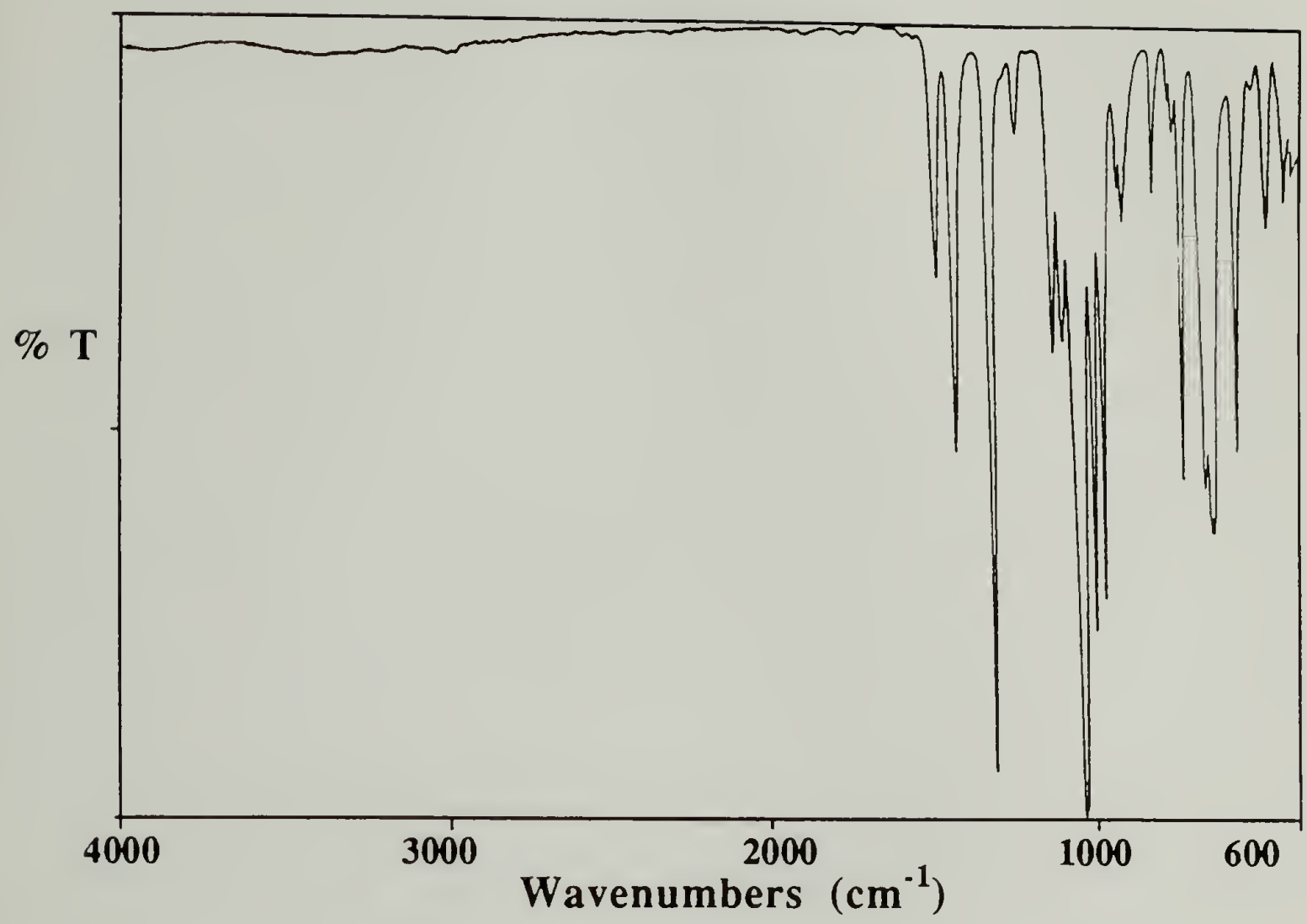

Figure 3.2. ATR-IR Spectrum of Semicrystalline PEEK.

energy) and the ketone oxygen (at lower binding energy). A small F_{1s} photoelectron line (700 eV) appears in the survey spectrum for virgin PEEK corresponding to 1-2 % atomic concentration. Microanalysis of PEEK film samples indicates 0.12 % fluorine content which means that an excess of fluorine is detected at the surface. PEEK is prepared by polycondensation reaction between 4,4'-difluorobenzophenone and hydroquinone[2-4] which suggests that the amount of fluorine detected by XPS is due to chain ends concentrating in the surface region.

All derivatized PEEK surfaces were characterized by XPS, ATR IR and contact angle measurements, and a number of them were analyzed by scanning electron microscopy (SEM), as well. Derivatized surfaces were analyzed by XPS at 15° and 75° takeoff angles (with respect to the plane of the surface) to assess the outer 11 and 40 Å of the sample, respectively. For nearly all samples, data are independent of takeoff angle which suggests that the outer 40 Å of the films are vertically homogeneous. Atomic concentration (and contact angle) data for derivatized surfaces are reported in tables included in this chapter. Rough reaction yields (for derivatizations) have been calculated from the 75° data with respect to the number of carbons in a theoretical 100 % reacted repeat unit. These yields have been calculated irrespective of variable amounts of fluorine detected on the surface. A number of derivatized surfaces contain somewhat higher concentrations of oxygen than our calculations would predict, especially when analyzed at the 15° takeoff angle. This could be attributed to slight surface oxidation of these samples or contamination with a silicon-containing compound (which would have oxygen associated with it). Analyses by ATR IR indicated no changes in samples upon surface

modification, and SEM micrographs indicated change in only one modified surface (oxidized surface). Although data obtained for these derivatized films do not allow determination of modified layer thickness, a rough estimate can be made from the XPS and ATR IR data. 75° takeoff angle XPS data indicate that most reactions proceed to depths of at least 40 Å (this is not true for some samples), and the lack of changes revealed by ATR IR indicates that depths do not exceed 200 Å.

Ketone Transformations

Standard ketone transformations were carried out on PEEK film using modifications of literature procedures for (high-yield) reactions with benzophenone, when available. PEEK films were cleaned by extraction in THF and dried to constant mass before use in surface chemical reactions. For each surface modification, experiments were carried out to maximize the yield, although careful kinetics were not obtained. Great care was taken in washing films after reaction (including use of Soxhlet extraction and soaking of films) because some unreacted reagents proved difficult to remove. Control reactions were run whenever possible.

PEEK-Hydrazone Synthesis. PEEK reacts with 2,4-dinitrophenyl-hydrazine to produce the hydrazone (PEEK~C=NNHØ$(NO_2)_2$) (eq. 3.1). XPS data for the hydrazone film exhibited two N_{1s} peaks at 406 eV $(NO_2)_2$ and 400 eV (C=**N**-**N**H). Figure 3.3 shows the XPS survey spectrum and N_{1s} region for the PEEK-hydrazone surface. The repeat unit expected for 100% reaction is $C_{25}O_6N_4$, and atomic composition data indicate a repeat unit of $C_{25}O_{6.4}N_{2.1}$, corresponding to a ~50% reaction yield. XPS data

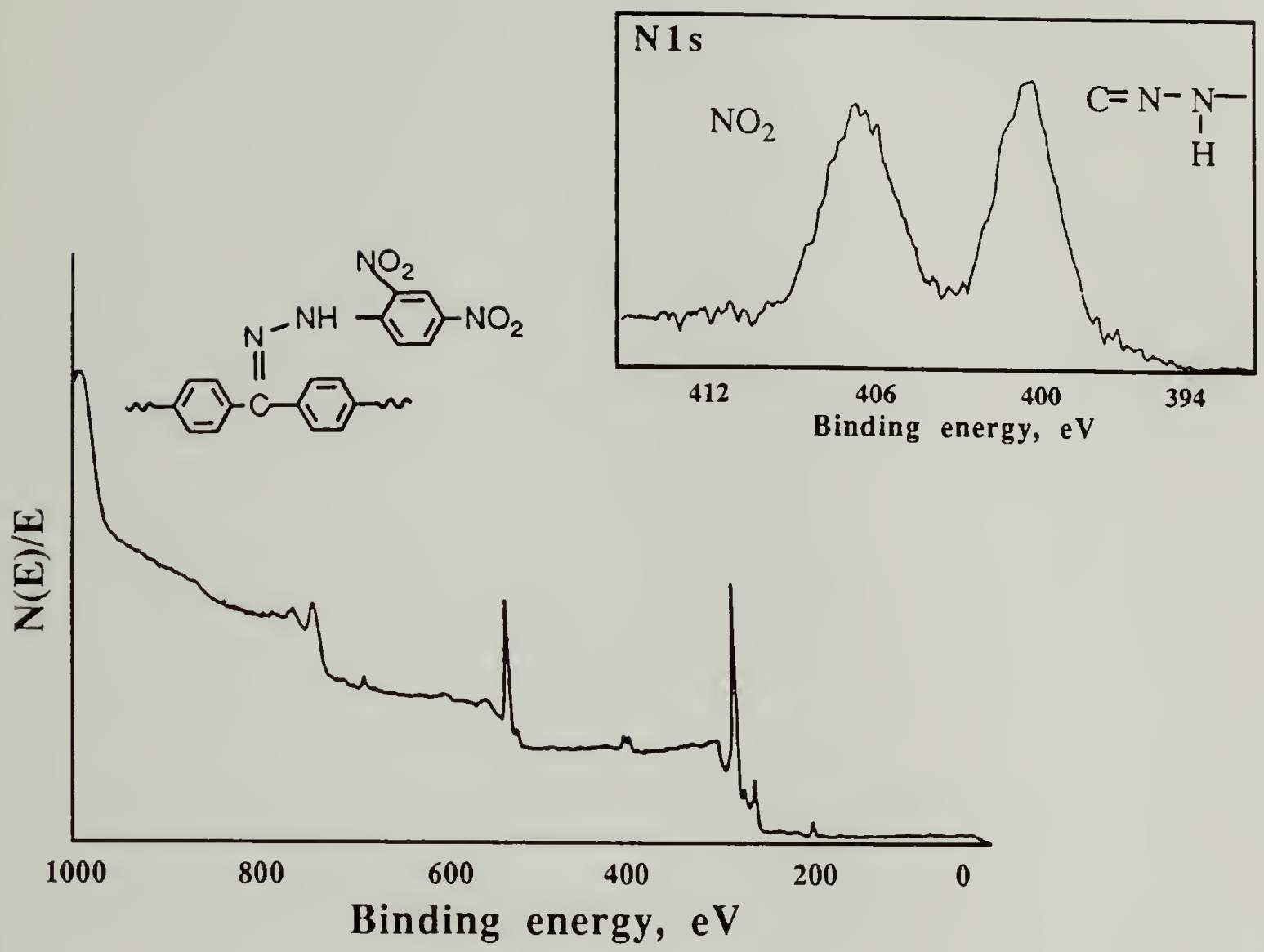

Figure 3.3. XPS Survey Spectrum and N_{1s} Region of PEEK-Hydrazone Surface.

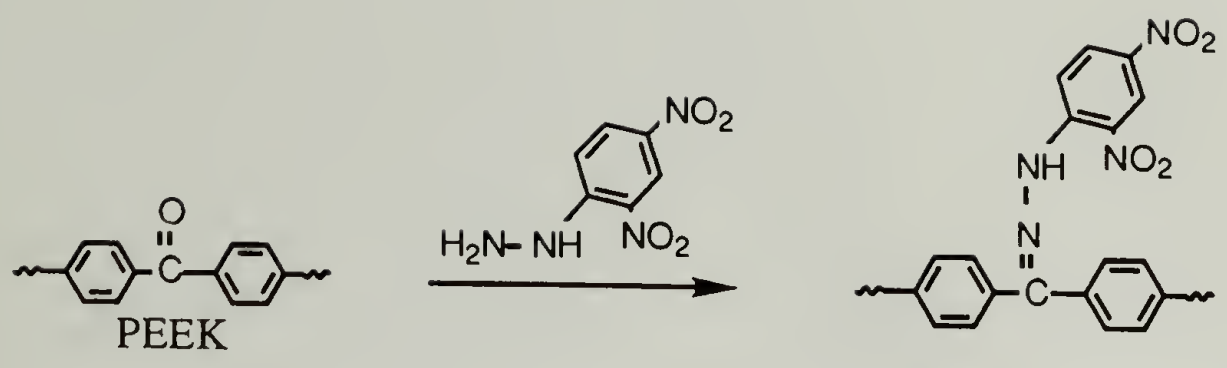

(3.1)

also indicate a small amount of chlorine on the surface (<1 %). Contact angles decrease slightly to $\theta_A/\theta_R = 78°/47°$ (side a), $\theta_A/\theta_R = 76°/40°$ (side b), which may be due to the introduction of nitro groups.

PEEK-Oxime Synthesis.[5] PEEK reacts with hydroxylamine to form surface-confined oximes (PEEK~C=NOH) (eq. 3.2). Contact angles for the

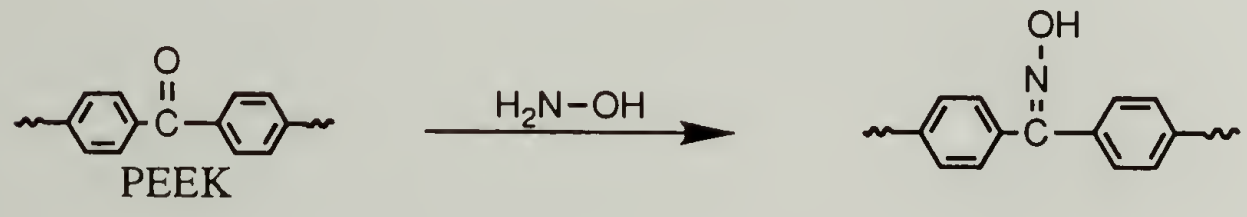

(3.2)

surface are fairly low: $\theta_A/\theta_R = 74°/40°$ (side a) and $\theta_A/\theta_R = 75°/35°$ (side b), which indicates increased wettability. XPS data for PEEK-oxime indicate an atomic composition of $C_{19}O_{3.9}N_{0.5}$ which corresponds to ~50% reaction yield in comparison to the theoretical repeat unit $C_{29}O_3N$. The literature procedure[5] for the preparation of benzophenone oxime indicated that a 5 min reflux time was sufficient to form the oxime. However, much longer reflux times were required for reaction with PEEK film; Table 2 contains XPS and contact angle data obtained for varied reflux times. These data indicate that very little increase in reaction occurs after 22 h of reflux. The data reported were obtained from samples that were cleaned with the optimum method developed (soaking in THF/MeOH); the XPS N_{1s}

Table 2. XPS and Contact Angle Data for PEEK-Oxime Reaction.

reflux time	XPS Atomic Conc. 15°/75° C	O	N	θ_A/θ_R side a	θ_A/θ_R side b
5 min.	82.9	16.5	.5	85/55	85/50
	83.6	16.3	.1		
10 min.				85/53	83/50
30 min.	82.5	16.7	.8	82/52	83/49
	84.0	15.3	.5		
60 min.	81.9	16.9	1.2	80/50	79/45
	82.4	16.6	1.0		
10 h.	81.0	17.3	1.7	78/46	77/42
	81.9	16.6	1.5		
22 h.	80.5	17.3	2.2	74/40	75/35
	81.4	16.6	2.0		
30 h.	80.3	17.5	2.0	74/39	73/35
	81.5	16.5	2.3		
48 h.				73/39	72/35
52 h.	80.3	17.6	2.0	71/36	69/33
	81.3	16.7	2.0		
72 h.	79.1	18.7	2.1	73/37	73/33
	81.3	16.6	2.0		

region indicated the presence of only one type of nitrogen. PEEK-oxime surfaces were reacted with benzenesulfonyl isocyanate[6] to confirm the presence of oxime functionality and assess its reactivity (eq. 3.3). Based on the 50% oxime reaction yield, the predicted atomic composition for the refunctionalized surface is $C_{45}O_9N_2S$, and observed composition is $C_{45}O_{9.5}N_{1.8}S$, indicating good yield for the urethanation reaction.

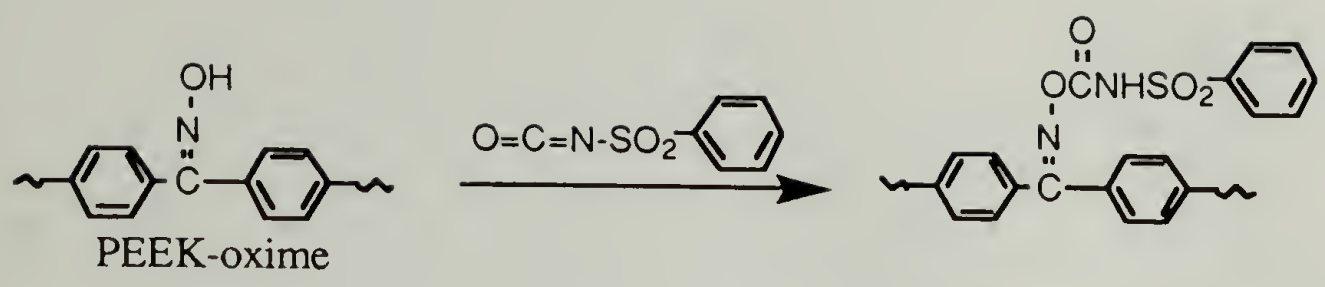

(3.3)

Figure 3.4 shows the XPS survey spectra for PEEK-oxime and the surface following urethanation. Control films (plain PEEK samples) contain no sulfur or nitrogen by XPS.

Oxidation of PEEK. PEEK can be oxidized with an aqueous potassium chlorate/sulfuric acid solution[7] to produce carboxylic acid and phenol-type functionality on the surface (eq. 3.4), and the presence of these functional groups is confirmed by reaction with thallous ethoxide[8] (eq. 3.5). This oxidation was one of only two non-carbonyl-specific reactions

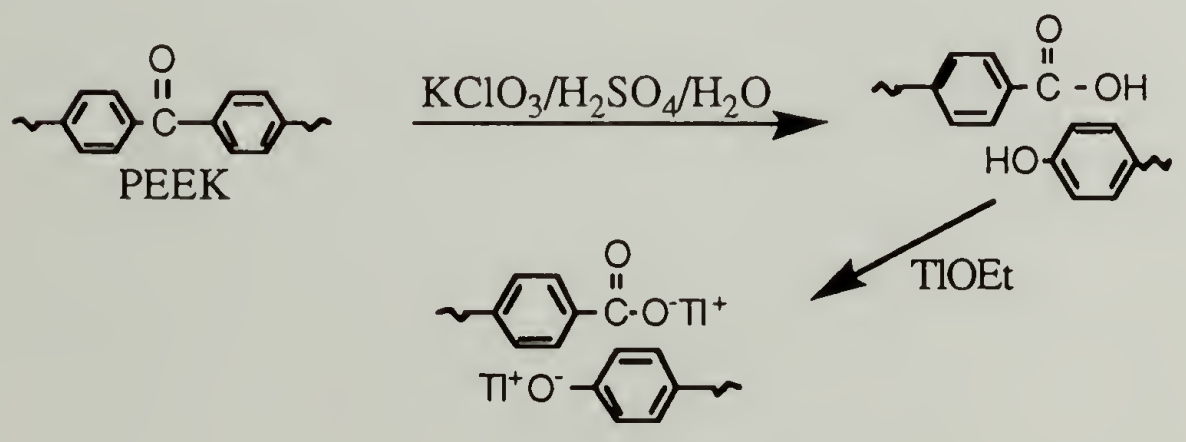

(3.4)

(3.5)

attempted with PEEK. The oxidation reaction was expected to cleave chains and degrade the surface somewhat because of the strength of reagents employed. SEM micrographs confirm the corrosive nature of this reaction and indicate formation of circular pits of 3000 - 6000 Å diameter on the surface. Initial attempts were made to carry out the oxidation reaction without dilution of the sulfuric acid (with water), and the film

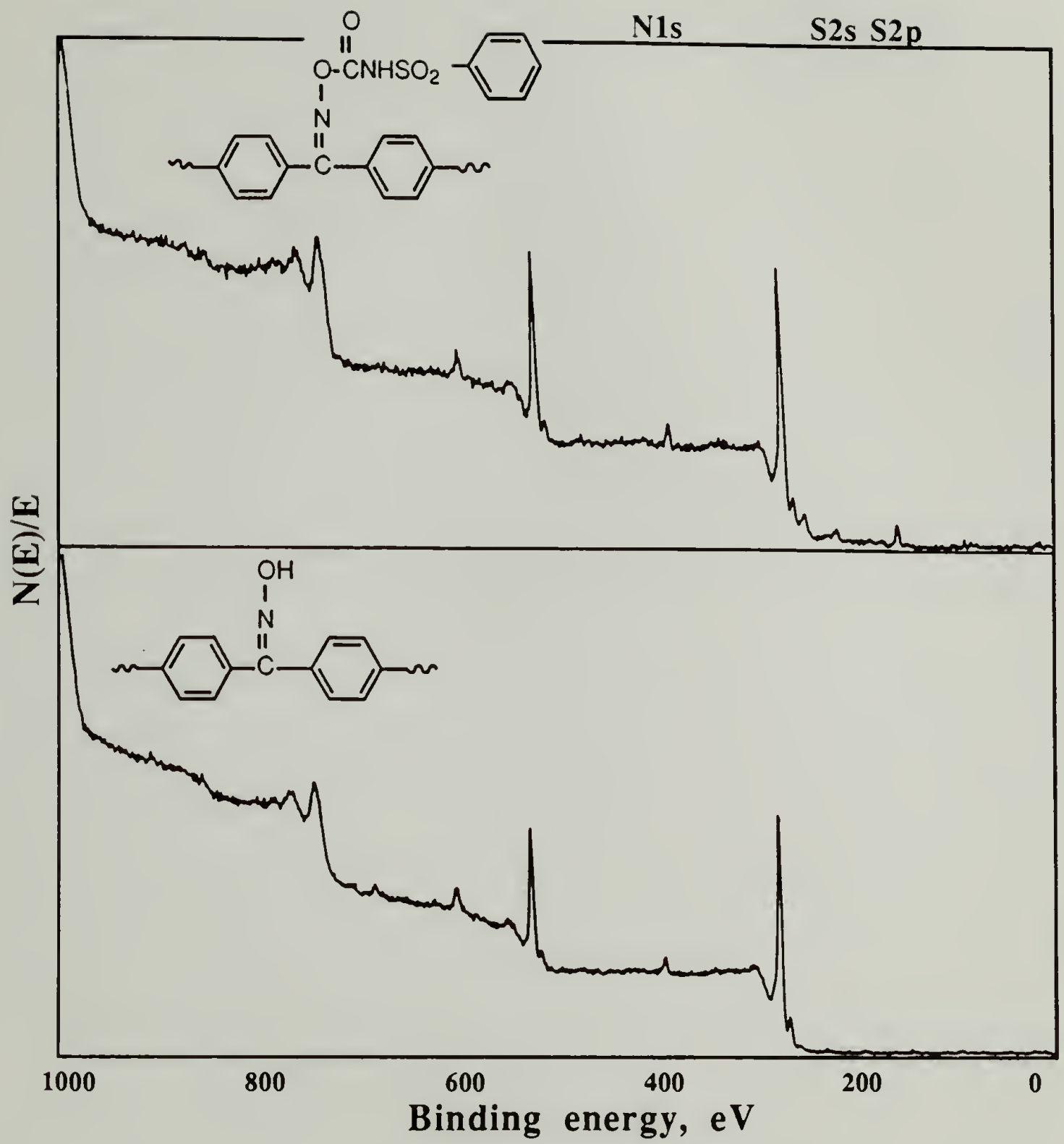

Figure 3.4. XPS Survey Spectra of PEEK-Oxime and PEEK-Oxime Labelled with Benzenesulfonyl Isocyanate.

dissolved. Different proportions of water and sulfuric acid were used (with 1.0 g $KClO_3$) for this reaction to determine the best combination for producing the most wettable and least contaminated (oxidized) surface. Contact angle data for these reactions are summarized in Table 3 with comments about the status of the product film samples. A 50:50 (v:v) ratio of water to sulfuric acid was determined as the optimum combination for the oxidation reaction. Contact angle data obtained for experiments varying the reaction time are summarized in Table 4; this information indicates that 30 min is sufficient time for extensive reaction. XPS data for oxidized PEEK samples indicate a significant increase in oxygen content and a small amount of chlorine is present, as well. Figure 3.5 shows XPS survey spectra for the oxidized surface and the thallium-labelled one.

Table 3. Contact Angle Data for PEEK-Oxidation Reaction for 1h Using 1g $KClO_3$ and Varied Amounts of H_2SO_4 in H_2O.

sample #	H_2O/H_2SO_4 (mL/mL)	% oxygen	θ_A/θ_R side a	θ_A/θ_R side b	comment
1	0/100	---	---	---	film dissolved
2	10/90	---	---	---	film brown, vy etched
3	20/80	---	---	---	film brown, vy etched
4	40/60	19.3	76/16	72/22	film etched, discolored
5	50/50	22.3	69/24	70/20	film sl. roughened
6	60/40	17.3	72/36	75/28	film same as before rxn
7	100/50	16.7	79/40	79/34	
8	125/50	18.4	76/35	77/30	used 1.5g $KClO_3$

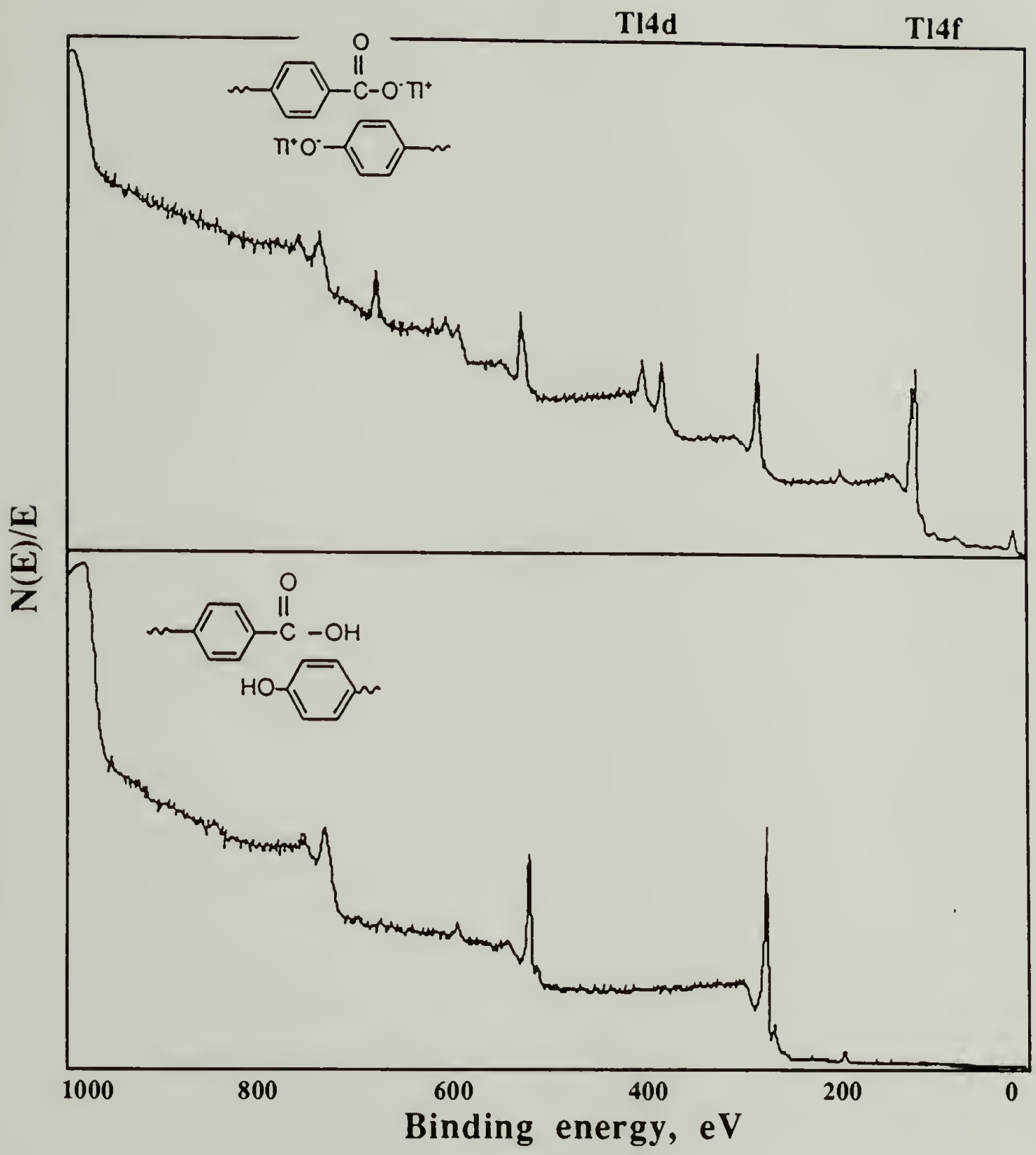

Figure 3.5. XPS Survey Spectra of Oxidized PEEK and the Oxidized Surface Labelled with Thallium.

Table 4. Contact Angle Data for PEEK-Oxidation Reaction Using 1g $KClO_3$ in 50mL H_2O/50mL H_2SO_4 for Different Times.

sample #	rxn time	% oxygen	θ_A/θ_R side a	θ_A/θ_R side b	comment
1	0 min.	13.6	85/55	85/50	plain PEEK
2	15 min.	17.1	79/40	81/38	
3	30 min.	22.5	69/22	67/18	
4	60 min.	21.3	69/24	70/20	film yellow
5	24 h.	24.1	71/24	74/19	film yellow vy brittle

Wittig Reaction.[9] PEEK reacts with methylenetriphenylphosphorane to convert the ketone groups to olefin moieties which react with molecular bromine (eqs. 3.6 - 3.7). The theoretical repeat unit for quantitative (Wittig) reaction is $C_{20}O_2$ and the observed atomic composition data

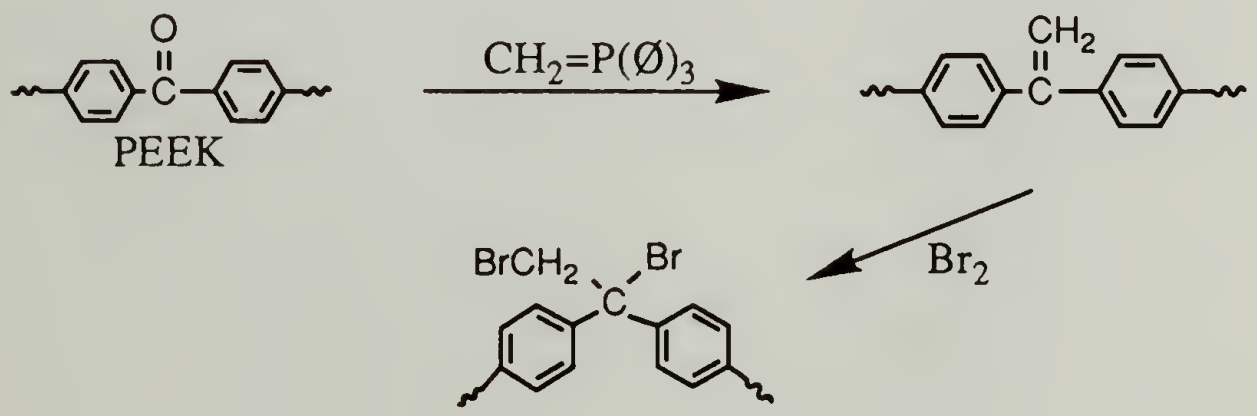

indicate a repeat unit of $C_{20}O_{2.5}$ which corresponds to ~50% yield. Curve-fit analysis of the O_{1s} region indicates a yield closer to 60%. Figure 3.6 shows XPS survey spectra of the olefin-containing and brominated surfaces. A surprising feature of the olefin-containing surface is that the

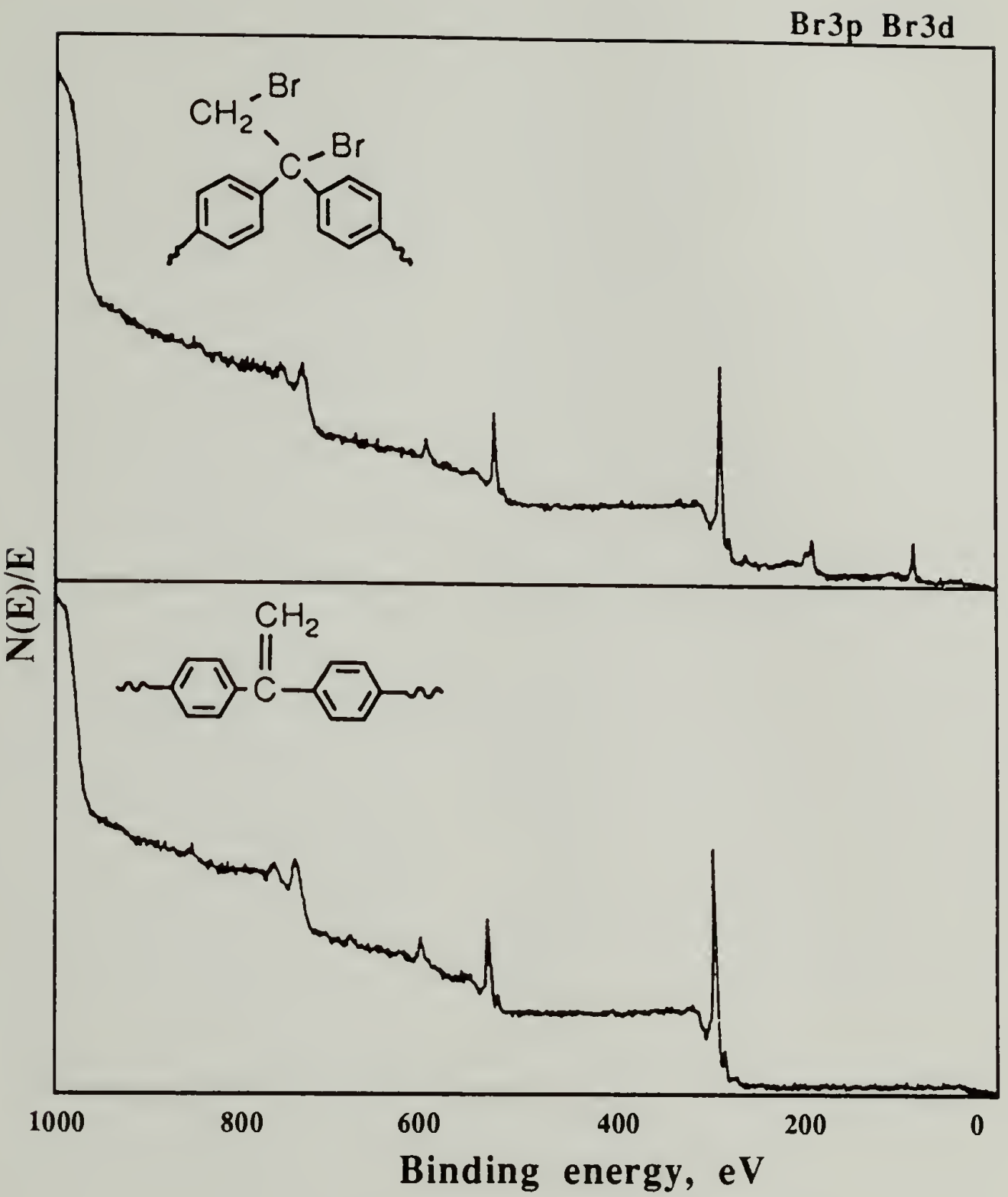

Figure 3.6. XPS Survey Spectra of PEEK-C=CH_2 and PEEK-CBr-CH_2Br Films.

contact angles decrease slightly (relative to unreacted PEEK). Although no phosphorous is detected by XPS (P_{2p} peak would appear at 133 eV, but phosphorous has a small cross-sectional area which makes detection of small amounts difficult), it is possible that some reaction byproducts (i.e. $Ø_3P{=}O$) contaminate the outermost layers of the surface and are detected only by contact angle. Bromination of the olefins increases contact angles, as expected, and the control film (PEEK) remains unaffected by the bromination reaction. Contact angle and XPS data for these samples are included in Tables 5 and 6 (on pages 55-56).

Reaction of PEEK with Dimsyl Sodium.[9] PEEK reacts with dimsyl sodium (eq. 3.8) to produce a surface containing alcohol and sulfoxide species. Contact angles decrease to $\theta_A/\theta_R = 70°/23°$ (side a) and $\theta_A/\theta_R = 72°/19°$ (side b) which is consistent with the expected structure. XPS data

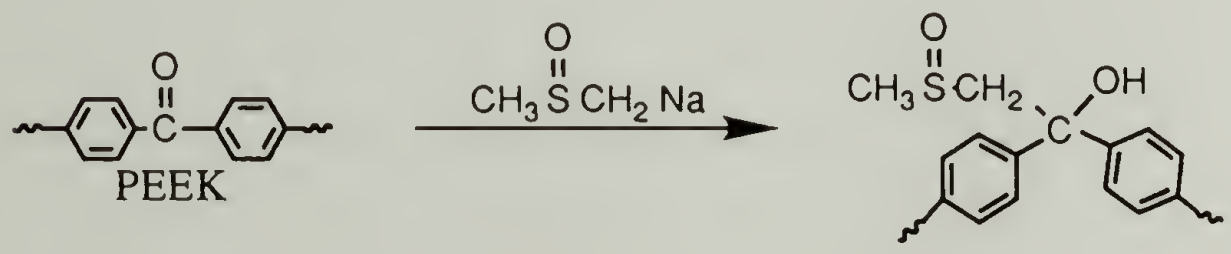

(3.8)

indicate S_{2s} and S_{2p} photoelectron lines at 230 and 167 eV, respectively, as expected. The theoretical repeat unit for quantitative reaction is $C_{21}O_4S$ and the observed atomic composition data indicate a repeat unit of $C_{21}O_{3.8}S_{0.6}$ which corresponds to ~60% yield.

Cyanosilylation of PEEK.[10] Reaction of PEEK with trimethylsilyl cyanide is shown in eq. 3.9. This reaction was carried out with the original

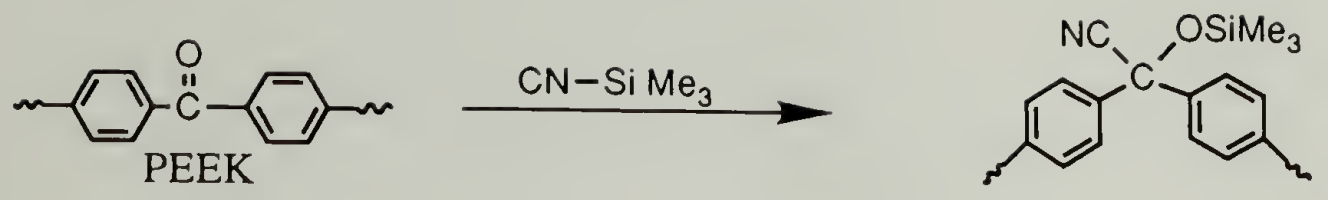

(3.9)

intention of converting the nitrile groups into carboxylic acid species, although this conversion was never successful. The 75° takeoff angle XPS data indicate that the cyanosilylation reaction proceeds to only 40% yield, although 15° data indicate a slightly higher yield, closer to 50%. This is one of the only examples of angle-dependent XPS data for derivatized PEEK samples. Contact angles for this surface are θ_A/θ_R = 79°/50° (side a) and θ_A/θ_R = 79°/48° (side b), slightly lower than those observed for PEEK.

Comments about Derivatized PEEK Samples

The experiments carried out to derivatize PEEK film indicate that the diaryl ketone can be used as a reactive handle to refunctionalize the surface. These experiments, in addition to others described at the end of this chapter, indicate that ketones at the PEEK-solution interface have somewhat different reactivity than benzophenone. Reactions which afford very high yields in solution (96 - 98% yield) render only 50% conversion of carbonyl groups on the film surface. These limited yields can be ascribed to several factors including the semicrystalline nature of the material (i.e. not all of the ketones in the surface region are accessed by derivatizing reagents) or differences in solvation of the reactive sites or orientation of the carbonyl moieties (which could hinder addition reactions). One drawback to modifying one functional group within a large repeat unit is that changes in the surface indicated by XPS are small.

Unfortunately, these changes occurred on PEEK at depths too shallow to be followed by ATR IR. Contact angle data were relied on to corroborate data obtained by XPS and to monitor changes in wettability of the derivatized surfaces. Incorporation of more polar functionality (such as NO_2 moieties) caused an increase in wettability. It is possible that some of the changes in wettability observed were influenced by the position and orientation of functional groups.[11] It is also possible that some of the reactions carried out changed the nature of the surface (caused some roughening) which would influence wettability, as well.[12,13] The 50% yields calculated for most of the reactions with PEEK indicate that these derivatized surfaces contain mixed functionality (i.e. 50% of diaryl ketones are still present in addition to the new functionality) and changes in surface properties most likely were influenced by this mixture. (Wettability is thought to be determined by the ratio of polar:nonpolar groups on a surface.[7]) It is interesting to see that changing only half of the functional groups still can have a dramatic effect on wettability. Contact angle and XPS data for representative samples (and control samples) from each reaction carried out are included in Tables 5 and 6 on pages 55 and 56.

In the fluoropolymer surface chemistry developed by the McCarthy group,[14-24] modified substrates resemble a two-dimensional array of functional groups covalently attached to an inert substrate. Manipulation of these groups leaves the bulk unaffected; reaction is confined to the surface region. This surface-selectivity ensures that any new properties that develop for the material can be attributed to the surface functionality. Ideally, the surface-selectivity can be controlled by choice of solvent and temperature. PEEK contains diaryl ketone functional groups throughout

the bulk which suggests that control over reaction could be effected by manipulating conditions such that different amounts of the surface region were solubilized, or accessed by the reaction solution. However, such control over the surface modification of PEEK was not achieved. Reaction depths never proceeded to the point where significant differences based on solvent and temperature conditions could be detected (although some differences were detected by contact angle).

Table 5. Contact Angle Data for PEEK Derivatives and Controls.

PEEK derivative	θ_A/θ_R side a	θ_A/θ_R side b
PEEK	85/55	85/50
PEEK-C=N-NHØ$(NO_2)_2$	78/47	76/40
PEEK-C=N-OH	74/40	75/35
PEEK-C=N-OC(O)NHSO$_2$Ø	78/38	79/34
control: PEEK in THF with BSI and DBTDL	85/53	85/50
PEEK-C=CH_2	78/38	77/33
PEEK-CBr-CH_2Br	87/56	90/51
control: PEEK in Br_2/CCl_4	85/55	85/50
PEEK-C(OH)CH_2S(O)CH_3	70/23	72/19
control: PEEK in DMSO	85/56	86/50
PEEK-C(CN)-OSiMe_3	79/50	79/48
PEEH-(OH)(CO_2H)	69/22	67/18
PEEK-(OTl)(CO_2Tl)	69/32	65/25
control: PEEK in TlOEt	85/55	85/50

Table 6. XPS Data for PEEK Derivatives and Controls.

PEEK derivative	XPS Atomic Conc. 15°/75° C	O	N	X[A]
PEEK	86.3 86.4	13.7 13.6		
PEEK-C=N-NHØ$(NO_2)_2$	72.7 74.5	21.1 19.2	6.2 6.3	
PEEK-C=N-OH	80.3 81.4	17.5 16.6	2.2 2.0	
PEEK-C=N-OC(O)NHSO$_2$Ø	78.0 78.3	16.3 16.7	3.8 3.2	2.1^{S} 1.7^{S}
control: PEEK in THF with BSI and DBTDL	85.9 86.4	14.1 13.6		
PEEK-C=CH_2	87.0 88.7	13.0 11.3		
PEEK-CBr-CH_2Br	82.2 85.3	14.1 11.0		3.7^{Br} 3.7^{Br}
control: PEEK in Br_2/CCl_4	86.0 86.3	14.0 13.7		
PEEK-C(OH)CH_2S(O)CH_3	80.9 82.7	16.7 14.9		2.3^{S} 2.4^{S}
control: PEEK in DMSO	86.2 86.5	13.8 13.5		
PEEK-C(CN)-OSiMe$_3$	82.1 84.0	13.4 13.1	2.4 1.5	2.1^{Si} 1.4^{Si}
PEEH-(OH)(CO_2H)	77.2 79.8	22.7 20.2		
PEEK-(OTl)(CO_2Tl)	73.6 73.8	21.3 21.1		5.0^{Tl} 5.0^{Tl}
control: PEEK in TlOEt	86.7 86.9	13.3 13.1		

Preparation of PEEK-Alcohol Surfaces

Several PEEK-alcohol surfaces were prepared with the objective of comparing reactivities of surface-confined hydroxyl groups based on structural differences, and making general comparisons with reactivities of alcohol groups in solution. The PEEK-alcohol (PEEK-OH) surfaces were characterized with XPS, ATR IR and contact angle measurements, and by reaction with "XPS visible"[8,25] reagents. Because XPS spectra for PEEK-OH surfaces are nearly indistinguishable, labelling reactions were used to differentiate between surfaces containing alcohol groups of different structures and different steric hindrance.

Reduction of PEEK. Reaction with sodium bis(2-methoxyethoxy) aluminum hydride[26] reduces the ketones in the surface region of PEEK to secondary alcohols (PEEK~$OH^{2°}$) (eq. 3.10). Contact angles indicate that this reduced surface is highly wettable: $\theta_A/\theta_R = 69°/23°$ (side a) and $\theta_A/\theta_R = 71°/18°$ (side b). Figure 3.7 shows 15° and 75° takeoff angle spectra for the O_{1s} region of PEEK~$OH^{2°}$ (compare these with the O_{1s} spectrum

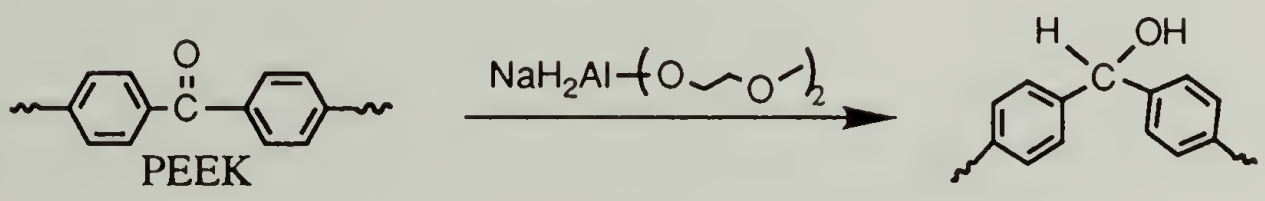

(3.10)

included in Figure 3.1). Curve-fitting analysis for (rough) determination of reaction yield indicates reduction of 90% of the ketones in the top 11 Å of the film (15° data) and 75% in the outer 40 Å (75° data). These data were obtained for PEEK film reduced at 40 °C in THF (for 3 h). Other reaction times and temperatures were investigated, as well, and the contact

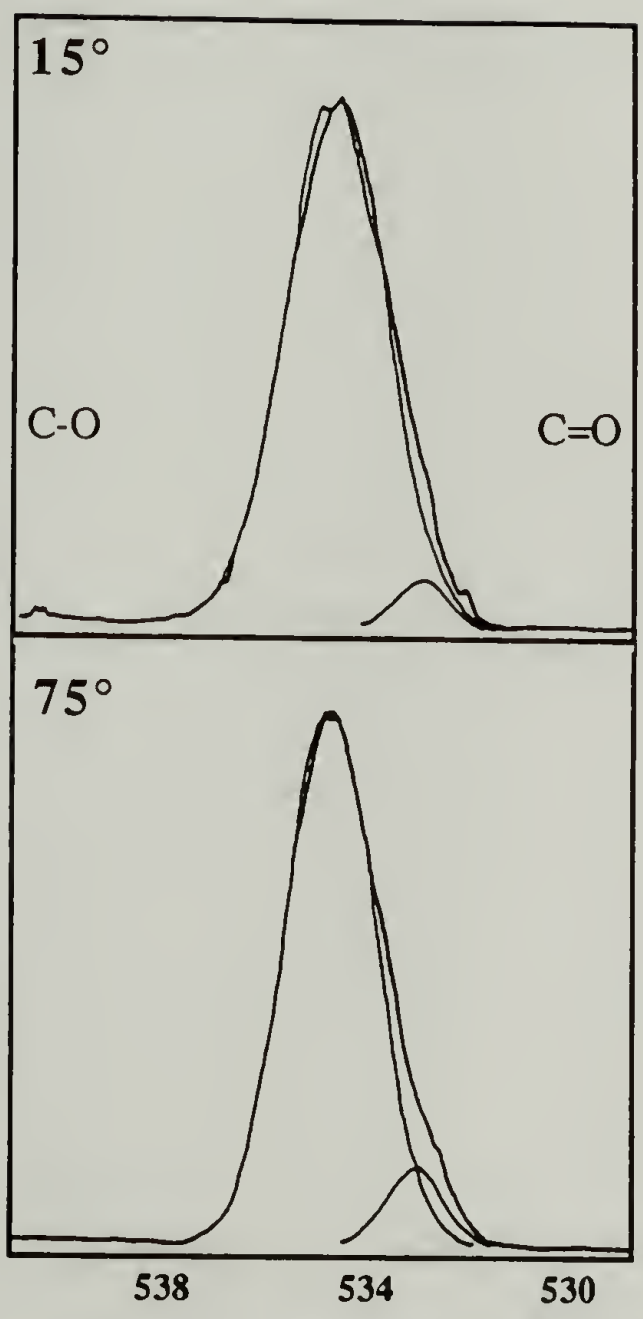

Figure 3.7. 15° and 75° Takeoff Angle Spectra for O_{1s} Region of Reduced Samples.

angle and O_{1s} region (curve-fit) XPS data obtained for these samples are summarized in Table 7. Reaction at room temperature produced fairly wettable surfaces, but curve-fit analysis of the O_{1s} region did not indicate that as much reduction occurred for these samples as for the films that were reduced at higher temperatures. Reaction at 50 °C produced samples that were contaminated with aluminum species that could not be extracted.

Table 7. Contact Angle Data for Reduction Reaction.

rxn temp.	rxn time	θ_A/θ_R side a	θ_A/θ_R side b	yield by curve fit, 15°/75°
RT	1 h.	67/28	70/25	~66%/50%
RT	2 h.	66/32	68/28	
RT	3 h.	68/25	69/21	~70%/65%
40 °C	2 h.	66/23	69/20	~80%/75%
40 °C	3 h.	66/20	70/16	~90%/75%
50 °C	3 h.	60/0	56/0	film couldn't be cleaned

XPS atomic composition data for the reduced surface indicate a repeat unit of $C_{19}O_{3.3}$ ($C_{19}O_{3.6}$ at 15°) although the formula should not deviate from $C_{19}O_3$, regardless of reaction yield. One explanation for the increase in the amount of oxygen detected is that the reduction reaction causes some reconstruction of the surface. Conversion of the sp^2 carbonyl to the sp^3 alcohol may move the oxygen-containing moiety closer to the surface (i.e the change in orientation facilitates detection by XPS). Orientation effects can be used to explain the difference between peak sizes

for $(NO_2)_2$ and C=N-N moieties in the N_{1s} XPS spectrum of the PEEK-hydrazone surface, as well (i.e. the peak corresponding to the nitrogen from the nitro groups is slightly larger). Otherwise, these data may indicate that some surface oxidation or contamination occurs during the reduction reaction. This reduction is among the simplest and most reproducible reactions carried out with PEEK, producing the most wettable surfaces and affording the highest reaction yields.

Reaction of PEEK with Methyllithium. Tertiary alcohol groups were produced on the surface (PEEK~$OH^{3°}$) by reacting PEEK with methyllithium under conditions similar to those used for the reduction reaction (eq. 3.11). Contact angles indicate increased wettability upon reaction: $\theta_A/\theta_R = 74°/35°$ (side a) and $\theta_A/\theta_R = 73°/32°$ (side b). Curve-

(3.11)

fitting analysis of the O_{1s} spectrum suggests that 52% of the ketones in the outer 40 Å have been converted to tertiary alcohols. The carbon:oxygen ratio should increase with addition of the methyl group to the repeat unit, but XPS atomic composition data indicate that the ratio changes more than the stoichiometry predicts. For quantitative yield, the predicted formula is $C_{20}O_3$, but a repeat unit of $C_{20}O_{2.7}$ is observed. The discrepancy in these data also may be attributed to reconstruction of the surface or orientation effects. For example, upon hybridization of the sp^2 (carbonyl) orbital, the tertiary alcohol group may be pointed away from the surface and is

detected less readily by XPS. (The discrepancies between the expected data and those obtained by XPS highlight limitations in relying on atomic composition data to compute surface reaction yields.)

Reaction of PEEK~OH$^{2°}$ and PEEK~OH$^{3°}$ with LDA and Ethylene Oxide. PEEK~OH$^{2°}$ and PEEK~OH$^{3°}$ films were reacted with lithium diisopropylamide (LDA) and ethylene oxide in an effort to "chain extend" the secondary and tertiary hydroxyl groups and convert them into primary

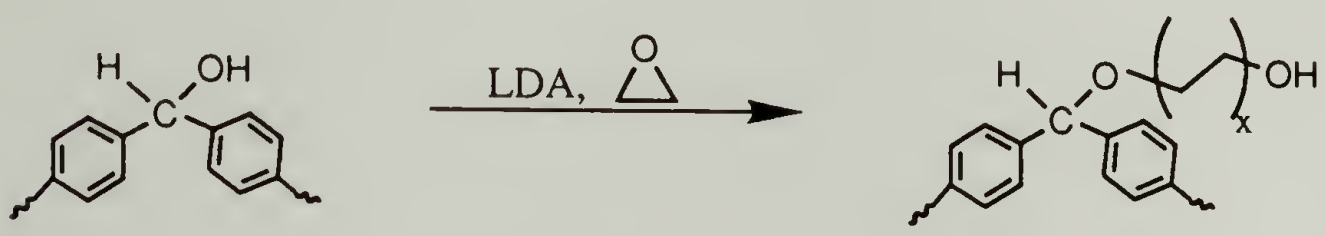

(3.12)

species (and thereby increase their reactivity)[20] (PEEK~ce-OH$^{2°}$ and PEEK~ce-OH$^{3°}$). It was expected that LDA, a nonucleophilic base, would deprotonate the alcohol species on the surface and the resulting lithium alkoxide would react to open an ethylene oxide ring. Equation 3.12 above describes the reaction for the PEEK~OH$^{2°}$ surface. In this case, 75° XPS atomic composition data indicate a C/O ratio ~5.25 which corresponds to x = .5 when the curve-fit data (indicating 75% reduction) and the repeat unit determined for the original PEEK~OH$^{2°}$ surface ($C_{19}O_{3.3}$) are taken into account. In other words, these data indicate that half of the secondary alcohols are converted to primary species. Contact angles for this chain-extended surface are similar to those observed for the original alcohol surface: θ_A/θ_R = 71°/30° (side a) and θ_A/θ_R = 70°/26° (side b). 75° XPS data for the PEEK~ce-OH$^{3°}$ surface indicate a C/O ~6.4 which corresponds

to conversion of 50% of the tertiary alcohol groups into primary species. Again this takes into account the original reaction yield (~52%) and the stoichiometry of the PEEK~$OH^{3°}$ surface ($C_{20}O_{2.7}$). Contact angles for PEEK~ce-$OH^{3°}$ indicate increased wettability upon chain extension reaction: $\theta_A/\theta_R = 68°/30°$ (side a) and $\theta_A/\theta_R = 69°/27°$ (side b). It is possible that the difference in contact angles observed between PEEK~$OH^{3°}$ and PEEK~ce-$OH^{3°}$ is due to the change in position of the hydroxyl group (relative to backbone). For the chain-extended surface, the hydroxyl may be more exposed because of the two-carbon spacer, whereas for the original surface, it may be hidden between the phenyl rings and beneath the methyl group.

Reaction of PEEK with Acetaldehyde Lithiopropyl Ethyl Acetal.[23] Primary alcohols were produced on the surface of PEEK (PEEK~$OH^{1°}$) by a more direct method using a protected alcohol-containing lithium reagent (eq. 3.13) and subsequent deprotection (eq. 3.14). XPS atomic composition

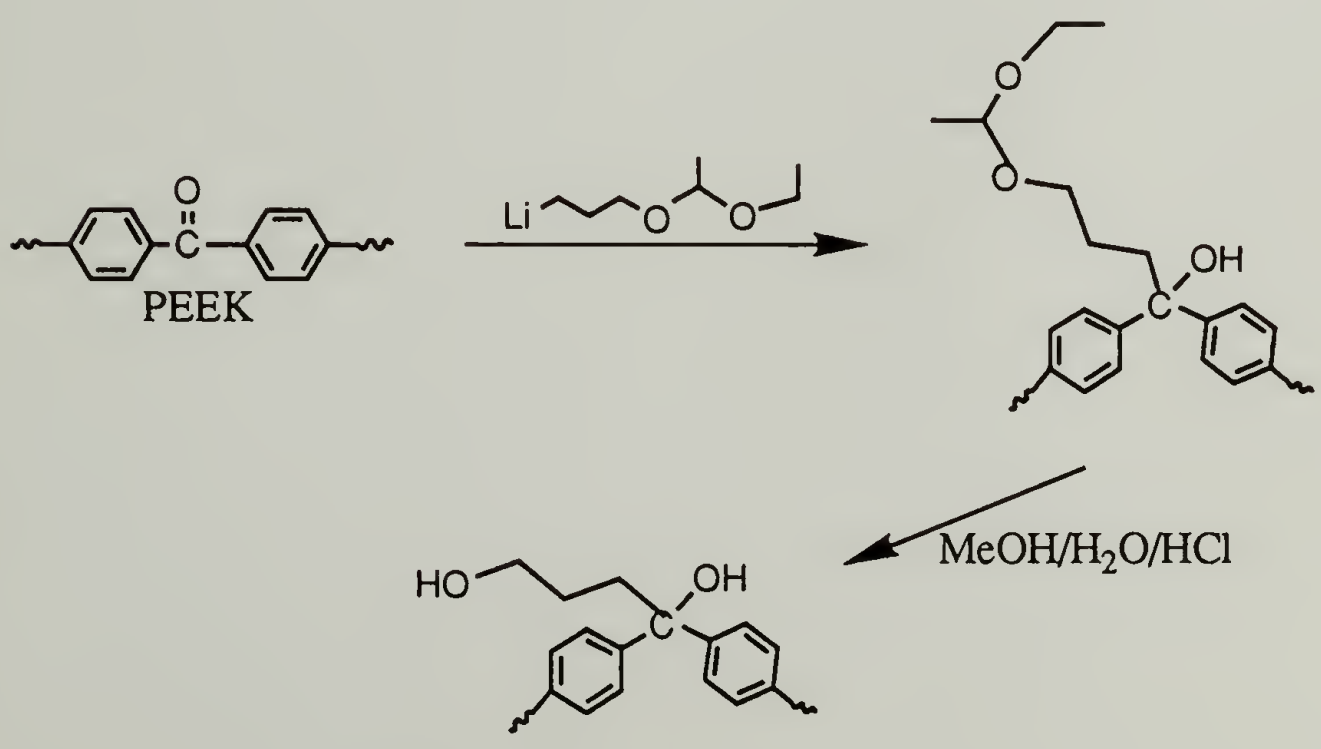

data indicate a large increase in oxygen content for the PEEK~OH$^{1°}$ surface suggesting a reaction yield (~90%) beyond that indicated by curve-fitting analysis of the O_{1s} spectrum (~45% yield). The discrepancy in these data suggests that this surface may contain some (oxygen) contamination; the 45% yield is more likely accurate. Reaction of PEEK with acetaldehyde lithiopropyl ethyl acetal was carried out in a THF/heptane mixture at 0 °C for 3 h. Longer reaction times produced samples that could not be cleaned, and shorter times and lower temperatures afforded less reaction (indicated by contact angle). Table 8 contains contact angle data for different reaction times and temperatures for PEEK-OPr and the deprotected surface. Contact angle values for PEEK~OH$^{1°}$ are not as low as expected, given that two hydroxyl groups (primary and tertiary) are obtained for each reacted ketone (suggesting that tertiary alcohol groups contribute less to surface wettability than hydroxyl groups of different structure).

Table 8. Reaction of PEEK with Acetaldehyde Lithiopropyl Ethyl Acetal, Followed by Deprotection Reaction.

		PEEK-OPr surface			after deprotection	
time (h)	temp (°C)	θ_A/θ_R side a	θ_A/θ_R side b	comment	θ_A/θ_R side a	θ_A/θ_R side b
1	RT	85/55	85/50	Li reagent decomposed	85/55	85/50
1	0	84/49	84/47		82/47	80/43
3	0	81/48	83/43		77/45	75/40
5	0	83/48	80/42	film dirty	76/45	77/42
1	-15					
3	-15	84/49	83/49		84/49	83/50

Reactions with PEEK-Alcohol Surfaces

The different PEEK-alcohol surfaces (designated PEEK-OH) were reacted with a variety of reagents in an effort to confirm hydroxylation reaction yields (estimated from curve-fit data) and to compare reactivity among these surfaces. All XPS and contact angle data for these reactions have been tabulated and are included at the end of this chapter. Control reactions were carried out with only PEEK~$OH^{2°}$ samples to establish appropriate cleaning procedures to use with all PEEK-OH films. The discussion below focusses on only two of the reagents used, trichloroacetyl chloride (TCAC) and trichloroacetyl isocyanate (TCAI). These two reagents were chosen for reaction with the PEEK-OH surfaces because each contains a trichloro group which is a better XPS label than a single-element functional group, so changes would be detected by XPS more readily. Incorporation of these trichloro groups was expected to increase the hydrophobic character of the surface (i.e. decrease the wettability) and these changes would be detectable by contact angle measurement. Structural differences between the two reagents cause differences in steric hindrance near the reactive (electrophilic) site, and these differences can be used to distinguish between alcohol surfaces of different structures.

Reaction of PEEK-OH with Trichloroacetyl Chloride (TCAC). Each of the PEEK-alcohol surfaces was reacted with TCAC (eq. 3.15 shows the

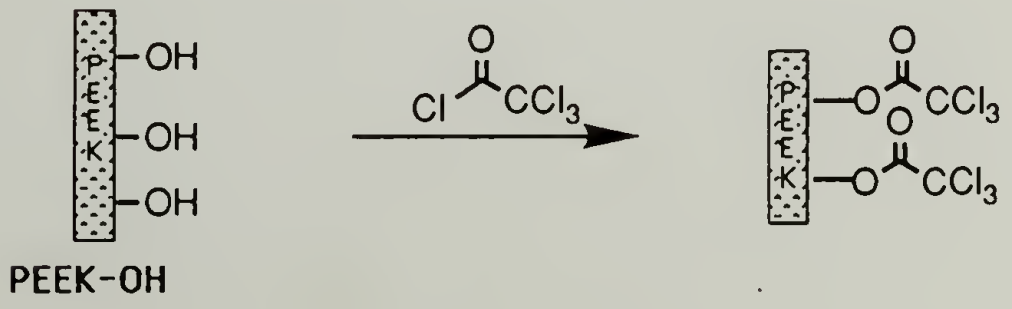

(3.15)

reaction with generic structures). In general, the esterified surfaces had higher contact angles than the original alcohol-containing ones. The (75°) atomic concentration data for the PEEK~OH$^{1°}$ surface indicate a repeat unit of $C_{24}O_{4.3}Cl_{0.9}$ which corresponds to roughly 30% yield when compared to the theoretical yield of $C_{24}O_5Cl_3$ (this is based on quantitative yield of reaction equations 3.13 and 3.14). This low esterification yield most likely indicates that the hydroxylation reaction yield is low because primary alcohol species are unhindered and high reactivity toward electrophiles would be expected. Contact angles indicate a slight decrease in wettability (relative to the OH surface): θ_A/θ_R = 81°/49° (side a) and θ_A/θ_R = 80°/46° (side b). The PEEK~OH$^{3°}$ surface did not react with TCAC to a significant degree. XPS data at 15° takeoff angle indicate incorporation of less than 1% chlorine to the surface, and 75° data show about 0.3%. Contact angles for this (unreacted) surface are θ_A/θ_R = 76°/35° (side a) and θ_A/θ_R = 76°/36° (side b), essentially the same as those for the PEEK~OH$^{3°}$ surface. The reduced surface, PEEK~OH$^{2°}$, reacts with TCAC to a limited extent. Atomic composition data indicate a repeat unit of $C_{21}O_{3.7}Cl_{0.8}$, corresponding to less than 30% yield. Contact angles increased to θ_A/θ_R = 81°/38° (side a) and θ_A/θ_R = 82°/32° (side b). Considering that curve-fit analysis of the O_{1s} spectrum for PEEK~OH$^{2°}$ indicates reduction of 75% of ketones on the surface, a 30% reaction yield with TCAC is very low. One explanation for these data is that the secondary alcohol groups are sterically hindered by their position between two phenyl rings, and this hindrance, coupled with that of TCAC (trichloro moiety is α to acyl group), prevents greater extent of reaction. The lack of reaction of the tertiary alcohol surface with TCAC is a more extreme case because of the additional

hindrance provided by the methyl group, but can be rationalized in a similar fashion.

Reaction of the chain-extended alcohol surfaces (PEEK~ce-$OH^{2°}$ and PEEK~ce-$OH^{3°}$) with TCAC highlights differences between these surfaces and the original ones (PEEK~$OH^{2°}$ and PEEK~$OH^{3°}$). Although characterization of the chain-extended alcohol surfaces by XPS and contact angle analyses indicates (somewhat) that these surfaces differ from the original alcohol samples, efforts were made to confirm the structure of the chain-extended species. In solution, lithium alkoxides are not reactive enough to polymerize ethylene oxide (i.e. in solvents of moderate polarity, like THF).[27] This lack of reactivity can be ascribed mainly to the strong association between lithium and oxygen ions and to the aggregation between alkoxide species. However, the lack of reactivity of lithium alkoxides toward ethylene oxide in solution (with respect to polymer formation) does not preclude reaction between surface-confined lithium alkoxides and ethylene oxide. Surface chemical reactions to chain-extend hydroxyl groups to produced alcohol species of increased reactivity have been reported by the McCarthy group, previously.[20]

The chain-extended PEEK-OH surfaces show much higher reactivity than the original alcohol surfaces toward TCAC. XPS data for reaction with PEEK~ce-$OH^{3°}$ indicate a repeat unit of $C_{24}O_{3.4}Cl_{1.3}$ (compared to the theoretical formula $C_{24}O_4Cl_3$) corresponding to ~45% yield. Contact angles for the esterified surface rise to $\theta_A/\theta_R = 81°/48°$ (side a) and $\theta_A/\theta_R = 82°/52°$ (side b), indicating an increase in the hydrophobicity of the surface. These data suggest that the chain extension reaction produces

alcohol groups of (most likely) higher reactivity and much less steric hindrance than the original tertiary hydroxyl species. Figure 3.8 shows XPS spectra for PEEK~$OH^{3°}$ and PEEK~ce-$OH^{3°}$ after reaction with TCAC. Similarly, PEEK~ce-$OH^{2°}$ reacts with TCAC to a greater extent than the (original) reduced surface. Atomic concentration data indicate a reaction yield of ~78% and contact angles increase to $\theta_A/\theta_R = 85°/52°$ (side a) and $\theta_A/\theta_R = 86°/46°$ (side b), indicating a dramatic decrease in the wettability of the surface, compared to PEEK~ce-$OH^{2°}$. Figure 3.9 shows XPS spectra for PEEK~$OH^{2°}$ and PEEK~ce-$OH^{2°}$ following reaction with TCAC.

Reaction of PEEK-OH with Trichloroacetyl Isocyanate (TCAI). PEEK-OH surfaces were reacted with TCAI to yield the surface-confined urethanes (eq. 3.16). Data from these reactions can be compared (in some respects) to those obtained from reaction with TCAC on the basis of

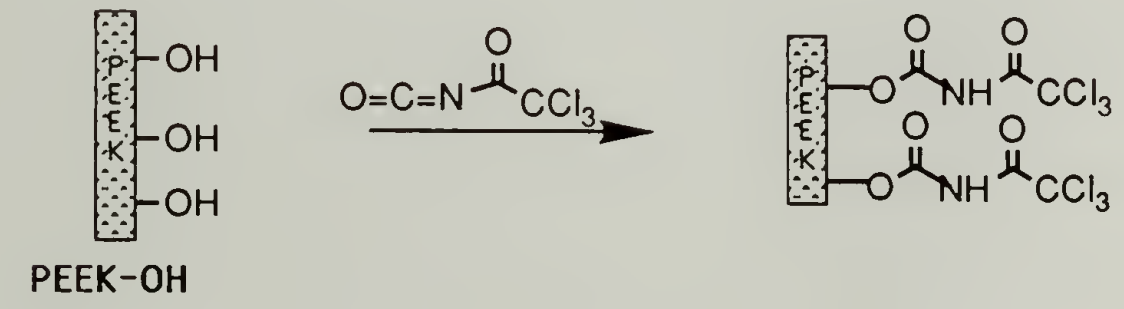

(3.16)

differences in steric hindrance. Compared to the hindrance near the acyl group in TCAC (because the trichloro group is in α position), the reactive site (isocyanate group) in TCAI is unhindered (trichloro group is γ). This difference suggests that the slightly hindered alcohol surfaces (i.e. reduced surface) may react with TCAI to a greater extent. PEEK~$OH^{1°}$ reacts with

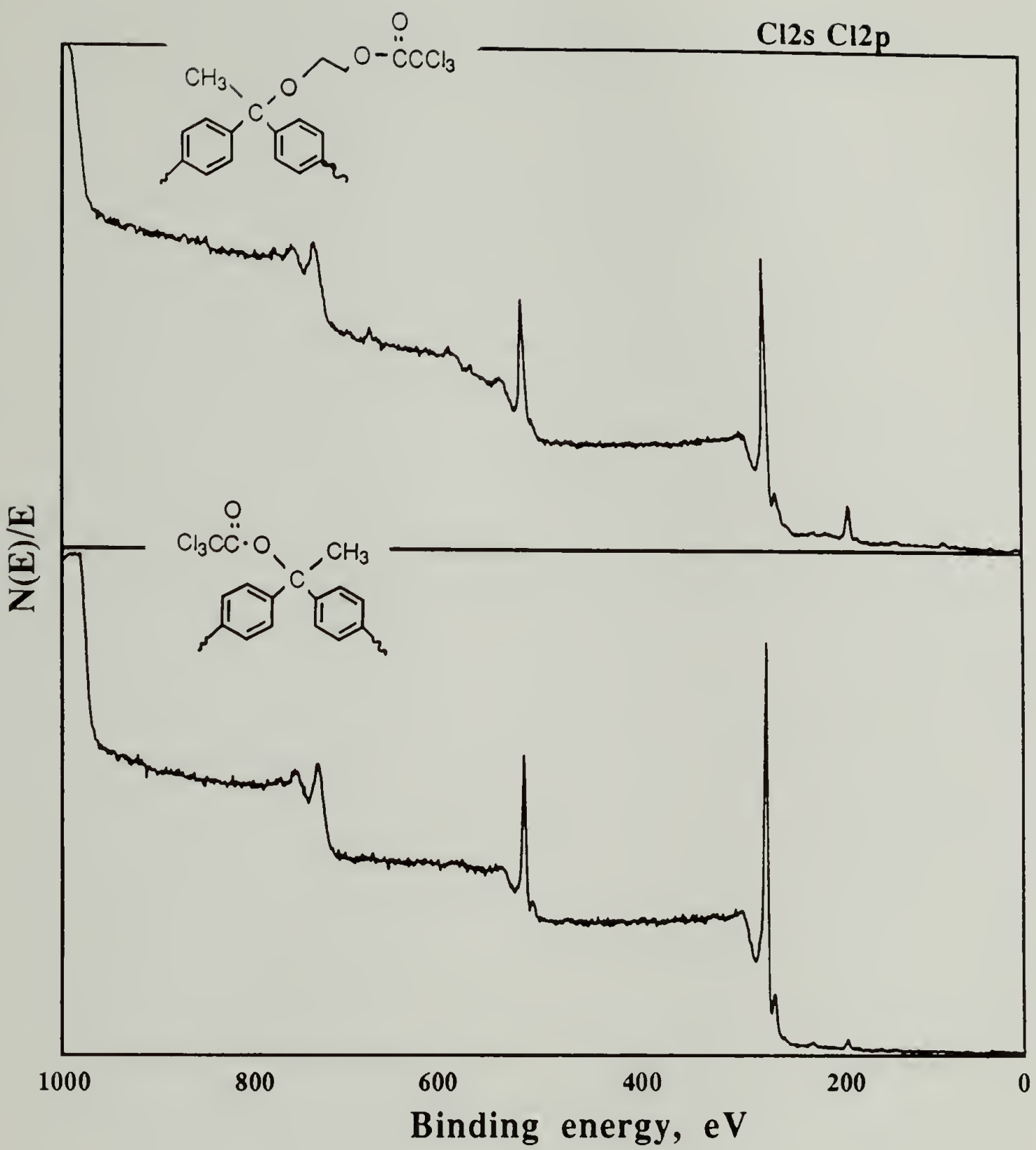

Figure 3.8. Comparison between XPS Survey Spectra for PEEK-$O^{3°}C(O)CCl_3$ and PEEK-ce-$O^{3°}C(O)CCl_3$ Films.

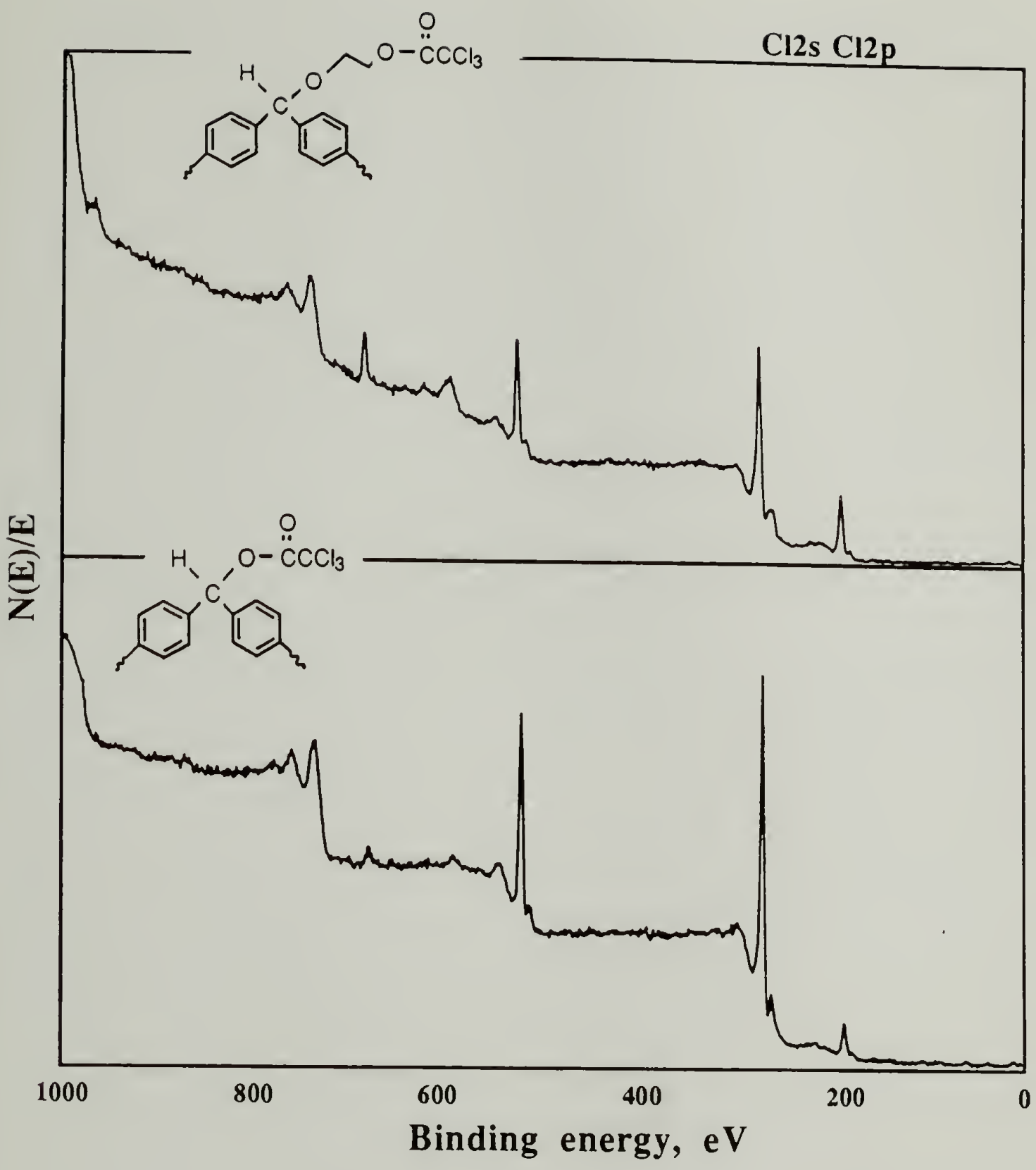

Figure 3.9. Comparison between XPS Survey Spectra for PEEK-$O^{2°}C(O)CCl_3$ and PEEK-ce-$O^{2°}C(O)CCl_3$ Films.

TCAI in fairly low yields. Quantitative (hydroxylation and) urethanation yields would render a repeat unit of $C_{25}O_5Cl_3$, and atomic composition data indicate $C_{25}O_{3.6}Cl_{0.6}$, corresponding to only ~20% reaction (at 15°, these data are considerably higher). Contact angles indicate increased hydrophobicity: $\theta_A/\theta_R = 82°/47°$ (side a) and $\theta_A/\theta_R = 81°/42°$ (side b). XPS data and contact angles indicate that the PEEK~$OH^{3°}$ surface does not react with TCAI. XPS spectra contain very little chlorine (~0.6%) and contact angles are unchanged. However, XPS data indicate that PEEK~$OH^{2°}$ reacts with TCAI in almost 60% yield. Atomic concentration reveals a repeat unit of $C_{22}O_{3.4}Cl_{1.7}$, and contact angles increase to $\theta_A/\theta_R = 85°/53°$ (side a) and $\theta_A/\theta_R = 87°/51°$ (side b), indicating a dramatic decrease in wettability of the surface (relative to the reduced surface). This reaction yield is nearly twice that observed for the reaction of PEEK~$OH^{2°}$ with TCAC, probably because of differences in steric hindrance near the reactive site.

Chain-extended alcohol surfaces react with TCAI in higher yields than the original alcohol surfaces (PEEK~$OH^{2°}$ and PEEK~$OH^{3°}$); however, these yields are slightly less than those obtained with TCAC. XPS atomic concentration data indicate slightly higher than ~30% yield for reaction with PEEK~ce-$OH^{3°}$ and contact angles for this surface increase to $\theta_A/\theta_R = 83°/49°$ (side a) and $\theta_A/\theta_R = 84°/45°$ (side b). Figure 3.10 shows XPS survey spectra for PEEK~$OH^{3°}$ and PEEK~ce-$OH^{3°}$ surfaces after reaction with TCAI. Similar to the data obtained from reaction of PEEK~$OH^{3°}$ and PEEK~ce-$OH^{3°}$ with TCAC, these data (with TCAI) indicate a dramatic increase in the reactivity of surface-confined alcohols after the chain-extension reaction. In the secondary alcohol case, the difference between

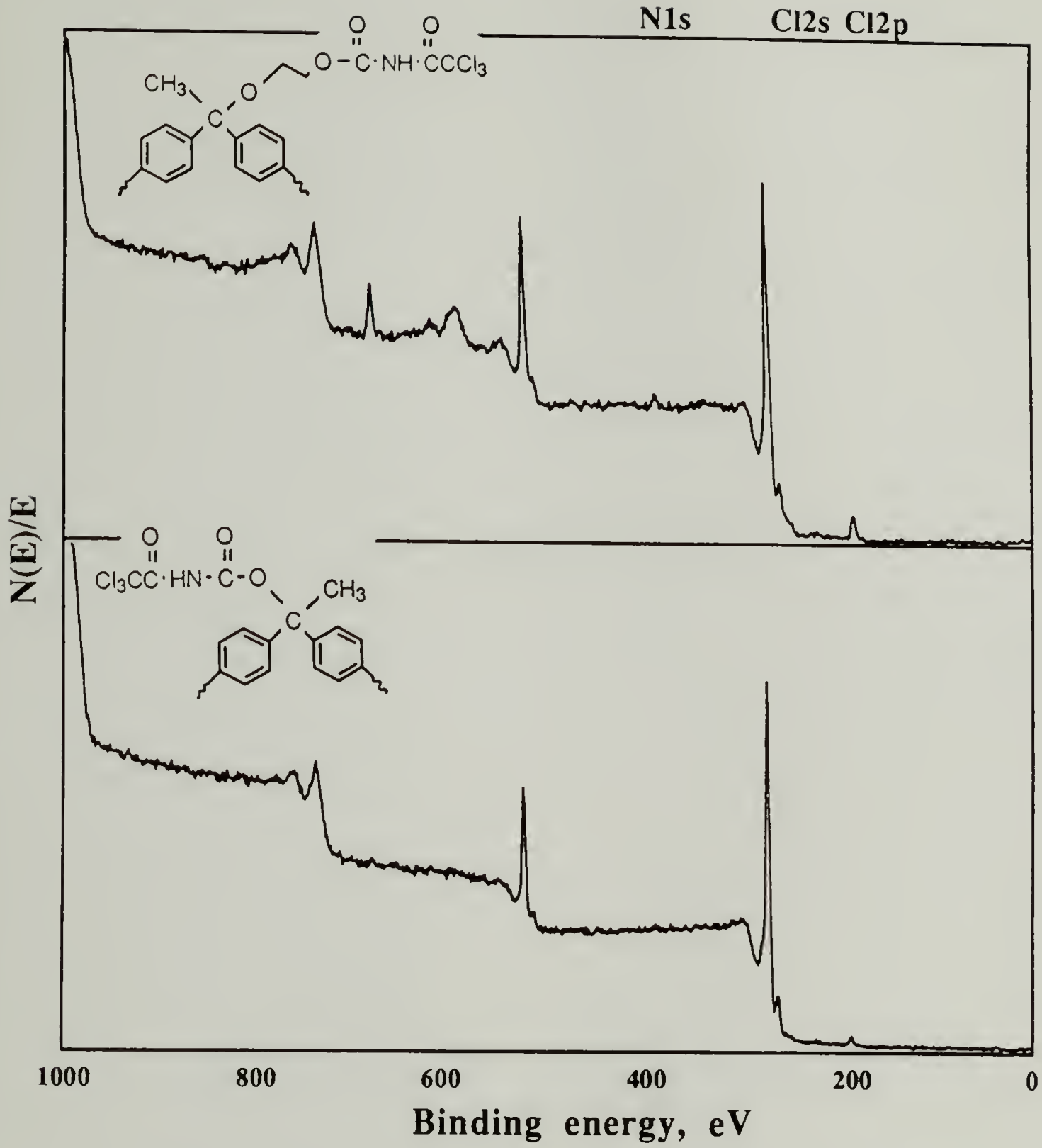

Figure 3.10. Comparison between XPS Survey Spectra for PEEK-$O^{3°}C(O)NHC(O)CCl_3$ and PEEK-ce-$O^{3°}C(O)$-$NHC(O)CCl_3$ Films.

the original surface and PEEK~ce-OH$^{2°}$ surface is slightly less dramatic, but significant changes are observed. Atomic composition data for the PEEK~ce-OH$^{2°}$ surface indicate a repeat unit of $C_{24}O_{4.9}Cl_{2.2}$, corresponding to ~73 % yield (when compared to quantitative repeat unit $C_{24}O_5Cl_3$). Contact angles increase to $\theta_A/\theta_R = 85°/52°$ (side a) and $\theta_A/\theta_R = 86°/46°$ (side b) indicating a dramatic increase in hydrophobicity of the surface. Figure 3.11 shows XPS survey spectra for PEEK~OH$^{2°}$ and PEEK~ce-OH$^{2°}$ surfaces after reaction with TCAI.

Reaction of PEEK-OH with Thionyl Chloride. PEEK-alcohol surfaces containing secondary, tertiary and chain-extended hydroxyl species were reacted with thionyl chloride[28] to convert the alcohol moieties to chlorides (eq. 3.17). Use of this reagent for reaction of alcohol groups

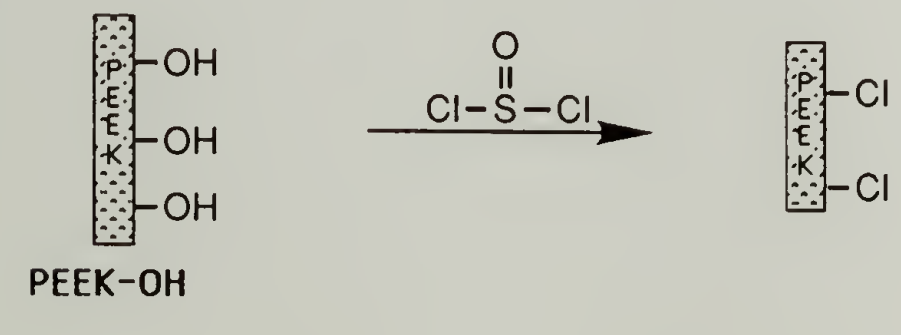

(3.17)

on PEEK has produced results very different than those observed for reaction on poly(chlorotrifluoroethylene) (PCTFE-OH).[23] PCTFE-OH reacts with thionyl chloride to produce the sulfite and no chlorine is observed. The reaction of PCTFE-OH with thionyl chloride provides an example in which the close proximity of functional groups on a surface can change the nature of a reaction. All PEEK-OH surfaces react in fairly high yields with thionyl chloride to give only the chlorinated product. No

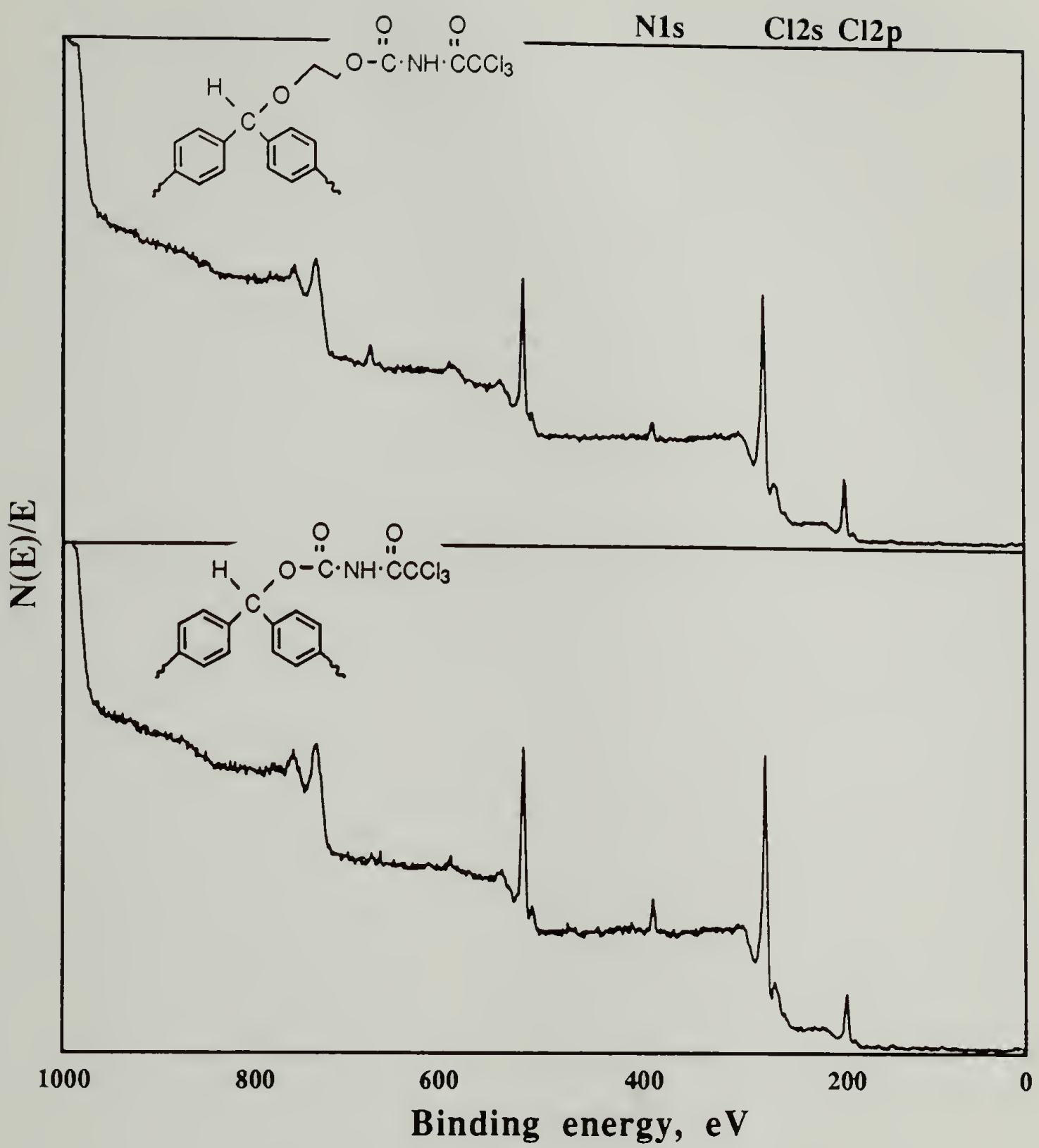

Figure 3.11. Comparison between XPS Survey Spectra for PEEK-$O^{2°}C(O)NHC(O)CCl_3$ and PEEK-ce-$O^{2°}C(O)$-$NHC(O)CCl_3$Films.

sulfur is detected by XPS and contact angles indicate decreased wettability of the surfaces. It is possible that the lower concentration of alcohols on PEEK allows better separation of these moieties and sulfite formation is not feasible. Based on the reaction yields observed for the PEEK~$OH^{2°}$, PEEK~ce-$OH^{2°}$ and PEEK~ce-$OH^{3°}$ surfaces with TCAC and TCAI, reasonably high reaction yields would be expected with thionyl chloride, as well; the only surprising data are those for PEEK~$OH^{3°}$. This surface reacts with thionyl chloride in (what appears to be) ~60% yield and produces an hydrophobic surface with fairly high contact angles: θ_A/θ_R = 84°/49° (side a) and θ_A/θ_R = 86°/44° (side b). One possible explanation for this (extensive) reaction with PEEK~$OH^{3°}$ is that some source of HCl is present in the thionyl chloride/THF solution. If thionyl chloride reacts with adventitious water in the system, the HCl generated would react rapidly with the tertiary hydroxyl species.[29] With this reaction pathway, each chlorine atom added to the surface would displace one molecule of water. Regeneration of water would promote formation of more HCl, and the cycle would continue. Use of this pathway would circumvent steric hindrance near the tertiary alcohol groups and allow extensive reaction. It is important to point out that the control film (PEEK) for this reaction is chlorinated by thionyl chloride to a small extent (~0.4 - 0.6% observed at 15° takeoff angle). No sulfur is detected on the surface which indicates that the reagent is not stuck in the film and suggests that some chlorination of the surface actually occurs. (Contact angles for the control film rise very slightly upon attempted reaction.) Similar data have been observed for other surface reactions in which HCl (or at least sources of chloride) came into contact with PEEK film (i.e. hydrazone reaction, oxidation reaction).

Failed Reactions with PEEK

Some of the reactions attempted with PEEK film were unsuccessful. In some cases, our analyses did not indicate significant changes in the samples and we concluded that little (or no) reaction occurred. In other cases, problems inherent to the reaction system precluded reaction or else caused extensive contamination of (or damage to) the surface.

Failed Attempt at PEEK~$C(NH_2)CN$. This reaction (Strecker synthesis) was carried out with the intention of introducing β-amino nitrile groups[30] to the surface of PEEK, although these efforts were not successful. (Although this procedure was not described in the literature for reaction with benzophenone, it was described as useful for reaction with aromatic ketones, namely acetophenone.) The reaction was initially carried out according to literature conditions[31] and several times at more dilute concentrations. In nearly all cases, an intractable black solid settled at the bottom of the flask, covering the PEEK film sample. Efforts to remove the black solid from the film (by chemical rather than physical methods) were in vain. At very dilute concentrations, the reaction solution grew orange and no solid appeared. XPS and contact angle analyses indicated no reaction with this film. One explanation for the appearance of the black solid rather than reaction with PEEK is that this reaction solution does not "wet" the surface of PEEK very well and the facile polymerization of HCN[32] occurs instead. From contact angle analyses on PEEK, we know that aqueous solutions do not wet the surface well and reactions at the PEEK-water interface would be expected to go to only shallow depths. However, in this case, it seems that side reactions occur much faster than reaction at the film-solution interface. It has been reported in the literature

that HCN will spontaneously polymerize in the presence of a bases, such as amines or ammonia, to form an intractable brownish/black solid.[32] The problems encountered in this reaction highlight the necessity of surface wetting for reaction at a solid-solution interface.

Failed Attempt at PEEK~$COCH_2$. The reaction between PEEK film and the sulfur ylide, dimethylsulfoxonium methylide, produced changes in the surface that were not consistent with epoxide formation. The purpose of this reaction was to convert the ketones into epoxide moieties which would be reactive to nucleophilic attack. A model reaction was carried out on benzophenone following a literature procedure[33] to test the feasibility of this reaction on such a diaryl ketone. The small molecule model reaction product was tested by melting point which agreed with the literature data.[33] Reaction with PEEK caused changes in the surface that were difficult to explain. Contact angles for the reacted surface were lower than those for PEEK film: θ_A/θ_R= 72°/30° (side a) and θ_A/θ_R = 75°/27° (side b), and the XPS data indicated that the surface contained sulfur which could not be extracted. The "functionalized" surface would not undergo further reaction with nucleophilic species like amines. It might be possible that steric hindrance at the film surface caused a secondary reaction to occur (resulting in the sulfur adduct) rather than the expected one, but we did not determine an alternate structure.

Failed Attempt at PEEK~CCl_2. Reaction of PEEK with PCl_5 did not produce any changes in the film surface. XPS and contact angle data gave no evidence of reaction. The literature indicated that this reaction would be successful for producing *gem*-dihalides on aliphatic ketones, but did not

indicate success for aromatic species. No attempt was made to generate the dihalide compound with benzophenone.

Failed Attempt at Friedel Crafts Acylations. Friedel Crafts acylations carried out on PEEK proved to be unsuccessful. Two acid chlorides (TCAC and HFBC) were used in attempts to acylate the phenyl ring between the two ether oxygens on PEEK; this was the only reaction (other than the oxidation reaction) that did not target the carbonyl group (specifically). These reactions were carried out at 65 °C, 30 °C and room temperature. At the highest temperature, the reaction caused visible roughening and pitting of the surface, but at 30 °C these physical changes did not occur. At all temperatures used for this reaction, the aluminum chloride (catalyst) penetrated the film and was very difficult to wash out. Surface contamination caused the contact angles to decrease (instead of increase with the incorporation of the halogen-containing groups, as would be expected) and XPS data did not indicate the presence of chlorine (without aluminum) or fluorine. Given the difficulties involved with cleaning up this surface and the apparent lack of reaction, this synthesis was not pursued very far.

The failure of these reactions tells us that not all reactions that can be carried out on ketones in solution will work at the solid-solution interface. Reactions that work with benzophenone may follow a different pathway when attempted with PEEK, and differences in solvation (of the ketone functional group) most likely come into play. Reactions that are not reported for benzophenone (i.e. formation of the *gem*-dihalide) may not be appropriate for use with PEEK.

Conclusion

Experiments carried out with semicrystalline PEEK film indicate that it is a suitable substrate for surface modification and that the carbonyl groups can function as reactive handles for derivatization of the surface. In general, the reactions carried out derivatize ~50 % of the diaryl ketones in the outer 40 Å of the material. Many of the reactions utilized were chosen from high yield reactions reported in the literature of benzophenone chemistry. The consistently low yields obtained for reaction with PEEK suggest that factors (or problems) inherent to surface reactions, namely varied solvation of functional groups (complicated by partial crystallinity of the material), steric hindrance caused by the solid surface, and the two dimensional nature of the surface environment strongly influence the reactivity of surface-confined functional groups. Alcohol groups with different structures were introduced to the surface of PEEK. Comparisons of wetting behavior and reactivity toward electrophiles of varied steric hindrance were made for the purpose of determining whether functional group structure influences these characteristics. The data obtained indicate that the more hindered alcohols show lower reactivity toward sterically hindered electrophiles and suggest that the more hindered (3°) alcohols contribute less to surface wettability.

Table 9. XPS Data for Reactions on PEEK-$OH^{2°}$ Surface.

PEEK derivative	XPS Atomic Conc. 15°/75° C	O	N	X[A]
PEEK-$OH^{2°}$	84.0	16.0		
	85.2	14.7		
PEEK-$O^{2°}C(O)NHSO_2Ø$	77.6	17.8	2.3	2.4^{S}
	76.3	19.2	2.2	2.3^{S}
control: PEEK in THF with BSI and DBTDL	85.9	14.1		
	86.2	13.8		
PEEK-$O^{2°}C(O)CCl_3$	80.0	17.0		3.0^{Cl}
	82.5	14.5		3.0^{Cl}
control: PEEK in THF with TCAC and pyr	85.7	13.9		$.4^{Cl}$
	86.0	14.0		
PEEK-$O^{2°}C(O)NHC(O)CCl_3$	83.7	14.0	2.2	6.0^{Cl}
	84.7	13.3	2.0	5.0^{Cl}
control: PEEK in THF with TCAI and DBTDL	86.2	13.8		
	86.4	13.6		
PEEK-$O^{2°}C(O)NH(CH_2)_2CH_3$	83.7	14.0	2.0	
	84.7	13.3	2.3	
control: PEEK in THF with $OCN(CH_2)_2CH_3$	86.2	13.8		
	86.5	13.5		
PEEK-$O^{2°}C(O)NHØ$	83.5	14.5	2.0	
	86.5	11.6	1.9	
PEEK-$Cl^{2°}$	84.0	13.0		3.1^{Cl}
	87.2	9.7		2.8^{Cl}
control: PEEK in THF with $SOCl_2$	86.0	13.4		$.6^{Cl}$
	86.2	13.5		$.3^{Cl}$

Table 10. Contact Angle Data for Reactions on PEEK-$OH^{2°}$ Surface.

PEEK derivative	θ_A/θ_R side a	θ_A/θ_R side b
PEEK-$OH^{2°}$	69/23	71/18
PEEK-$O^{2°}C(O)NHSO_2Ø$	78/38	79/32
control: PEEK in THF with BSI and DBTDL	85/55	85/50
PEEK-$O^{2°}C(O)CCl_3$	81/38	82/32
control: PEEK in THF with TCAC and pyr	85/56	85/50
PEEK-$O^{2°}C(O)NHC(O)CCl_3$	85/53	87/51
control: PEEK in THF with TCAI and DBTDL	85/55	85/50
PEEK-$O^{2°}C(O)NH(CH_2)_2CH_3$	79/44	81/41
control: PEEK in THF with $OCN(CH_2)_2CH_3$	85/55	85/50
PEEK-$O^{2°}C(O)NHØ$	80/45	81/40
PEEK-$Cl^{2°}$	79/47	81/42
control: PEEK in THF with $SOCl_2$	86/57	86/50

Table 11. XPS Data for Reactions on PEEK-$OH^{3°}$ Surface.

PEEK derivative	XPS Atomic Conc. 15°/75° C	O	N	X^A
PEEK-$OH^{3°}$	87.8 88.3	12.2 11.7		
PEEK-$O^{3°}C(O)NHSO_2Ø$	84.5 83.2	15.5 16.7	0 0	0^S 0^S
PEEK-$O^{3°}C(O)CCl_3$	88.0 85.0	10.8 14.7		$<1.0^{Cl}$ $.3^{Cl}$
PEEK- $O^{3°}C(O)NHC(O)CCl_3$	87.8 89.4	11.6 10.0	0 0	$.6^{Cl}$ $.6^{Cl}$
PEEK- $O^{3°}C(O)NH(CH_2)_2CH_3$	83.4 84.2	16.6 15.8	0 0	
PEEK-$O^{3°}C(O)NHØ$	86.6 86.9	13.2 13.1	.2 0	
PEEK-$Cl^{3°}$	85.7 86.5	11.0 10.8		3.2^{Cl} 2.7^{Cl}
control: PEEK in THF with $SOCl_2$	86.0 86.2	13.6 13.6		$.4^{Cl}$ $.2^{Cl}$

Table 12. Contact Angle Data for Reactions on PEEK-$OH^{3°}$ Surface.

PEEK derivative	θ_A/θ_R side a	θ_A/θ_R side b
PEEK-$OH^{3°}$	74/35	73/32
PEEK-$O^{3°}C(O)NHSO_2Ø$	73/33	73/29
PEEK-$O^{3°}C(O)CCl_3$	76/35	78/36
PEEK-$O^{3°}C(O)NHC(O)CCl_3$	76/34	78/35
PEEK-$O^{3°}C(O)NH(CH_2)_2CH_3$	72/33	73/30
PEEK-$O^{3°}C(O)NHØ$	75/40	76/39
PEEK-$Cl^{3°}$	84/49	86/44

Table 13. XPS Data for Reactions on PEEK-$OH^{1°}$ Surface.

PEEK derivative	XPS Atomic Conc. 15°/75° C	O	N	X^{A}
PEEK-OPr	80.0 87.0	20.0 13.0		
PEEK-$OH^{1°}$	84.0 85.0	16.0 15.0		
PEEK-$O^{1°}C(O)NHSO_2Ø$	77.1 78.0	20.0 18.8	1.3 1.5	1.4^{S} 1.6^{S}
PEEK-$O^{1°}C(O)CCl_3$	82.5 83.0	14.5 15.0		3.0^{Cl} 2.0^{Cl}
PEEK- $O^{1°}C(O)NHC(O)CCl_3$	84.0 85.4	12.0 12.4	1.0 .6	3.0^{Cl} 1.6^{Cl}
PEEK- $O^{1°}C(O)NH(CH_2)_2CH_3$	81.5 82.1	17.1 16.6	1.4 1.3	
PEEK-$O^{1°}C(O)NHØ$	82.2 84.7	16.2 14.0	1.3 1.4	

Table 14. Contact Angle Data for Reactions on PEEK-$OH^{1°}$ Surface.

PEEK derivative	θ_A/θ_R side a	θ_A/θ_R side b
PEEK-OPr	81/48	83/43
PEEK-$OH^{1°}$	77/45	75/40
PEEK-$O^{1°}C(O)NHSO_2Ø$	77/44	78/40
PEEK-$O^{1°}C(O)CCl_3$	81/49	80/46
PEEK-$O^{1°}C(O)NHC(O)CCl_3$	82/47	81/42
PEEK-$O^{1°}C(O)NH(CH_2)_2CH_3$	80/44	79/41
PEEK-$O^{1°}C(O)NHØ$	79/43	80/40

Table 15. XPS Data for Reactions on PEEK-ce-$OH^{2°}$ Surface.

PEEK derivative	XPS Atomic Conc. 15°/75° C	O	N	X^A
PEEK-ce-$OH^{2°}$	82.0 84.0	18.0 16.0		
PEEK-ce-$O^{2°}C(O)NHSO_2Ø$	79.1 80.1	17.6 15.7	2.0 1.5	1.9^S 1.4^S
PEEK-ce-$O^{2°}C(O)CCl_3$	77.0 77.0	16.5 15.0		6.5^{Cl} 8.0^{Cl}
PEEK-ce-$O^{2°}C(O)NHC(O)CCl_3$	75.0 75.3	15.8 15.3	2.1 2.3	7.0^{Cl} 6.9^{Cl}
PEEK-ce-$O^{2°}C(O)NH(CH_2)_2CH_3$	81.6 82.0	16.3 15.9	2.4 2.2	
PEEK-ce-$O^{2°}C(O)NHØ$	84.6 85.6	13.2 12.5	2.2 2.0	
PEEK-ce-$Cl^{2°}$	81.6 84.3	15.1 12.6		3.4^{Cl} 3.1^{Cl}

Table 16. Contact Angle Data for Reactions on PEEK-ce-$OH^{2°}$ Surface.

PEEK derivative	θ_A/θ_R side a	θ_A/θ_R side b
PEEK-ce-$OH^{2°}$	71/30	70/26
PEEK-ce-$O^{2°}C(O)NHSO_2Ø$	76/37	78/32
PEEK-ce-$O^{2°}C(O)CCl_3$	85/52	86/46
PEEK-ce-$O^{2°}C(O)NHC(O)CCl_3$	85/52	86/46
PEEK-ce-$O^{2°}C(O)NH(CH_2)_2CH_3$	78/46	79/41
PEEK-ce-$O^{2°}C(O)NHØ$	83/47	82/42
PEEK-ce-$Cl^{2°}$	85/49	84/46

Table 17. XPS Data for Reactions on PEEK-ce-$OH^{3°}$ Surface.

PEEK derivative	XPS Atomic Conc. 15°/75° C	O	N	X^A
PEEK-ce-$OH^{3°}$	84.0 86.5	16.0 13.5		
PEEK-ce-$O^{3°}C(O)NHSO_2Ø$	77.1 80.4	19.1 16.7	1.3 1.5	1.1^S 1.3^S
PEEK-ce-$O^{3°}C(O)CCl_3$	82.3 83.6	12.4 12.0		5.4^{Cl} 4.3^{Cl}
PEEK-ce-$O^{3°}C(O)NHC(O)CCl_3$	78.8 80.0	16.6 16.0	1.1 1.0	3.5^{Cl} 3.0^{Cl}
PEEK-ce-$O^{3°}C(O)NH(CH_2)_2CH_3$	82.4 83.2	15.8 15.0	1.8 1.8	
PEEK-ce-$O^{3°}C(O)NHØ$	84.0 86.1	14.6 12.6	1.4 1.3	
PEEK-ce-$Cl^{3°}$	85.4 85.8	12.3 11.8		2.4^{Cl} 2.5^{Cl}

Table 18. Contact Angle Data for Reactions on PEEK-ce-$OH^{3°}$ Surface.

PEEK derivative	θ_A/θ_R side a	θ_A/θ_R side b
PEEK-ce-$OH^{3°}$	68/30	67/27
PEEK-ce-$O^{3°}C(O)NHSO_2Ø$	77/38	76/34
PEEK-ce-$O^{3°}C(O)CCl_3$	81/48	82/52
PEEK-ce-$O^{3°}C(O)NHC(O)CCl_3$	83/49	84/45
PEEK-ce-$O^{3°}C(O)NH(CH_2)_2CH_3$	80/42	71/38
PEEK-ce-$O^{3°}C(O)NHØ$	80/43	81/39
PEEK-ce-$Cl^{3°}$	83/48	82/42

References

1. Technical data sheet from ICI, Americas.
2. Attwood, T.E.; Dawson, P.C.; Freeman, J.L.; Hoy, L.R.J.; Rose, J.B.; Staniland, P.A. *Polymer* **1981**, *22*, 1006.
3. Clendinning, R.A.; Farnham, A.G.; Johnson, R.N. *Polym. Prepr. (Am. Chem. Soc., Div. Polym. Chem.)* **1986**, *27(1)*, 478.
4. Rose, J.B. *Polym. Prepr. (Am. Chem. Soc., Div. Polym. Chem.)* **1986**, *27(1)*, 480.
5 Lachman, A. In *Organic Syntheses*; Blatt, A.H., ed. John Wiley & Sons: New York, 1943, Collect. Vol. II, p. 70.
6. McFarland, J.W.; Howard, J.B. *J. Org. Chem.* **1965**, *30*, 957.
7. Baskin, A.; Ter-Minassian-Saraga, L. *J. Polym. Sci. Part C* **1971**, *34*, 243.
8. Batich, C.D.; Wendt, R.C. In *Photon, Electron, and Ion Probes of Polymer Structure and Properties*; Dwight, D.W.; Fabishi, T.J.; Thomas,H.R., eds. *ACS Symp. Ser.*, 1981, *162*, Ch. 15.
9. Corey, E.J.; Chaykovsky, M. *J.Am. Chem. Soc.* **1962**, *84*, 866.
10. Evans, D.A.; Truesdale, L.K.; Carroll, G.L. *Chem. Commun.* **1973**, 55.
11. Andrade, J.D.; Gregonis, D.E.; Smith, L.M. In *Surface and Interfacial Aspects of Biomedical Polymers*; Andrade, J.D. ed. Plenum: New York, 1986, Vol. 1, Ch. 2.
12. Reference 11, Ch. 5.
13. Reference 11, Ch. 7.
14. Dias, A.J.; McCarthy, T.J. *Macromolecules* **1984**, *17*, 2529.
15. Brennan, J.V.; McCarthy, T.J. *Polym. Prepr. (Am. Chem. Soc., Div. Polym. Chem.)* **1988**, *29(2)*, 338.
16. Brennan, J.V.; McCarthy, T.J. *Polym. Prepr. (Am. Chem. Soc., Div. Polym. Chem.)* **1989**, *30(2)*, 152.
17. Shoichet, M.S.; McCarthy, T.J. *Macromolecules* **1991**, *24*, 982.
18. Costello, C.A.; McCarthy, T.J. *Macromolecules* **1987**, *20*, 2819.

19. Costello, C.A.; McCarthy, T.J. *Macromolecules* **1984**, *17,* 2940.

20. Bening, R.C.; McCarthy, T.J. *Macromolecules* **1990**, *23*, 2648.

21. Bee, T.G..; McCarthy, T.J. *Macromolecules* **1992**, *25*, 2093.

22. Lee, K.-W.; McCarthy, T.J. *Macromolecules* **1988**, *21*, 2318.

23. Dias, A.J.; McCarthy, T.J. *Macromolecules* **1987**, *20*, 2068.

24. Dias, A.J.; McCarthy, T.J. *Macromolecules* **1985**, *18*, 1826.

25. Everhart, D.S.; Reilley, C.N. *Anal. Chem.* **1981**, *53*, 665.

26. Capka, M.; Chvalovsky, V.; Kochloefl, K.; Kraus, M. *Coll. Czech. Chem Commun.* **1969**, *34*, 118.

27. Quirk, R.P.; Seung, N.S. In *Ring Opening Polymerization*; McGrath, J.E. ed. Plenum: New York, 1986, Vol. 1, Ch. 2.

28. Pizey, S.S. *Synthetic Reagents*, John Wiley & Sons: New York, 1974, Vol. 1, Ch. 4.

29. Carey, F.A.; Sundberg, R.J. *Advanced Organic Chemistry Part B: Reactions and Synthesis*, Plenum Press: New York, 1983.

30. March, J. *Advanced Organic Chemistry*, 3rd ed. Wiley-Interscience: New York, 1985.

31. Steiger, R.E. In *Organic Syntheses*; Blatt, A.H., John Wiley and Sons: New York, **1965**, Coll. Vol. III, p. 66.

32. Matthew, C.N.; Ludicky, R. *Polym. Prepr. (Am. Chem. Soc., Div. Polym. Chem.)* **1987**, *28 (2)*, 104.

33. Corey, E.J.; Chaykovsky, M. *J. Am. Chem. Soc.* **1965**, *87*, 1353.

CHAPTER IV

ADSORPTION/MIGRATION OF SELECTIVELY-FUNCTIONALIZED POLYSTYRENES FROM A POLYSTYRENE MATRIX: INTRODUCTION

Previous research in the McCarthy group has concentrated on the preparation of specifically functionalized and well-characterized polymer surfaces with the objective of studying polymer surface structure-property relationships. Among the approaches to surface modification used by the group are chemical modification, polymer adsorption from solution and surface reconstruction. Reconstruction is a unique approach to surface modification because changes in surface properties are environmentally induced. Surface reconstruction experiments have been carried out by first chemically modifying poly(chlorotrifluoroethylene) (PCTFE)[1] or polyethylene (PE)[2] film samples to introduce polar functional groups to the surface, followed by annealing treatments under vacuum or in an aqueous environment. Surface analyses, including X-ray photoelectron spectroscopy (XPS) and contact angle measurements, were carried out to monitor changes in both surface structure and macroscopic surface properties that occur upon manipulating the annealing environment. Other examples of surface reconstruction experiments now include the study of heat-treated films cast from toluene solutions of polystyrene that contain varied concentrations of surface-active polymers. The purpose of these

experiments was to examine molecular and environmental parameters that influence surface reconstruction.

Reconstruction of Polymers

The mobility of the chains in a given polymer sample under the appropriate conditions gives the material the ability to reconstruct in response to environmental changes and to minimize the surface free energy; this characteristic sets polymers apart from other materials. Reconstruction of polymer surfaces (and interfaces) to minimize interfacial free energy has been reported in the literature[3] fairly extensively from both the theoretical[4-10] and experimental[11-30] perspectives; the phenomenon of surface reconstruction is becoming fairly well known. Experiments employing small molecule surface-active agents,[11-12] diblock[13-24] (or triblock[25]) copolymers, polymer blends[26-30] and surface modified polymers[1,2] have demonstrated that polymer surfaces are dynamic. Under the appropriate (annealing) conditions, a polymer surface will reorganize to allow preferential segregation (or adsorption[3]) of the lowest energy component to that interface.[17-27] Surface structure and composition depend on several factors including bulk composition,[22,25,26,30] incompatibility of system components,[23-26,30-32] annealing time,[1] annealing temperature,[1,17] casting solvent,[17,22,26,30,34] polymer molecular weight,[28,29,33] and temperature of measurement.[28] Other factors, such as the structure of the surface-migrating species,[35] the orientation of specific groups at the surface[36-38] and the proximity of other chain ends in the sample to the surface are important factors, as well. As a result of surface

reconstruction, the surface of a polymer can differ dramatically from the bulk material in composition, structure and properties.

Environmental Influences

Polymer surfaces are nonequilibrium solids[36] which have time and temperature-dependent properties and, for this reason, can exhibit relaxation properties in response to the environment. Mobility of chains in a sample can result in a preferred bond orientation which can affect the properties of a surface,[36,39] as well as the reactivity.[40] Experiments with preformed polymer films indicate that exposure to various (chemical) environments,[41,42] molding against high[43-46] (or low)[44,46] energy substrates, or annealing in vacuum[1,47] can dramatically change the wetting properties of the material. In general, reconstruction or bond orientation in the sample serves to concentrate the component at the surface that is most similar (energetically) to the phase above the material; changes in contact angle measurements reflect changes in wettability with reconstruction and reorientation.[1,45] Studies of reconstruction (or functional group migration) in preformed films include annealing experiments with oxidized poly(ethylene)[2] and copolymers of tetrafluoroethylene-perfluoro(propyl vinyl ether).[47] Experiments to determine the effects of annealing films against various substrates were carried out with poly(ethylene)[45] and copolymers of ethylene-acrylic acid.[46] Surface energy determinations based on bulk composition were done on vinyl alcohol-vinyl acetate[48] and ethylene-vinyl acetate[49] copolymer films.

Surface Adsorption/Migration of Low Energy Component

Solution-cast films of homopolymers, blends or block copolymers often will exhibit surface properties that differ dramatically from the properties of the bulk due to segregation of the lower energy component to the surface to reduce the surface energy. This surface segregation can occur during film casting, heat processing or annealing. The Gibbs adsorption equation has been used to describe changing surface tension (γ) with surface-migration[3]

$$-d\gamma = \sum_i \Gamma_i d\mu_i \qquad \text{where } \Gamma_i = \frac{N_i}{A_s} \tag{4.1}$$

and represents the number of species i per area A. The chemical potential μ describes the free energy change with each species adsorbed to the surface, and in this sense, can describe surface energy differences between two molecular species in a given material. The air phase above a polymer is considered an energetically neutral surface (can be thought of as a wall),[10] but surface energy differences between components of the bulk cause preferential segregation of one component. The presence of the "wall" causes a loss of potential energy for whichever species migrates to the surface because the next-nearest neighbor interactions have been reduced (removed on one side). The loss of potential energy for the two types of segments also can be related to energetic interactions in the bulk between two of the same chemical species (e.g. A-A segments and B-B segments), using the mean-field lattice formulation developed by Scheutjens and Fleer.[10,50] The chemical potential difference between two species in a

blend can determine which species will segregate to the surface and can be calculated from bulk property information.

Experiments using diblock and triblock copolymers and homopolymer blends indicate that surface-segregation of one component depends on surface energy and compatibility differences (i.e. segregation limit) between the components, as well as the bulk composition. XPS studies of polystyrene-poly(methyl methacrylate) diblock copolymer film samples[24] indicate that the polystyrene component dominates the surface but forms an incomplete surface overlayer (termed incomplete wetting[51]). The surface excess of polystyrene (Φ_{ps}) increased with molecular weight (N) and was described with the following relationship:

$$\Phi_{PS} = a - \frac{b}{\sqrt{N}} \qquad (4.2)$$

where a and b are constants. (Using the theory of Fredrickson,[51] the dependence of surface segregation on N arises from the range of interactions in a polymer system (e.g. correlation length in ordered phase) that vary ~$N^{1/2}$.) The incomplete wetting phenomenon has been observed in other weakly segregated copolymer systems, such as polystyrene-poly(ethylene oxide)[22,25] and polycarbonate-poly(dimethylsiloxane).[18] One explanation offered for the incomplete coverage was that the molecular weights used in these systems are very low which means χN (which is essentially a measure of compatibility) is too low for strong segregation behavior between components. These results emphasize that surface energy differences alone do not give accurate predictions of surface composition.

Another interesting point is that films prepared from these same polymers as homopolymer blends[26,30] showed much stronger segregation behavior than the copolymer samples, and this reveals the importance of polymer structure in phase behavior (and ultimately surface segregation behavior).

Surface Tension

The surface tension of polymer samples depends on the molecular weight and polydispersity of the bulk, as well as the temperature of measurement. In general, surface (or interfacial) tension decreases in a linear fashion with temperature[28] and increases with molecular weight. Experiments with poly(isobutylenes)[52] in the molecular weight range 400-3000 have shown that surface tension varies as $Mn^{-2/3}$ although other data with poly(dimethylsiloxane)[33] indicate that surface tension varies as Mn^{-1} in the molecular weight range above 770. Other researchers[28] have suggested the power law $C_1 + C_2Mn^{-z}$ to fit interfacial tension in polystyrene-poly(methyl methacrylate), polybutadiene-poly(dimethylsiloxane) and polystyrene-hydrogenated 1,2-polybutadiene systems (where the asymptotic regime of $z = 1$ is not reached[8] up to a molecular weight of 43,700). The relationship of molecular weight to surface tension reflects that lower molecular weight samples would have lower surface tension; this could be due to a concentration of chain ends at the surface. It is argued that shorter chains in a polymer sample partition preferentially to the surface for entropic reasons.[6,10] The (conformational) entropy lost by longer chains at a surface would exceed that lost by the shorter ones because of chain connectivity; adsorption of the shorter chains in place of the longer ones would maximize the entropy of the system.[6,10] Adsorption of the shorter

chains in combination with the $Mn^{-2/3}$ dependence of surface tension suggests that the polydispersity of a polymer sample would have important consequences on its surface properties.

Surface tension measurements made by the pendant drop method for homopolymer mixtures (blends) for a variety of polyethers[53] indicate that the surface excess of the lower surface energy component increases with the molecular weight (of both components) rather than the fractional bulk composition of the surface-active species. Because surface tension (in general) increases with molecular weight, these results imply that the increasing surface tension was the driving force for increasing the surface excess.

Bulk Order

The bulk morphology, as well as the surface structure of a given polymer material, is determined by the compatibility[17,35] and relative amounts[24,35] of the components and structural factors like chain architecture (i.e. block copolymer vs. homopolymer blend). For example, (incompatible) symmetric diblock copolymers (each volume fraction, ϕ is .5) phase segregate into spatially periodic structures (lamellae) whereas systems in which one volume fraction is less than .2 will form spherical domains within the matrix of the other component.[24,35] Experimental data of copolymer blends of polystyrene-poly(methyl methacrylate) indicate that near critical points (with respect to segregation), surface and bulk properties are coupled (i.e. surface-segregation induces order in the

bulk).[17] Researchers have found that the lower surface energy component forms a surface overlayer to an extent that depends on the segregation limit (i.e. χN), as well as surface energy differences.[7,17,23,26] In cases in which both system components were found at the surface, the morphology of the bulk was determined to be vertically aligned lamellae.[18,24,32] Other (theoretical) papers in the literature indicate that when two components have similar affinities for the surface, the material has a small value of χ_s, the surface interaction parameter, and both components will lie parallel to the surface. At higher values of χ_s, the component with higher surface affinity will be preferentially partitioned to the surface.[7] χ_s has been defined as a measure of differential affinity between A and B segments for the surface:[5]

$$\chi_s = \chi_S^A - \chi_S^B = -\frac{u_S^A - u_S^B}{kT} \qquad (4.3)$$

where u_S is the surface adsorption energy. Calculations of the theoretical end-segment densities of the two components suggest that the component with lower surface affinity would preferentially partition end segments to the surface, rather than middle ones.[7]

Fredrickson[51] has developed a theory to address the contribution of surface effects to the bulk properties of a symmetric (ϕ = .5) diblock copolymer film sample in the weak segregation limit. (Despite the restrictions on this theoretical model, discussion of some of the important physical parameters should shed light on factors controlling surface-

segregation systems, in general.) A surface free energy term, $F_s(\psi)$which relates to a surface energy density $f_s(\psi)$, can be added to the bulk free energy term for an overall system free energy

$$[F(\psi) = F_b(\psi) + F_s(\psi)]. \tag{4.4}$$

The surface energy density is described as

$$f_s(\psi) = \frac{\left[-H_1\psi(\mathbf{r}) + a_1\psi^2(\mathbf{r})\left(\frac{1}{2}\right)\right]}{N} \tag{4.5}$$

where the order parameter $\psi(\mathbf{r}) = <\rho_A(\mathbf{r})>/(\rho - \phi)$ represents the deviation of one diblock copolymer component (at point $\mathbf{r}$) from the average density of the bulk. The terms a_1 and H_1 are proportional to N, the size of the chain, and they describe how the bulk thermodynamic potential is affected by the film surface. H_1 is a "field" (assumed to be small) that is related to the chemical potential difference between the two system components that favors one component at the surface over the other. Because in most cases, one component of a system will exhibit a preference for the surface (surface affinity), the field is nonzero: $/H_1/ > 0$. The parameter a_1 describes how the surface modifies the (local) Flory interaction parameter χ between segments of the two system components near the surface. When $a_1 < 0$, the local interaction parameter is less than the bulk value and the surface energy will be decreased by segregation of one component to the surface, independent of disorder in the bulk. Likewise, if $a_1 > 0$, meaning that χ_{local} exceeds χ_{bulk}, surface segregation would increase the surface energy and is therefore unlikely.

Segregation to Interfaces

In the same fashion that surface-segregation of surface-active species is driven by surface free energy minimization, the driving force for segregation of diblock copolymers to interfaces between homopolymers in blends is a reduction of interfacial tension; this results in a reduction in the overall free energy of the system. Block copolymers exhibit an emulsifying effect and facilitate mixing of the homopolymer phases by reducing interfacial tension[54] and effectively increase the width of the interface.[19,20] The mechanical properties of such a blend are increased by the addition of the copolymer (of large enough molecular weight[29]) because of the increase in the number of entanglements between the two phases. A number of experiments have been carried out using small amounts of block copolymers of polystyrene and poly(2-vinyl-pyridine)[14,19,29] to study the segregation to the interfacial region between the two corresponding homopolymers. It is argued that in some of these experiments[14,19] the formation of block copolymer micelles in the bulk interferes with the segregation of the copolymers to interfacial regions because of the strong tendency of the micelles to segregate to the free surface. Other experiments designed to pinpoint the critical molecular weight necessary for segregated diblock copolymers to improve the mechanical properties of blends were carried out, as well.[29] Experiments studying the adsorption of polystyrene-poly(methyl methacrylate)[20,55] diblock copolymers to the interfacial regions of the corresponding homopolymers were carried out to examine the driving force for segregation,[20] as well as to determine the width of the interface[55] In the limit of infinite molecular weight, interfacial thickness, D, can be related to the interaction parameter for the two system components A and B as[8]

$$D_\infty = \frac{2a}{\sqrt{6\chi_{AB}}} \qquad (4.6)$$

where a represents the statistical monomer length. The width of the interface is an indication of the extent of penetration of polymer chains into the region between two phases. (A "minor" reptation model can be used to calculate the rate and extent of diffusion of one species into the other.[56])

Surface-Activity in Fluorinated Polymers

A number of polymers containing fluorinated moieties have been developed recently to study surface activity effects. This work stems from recognition of the amphiphilic properties and preferential surface-adsorption of fluorinated surfactants (also called semifluorinated alkanes)[57] $[F(CF_2)_m(CH_2)_nH]$ which resemble block copolymers[58] of very low molecular weight, as well as knowledge of the strong incompatibiltiy between fluorinated and hydrocarbon segments. XPS data from experiments comparing fluorine surface-enrichment between methacrylate polymers containing fluorinated side groups of different lengths[59] indicate that the longer fluoroalkyl group allowed greater surface enrichment; coating thickness was also found to be important. In a similar fashion, experiments with polystyrenes carrying C_4F_9 and C_8F_{17} substituents (in various mole percents)[60] indicated that the longer substituent provided a greater reduction in surface energy for the material (as evidenced by contact angle data). The difference in surface energy reduction was attributed to the ability of the longer fluoroalkyl groups to order on the surface. Tremendous reduction in surface energy due to the packing of

CF_3 groups on a surface has been reported previously[12] and in other cases, further reductions in surface energy (beyond that provided by CF_2 groups) have been attributed to just the presence of CF_3 groups on the surface.[47] XPS studies of the surface structure of segmented poly(ether urethanes) and poly(ether urethane ureas)[61] containing fluorinated main-chain moieties indicated that the surface-segregation of the fluorinated (hard) segments was influenced by steric and conformational restraints and depended on the extent of phase separation/segregation in the material.

Theory and Predictions for Surface-Active Molecules

A theoretical site lattice model approach has been developed by Theodorou[4,5,62,63] to describe the thermodynamic properties and microscopic structure of bulk polymers at interfaces. For the most part, these theories are extensions of the Scheutjens-Fleer[50] solution adsorption model which is itself an adaptation of Flory-Huggins theory to systems in which properties are variant along a principal lattice direction because of the interface present.[62] In particular, Theodorou has developed a lattice model that can be used to shed light on the structure, in terms of local composition and chain shape, and interfacial properties, namely interfacial tension, of surface-active polymers adsorbing at a surface from the bulk;[63] the exact nature of the interface (polymer-air vs. polymer-solid) is irrelevant.

In Theodorou's model,[63] structural and thermodynamic parameters were examined with respect to chain length (r) and relative surface-

adsorption affinity of the system components (χ_s). The model describes the surface-adsorption behavior of linear polymers of the structure AB_{r-1} in which the A segments are surface-active and $r_A = 1$; this means that the surface interaction parameter is positive ($\chi_s > 0$). Some of the assumptions made in this model are that segment density in the sample is constant and all lattice sites are occupied (no voids or inconsistencies exist), the Flory interaction parameter χ is zero, and that the flexible, freely jointed chains at the interface are in equilibrium with the unconstrained bulk polymer (beneath or adjacent).

Calculations within this model[63] have led to several predictions about the adsorption behavior for polymer chains containing a surface-active endgroup. Plots of the spatial distribution of A segments in the samples (as a function of depth) for different chain lengths (r = 10, 25, 50, 100 and 300) and different χ_s values (χ_s = 0, 5, 10, 20 and 27) indicate the prediction that the surface excess (of headgroups) increases with increasing r, and that a depletion layer exists immediately beneath the surface, caused by the necessity of having B segments attached to the surface-active A segments. The number of depleted layers increases with increasing r because of the larger number of B segments. Greater surface excesses and deeper depletion layers are predicted for larger χ_s values for all chain sizes. Theodorou[63] also predicts a tremendous decrease in interfacial tension with adsorption of the surface-active moieties. For homopolymers, the lattice model[62] predicts increasing interfacial tension with molecular weight which has been shown to be accurate experimentally.[28,52] In the surface-active polymer system, the interfacial free energy is predicted to

decrease with molecular weight and scale with χ_s; this means that interfacial tension is a parameter that can be used to characterize segment-surface interactions (e.g. surface analysis by contact angles) on the molecular level.

Theodorou's[63] model predicts that migration of surface-active chains to an interface perturbs their natural conformation. In the homopolymer case, the chains are expected to lie parallel to a surface (as if flattened out) because of entropic constraints.[62] However, in the case of the surface-active chains, the tendency is for the chains to crowd the surface to maximize the surface excess.[63] Plots of the surface-active chain shape profiles indicate that chain segments occupy fewer lattice sites per layer near the surface than in the unperturbed bulk which means that the chains are elongated in the direction perpendicular to the plane of the surface. The data also indicate that shape perturbations extend to deeper layers with increasing r, but that the extent of chain narrowing reaches a limit at high molecular weight. The thickness of the interfacial (perturbed) region is predicted to vary roughly with $(r)^{1/2}$. Chain-packing at the surface (i.e. packing of surface-active groups) is not predicted by this model, even at very high χ_s values. The assumption that chains at an interface are in equilibrium with (unconstrained) bulk polymer means that perfect orientation of the surface-active polymers (at that interface) is nearly impossible.

Objective

The experimental research described here examines the more fundamental aspects of polymer surface reconstruction through careful selection and manipulation of variables and through appropriate polymer design. Data in the literature indicate that polymers will reconstruct to minimize interfacial free energy, given sufficient chain mobility, however, the parameters that actually influence and control surface reconstruction are less well understood. With some knowledge about small molecule surfactant phenomena and surface reconstruction in polymers, we have chosen a well-defined and controlled system in which reconstruction is likely to occur and have manipulated variables with the objective of studying how certain molecular and environmental parameters affect adsorption of surface-active polymers.

This work examines the rate and extent of surface migration (adsorption) through (from) a polystyrene matrix (Mn = 10,000) by surface-active polystyrene molecules (SAPs) functionalized with perfluoroalkyl groups. Blends containing varied amounts of surface-active polymer in the matrix polymer were prepared as films and heat-treated to facilitate migration of the fluorinated species. Kinetics and temperature variation studies were carried out on end-functionalized SAP polymers of different molecular weights to determine optimum annealing conditions for each SAP sample series and to pinpoint maximum surface reconstruction while examining reconstruction rates. Two SAP polymers, one with a different chain architecture and the other with a larger surface-active group size, also were prepared and studied. Below is a graphic depiction of a reconstructed film sample using balloons to represent the surface-

active moiety on the SAP chains, as well as models to describe the structures of the SAP chains used in these experiments.

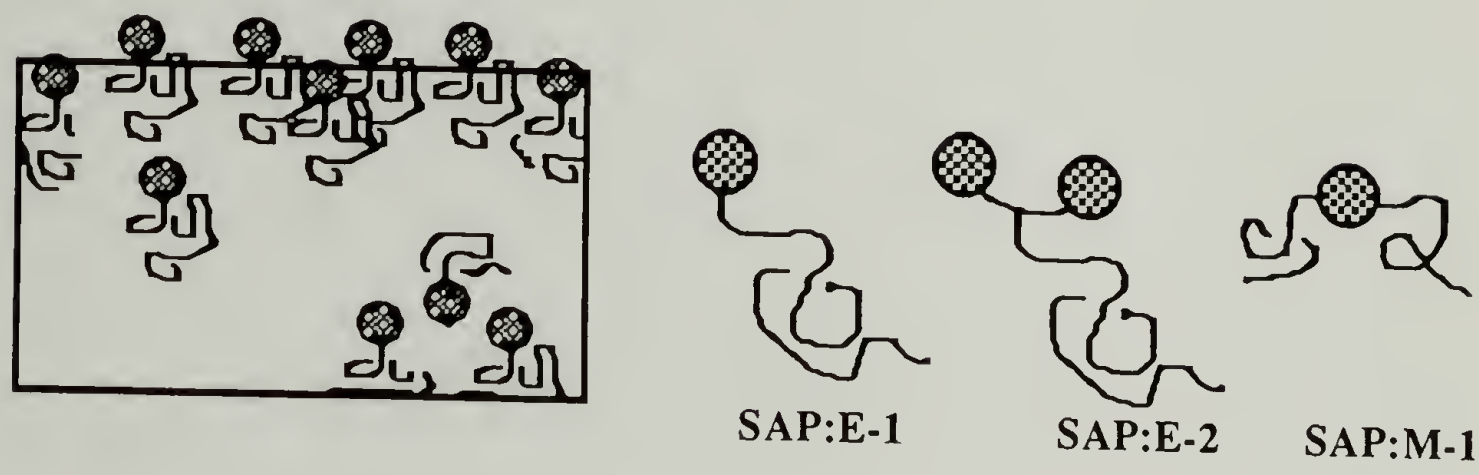

Reconstructed film samples were analyzed by XPS and contact angle measurements to assess changes in atomic composition, as well as changes in surface properties, namely the wettability, with adsorption. This system is appropriate for such experiments because detection of fluorine by XPS and concommitant decreasing wettability can be ascribed only to the presence of the functionalized (SAP) polymers at the surface. With few components in the system, XPS data are simplified: new peaks in the C_{1s} region are due to CF_2 and in some cases, CF_3 groups, and the survey spectra contain only carbon, fluorine and very small amounts of oxygen which allow us to present our data in terms of F/C atomic concentration ratios that accurately represent the composition of the surface. The experiments carried out were designed with the objectives of observing molecular weight effects in surface reconstruction as well as determining the importance of chain architecture and surface-active group size. Basic knowledge concerning the extent and the kinetics of reconstruction, as well as the conditions required to induce reconstruction, were sought. The final

goal of this work was to obtain information regarding the driving force for and limitations in surface reconstruction, and possibly shed some light on the mechanism of surface-migration of SAP chains in this system.

Properties of Polystyrene

The main advantage in using polystyrene in these experiments is that it is easily prepared by anionic techniques with (almost) complete control over the molecular weight and molecular weight distribution. Typically target molecular weights are obtained with polydispersity indices of less than ~1.05. Anionically polymerized polystyrene is atactic, with a Tg ~100 °C (depending on molecular weight[64]). These polymers can be end-functionalized relatively easily by reacting the polystyryllithium species with an ethylene oxide-type moiety. Attempted reactions of polystyryllithium with halogen-containing reagents have been less successful, resulting in a fair amount of oxidatively coupled polymer. Polystyrene is soluble in a range of solvents which is only somewhat advantageous because it means that films of this material have low solvent resistance. Polystyrene has the distinct disadvantage of having poor mechanical properties as well as being susceptible to both thermal and photo-induced oxidation.[65] For these reasons, the polystyrene samples used in these experiments were supported on glass (free standing films were too brittle) and stored in the dark under an inert atmosphere. The critical surface tension of polystyrene (γ_{crit}) is 33 dyn/cm,[66] the solubility (δ) parameter is 17.6 $[(J/cm^3)^{1/2}]$[67] and the density of amorphous polymer is ~1.05 g/cm^3.[68] The (self-) diffusion constant measured for radioactive-labelled 80 K polystyrene in matrices of higher molecular weight (186 K,

410 K or 1060 K) was determined to be 1.6 ±0.5 * 10^{-10} cm^2/sec at 237 °C with no dependence on matrix molecular weight observed.[69] Experiments attempting to measure the diffusion rate of 100 K polystyrene at 150 °C indicated such slow diffusion that no significant diffusion occurred over weeks.[70] The critical entanglement weight (M_e) of polystyrene is around 30 K.[69,71] Below this molecular weight entanglements are not expected to retard diffusion processes extensively.[69]

Perfluoroalkyl Groups

The incompatibility of the perfluoroalkyl groups[56] with the polystyrene matrix is an essential feature which facilitates surface reconstruction in these experiments. In general, fluorinated species tend to be oleophobic and the discrepancy between the solubility parameters of polystyrene and poly(tetrafluoroethylene) (teflon) (δ = 12.7 [$(J/cm^3)^{1/2}$])[67] reflects this. Polymer blends of polymers comprised of highly incompatible monomers have large χN values at most compositions and will phase separate.[24,35,51] The morphology of the sample after phase separation will depend on bulk composition as well as chain architecture.[26,30] In general, interfacial tension will cause a reduction in surface area resulting in macroscopic segregation with the lower energy component at the air-polymer interface. The critical surface tension of teflon is 18 dyn/cm,[66] so it would be expected that the perfluoroalkyl groups would be favored over the polystyrene segments at the film surface in these experiments. Attachment of the perfluoroalkyl groups to the polystyrene segment will modify segregation to the surface, will prevent

phase separation (only phase segregation is possible) and will prevent complete diffusion out of the samples.[12,13,46]

Surface Analyses

The incompatibility between the perfluoroalkyl groups and polystyrene matrix of these samples, in combination with the very low surface tension of fluorinated species, gives rise to the expectation that the reconstructed polymer films will have fluorine concentrated in the outermost regions of the surface. In keeping with Theodorou's theoretical predictions,[63] a depletion layer is expected to lie immediately below the concentrated surface layer. Given the small size of the perfluoroalkyl groups (roughly 13 Å long and 5 - 6 Å across), the transition between the highly concentrated fluorinated surface layer and the depleted polystyrene layer is expected to occur at very shallow depths, less than 10 Å into the material. For this reason, surface analytical techniques which are particularly sensitive to this outer region were employed for analysis of these substrates. These techniques include variable angle X-ray photoelectron spectroscopy (XPS) which can probe the surface at depths up to 42 Å, and contact angle which samples only the outermost few angstroms of the material. Other surface analyses, such as that provided by attenuated total reflectance infrared spectroscopy (ATRIR), probe the substrate at depths on the order of microns which is not surface-selective enough for these experiments because it samples too much of the bulk material.

References

1. Cross, E.M.; McCarthy, T.J. *Macromolecules* **1990**, *23*, 3921.
2. Gagnon, D.R.; McCarthy, T.J. *J. Appl. Polym. Sci.* **1984**, *29*, 4335.
3. For a review, see Koberstein, J.T. In *Encyclopedia of Polymer Science and Engineering*, 2nd ed.; Mark, H.F.; Bikales, N.M.; Overberger, C.G.; Menges, G.; Kroschwitz, J.I., eds.; John Wiley and Sons: New York, 1989; Vol. 8, p. 237.
4. Theodorou, D.N. *Macromolecules* **1988**, *21*, 1391.
5. Theodorou, D.N. *Macromolecules* **1988**, *21*, 1411.
6. Hariharan, A.; Kumar, S.K.; Russell, T.P. *Macromolecules* **1990**, *23*, 3584.
7. Hariharan, A.; Kumar, S.K.; Russell, T.P. *Macromolecules* **1991**, *24*, 4909.
8. Broseta, D.: Fredrickson, G.H.; Helfand, E.; Leibler, L. *Macromolecules* **1990**, *23*, 132.
9. Kumar, S.K.; Vacatello, M.; Yoon, D.Y. *Macromolecules* **1990**, *23*, 2189.
10. Kumar, S.K.; Russell, T.P. *Macromolecules* **1991**, *24*, 3816.
11. Jarvis, N.L.; Fox, R.B.; Zisman, W.A. *Adv. Chem. Ser.* **1964**, *43*, 317.
12. Torstensson, M.; Ranby, B.; Hult, A. *Macromolecules* **1990**, *23*, 126.
13. Shull, K.R.; Kramer, E.J.; Bates, F.S.; Rosedale, J.H. *Macromolecules* **1991**, *24*, 1383.
14. Shull, K.R.; Winey, K.I.; Thomas, E.L.; Kramer, E.J. *Macromolecules* **1991**, *24*, 2748.
15. Gaines, G.L., Jr. *Macromolecules* **1979**, *12*, 1011.
16. Gaines, G.L., Jr.; Bender, G.W. *Macromolecules* **1972**, *5*, 82.
17. Green, P.F.; Christensen, T.M.; Russell, T.P. *Macromolecules* **1991**, *24*, 252.
18. Schmitt, R.L.; Gardella, J.A., Jr.; Magill, J.H.; Salvati, L., Jr.; Chin, R.L. *Macromolecules* **1985**, *18*, 2675.

19. Shull, K.R.; Kramer, E.J.; Hadziioanou, G.; Tang, W. *Macromolecules* **1990**, *23*, 4780.

20. Green, P.F.; Russell, T.P. *Macromolecules* **1991**, *24*, 2931.

21. LeGrand, D.G.; Gaines, G.L., Jr. *Polym. Prepr. (Am. Chem. Soc., Div Polym. Chem.)* **1970**, *11*, 442.

22. Thomas, H.R.; O'Malley, J.J. *Macromolecules* **1979**, *12*, 323.

23. Clark, D.T.; Peeling, J.; O'Malley, J.M. *J. Polym. Sci., Polym. Chem.* **1976**, *14*, 543.

24. Green, P.F.; Christensen, T.M.; Russell, T.P.; Jérôme, R. *Macromolecules* **1989**, *22*, 2189.

25. O'Malley, J.J.; Thomas, H.R.; Lee, G.M. *Macromolecules* **1979**, *12*, 996.

26. Schmitt, R.L.; Gardella, J.A., Jr.; Salvati, L., Jr. *Macromolecules* **1986**, *19*, 648.

27. Schmidt, J.J.; Gardella, J.A., Jr.; Salvati, L., Jr. *Macromolecules* **1989**, *22*, 4489.

28. Anastasiadis, S.H.; Gancarz, I.; Koberstein, J.T. *Macromolecules* **1988**, *21*, 2980.

29. Creton, C.; Kramer, E.J.; Hadziioannou, G. *Macromolecules* **1991**, *24*, 1846.

30. Thomas, H.R.; O'Malley, J. M. *Macromolecules* **1981**, *14*, 1316.

31. Clark, M.B., Jr.; Burkhardt, C.A.; Gardella, J.A., Jr. *Macromolecules* **1989**, *22*, 4495.

32. Clark, M.B., Jr.; Burkhardt, C.A.; Gardella, J.A., Jr. *Macromolecules* **1991**, *24*, 799.

33. Sauer, B.B.; Dee, G.T. *Macromolecules* **1991**, *24*, 2124.

34. Rosen, M.J. *Surfactants and Interfacial Phenomena*, John Wiley & Sons, NY, 1978, Ch. 2.

35. Bates, F.S. *Science* **1991**, *251*, 898.

36. Andrade, J.D.; Gregonis, D.E; Smith, L.M. In *Surface and Interfacial Aspects of Biomedical Polymers*; Andrade, J.D. ed. Plenum: New York, 1986, Vol. 1, Ch. 2.

37. Andrade, J.D. *Surf. Interf. Anal.* **1986**, *8*, 253.

38. Andrade, J.D. *Polymer Surface Dynamics*; New York, Plenum: 1988.

39. Yasuda, H.; Sharma, A.K.; Yasuda, T. *J. Polym. Sci., Polym. Phys. Ed.* **1981**, *19*, 1285.

40. Swalen, J.D.; Allara, D.L.; Andrade, J.D.; Chandross, E.A.; Garoff, S.; Israelachvili, J.; McCarthy, T.J.; Murray, R.; Pease, R.F.; Rabolt, J.F.; Wynne, K.J.; Yu, H. *Langmuir* **1987**, *3*, 932.

41. Ruckenstein, E.; Gourisankar, S.V. *J. Coll. and Interf. Sci.* **1985**, *107*, 488.

42. Ruckenstein, E.; Gourisankar, S.V. *J. Coll. and Interf. Sci.* **1986**, *109*, 557.

43. Pennings, J.F.M.; Bosman, B. *Coll. and Polym. Sci.* **1979**, *257*, 720.

44. Pennings, J.F.M. *Coll. and Polym. Sci.* **1978**, *256*, 78.

45. Schonhorn, H. *Macromolecules* **1968**, *1*, 145.

46. Azrak, R.G. *J. Coll. and Interf. Sci.* **1974**, *47*, 779.

47. Reardon, J.P.; Zisman, W.A. *Macromolecules* **1974**, *7*, 920.

48. Scholtens, B.J.R.; Bijsterbosch, B.H. *J. Coll. and Interf. Sci.* **1980**, *77*, 162.

49. Matsunaga, T. Tamai, Y. *J. Appl. Polym. Sci.* **1978**, *22*, 3525.

50. Scheutjens, J.M.H.M.; Fleer, G.J. *J. Phys. Chem.* **1979**, *83*, 1619; *J. Phys. Chem.* **1980**, *84*, 178; *Macromolecules* **1985**, *18*, 1882.

51. Fredrickson, G.H. *Macromolecules* **1987**, *20*, 2535.

52. LeGrand D.G.; Gaines, G.L. *J. Coll. and Interf.* **1969**, *31*, 162.

53. Rastogi A.K.; St. Pierre L.E. *J. Coll. and Interf. Sci.* **1969**, *31*, 169.

54. Noolandi, J.; Hong, K.M. *Macromolecules* **1982**, *15*, 482.

55. Russell, T.P.; Anastasiadis, S.H.; Menelle, A.; Felcher, G.P.; Satija, S.K. *Macromolecules* **1991**, *24*, 1575.

56. Foster, K.L.; Wool, R.P. *Macromolecules* **1991**, *24*, 1397.

57. Gaines, G.L. *Langmuir* **1991**, *7*, 3054.

58. Rabolt, J.F.; Russell, T.P.; Twieg, R.J. *Macromolecules* **1984**, *17*, 2786.

59. Phillips, R.W.; Dettre, R.H. *J. Coll. and Interf. Sci.* **1976**, *56*, 251.

60. Höpken, J.; Möller, M. *Macromolecules* **1992**, *25*, 1461.

61. Yoon, S.C.; Ratner, B.D. *Macromolecules* **1986**, *19*, 1068.

62. Theodorou, D.N. *Macromolecules* **1988**, *21*, 1400.

63. Theodorou, D.N. *Macromolecules* **1988**, *21*, 1422.

64. Fox, T.G., Jr. Fory, P.J. *J. Appl. Phys.* **1950**, *21*, 581.

65. Fox, R.B.; Price, T.R.; Cain, D.S. *Adv. Chem. Ser.* **1968**, *87*, 72. Grassie, N.; Weir, N.A. *J. Appl. Polm. Sci.* **1965**, *9*, 975, 999.

66. Zisman, W.A. *Adv. Chem. Ser.* **1964**, *43*, 1.

67. Billmeyer, F.W. *Textbook of Polymer Science*, 3rd ed. Wiley Interscience, New York, 1984, p. 153.

68. Brandup, J.; Immergut, E.H. eds. *Polymer Handbook*, 2nd ed. Wiley Interscience, New York, 1975, p. V-59.

69. Bueche, F. *J. Chem. Phys.* **1968**, *48*, 1410.

70. Bueche, F.; Cashin, W.M.; Debye, P. *J. Chem. Phys.* **1952**, *20*, 1956.

71. Aklonis, J.J.; MacKnight, W.J. *Introduction to Polymer Viscoelasticity*, 2nd ed. Wiley Interscience, New York, 1983, p. 41.

CHAPTER V

EXPERIMENTAL

Materials

Benzene (Aldrich) was distilled from calcium hydride.

Cyclohexane (Aldrich) was distilled from calcium hydride.

Dichloromethane (Fisher) was distilled from calcium hydride.

3,4-Dihydro-2*H*-pyran (Aldrich) was stirred over CaO for several hours and then decanted and fractionally distilled from phosphorous pentoxide.

Ethylene oxide (Kodak) was purified by freeze-pump-thaw cycles and trap-to-trap distillation from calcium hydride.

Glycidol (Aldrich) was stirred over CaO for several hours and then decanted and distilled (70 °C, 18 mm).

Hexadecane (Aldrich) was distilled from calcium hydride (125 °C, 2-4 mm).

Pyridine (Aldrich) was distilled from calcium hydride.

Styrene (Aldrich) was distilled from calcium hydride (50 °C, 20 mm) and subsequently refrigerated in darkness. Immediately prior to use, 15-20 mL styrene was stirred over dibutylmagnesium until yellow and then degassed with three freeze-pump-thaw cycles and distilled (trap-to-trap).

Tetrahydrofuran (Aldrich) was distilled from sodium benzophenone dianion.

Toluene (Aldrich) was distilled from calcium hydride.

Water (house distilled) was redistilled using a Gilmont still.

sec-Butyllithium (1.3M in cyclohexane), nonadecafluorodecanoic acid, phosphorous pentachloride, and *p*-toluenesulfonic acid monohydrate were obtained from Aldrich and used as received. Hexadecafluorosebacic acid was obtained from PCR and used as received. Tech. grade methanol used for precipitating polymers was not purified.

Materials Handling

All solvents and distilled reagents were either used immediately or stored under nitrogen for short periods of time in Schlenk flasks. All transfers of reagents and solvents were done by cannula or syringe.

Reaction Methods

All distillations and reactions were performed under nitrogen. All polymerizations were carried out in 250 or 500 mL round-bottom flasks equipped with a Schlenk arm (with a teflon stopcock and a 14/20 female ground-glass joint) and another (male or female) ground-glass joint (size 24/40) to facilitate access for cleaning flask. Polymerization reactions were stirred with glass-covered stirbars, and all other reaction solutions were stirred with teflon-covered stirbars.

Polymers

All of the polymers prepared in this work were based on polystyrene. The matrix polymer (MP) used was polystyrene with Mn = 10 K. The surface-active polymers (SAPs) prepared were polystyrenes selectively-functionalized with perfluoroalkyl groups. These polymers were prepared with specific chain architectures: the first with a monofunctional endgroup, another with two fluorinated endgroups and the third middle-functionalized. The three SAPs have been termed SAP:E-1, SAP:E-2 and SAP:M-1, respectively. The SAP:E-1 polymers were prepared with Mn = 1, 5, 10, 40 and 100 K, and the SAP:E-2 and SAP:M-1 polymers with Mn = 10 K.

Polymer Mixtures and Solutions

Film samples were prepared at several concentrations, each determined by the mmol SAP (of given molecular weight and structure) in 10 K MP (plain polystyrene). All samples were based on a 200 mg "mixed

polymer" sample size. The 200 mg sample was treated as a volumetric flask; X mmol SAP were put into a 25 mL round-bottom flask and [200 mg - X mmol(SAP mw)] of matrix polymer were added. Powders of SAP and MP were weighed in air, and then each flask was capped with a septum and purged for 15 min with N_2. Toluene (1 mL purified as described above) was added to each flask; the concentration of all polymer solutions prepared was 200 mg mixed polymer per 1 mL toluene.

Samples containing different molecular weight SAPs of the same structure can be related by mmol polymer or mmol surface active group (SAG) per 200 mg, and by percent SAP chains per sample, using the relationship:

$$\% \text{ chains} = \text{mmol SAP}/(\text{mmol SAP} + \text{mmol MP}). \qquad (5.1)$$

In the case of samples that contain SAPs with more than one surface-active group, the percent chains and mmol SAG relationships still hold. Most often the blended film samples will be referred to by the molecular weight and structure of the SAP they contain.

Sample Preparation

Polystyrene and blended films were supported on glass slides (1 cm x 2 cm size) cut from microscope slides. These glass slides were cleaned by immersion in a 10% aqueous NaOH solution for 1 h, followed by several rinses with distilled water and a final rinse with acetone. The slides were dried for 3 - 4 h in the glassware oven and used immediately afterwards.

Film samples were prepared in a N_2 atmosphere using a Headway Research Spin Coater enclosed in a sealed glove bag. A pipette was used to make three one-droplet additions of polymer solution to a glass slide supported on the spin-coater. After each addition the slide was spun at 500 rpm for five seconds (not timed) for the purpose of laying a thin coat of polymer that would adhere to the slide. After the initial layer was coated, the slide was transferred aside and several more drops of polymer solution were added until the sample had rounded edges (bulged). Care was taken not to cause the solution to overflow the substrate. The films sat in the inert environment for at least 1 h before transfer to the oven.

Heat Treatment of Samples

The blended film samples were subjected to various heat treatments to observe the effect of temperature on surface reconstruction and to ascertain the optimum conditions (for time as well as temperature) for maximizing surface reconstruction while keeping surface oxidation to a minimum. Complete kinetics and temperature variation data were obtained for 1, 10 and 100 K SAP:E-1 film samples and some time and temperature variation data were obtained for the 5 K samples. For experiments designed to explore annealing conditions usually two samples were studied, one at low concentration (10% SAP chains) and the other at maximum concentration (100% SAP chains, or 71% in the 1 K case). Occasionally an intermediate concentration was used, as well. Under the optimum heating conditions for each molecular weight, an isotherm was constructed for each SAP sample series to show changing F/C with concentration.

All film samples were heated under reduced pressure (0.05 mm) in a vacuum oven equilibrated at a specified temperature for different lengths of time or held at room temperature under vacuum. The highest temperatures tested were 180 °C and 150 °C, and the longest times were 192 h and two weeks. All XPS and contact angle data has been tabulated and are included in Appendix B. 1, 5 and 10 K samples were annealed at 180 °C for 24 h (7:76-78)[1] and at 150 °C for 24 h (6:64-70) and 72 h (7:66-70, 71-74). The XPS and contact angle data for these annealing experiments are in Tables 25, 26, 34, 36, 40 and 41.

The lowest molecular weight SAP samples studied contained 1 K SAP:E-1 polymers. Concentrations for these samples ranged from 10% (0.002 mmol) to 71% SAP (0.04 mmol). No higher concentrations were studied because above 0.04 mmol the bulk F/C ratio begins to shoot up towards 2 (the sample looks too much like just the endgroup). The 1 K samples were annealed at 110 °C for 24 h (7:17-20, 85-90; 8:121-131), 48 h (7:57-65, 143-149), 72 h (8:19-29, 30-36, 48-58, 71-80), 96 h (9:116; 10:16) and 120 h (10:17) to observe the length of heating time required for maximum surface reconstruction. XPS and contact angle data for these experiments are in Tables 27 and 28. The 1 K samples also were heated at 60 °C for 72 h (8:48-58, 71-80) to see if any reconstruction occurred below Tg of the film samples. XPS and contact angle data for these experiments are in Tables 31 and 32. An isotherm was constructed from data taken from several 1 K samples (of several concentrations) annealed at 110 °C for 72 h (135-150; 9:5-17, 28-35). XPS and contact angle data for these samples are in Tables 29 and 30. In an effort to shed light on variations in fluorine concentration with distance from the surface of a

71% 1 K SAP chain sample (heated at 110 °C for 72 h), XPS data was acquired at several angles to provide a depth profile (9:14-17, 69-79). These data are in Table 33. XPS data for the backside and glass surface from some 1 K samples (heated at 110 °C for 72 h) are in Table 34 (9:107, 118-122; 10:27-33).

The 10 K SAP samples were studied more extensively than the other molecular weights (because there are three SAP polymer architectures for this molecular weight). SAP:E-1 samples were held at room temperature for 72 h (6:38-50; 7:30-33) to study the effects of not supplying heat for reconstruction, and these data are in Tables 40 and 41. SAP:E-1 samples were heated at 110 °C for 24 h (7:17-20, 85-90; 9:49-57), 48 h (7:34-37, 57-65, 143-150; 9:57-68), 72 h (6:36, 38-42, 43, 80-85, 92-96; 7:12-17; 8:19-29), 96 h (9:116; 10:12-13), 120 h (9:117; 10:18, 33-34), 144 h (10:19, 25), 168 h (10:20, 25-26), 192 h (10:20), and two weeks (7:78-84) to determine optimum heating times for this temperature. XPS and contact angle data for these experiments are in Tables 42 and 43. An attempt was made to hydrolyze the fluorinated ester groups on the surface of 100% 10 K SAP:E-1 films (9:79-80, 84). XPS and contact angle data for the original and reacted surfaces are in Tables 21 and 22. XPS data for the backside of some of the 10 K SAP:E-1 samples are in Table 46 (9:107, 118-122, 143-151). Isotherm data were taken for all of the 10 K SAP samples heated at 110 °C for 72 h. The data for the SAP:E-1 samples (7:143-150; 9:35-49) are in Tables 44 and 45, data for SAP:E-2 (11:73-86, 87-98, 109-118) are in Tables 53 and 54 and data for SAP:M-1 (11:99-108, 119-127) are in Tables 55 and 56.

The highest molecular weight polymer studied in these experiments was 100 K SAP:E-1. The 100 K samples were annealed at 24 h (9:17-24), 48 h (7:143-149), 72 h (9:85-96; 10:9-10), 96 h (10:11-12), 120 h (10:21, 33-34, 102, 124), 144 h (10:22), 168 h (10:23-24) and 192 h (10:23-24) to determine the length of heating time required for maximum surface reconstruction. XPS and contact angle data for these experiments are in Tables 49 and 50. Isotherm (XPS and contact angle) data taken for 40 K (10:101-112, 123-132) and 100 K (10:35-45, 71-84) SAP:E-1 samples heated at 110 °C for 120 h, are in Tables 47 and 48 and 49 and 50. Film samples containing 5 K SAP:E-1 polymers were annealed at 110 °C for 24 h (7:17-20, 85-90), 48 h (7:57-65), 72 h (7:12-17; 8:19-29, 30-36), 96 h (10:12-13), 120 h (10:12-15) and144 h (10:16). XPS and contact angle data for these samples are in Tables 36 and 37. An isotherm was constructed from data taken from 5 K samples heated at 110 °C for 72 h (9:108-116, 137-142). These data are in Tables 38 and 39. Table 57 provides F/C plateau and maximum surface excess data for comparisons among SAPs of each molecular weight and structure.

Methods of Analysis

Molecular weights and polydispersities of polymers were determined by gel permeation chromatography (GPC) using a system equipped with Polymer Laboratories PL gel columns (10^4, 10^3, 10^2 Å), a Rainin Rabbit solvent pump with THF as the mobile phase, and an IBM LC9563 Variable UV detector interfaced with an IBM 386 computer. Molecular weight data reported are relative to calibration with polystyrene. Proton nuclear magnetic resonance (^{1}H NMR) spectra of deuteriochloroform solutions

were recorded on a Bruker NR/80AF spectrometer. Transmission infrared spectra were obtained using an IBM 44 FTIR spectrometer equipped with a MCT detector. Thin layer chromatography data was obtained using mylar-backed silica gel TLC plates purchased from Kodak and Whatman glass-backed silica gel TLC plates purchased from Fisher. In all cases, the plates (250 μm thick silica gel with 60 Å pore size) were heated (~200 °C) in the glassware oven for several days prior to use, and toluene (purified as described above) was the eluent. Differential Scanning Calorimetry (DSC) data were obtained using a Perkin Elmer DSC7 calibrated with an indium standard. Thermal Gravimetric Analyses (TGA) were made using a General V4.1C DuPont 2000. X-ray photoelectron spectra (XPS) were recorded using a Perkin Elmer-Physical Electronics 5100 spectrometer with Mg K_α excitation (400 W). Spectra typically were recorded at two takeoff angles, 15° and 75°, from the plane of the sample surface. Contact angle measurements were made with a Ramé-Hart telescopic goniometer using a Gilmont syringe with a 24-gauge flat-tipped needle. Water and hexadecane purified as described above were used as the probe fluids. Dynamic advancing and receding angles were measured while adding or withdrawing probe fluid to or from the drop. The values reported are averages of five measurements made at random points on the surface. Separate substrates were prepared for XPS and contact angle analyses.

Synthesis of Polystyrene and SAP:E-1 Polymers

Synthesis of polystyrene and alcohol-terminated polystyrene have been reported in the literature, but for the sake of completeness, they have been included here, as well. The SAP:E-1 polymers were prepared by

esterifying the alcohol terminus of PS-OH. This reaction is shown in Scheme 5.1.

Polystyrene (PS-H). (6:31, 72-73, 97, 106; 7:38, 49, 51, 74-75, 117-119, 120-123; 8:65, 83: 9:25, 73)

Actual quantities of *sec*-butyllithium and styrene used in this procedure depended on molecular weight and amount of polymer desired. *sec*-Butyllithium was introduced via syringe to a flask containing 45-50 mL freshly distilled cyclohexane. After this solution stirred for approximately 5 min, styrene was added via syringe and an orange color developed within 30-60 s. Polymerizations generally were stirred overnight (for convenience) and worked up the following morning by adding a few mL methanol (degassed by either three freeze-pump-thaw cycles or 20 min of

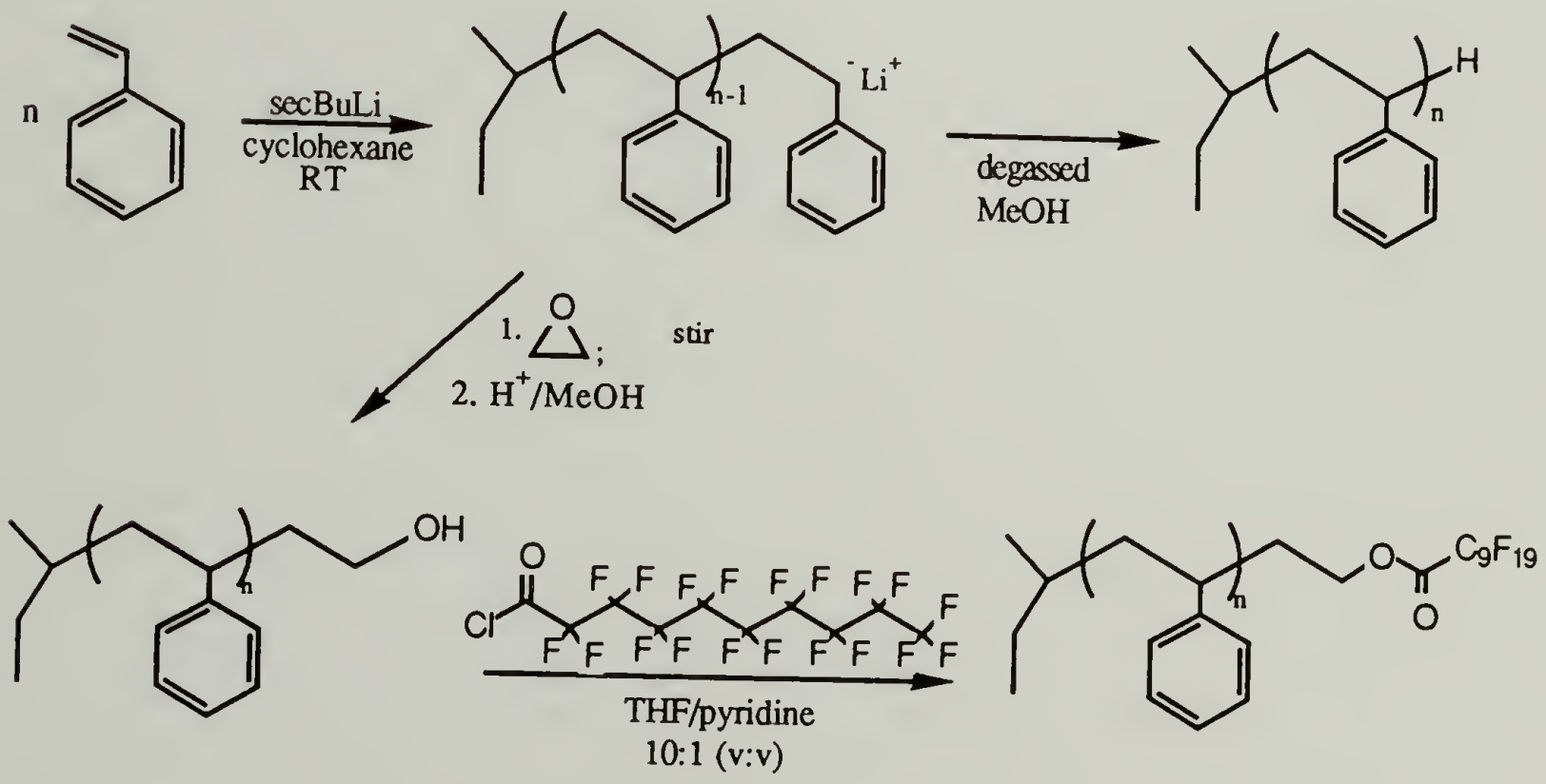

Scheme 5.1. Preparation of SAP:E-1 Polymers

sparging with N_2) to convert polystyryllithium (PSLi) to PS-H. A portion of the cyclohexane was pulled off (and trapped for recycling) to reduce the volume of solvent and facilitate precipitation of the polymer in methanol. After precipitation, the polymer was filtered and dried at reduced pressure (opaque container, room temperature, 0.05 mm, 24 h) and stored under nitrogen (opaque container).

2-(Polystyryl)ethanol (PS-OH). (6:16-18, 31, 62-63, 73, 98, 106; 7:5-8, 39-40, 127-130, 136-138; 8:84-86; 11:60)

In the same fashion as described above, PSLi was prepared in cyclohexane and allowed to stir overnight. A tube of freshly degassed (and still frozen) ethylene oxide was attached to the polymerization flask via cannula. The ethylene oxide was allowed to warm up and volatilize into the polymerization flask to react with the PSLi and discharge the orange color. After complete disappearance of color, the ethylene oxide tube was removed and the solution was stirred for ~8 h to insure completion of the endcapping reaction. Slightly acidic methanol (3 drops HCl in 3 mL methanol) was added to the reaction solution to protonate the alkoxide species. A portion of the cyclohexane was pulled off (and trapped for recycling) to reduce the volume of solvent and facilitate precipitation of the polymer in methanol. After precipitation, the polymer was filtered, dried at reduced pressure (opaque container, room temperature, 0.05 mm, 24 h) and stored under nitrogen (opaque container).

Perfluorodecanoyl Chloride.[4] (6:18-21, 78-79; 7:21-22, 124-125; 11:61) Nonadecafluorodecanoic acid (~10 g) and a 3 x molar excess of phosphorous pentachloride (~15 g) were introduced into a 250 mL round-bottom flask equipped with a condenser (with a teflon sleeve in the ground-glass joint connection instead of grease). Benzene (75 mL) was introduced via cannula with the flask cooling in an ice bath. After complete addition of the solvent, the ice bath was removed and the mixture stirred for 1 h at room temperature. The reaction mixture was heated slowly to a mild reflux which was maintained overnight. After ~14 h of reaction, the solution was allowed to cool slowly to room temperature and then cooled with an ice bath. The top (yellow) phase of the mixture was removed by cannula leaving white/clear crystals behind. Fresh benzene was added to the pot and the contents of the flask were warmed and transferred to a fresh, N_2-purged flask. The flask was cooled with ice to crystallize the acid chloride out and the benzene was removed. The acid chloride was recrystallized 3 - 4 times for purification (mp = 28 °C) and stored in the refrigerator.

2-(Polystyryl)ethyl-1-perfluorodecanoate (SAP:E-1). (6:22-23, 63, 76-77, 99-101, 112-113; 7:8-11, 28, 29, 41-42, 140-142; 8:36) Alcohol-terminated polystyrene and a 2 x molar excess of perfluoro-decanoyl chloride were introduced to a round-bottom flask which was then carefully purged with N_2. THF (30 - 40 mL) was added, followed by 2 - 3 mL pyridine, and the (slightly yellow) solution was stirred overnight. The endcapped polymer was precipitated in methanol and then redissolved in THF several times to insure removal of any methyl ester (that may have formed upon reaction with MeOH). After 3 - 4 washings/precipitations,

the polymer was filtered and dried at reduced pressure (opaque container, room temperature, 0.05 mm, 24 h) and stored under nitrogen (opaque container). GPC, TLC, DSC and elemental analysis data for the polymers prepared in this section are summarized in Tables 19 and 20, which appear in Chapter 6.

Attempted Hydrolysis. (9:79-80, 84) An attempt was made to hydrolyze the fluorinated esters on the surface of 100 % 10 k SAP:E-1 samples by immersing them in a slighly acidic methanol/water solution (25 mL HCl/15 mL MeOH/10 mL H_2O) at 35 °C for 3 h. After this time, the solution was removed and the films were carefully rinsed with water (2 x 20 mL), methanol (2 x 20 mL) and hexane (1 x 20 mL) and then dried (room temperature, 0.05 mm, 24 h). XPS and contact angle data for the original and the reacted surfaces are in Tables 21 and 22, included in Chapter 6.

Removal of Film Samples from Glass. (9:107, 118-122, 143-151; 10:27-33) Some of the SAP:E-1 samples were removed from the glass substrate by laying a piece of double-stick tape on the top and flipping the sample over so that it stuck to an XPS sample holder. The glass was pulled off with out touching the bottom surface of the film. XPS data for the backside of some of the 10 K SAP:E-1 samples as well as the (opposite) glass surface are in Table 46.

Synthesis of SAP:E-2 Polymers

The SAP:E-2 polymers were made by reacting polystyryllithium with epoxypropyltetrahydropyranyl ether and subsequent deprotection of the THP group. The idea for this endcapping reaction came from a paper in the literature describing an endcapping reaction for polyethylene oxide,[5] although no procedure was given for synthesis of the ether. These reactions are found in Scheme 5.2.

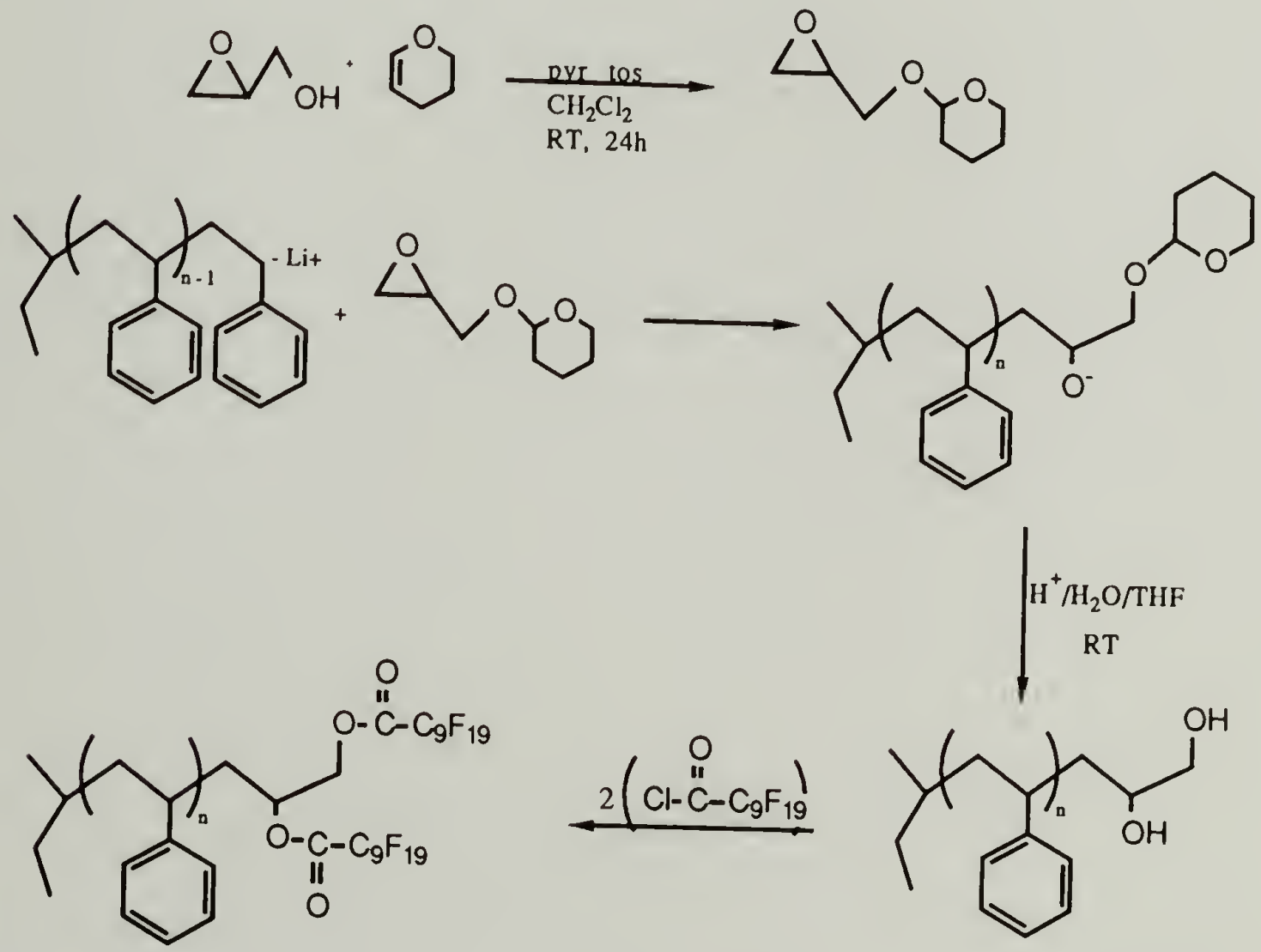

Scheme 5.2. Preparation of SAP:E-2 Polymers.

Pyridinium p-Toluenesulfonate (Pyr Tos).[6] (11:9, 19, 33) *p*-Toluenesulfonic acid monohydrate (5 g) was introduced to a round-bottom flask and pyridine (10 mL) was added. The resulting solution was stirred at room temperature for 30 min and the remaining pyridine was pulled off (and trapped). The grayish granules were recrystallized from acetone to produce large, reflective white crystals (mp = 121 °C).

Epoxypropyltetrahydropyranyl Ether. (11:19-20, 23-32, 33, 34, 35-36, 38-42) Glycidol (5.8 mL) and dihydropyran (12.0 mL) were introduced via syringe to a flask containing 20 mol % pyr tos in methylene chloride (50 mL). The solution was heated to 34 °C with a water bath for 24 h and then diluted with diethyl ether and washed with half saturated brine to remove the catalyst. After extraction, the solution was stirred over magnesium sulfate and decanted. Low boiling components were pulled off (and trapped) and the remaining liquid was distilled (118 °C, 10 - 12 mm). The ether was purified by trap-to-trap distillation from calcium hydride immediately prior to use.

3-(Polystyryl)propane-1,2-diol (PS-2(OH)). (11:45-59) In the same fashion as described above, PSLi was prepared in cyclohexane and allowed to stir overnight. A 2 x molar excess of epoxypropyltetra-hydropyranyl ether was introduced to the flask via syringe and the orange color disappeared. Most of the cyclohexane was pulled off (and trapped for recycling) and a degassed (with N_2), acidic solution of water, methanol and THF (1 mL HCl/ 5 mL H_2O/ 5 mL MeOH/ 50 mL THF) was added. This polymer/hydrolysis solution was stirred at 50 °C for 5 h to cleave the THP group. After hydrolysis, the polymer was precipitated in methanol

and redissolved in THF (3 - 4 washings) and then was finally filtered, dried at reduced pressure (opaque container, room temperature, 0.05 mm, 24 h) and stored under nitrogen (opaque container).

3-(Polystyryl)propyl-1,2-di(perfluorodecanoate) (SAP:E-2). (11:50-52) Esterification reaction conditions for SAP:E-2 polymers were identical to those described above for the monofunctional polymers except that twice as much acid chloride and pyridine were used in the SAP:E-2 case. GPC, TLC and elemental analysis data for the polymers prepared in this section are in Table 24 included in Chapter 6.

Synthesis of SAP:M-1 Polymers

The SAP:M-1 polymers were made by coupling two alcohol-terminated polystyrenes with perfluorosebacoyl chloride. This reaction is shown in Scheme 5.3.

Perfluorosebacoyl Chloride. (11:63-64, 67-69) Perfluorosebacic acid (2.6 g) and a 6 x molar excess of phosphorous pentachloride (6.4 g) were introduced into a 250 mL round-bottom flask equipped with a condenser (with a teflon sleeve in the ground-glass joint connection instead of grease). Benzene (40 mL) was introduced via cannula with the flask cooling in an ice bath. After complete addition of the solvent, the ice bath was removed and the mixture stirred for 1 h at room temperature. The reaction mixture was heated slowly to a mild reflux which was maintained overnight. After ~24 h of reaction, the solution was cooled and the solvent and $POCl_3$ were removed. The remaining liquid was distilled(34 °C,

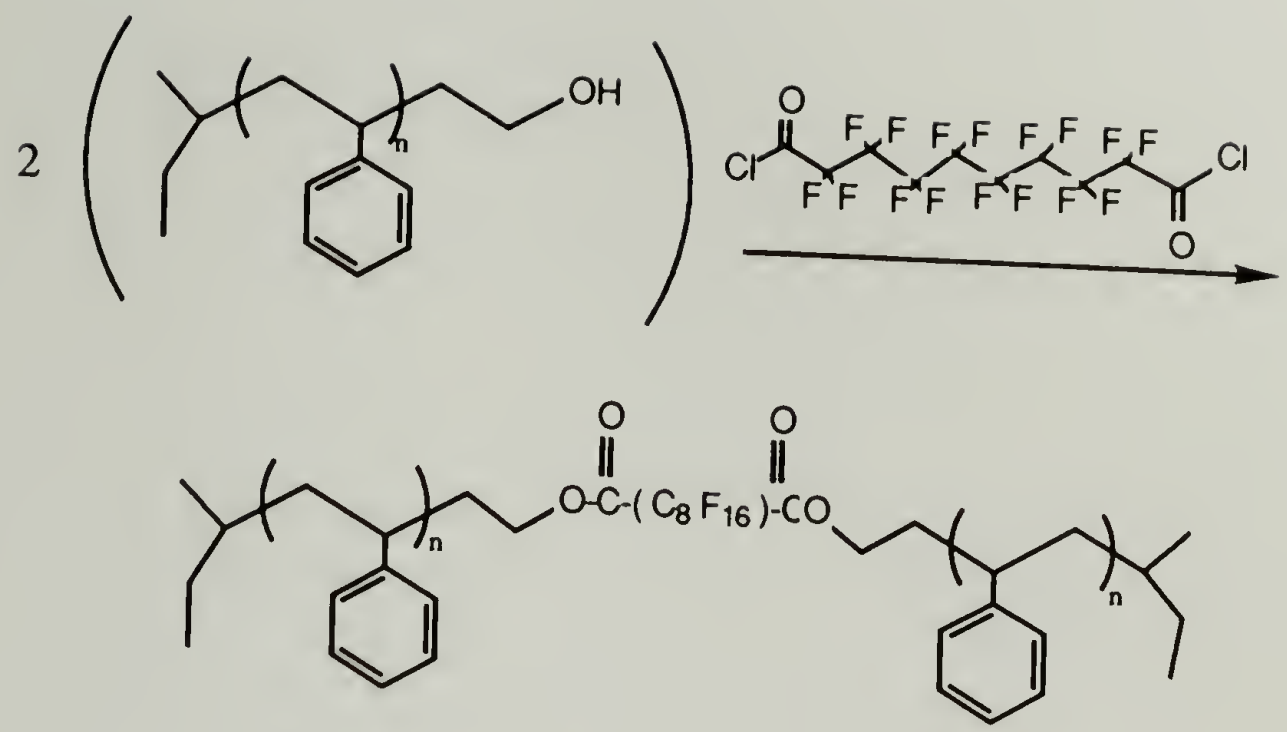

Scheme 5.3. Preparation of SAP:M-1 Polymers.

1 mm). Two immiscible liquids were isolated and infrared analysis indicated one to be the half-acid/half-acid chloride and the other the diacid chloride.

Perfluorosebacate-Coupled Polystyrene (SAP:M-1). (11:65-72, 130-131) Alcohol-terminated polystyrene (at half the desired molecular weight) was introduced to a round-bottom flask which was then carefully purged with N_2. THF (30 - 40 mL) was added, followed by 5 mL pyridine and slightly less than 0.5 molar equiv. of perfluorosebacoyl chloride. The (slightly yellow) reaction solution was stirred overnight. The endcapped polymer was precipitated in methanol and then redissolved/reprecipitated in THF/MeOH several times to insure removal of unreacted reagents and to fractionate the remaining uncoupled polymer out of the mixture. After 3 - 4 washings/precipitations, the polymer was filtered, dried at reduced

pressure (opaque container, room temperature, 0.05 mm, 24 h) and stored under nitrogen (opaque container). GPC, TLC and elemental analysis data for the polymers prepared in this section are in Table 23, included in Chapter 6.

References

1. The numbers in parentheses refer to notebook numbers and pages.
2. This procedure has been modified from Tim Bee's adaptation of the procedure described in Bonafini, J. Master of Science Thesis, Univ. of Mass., 1985, p. 81.
3. Yang, J.; Wegner, G. *Macromolecules* **1992,** *25*, 1791.
4. Miyashita, N.; Yoshikoshi, A.; Grieco, P.A. *J. Org. Chem* **1977**, *42*, 3772.

CHAPTER VI

RESULTS AND DISCUSSION

XPS and contact angle measurements were used to follow surface reconstruction in heat-treated film samples containing specific concentrations of surface-active polymer in a polystyrene (Mn = 10 K) matrix. The surface-active polymers (SAPs) were prepared with different molecular weights and with different chain architectures by selectively functionalizing polystyrene molecules with perfluoroalkyl groups. Several variables are possible for this system, but only a few were chosen for manipulation, namely, time and temperature of heating to allow reconstruction, molecular weight of SAP polystyrene "tails", concentration of SAPs in the film samples, size of the surface-active group, and chain architecture of the SAP. Experiments utilizing these variables were designed with the objective of elucidating how certain molecular and environmental parameters influence the rate and extent of surface reconstruction of films of this type.

The goal in heat-treating these samples was to maximize surface reconstruction while keeping surface oxidation to a minimum. Surface oxidation is particularly detrimental in that it changes the surface to something different than polystyrene and undermines comparisons drawn between samples. Preliminary experiments with elevated temperatures and long heating times resulted in an increase in the amount of oxygen detected on the surface by XPS. Samples that were not heated did not indicate

significant reconstruction. Samples heated at 110 °C exhibited significant fluorine surface-enrichment without extensive oxidation; hence most of the experiments were carried out at this temperature.

Film samples were prepared from toluene solutions of blends containing the desired amounts of SAP and matrix polymer (MP) and were supported on glass substrates cut to an appropriate size for XPS analyses. Below is a graphic depiction of a reconstructed film sample plus idealized models of the surface-active polymers prepared and used in these studies.

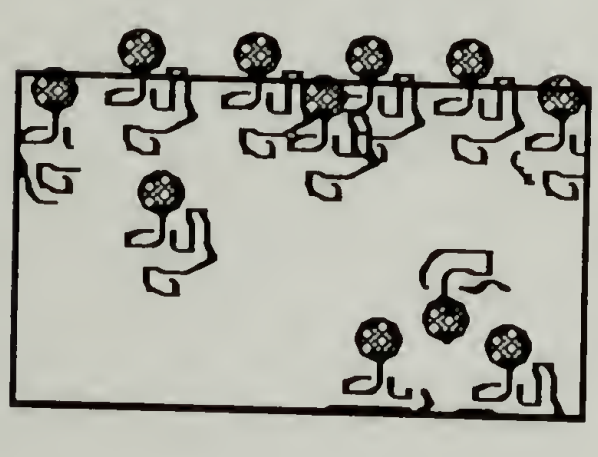

SAP:E-1

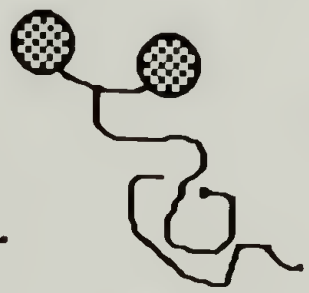

SAP:E-2

SAP:M-1

SAP:E-1 Polymers

In the first section of this work, 2-(polystyryl)ethyl-1-perfluorodecanoate (SAP:E-1) polymers (with Mn = 1, 5, 10, 40 and 100 K) were prepared by reacting alcohol-terminated polystyrene with perfluorodecanoyl chloride in THF with pyridine catalyst (eq. **1**).

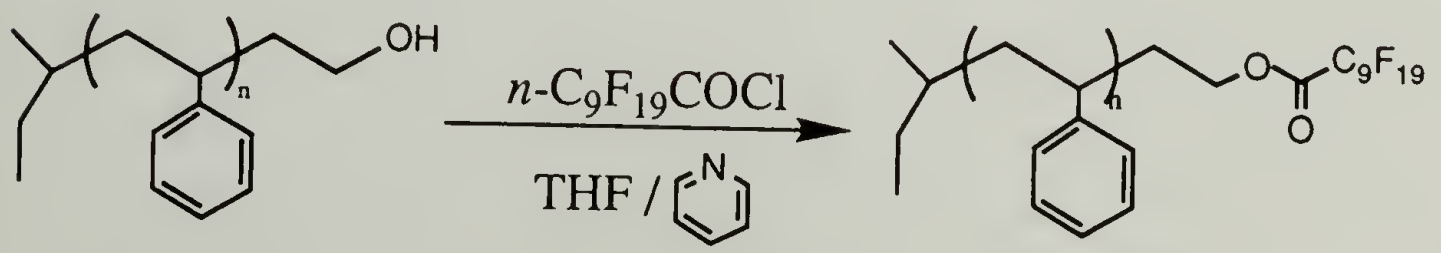

SAP:E-1 **(1)**

Characterization. The lowest molecular weight polymer (1 K) was used for spectroscopic characterization to prove the SAP:E-1 structure. The IR and NMR spectra for polystyrene (PS-H), alcohol-terminated polystyrene (PS-OH) and the SAP:E-1 polymer are shown in Figures 6.1 and 6.2. Comparison of the IR spectra for PS-H and PS-OH indicates for PS-OH, the presence of hydroxyl stretching (two peaks are observed, indicative of free hydroxyl (sharp, 3650 cm^{-1}) and H-bonded hydroxyl (broad, ~3500 cm^{-1})), an increased intensity (relative to PS-H) in the C-H methylene stretching at 2970 cm^{-1} and the presence of C-O stretching at 1050 cm^{-1}. The SAP:E-1 IR spectrum has no hydroxyl absorbance and new features include a large peak at 1787 cm^{-1} due to the carbonyl group on the fluorinated ester and very strong absorbances in the 1150-1350 cm^{-1} region, indicative of C-F stretching. The differences among the NMR spectra are fewer: the PS-OH spectrum differs from the PS-H in that it has a peak at 3.2 ppm (due to the CH_2-OH) which shifts downfield to 3.7 ppm upon conversion of the alcohol to the fluorinated ester. Representative GPC chromatograms for each molecular weight SAP:E-1 polymer as well as polystyrene (Mn = 10 K) are shown in Figure 6.3, and molecular weight, polydispersity, thin layer chromatography (TLC), and Tg data for these polymers are in Table 19.

A sketch of the TLC (silica/toluene) data for these polymers is shown in Figure 6.4. The data indicate that SAP:E-1 polymers with Mn = 1, 5 and 10 K elute slightly further than PS-H of corresponding molecular weight and that the two higher molecular weight polymers (Mn = 40 and 100 K) elute further than the smaller ones, in general. One explanation for the difference in R_f values based on molecular weight is size exclusion on

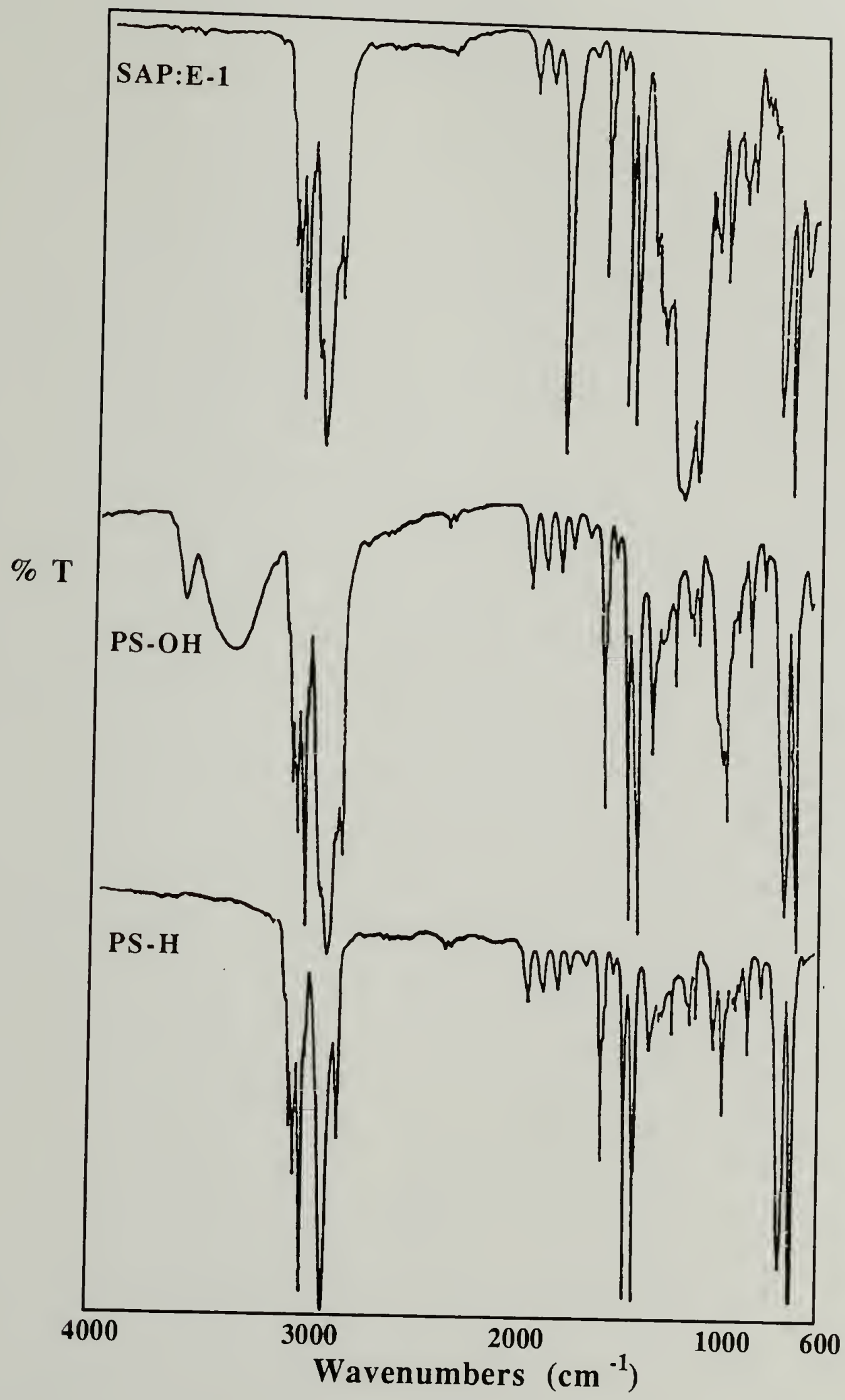

Figure 6.1. IR Spectra of Polystyrene, PS-OH and SAP:E-1.

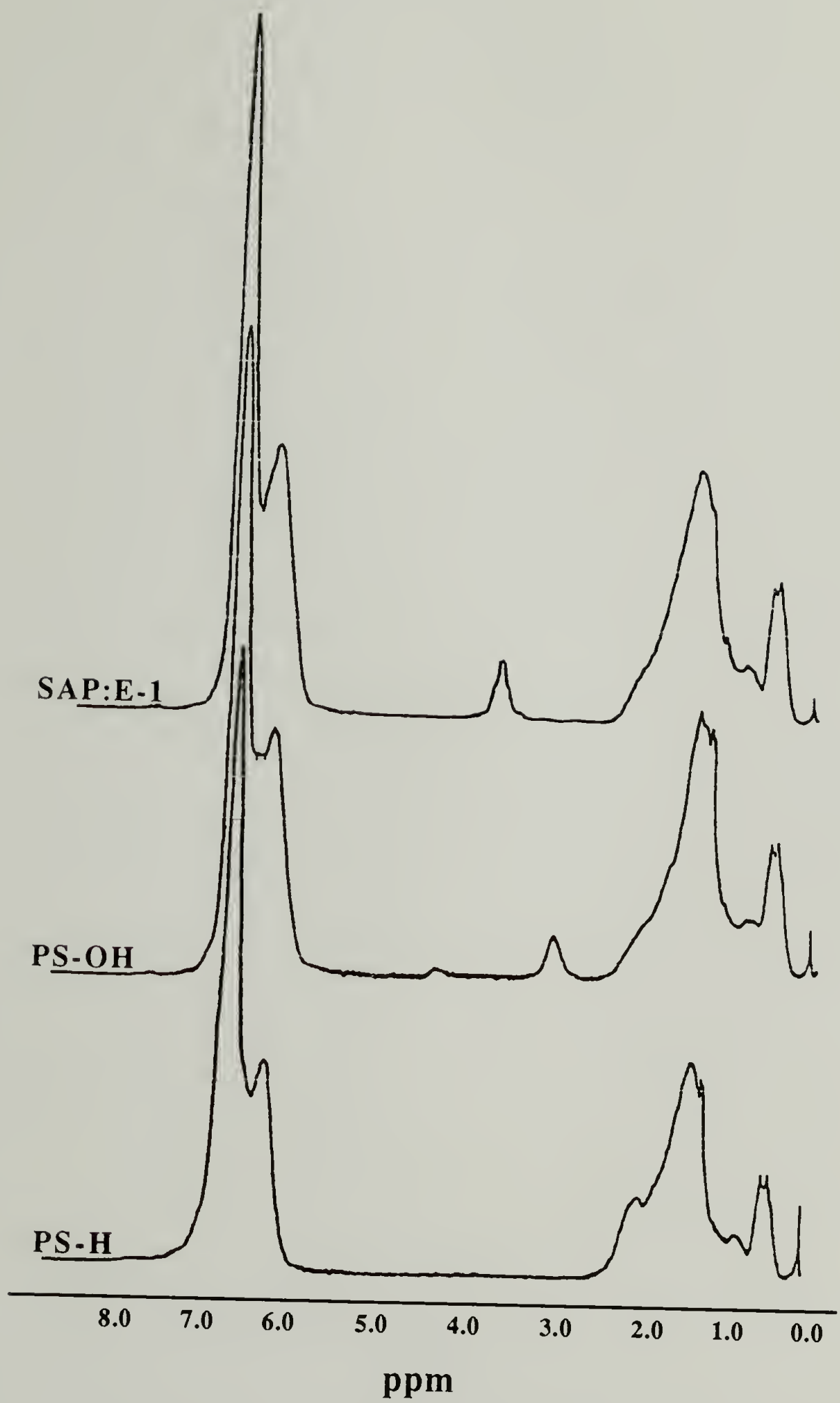

Figure 6.2. NMR Spectra of Polystyrene, PS-OH and SAP:E-1 Polymers (Mn = 1 K).

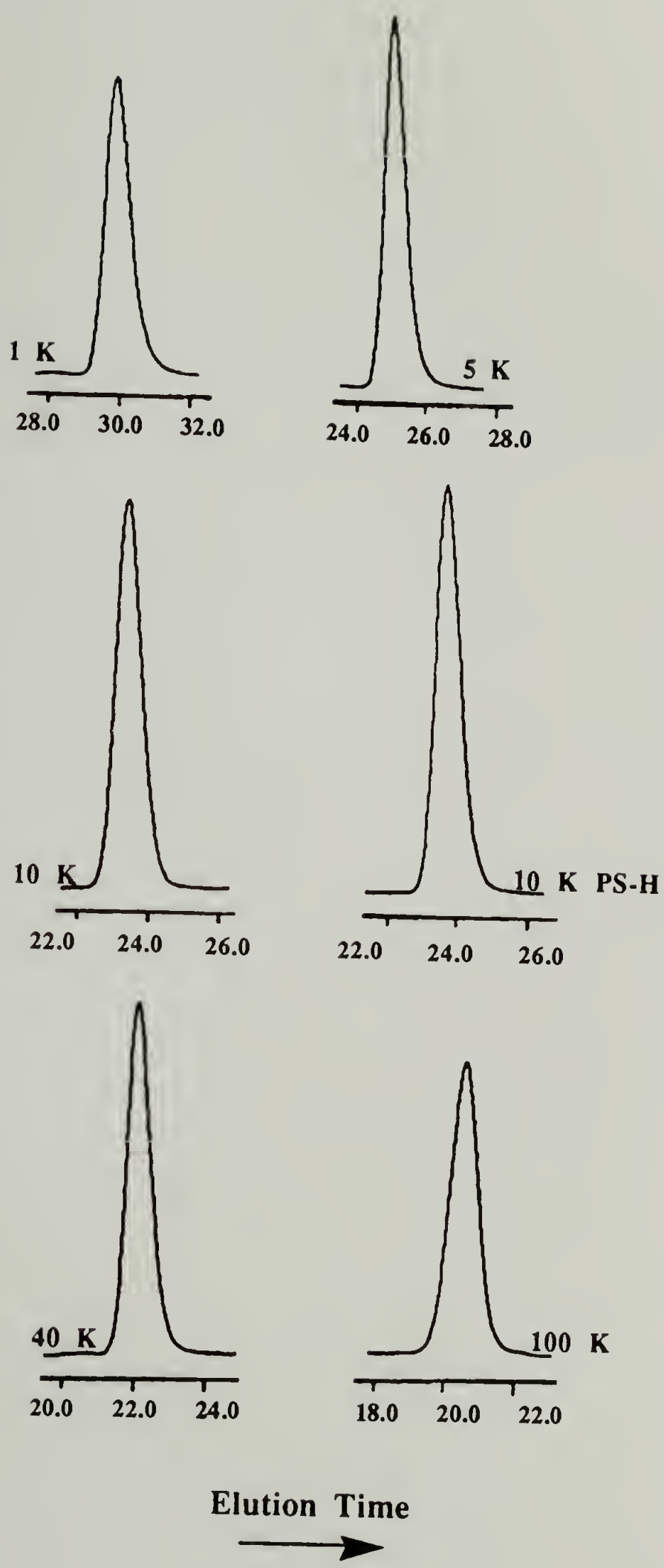

Figure 6.3. GPC Data for SAP:E-1 Polymers of Each Molecular Weight: Mn = 1 K, 5 K, 10 K (and 10 K Polystyrene), 40 K and 100 K.

Table 19. Molecular Weight (Mn), Polydispersity, Rf and Tg Values for SAP:E-1 Polymers.

Target molec. wt.	Polymer	Mn	PDI	Rf	Tg (°C)
.5 K	PS-H	750	1.065*	.70	42
(1 K)	PS-OH	790	1.063*	.06	
	PS-OF	1,363	1.044*	.75	14
5 K	PS-H	4,656	1.040	.90	86
	PS-OH	4,534	1.037	.20	56
	PS-OF	5,160	1.032	.95	72
10 K	PS-H	9,298	1.026	.96	94
	PS-OH	9,338	1.026	.30	
	PS-OF	10,054	1.026	1.0	100
40 K	PS-H	39,275	1.020	1.0	
	PS-OH	39,621	1.024	.52	
	PS-OF	40,281	1.020	1.0	
100 K	PS-H	104,938	1.039	1.0	105
	PS-OH	106,441	1.036	.67	
	PS-OF	108,757	1.041	1.0	107
annealed film sample (5K PSOF in 10K PS-H)					78
blend of powders (5K PSOF in 10K PS-H)					**1.** 13 **2.** 94

*out of gpc calibration range

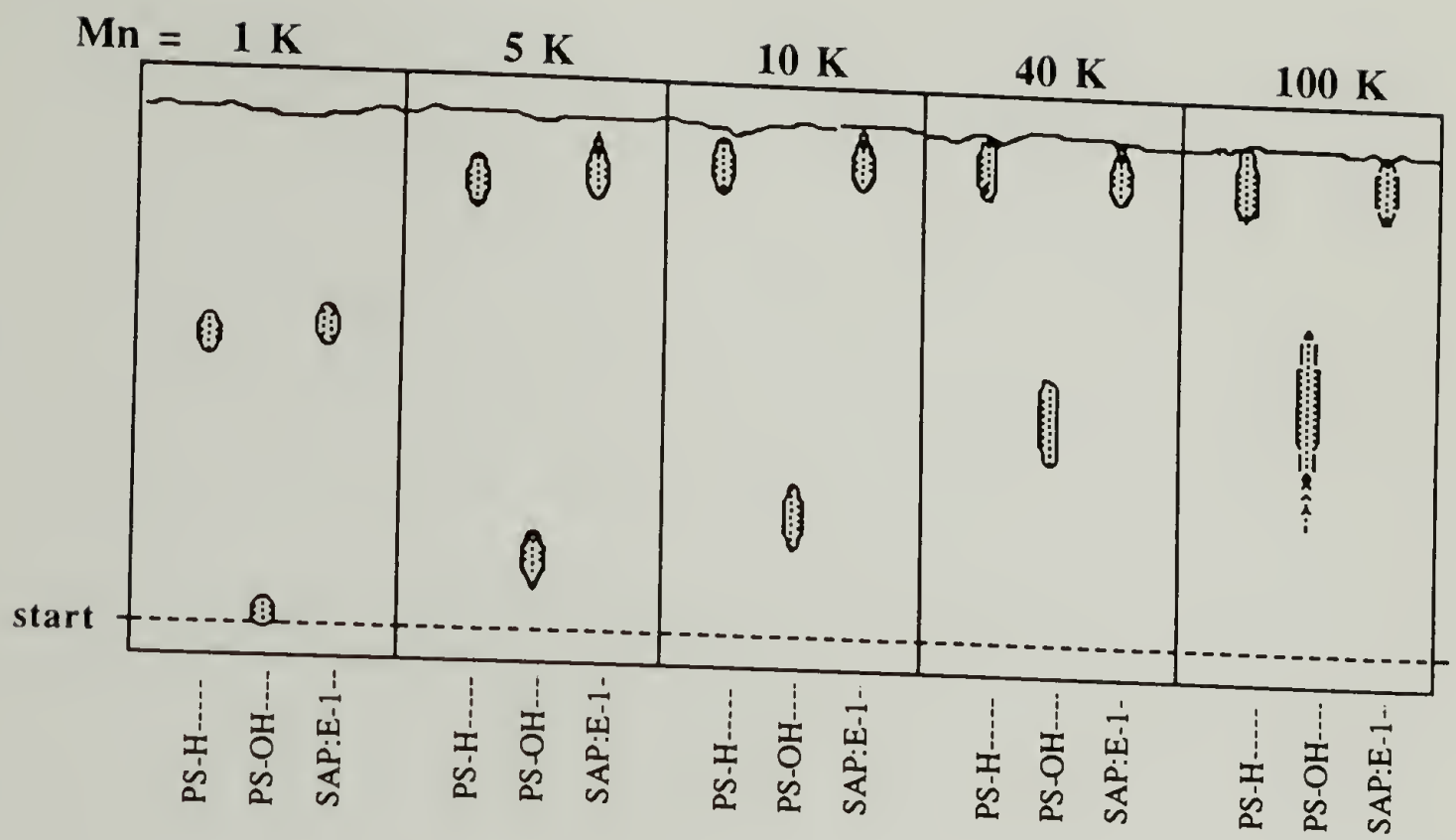

eluent: toluene
plate: mylar-backed silica

Figure 6.4. TLC Data for Polystyrene, PS-OH and SAP:E-1 Polymer at Each Molecular Weight.

the TLC plate (mean pore size for silica gel is 60 Å diameter).[1] A rationalization for the difference in R_f values for the lower molecular weight polymers based on the perfluoroalkyl endgroup is that this species increases the effective coil size of the smaller polymers such that size exclusion on the plate is changed. (The higher molecular weight polymers already are (size) excluded from the pores on the plate.) GPC data contained in Table 19 indicate that addition of the fluorinated endgroup causes a significant increase in the effective coil sizes of all the SAP:E-1 polymers with greater increases observed for higher molecular weights. Examination of the PS-OH TLC data indicates that the 1 K polymer hardly elutes. With increasing molecular weight, PS-OH polymers elute further and the spots become smeared. One explanation for this is that at lower molecular weights, the single alcohol group functions well as a sticky foot and all polymers in the spot adsorb to the silica. At higher molecular weights the stickiness is diluted by the extra styrene units and the polymers in the spot adsorb to and desorb from the silica gel, and the net result is that the polymers in the spot stick at slightly different times. Elemental analysis of 5 K SAP:E-1 polymers, shown in Table 20, indicates that the endcapping reaction (esterification) affords high yields; this corroborates the data observed by TLC.

Thermal analyses were carried out on the SAP:E-1 polymers to determine whether decomposition would occur at any given temperature (i.e. would the ester groups pyrolyze) and to determine the influence of the fluorinated endgroup on Tg. Results from TGA analysis carried out for SAP:E-1 polymers with Mn = 1, 5 and 10 K indicate that no decomposition (indicated by mass loss) occurs for these polymers before the polystyrene

Table 20. Elemental Analysis Results for PS-H, PS-OH and SAP:E-1 Polymer with Mn = 5 K.

5 K Polymer		Elemental Analysis (%) C	H	O	F	Empirical Formula
PS-H	theoretical	92.22	7.78	--	--	
	experimental	91.79	8.20	.01	--	$C_{404}H_{409}$
						$C_{404}H_{433}$
PS-OH	theoretical	91.88	7.81	.30	--	
	experimental	91.93	7.78	.29	--	$C_{406}H_{414}O_1$
						$C_{406}H_{412}O_{.96}$
PS-OF	theoretical	86.10	7.12	.55	6.23	
	experimental	85.61	7.16	1.06	6.17	$C_{416}H_{413}O_2F_{19}$
						$C_{421}H_{423}O_4F_{19}$

segment itself degrades at ~425 °C. The boiling point of perfluorodecanoic acid is 218 °C at 740 mm Hg, indicating that the acid, if present as such in our system, would have volatilized at temperatures slightly higher than this. Pyrolysis and volatilization of the endgroup would have resulted in a 50% mass loss for the 1 K samples. The TGA data do indicate a very slight mass loss (~2%) around 220 °C for the 1 K samples which could be due to decomposition of polymers with DP = 1 or 2, or small amounts of methyl perfluorodecanoate in the sample (the 1 K polymer was difficult to purify). These data do not indicate cleavage of the fluorinated endgroup, or at least not to a significant degree.

The DSC data for the SAP:E-1 polymers indicate that the perfluoroalkyl group had a slightly exaggerated "endgroup effect" on Tg for the lower molecular weight polymers. A plot of these data is shown in Figure 6.5. The Tg for polystyrene varies as

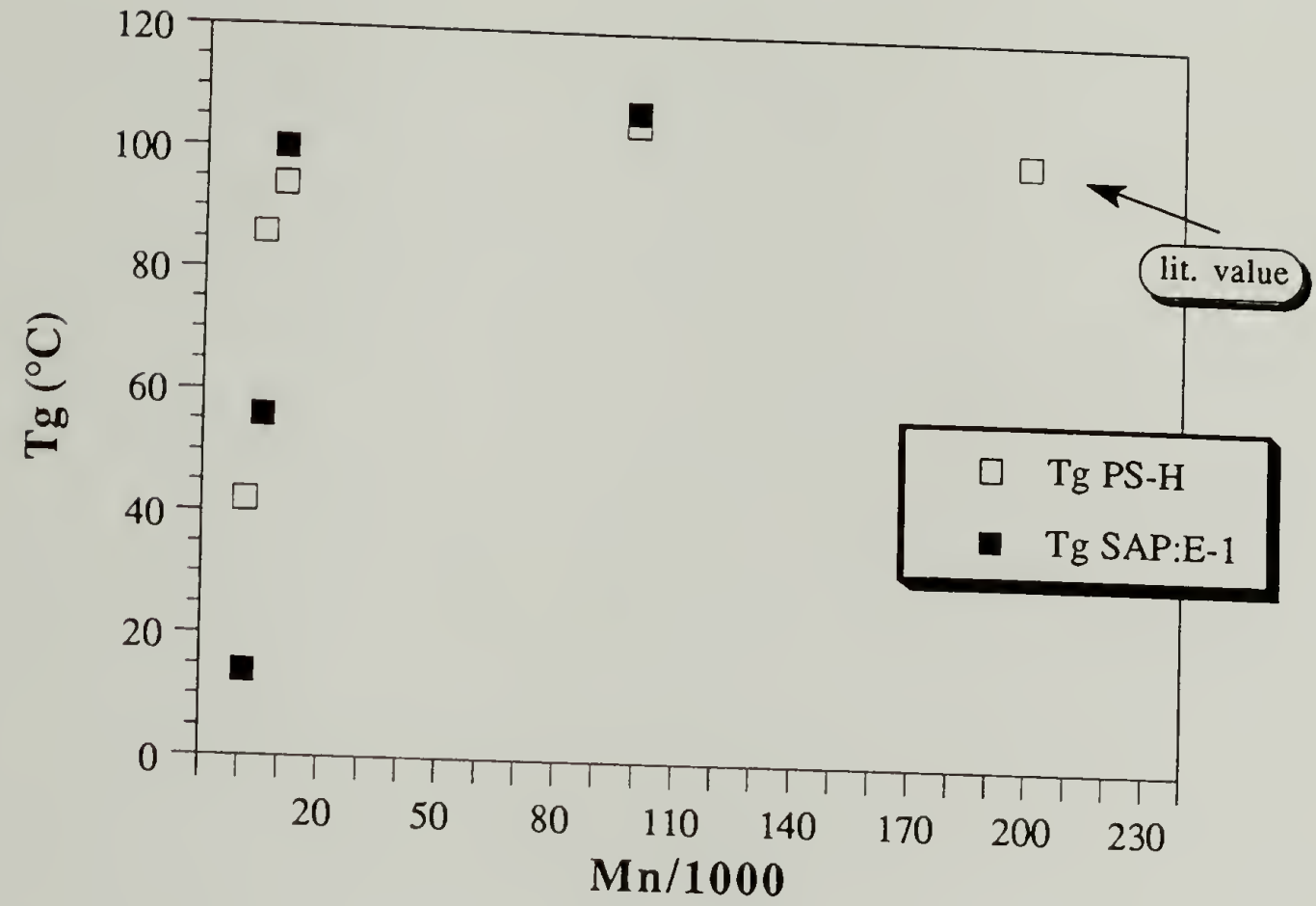

Figure 6.5. DSC Data for SAP:E-1 Polymers in Comparison with Data for Polystyrenes of Corresponding Molecular Weight.

$$Tg = 100 - \frac{1.7 * 10^5}{Mn} \qquad (6.1)$$

and becomes independent of molecular weight above 25 K.[2] With decreasing molecular weight, Tg is depressed by the increasing concentration of chain ends in a sample because this allows more chain mobility.[3] In the case of polymers with Mn = 1 and 5 K, the Tg values of the perfluoroalkyl group-functionalized polymers are 14 °C and 72 °C, respectively. These values are much lower than those obtained for the regular polystyrene samples of the same molecular weights: 42 °C and 86 °C. The endgroup effect diminishes for the polymers with molecular weights greater than 10 K. The SAP:E-1 polymer with Mn = 10 K has a slightly higher Tg than polystyrene, but at 100 K the two polymers have essentially the same value. These data suggest that Tg depression depends on the relative amounts of styrene and perfluoroalkyl segments in the sample.[4] DSC analysis of 1 K SAP:E-1 film samples that were annealed (for surface reconstruction experiments) indicates a single, intermediate Tg value of ~78 °C (between Tg for 10 K PS-H and that for 1 K SAP:E-1, data are in Table 19). This single value suggests that the sample consists of only one phase. (It should be noted that these DSC data were taken at a fairly fast ramp rate (20 °C/min) which would bias the temperature data a little high because of a slight lag in sample heating.)

Experiments with SAP:E-1 Film Samples. Polymers and variables were chosen for this first section of work with the objective of laying a foundation for studying the surface segregation of perfluoroalkyl group-

functionalized polymers in polystyrene-based film samples. SAP:E-1 film samples were subjected to various heat treatments to observe the effects of temperature and heating time on surface reconstruction and to ascertain optimum conditions for maximizing this reconstruction. Different molecular weight surface-active polymers were used in these experiments to investigate the effect of polystyrene tail-length on the rate and extent of surface segregation by these molecules. Several concentrations of SAP were used for each sample series to shed light on how surface reconstruction is influenced by bulk composition.

Polystyrene. Polystyrene films were prepared and annealed at 110 °C for 72 h to establish baseline values for contact angle measurements and XPS spectra. The survey and C_{1s} region XPS spectra for polystyrene are shown in Figure 6.6. Atomic concentration data for this surface indicates ~0.4% oxygen and ~0.1% silicon contamination. Polystyrene can oxidize by thermal as well as light-induced processes,[5,6] so care was taken to keep film samples in a dark and oxygen-free atmosphere; unfortunately most film samples still contain some amount of oxygen. The C_{1s} spectrum indicates a low binding energy peak at 285 eV and a π-π^* shakeup peak about 7 eV higher. Contact angles for polystyrene are (advancing angle/receding angle) $\theta_A/\theta_R = 87°/72°$ using water as the probe fluid, and $\theta_A/\theta_R = 10°/8°$ using hexadecane. Contact angles for teflon are $\theta_A/\theta_R = 120°/89°$ (water)[7] and 52°/45° (hexadecane). Both of these liquids were used as contact angle probe fluids in these experiments because the range in contact angle values between polystyrene and teflon is slightly larger

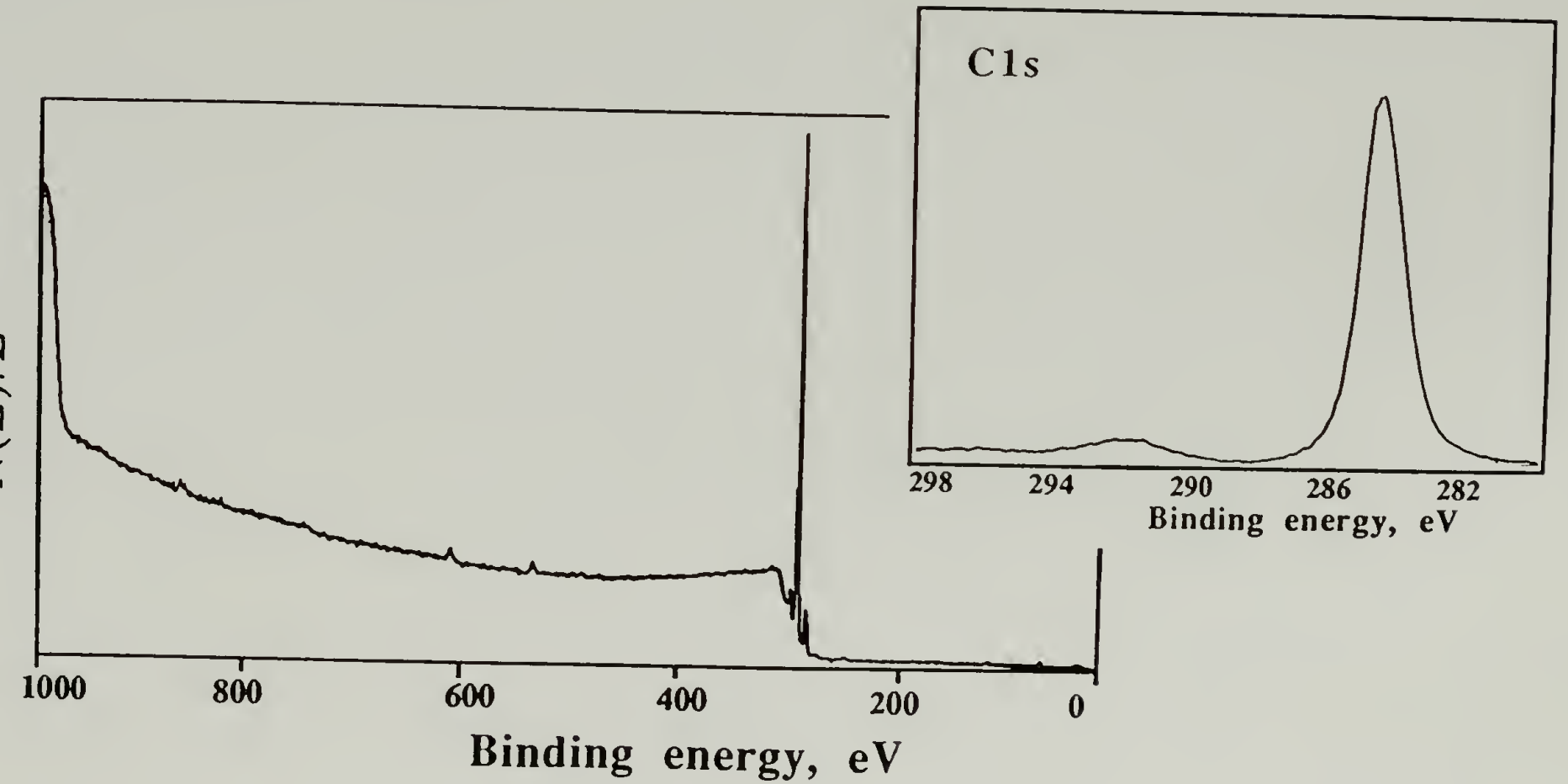

Figure 6.6. XPS Survey Spectrum and C1s Region for Polystyrene Film.

between polystyrene and teflon is slightly larger using hexadecane. Differences between advancing and receding contact angles is termed hysteresis and this usually reflects chemical heterogeneity or roughness in the surface. All of the film samples prepared for these experiments exhibited contact angle hysteresis; plain polystyrene samples showed the least difference.

Driving Force for Reconstruction. Differences in critical surface tension values between polystyrene (γ_{crit} = 33 dyn/cm) and teflon (γ_{crit} = 18 dyn/cm)[8] give rise to the expectation that a sample comprised of these two polymers (and assuming sufficient chain mobility) would contain only teflon segments at the surface for a minimization in overall free energy of the system. Complete phase separation of these polymers also would be expected. When the cohesive energy density (CED) is measured in joules, the solubility parameter (δ) for polystyrene is 17.6 [$(J/cm^3)^{1/2}$] and that for teflon is 12.7 [$(J/cm^3)^{1/2}$].[9] Polymers with even small solubility parameter differences (.7 at 10 K, or .2 at 100 K, for example) will not be miscible over the entire composition range.[10] In our surface-active polymer system where polystyrene molecules have been functionalized with perfluoroalkyl groups, the same principles apply to a certain extent. A driving force for surface reconstruction would be surface energy minimization and the polystyrene and fluorinated species should not be compatible although phase separation cannot occur for species that are chemically linked. Instead, phase segregation should occur and part of this would be manifest as segregation of the perfluoroalkyl groups at the film surface.

We have chosen to view surface reconstruction in the polystyrene film samples as an adsorption (or migration) of perfluoroalkyl groups from (or through) the polystyrene matrix. Migration or adsorption of any species to an interface is governed by thermodynamics; a reduction in surface energy must compensate for entropy lost by the adsorbed species. In analogy with a small molecule soap system, SAPs can be thought of as surfactants comprised of a lyophobic headgroup and a lyophilic tail. Compatibility of the polystyrene tail with the matrix gives our system an advantage over other film systems that contain small molecule additives in that our surface-active group cannot diffuse out of the sample entirely.[8] The Tg of polystyrene is roughly 100 °C (depending on molecular weight), so heating the samples at 110 °C gives the chains increased mobility to facilitate reconstruction. In contrast with the adsorption of soap molecules to the surface of a liquid which occurs on a very short time scale, reconstruction of polystyrene samples is very slow and occurs over days. Our methods of analyses are amenable to the study of solid surfaces and we are interested in assessing changes in wettability that occur with changes in surface chemical structure; this is why we have designed our system in this fashion.

Adsorption Isotherms. Data for adsorption experiments are most often reported as isotherms showing changes in the amount adsorbed with concentration and we have reported our surface reconstruction data in a similar fashion. XPS data indicating the atomic composition of the reconstructed surfaces have been "boiled down" to F/C values (which reflect the amount of surface-active groups adsorbed) and samples are

compared on this basis. Isotherms have been constructed for each SAP sample series, showing increasing F/C against concentration of surface-active polymer. Trends in the data for surface reconstruction mimic those seen for (polymer) adsorption from solution because the amount adsorbed (fluorine surface-enrichment) increases with concentration up to a point, and then remains constant. The most important data obtained from these experiments include F/C plateau values for each molecular weight, position of the "knee" for each isotherm, surface excess observed and comparison of F/C between different molecular weight SAPs at any given concentration.

One important parameter to consider for film samples containing surface-active polymers is the bulk fluorine to carbon ratio (F/C value) which functions as a reference point for the XPS data. Comparison of the surface F/C ratio (obtained from 15 ° takeoff angle XPS data) and 75 ° takeoff angle data with regard to the bulk F/C value describes more accurately the changes occurring in the surface of the film (or in the outer 40 Å). Figure 6.7 shows bulk F/C values plotted against concentration of SAP:E-1 polymer; this plot holds for any molecular weight SAP:E-1 polymer using a 200 mg sample size. None of the samples prepared in these experiments contained amounts of SAP:E-1 polymer greater than 0.04 mmol because after this point the bulk F/C value shoots up toward 2 as it would be for a sample containing only the endgroup. For a study of surface segregation of perfluoroalkyl groups, this species should be a minor component of the sample.

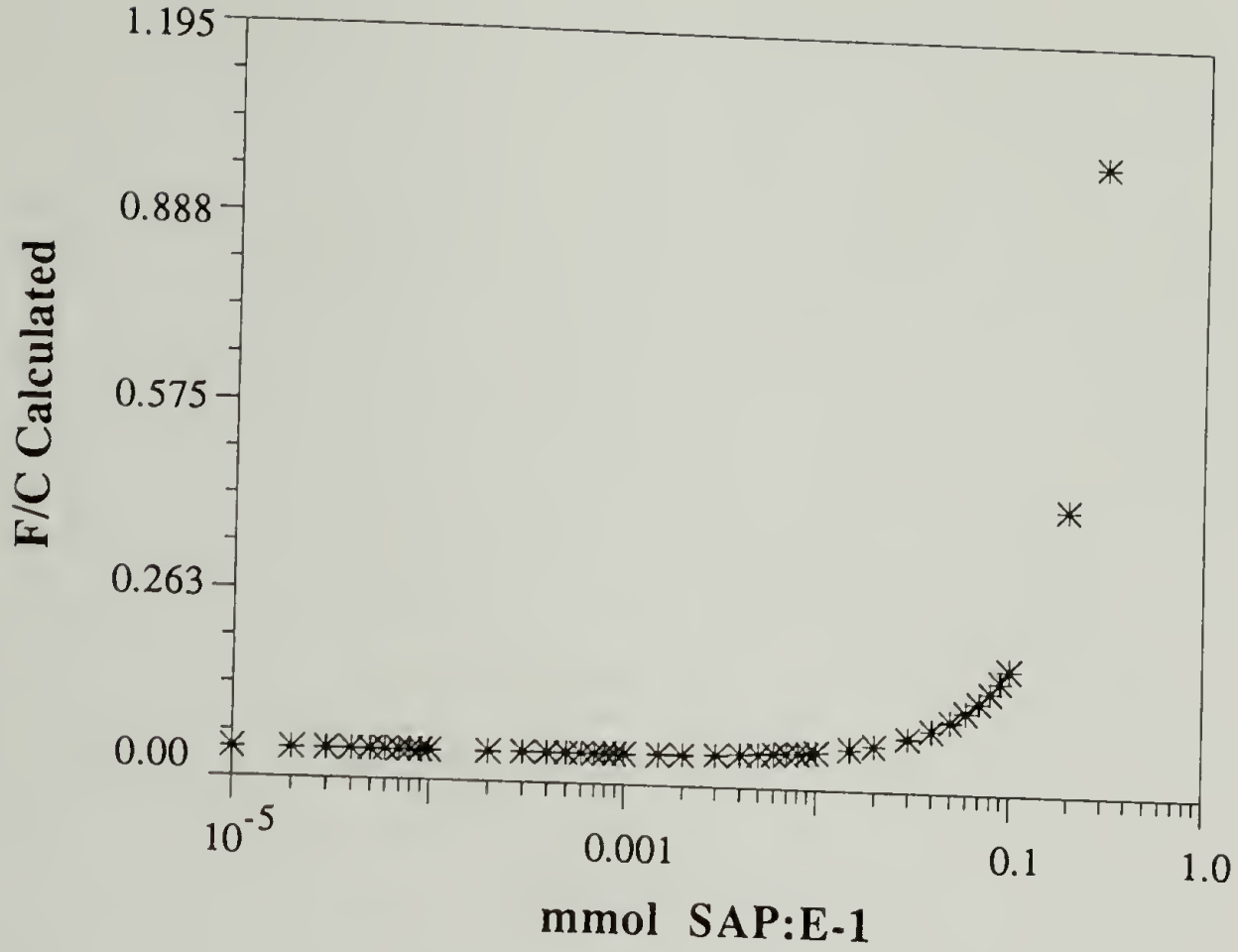

Bulk **F/C**:

$$F = (\text{mmol SAP})\ 19F$$

$$C = \left[\left(.2g - \frac{\text{mmolSAP}}{1000}(598\text{g/mol})\right)\frac{8C}{104\text{g/mol}} + \frac{\text{mmolSAP}}{1000}16C\right]1000$$

Figure 6.7. Calculated (Bulk) F/C Data for All Concentrations of SAP:E-1 Polymers.

Heat Treatment of SAP:E-1 Film Samples. Preliminary experiments were carried out to determine whether heat had to be supplied to film samples for reconstruction to occur. 10 K SAP:E-1 samples at a low and a high concentration were kept at room temperature under reduced pressure for 72 h and then analyzed by XPS and contact angles. Films prepared in this fashion were not smooth, like the heated ones, but were slightly crusty. Contact angle and XPS analyses indicate no surface reconstruction at the lower concentration, and very little at the higher one. Contact angle analyses were complicated by a wicking action on parts of the films.

After it had been determined that samples must be heated to facilitate reconstruction and that 110 °C was the optimum temperature for heating, kinetics data were obtained for SAP:E-1 polymers with Mn = 1, 10 and 100 K; 5 and 40 K SAP:E-1 samples were annealed under optimum conditions chosen for 10 and 100 K polymers, respectively. The data indicate that samples containing polymers with Mn = 1 and 10 K finish reconstructing after ~72 h of heating at 110 °C, but 100 K samples require 120 h. Samples were heated for very long times to insure that no further reconstruction would occur. Times shorter than 24 h were not investigated because residual solvent in the samples was volatilized upon irradiation by X-rays in the XPS causing the pressure to rise and shut the system down.

Surface Reconstruction Data for SAP:E-1 Samples. Isotherm data were obtained for each SAP:E-1 sample series under optimum annealing conditions to observe how F/C changes with concentration for different

molecular weights. Isotherm plots that were constructed from XPS data for samples containing SAP:E-1 polymers with Mn = 1, 5 and 10 K are shown in Figures 6.8, 6.9 and 6.10, respectively. In general, these plots show increasing F/C with concentration and then a plateau indicating no further reconstruction. An important feature in all of these plots is the discrepancy between the F/C values reported for 15° takeoff angle XPS data and those reported for 75°. Data from the 15° takeoff angle represent the composition of the top 11 Å of the film sample (94 % of the photoelectrons detected originate from this region). Electrons travel only short distances through matter due to inelastic scattering, which means that XPS sensitivity decreases as $\sim e^{-(t/\lambda \sin\theta)}$ where t is thickness of material traversed, λ is mean free path of an electron in a given material and θ is the angle to the detector. Spectra recorded at the 75° takeoff angle are representative of the outer 40 Å of a surface (95 % of photoelectrons detected are ejected from this region) and 54 % of the electrons measured at this angle actually originate from the top 11 Å. For samples in these experiments, data obtained at 75° indicate fluorine concentrations that are less than 54 % of the amount observed at 15°. This means that the top 11 Å of the samples is not homogeneous in fluorine composition, but rather the fluorine is concentrated in the outer few angstroms. Concentration of fluorine in the outermost surface layers would bias the 15° takeoff angle XPS data high in fluorine; these data will not reflect an average composition of the top 11 Å. The relatively low fluorine concentration detected at 75° suggests that a depletion layer exists below the region at the film surface.

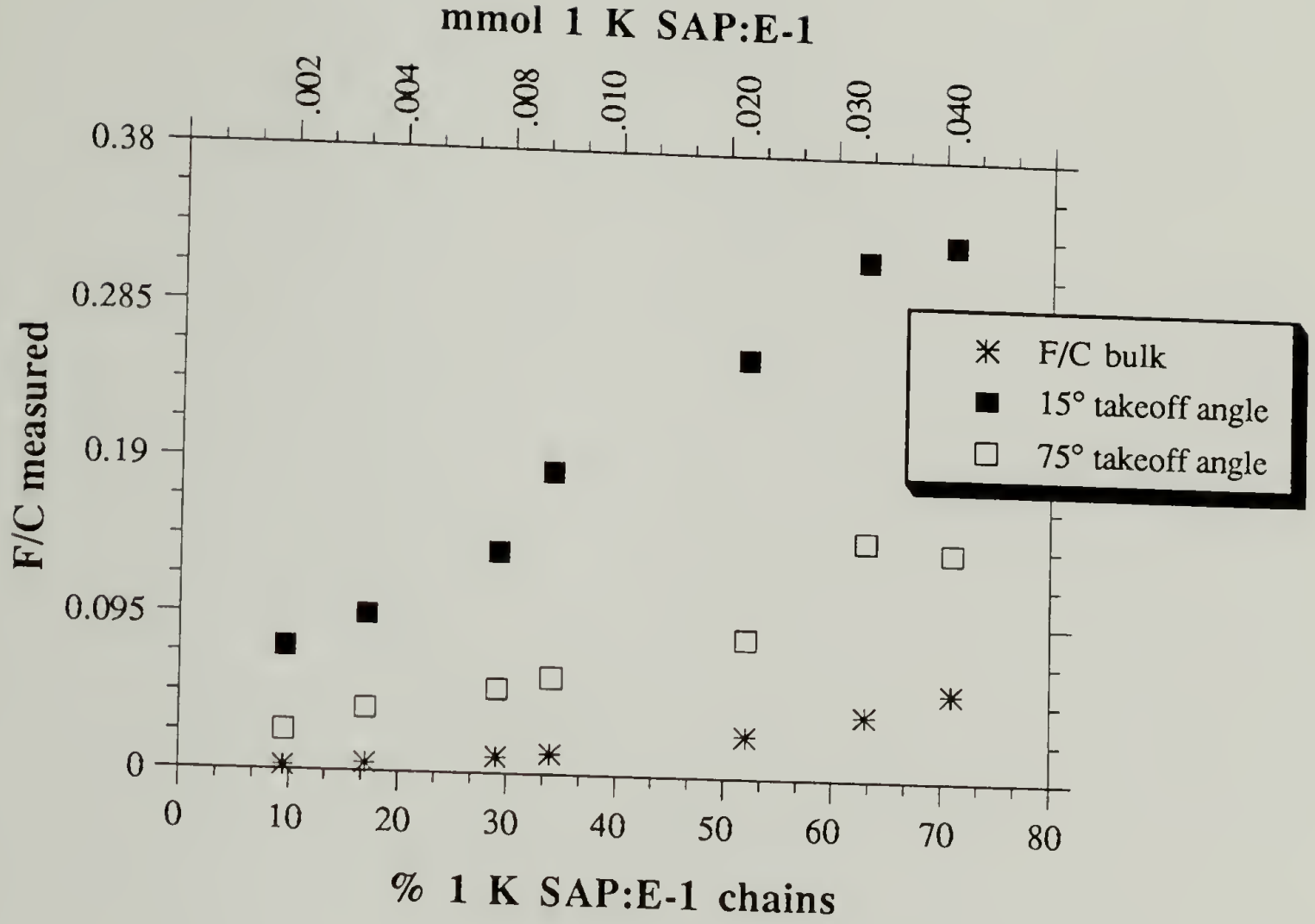

Figure 6.8. Changes in F/C with Concentration for 1 K SAP:E-1 Samples Heated at 110 °C for 72 Hours.

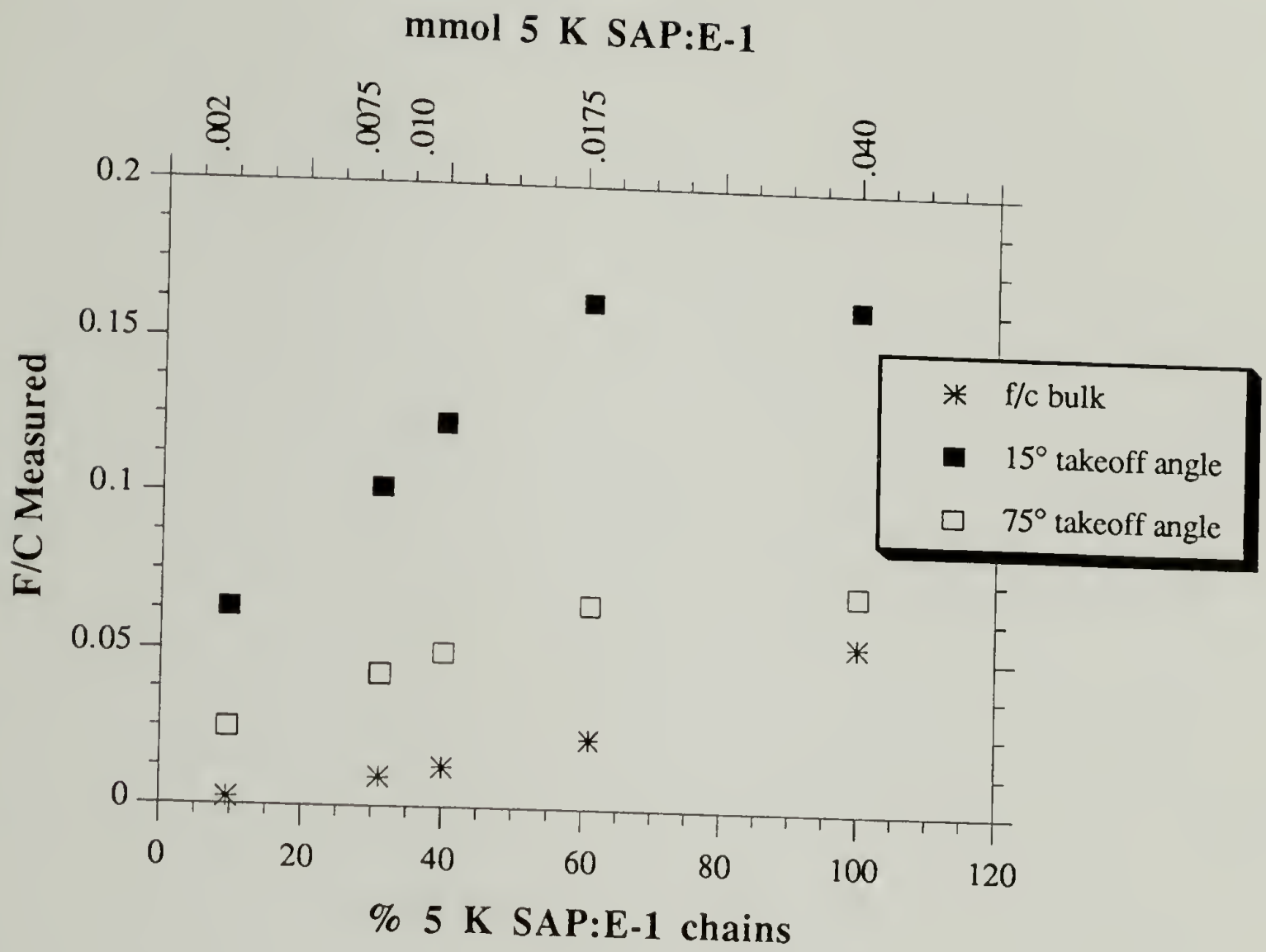

Figure 6.9. Changes in F/C with Concentration for 5 K SAP:E-1 Samples Heated at 110 °C for 72 Hours.

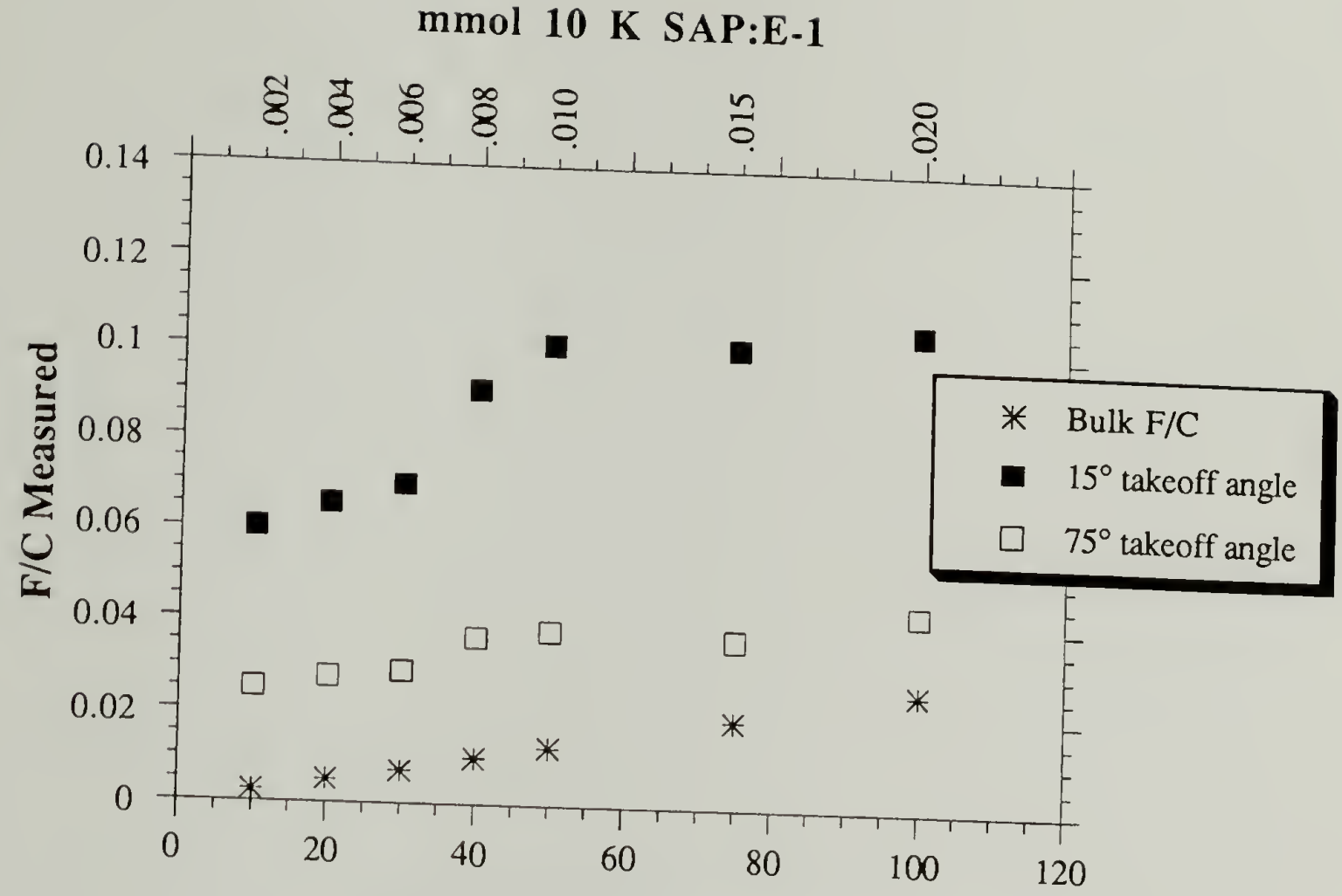

Figure 6.10. Changes in F/C with Concentration for 10 K SAP:E-1 Samples Heated at 110 °C for 72 Hours.

Among the SAP:E-1 polymers, the 1 K samples were expected to show the greatest amount of surface fluorine enrichment because in general, small chains tend to adsorb at interfaces and more of these chains would fit in any given space (at the surface). The isotherm data for the 1 K SAP:E-1 samples indicate a maximum F/C value of .329, occurring around 63% SAP chain concentration (0.03 mmol). This is the highest F/C value observed for SAP:E-1 samples, corresponding to a maximum surface excess of 8.2 times the bulk F/C value. Surface excess is defined for these experiments as the difference between bulk and surface F/C values; maximum surface excess occurs at the point of greatest difference between surface and bulk F/C. The maximum F/C value for the 1 K data obtained at 75° is ~.142 which is about 2.6 times bulk F/C value. Data from the 5 K isotherm indicate a plateau that begins at ~60% SAP chains (0.0175 mmol). The 1 and 5 K samples have the same maximum concentration (0.04 mmol) which is 100% 5 K SAP chains and 71% 1 K chains. The plateau value for 5 K is .163, almost exactly half that observed for 1 K, and the maximum surface excess is 10.9 times the bulk value. The plateau in the isotherm for 10 K SAP:E-1 data occurs at F/C = .105 and the knee occurs at ~50% SAP chains (0.01 mmol). Maximum concentration for the 10 K samples is 0.02 mmol (100% chains). The surface excess for 10 K samples at the plateau is 9.5 times bulk F/C.

XPS survey spectra for 10, 5 and 1 K samples at maximum concentration are shown in Figure 6.11 and the C_{1s} regions from these spectra are in Figure 6.12. The C_{1s} data indicate a low binding energy peak at 285 eV that is slightly broader than that seen for polystyrene due to carbon bonded to oxygen in the sample and the π-π^* peak at 292 eV is

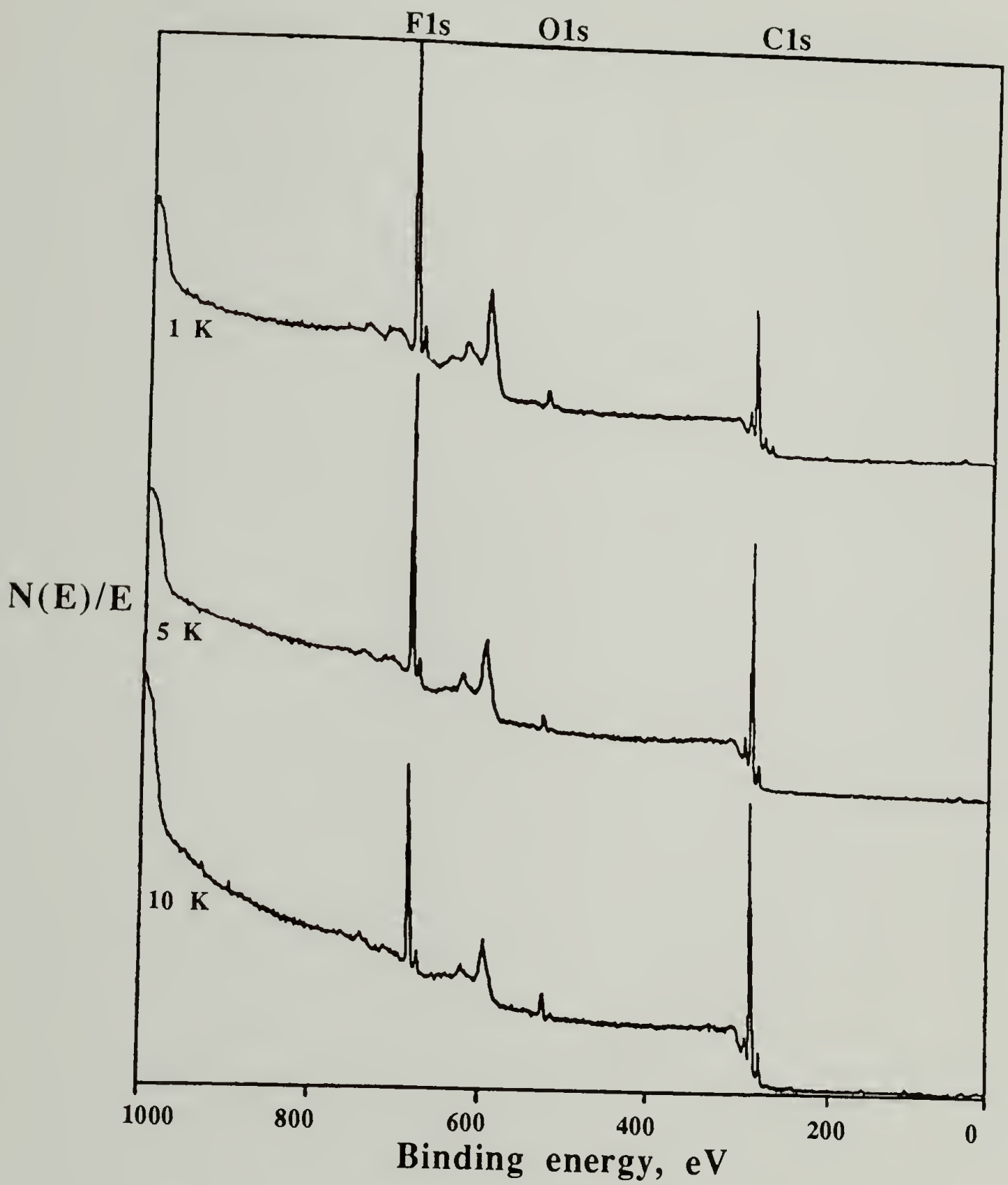

Figure 6.11. Comparison of XPS Survey Spectra for SAP:E-1 Samples (Mn = 10, 5 and 1K) at Maximum Concentration.

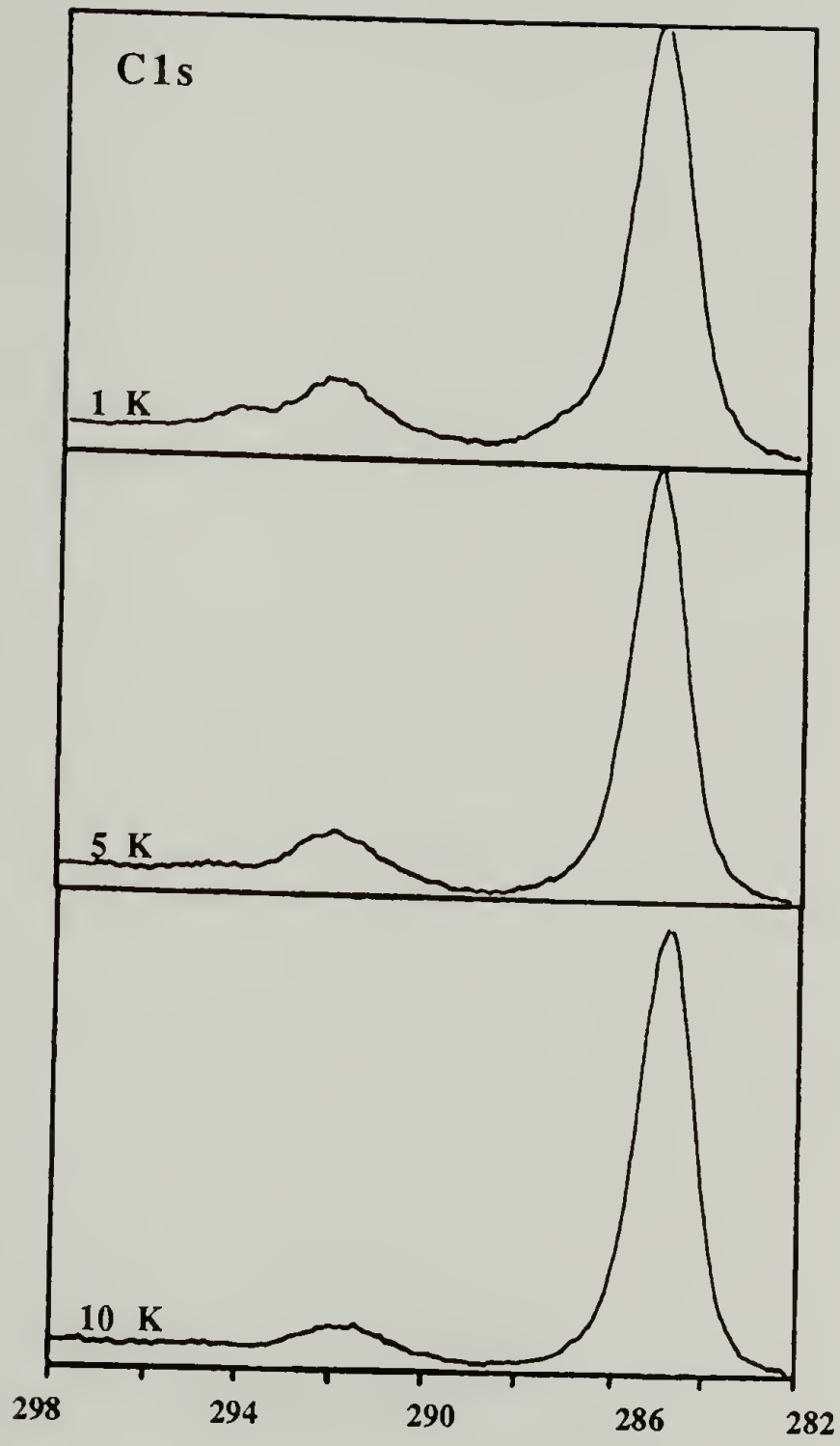

Figure 6.12. Comparison of C_{1s} Regions for SAP:E-1 Samples (Mn = 10, 5 and 1 K) at Maximum Concentration.

augmented by CF_2 carbon. In the 1 K, and to a slight degree the 5 K spectra, a small peak has appeared at 294 eV due to CF_3 species.

The F/C isotherm plots obtained for 40 and 100 K SAP:E-1 samples were similar to the data for the lower molecular weight samples; these plots are in Figures 6.13 and 6.14. The 100 K data show a surface F/C plateau value ~0.071 and the 40 K plateau is slightly lower (~0.066). The knee occurs in the 40 K plot at ~40% SAP chain concentration (0.00375 mmol) and at ~20% SAP chains in the 100 K case (0.0014 mmol). The maximum surface excess is 15.7 times the bulk F/C value for the 40 K films and 36.6 for the 100 K samples. A significant discrepancy exists between the 15° and 75° takeoff angle data and this difference is larger for 100 K samples than 40 K ones.

Some general trends have been observed among data obtained from the SAP:E-1 samples. Higher molecular weight samples take longer to reconstruct than the lower molecular weight ones, but reconstruction in the lower molecular weight samples results in higher F/C values and higher contact angles. In part, these higher values arise because greater amounts of surface-active polymer will fit into the 200 mg sample size at lower molecular weights. Surface reconstruction stops at lower concentrations of SAP chains with increasing molecular weight. In other words, the knee in the isotherms moves forward with increasing molecular weight, and this might reflect a chain-packing or surface-crowding phenomenon or it could reflect a minimization in surface energy. Surface reconstruction in these samples could possibly be controlled by a combination of these two effects and their relative importance may depend on molecular weight (especially

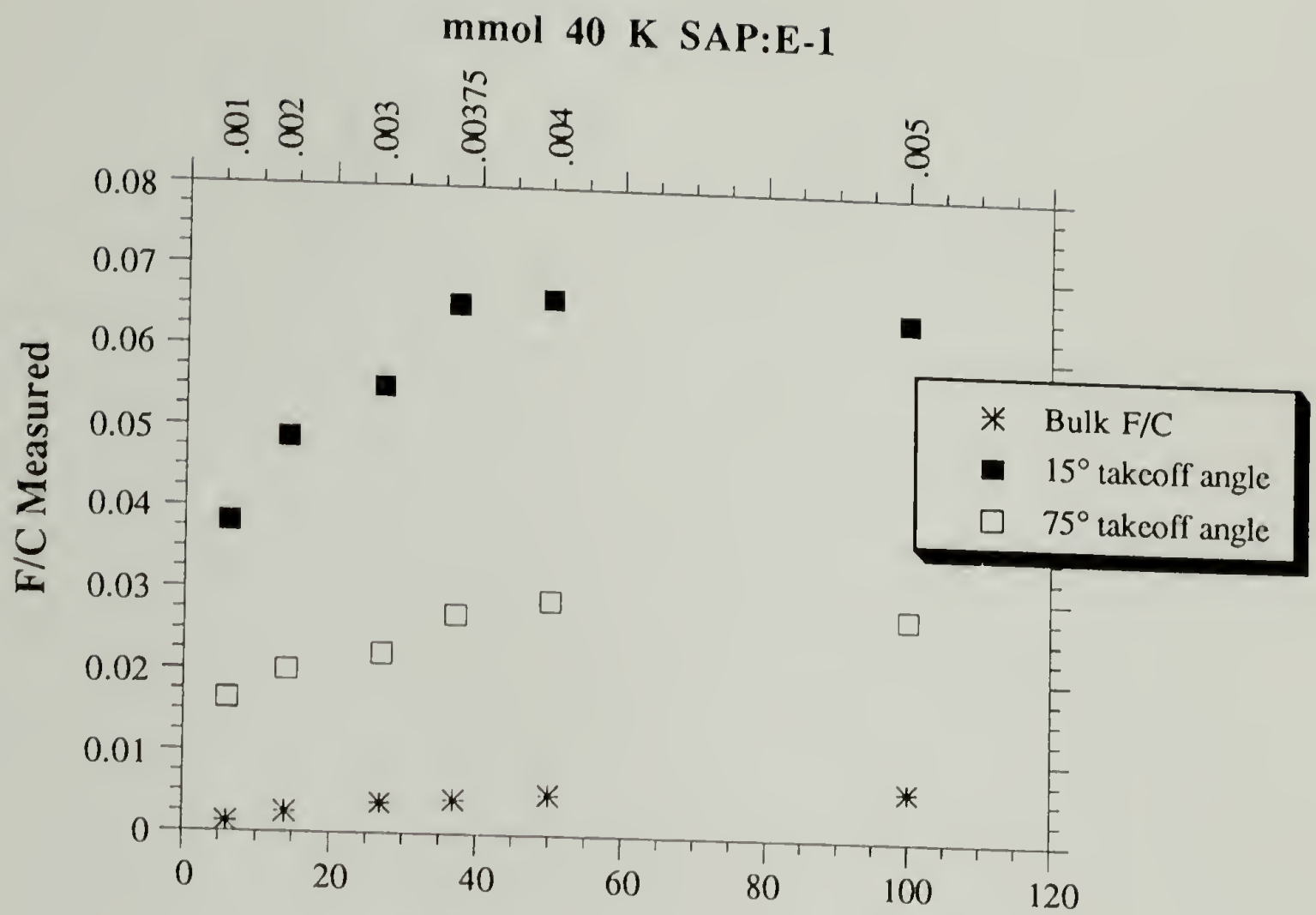

Figure 6.13. Changes in F/C with Concentration for 40 K SAP:E-1 Samples Heated at 110 °C for 120 Hours.

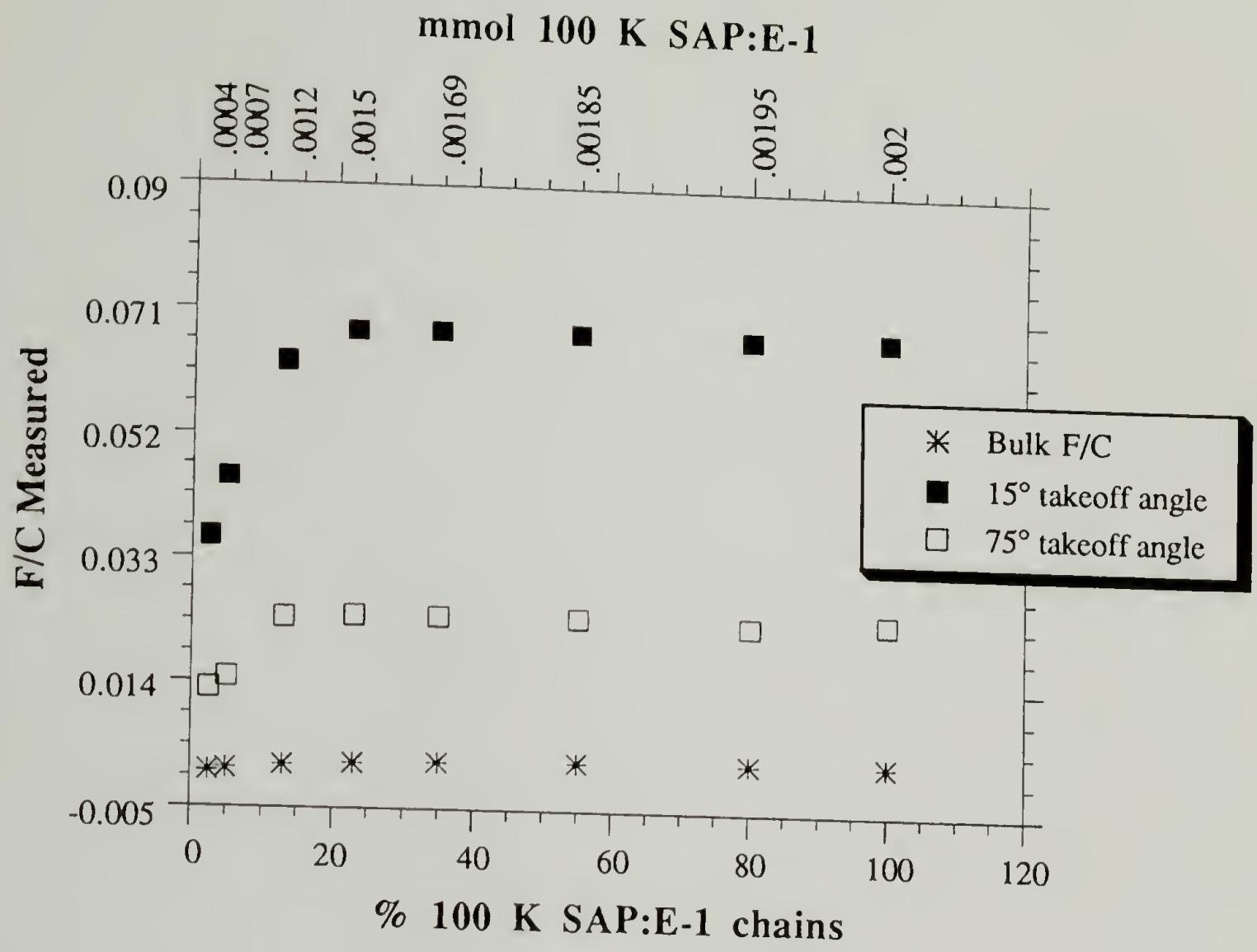

Figure 6.14. Changes in F/C with Concentration for 100 K SAP:E-1 Samples Heated at 110 °C for 120 Hours.

relative to the matrix polymer molecular weight). Another important feature of these isotherms is that the higher molecular weight SAP:E-1 samples exhibit greater surface excess values than the lower molecular weight samples.

Patterns in the contact angle data for all of the SAP:E-1 samples follow the trends seen in the XPS data. Contact angles increase (wettability decreases) with concentration up to a point and then remain constant. These data are plotted in the same fashion as the F/C isotherm data to allow comparison of plot shape and knee position. In general, the plot shapes are the same, athough the receding angle data are slightly less consistent (numbers jump around more, especially at 1 K). The advancing contact angle data indicate that surface reconstruction ceases (i.e. surface wettability stops decreasing) at roughly the same concentration that the XPS data indicate. Figure 6.15 shows the advancing contact angle data for SAP:E-1 polymers (with Mn = 1, 5, 10, 40 and 100 K) obtained using water as the probe fluid and Figure 6.16 shows the data obtained using hexadecane as the probe fluid.

In general, higher contact angles are expected for samples containing more fluorine at the surface. Water contact angles for the 1 K samples at the plateau are $\theta_A/\theta_R = 101°/81°$ and for hexadecane $\theta_A/\theta_R = 46°/33°$. Values obtained for the 5 and 10 K samples at the plateau are similar to one another, despite differences in surface F/C values: water contact angles for 5 K are $\theta_A/\theta_R = 98°/79°$ and for 10 K are $\theta_A/\theta_R = 98°/81°$, and hexadecane contact angles for 5 K are $\theta_A/\theta_R = 36°/26°$ and for 10 K are $\theta_A/\theta_R = 36°/28°$. Comparison of XPS data for these two molecular weight samples

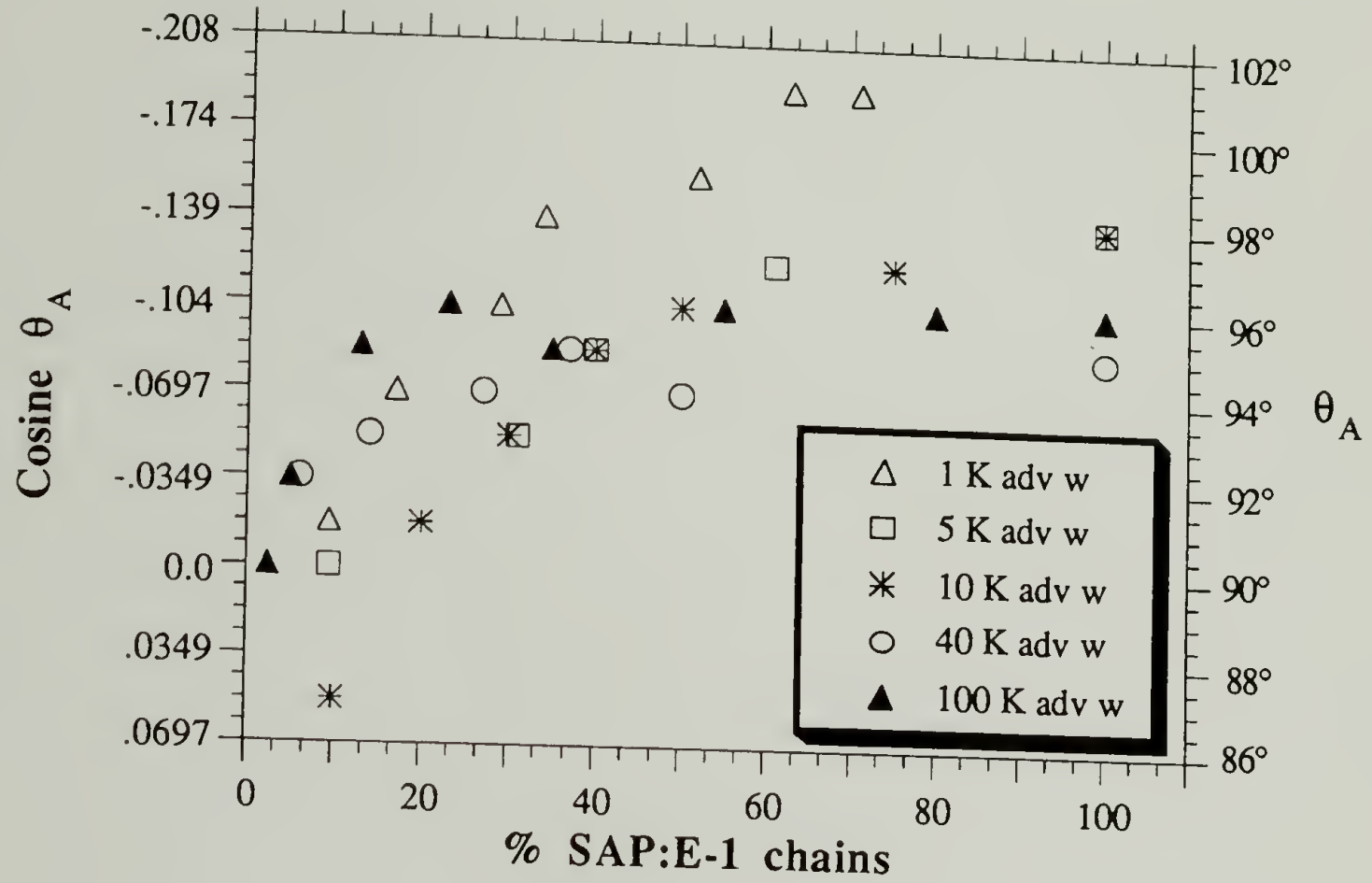

Figure 6.15. Comparison of Advancing Contact Angle Data for SAP:E-1 Polymers (Mn = 1, 5, 10, 40 and 100 K) Using Water as the Probe Fluid.

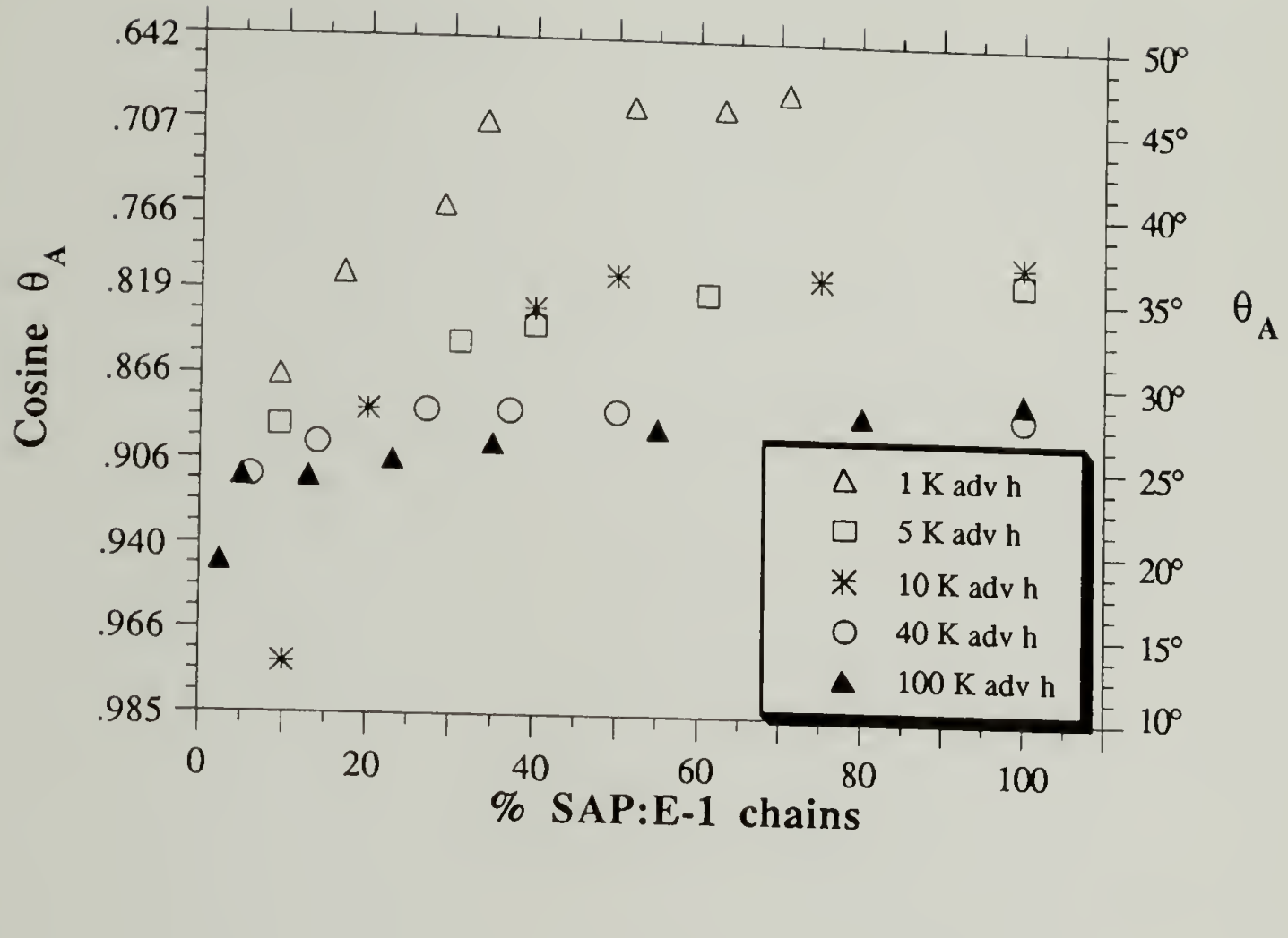

Figure 6.16. Comparison of Advancing Contact Angle Data for SAP:E-1 Polymers (Mn = 1, 5, 10, 40 and 100 K) Using Hexadecane as the Probe Fluid.

indicates that the difference between 15° and 75° takeoff angle data (for each molecular weight) is roughly the same, suggesting that the distribution of fluorine in the surface region is similar for these films. However, the 15° data indicate that 10 K samples contain less fluorine in the outer 11 Å of the surface relative to the 5 K samples. These data, in combination with the information obtained from the contact angle data (which are more sensitive to the outermost surface region), suggest that the perfluoroalkyl groups are closer to the surface in the 10 K samples. The plateau F/C values for 100 K and 40 K SAP:E-1 samples are similar (around 0.07), and the contact angle data for these surfaces are comparable, as well. Water contact angles for the 100 K samples at the plateau are θ_A/θ_R = 96°/81° and with hexadecane, θ_A/θ_R = 29°/23°. Water contact angles for 40 K samples at the plateau are θ_A/θ_R = 95°/77° and with hexadecane, θ_A/θ_R = 28°/24°.

Attempted Hydrolysis. To determine whether the fluorinated ester groups could be hydrolyzed during water contact angle measurements, hydrolysis experiments were attempted on 100% 10 K SAP:E-1 samples that had been annealed under the same conditions used to determine isotherms. In the first experiment, the samples were subjected to appropriate hydrolysis conditions (i.e. acidic methanol/water, 35 °C, 3 h) which actually are much stronger than those presented by a water droplet. Under these conditions, no fluorine loss was observed by XPS for these films, although the amount of oxygen detected increased. The contact angle data obtained using water as the probe fluid indicated a drop in contact angles θ_A/θ_R = 98°/81° to 92°/75°. Similarly, a decrease was detected by hexadecane contact angles: θ_A/θ_R = 37°/29° dropped to

27°/20°. Despite this decrease in values, the contact angles measured with both probe fluids are higher than would be expected for a plain polystyrene surface (or an alcohol-containing surface). These data suggest that either only some of the ester groups were hydrolyzed under these conditions (e.g. those in the region accessed by contact angle measurements but not those in the region assessed by XPS) or perhaps some reorientation[11] (at 35 °C, maybe with penetration of solvent) occurred on the very surface of these films (e.g. the fluorinated groups were turned under and ester groups were put next to the aqueous phase). XPS data for these samples (before and after) are contained in Table 21, and the contact angle data are in Table 22. In hindsight, this was not a good experiment for testing for water droplet-induced hydrolysis because it introduces new variables. However, the data obtained do highlight the surface-sensitivity of contact angle measurements relative to XPS.

Table 21. XPS Data and F/C Values for SAP:E-1 Samples (Mn = 10 K) Before and After Attempted Hydrolysis.

			XPS Atomic Composition 15°/75°						
% chains	time h	T °C	C	π–π* C	O	F	Si	F/C expt.	comment
Before Hydrol.			78.1	10.1	2.0	9.7	.2	.110	
100	72	110	87.4	7.4	1.2	3.9	0	.0411	
After Hydrol.			76.9	8.4	3.3	10.0	1.3	.117	amt F same, see increase in amt oxygen
100	72	110	86.6	6.1	2.8	4.2	.3	.0453	

Table 22. Water and Hexadecane Contact Angle Data for SAP:E-1 Samples (Mn = 10 K) Before and After Attempted Hydrolysis.

% chains	time h	T °C	θ_A/θ_R water	avg.	θ_A/θ_R hexadecane	avg.
Before Hydrolysis						
100	72	110	98/82, 97/80 99/80, 97/83 98/83, 98/81	98/81	38/31, 37/29 38/30, 38/29 37/30, 36/28	37/29
After Hydrolysis						
100	72	110	93/72, 92/74 91/75, 92/74	92/75	28/22, 27/20 27/18, 28/19	27/20

A more realistic method of testing for water droplet-induced hydrolysis was carried out by placing a large droplet of water on the film for a few seconds and then removing it and drying the film under vacuum; this approach uses water at room temperature on a very short time scale. The contact angle measurements for these films were similar to the original values: water $\theta_A/\theta_R = 98°/79°$ and hexadecane $\theta_A/\theta_R = 35°/27°$. Real changes in these films would be more readily detected by hexadecane measurements than by water, but the decrease in values using either fluid is fairly small. These data indicate that very little (if any) change occurs in the films during water contact angle measurements. (It also should be mentioned that normally contact angle measurements obtained with hexadecane would not be affected by hydrolysis because these measurements are taken on a different section of the film.)

Comparison of Unperturbed Dimensions with Experimental Data. We have made a rough calculation to determine the extent of SAP:E-1 chain stretching caused by migration of the perfluoroalkyl groups to the surface. We calculated dimensions for unperturbed chains (with Mn = 1, 5, 10, 40 and 100 K) and compared these values to the dimensions calculated from the XPS data of reconstructed films (F/C ratios). To find the unperturbed dimensions, we assumed (for each molecular weight) that the chains form a layer of interpenetrating coils at the surface and that the layer thickness, t_o, equals the radius of gyration for the chain (R_g). We carried out one set of calculations to determine the surface area per chain (SA_o) from the number of endgroups counted in a (1000 Å)^2 area with the additional assumption that each "unperturbed" chain contributes one end to the surface. (This is the most likely conformation, and even if the chains are not stretched in the "final state", the fluorinated endgroups would have to be at the surface to be detected by XPS.) End-to-end dimensions (R_o) have been determined for each molecular weight SAP using the characteristic ratio[12] for polystyrene, $C_\infty = 10$, and from these values R_g was determined. (Chains are Gaussian in the bulk which means that the number (n) and length (l) of the chain segments can be used to approximate coil size[13] and C_∞ is used to incorporate bond angle restrictions.) A second set of calculations were completed assuming the initial thickness (denoted t_i in this case) is equal to the linear dimension of a cube of polymer with no specifications about the location of the endgroup.

The perturbed chain dimensions were determined from the XPS data obtained. F/C values were converted first into a ratio of the number of perfluoroalkyl groups per number of styrene units which (using $\rho = 1.05$

g/cm^3 as the density of polystyrene[14]) translates into a ratio of perfluoroalkyl groups per volume. The final surface area (SA_o) was determined from this volume using the limiting depth dimension of 11 Å, the XPS sampling depth. A final chain thickness, t_f, was determined from

$$t_f = t_o \frac{(SA_o)^2}{(SA_f)^2} \qquad (6.2)$$

where the volume is conserved. Table 23 contains the dimension values calculated for each of the SAP:E-1 chains. Comparison of the t_f/t_o values for these polymers gives an indication of the chain extension in the z direction (i.e. into the film) relative to the initial structure. This ratio shows that chain stretching increases dramatically with molecular weight.

Table 23. Dimensions Calculated for SAP:E-1 Chains in Perturbed and Unperturbed States.

SAP (mw)	t_o (Rg)	t_i	$SA_o^{1/2}$ (Å)	$SA_f^{1/2}$ (Å)	t_f	t_f/t_o	t_f/t_i	# sty/ 1 perfgp
1 K	12 Å*	12 Å	12	10	16	1.3	1.3	6.5
5 K	23 Å	20 Å	18.5	15	35	1.5	1.75	14.5
10 K	32 Å	25 Å	22	18	48	1.5	1.9	22
40 K	64 Å	40 Å	31	23	116	1.8	2.9	35
100 K	101 Å	55 Å	41	22	33	3.3	6.1	33

* calculated as volume of seven styrenes plus the endgroup, i.e. as t_i

The extent of stretching observed for the 1 K polymer is very limited (1.3), whereas the 100 K chain stretches by a factor of three, at least. Comparison of the t_f/t_i values among the molecular weights show this same trend, but the stretching ratios are larger because of the smaller t_i values. (The numbers in the column headed #sty/1 perfgp were calculated from the XPS data as 1 perfluoroalkyl group per number styrene units.) These calculations are somewhat rough, but they do indicate that the SAP chains have stretched a fair amount to put the perfluoroalkyl groups at the surface, especially in the 100 K polymer case, and that the "final state" structures are not the same as the original (or initial) ones. The graphics below depict a given polymer chain in its unperturbed state (resting comfortably in a cube) and in the elongated conformation that our calculations indicate. The calculated numbers suggest that surface energy minimization is a strong driving force and that a field related to the chemical potential difference between the two system components actually attracts chains to the surface. It seems less likely that such chain stretching would be observed if fluorinated groups migrated to the surface by chance.

Unperturbed

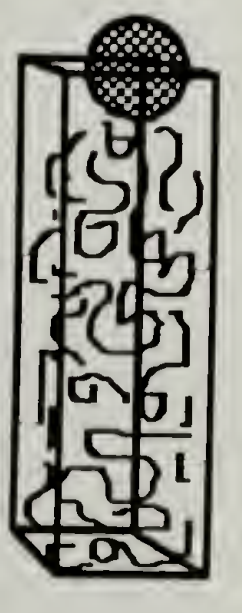

Elongated

Application of Theoretical Surface-Active Polymer Model. Theodorou[15] has developed a site lattice model that can be used to shed light on the structure, in terms of local composition and chain shape, and interfacial properties, namely interfacial tension, of surface-active polymers adsorbing at a surface from the bulk. In this model the surface is considered solid, but the model should still be valid when extended to a polymer-air interface. In Theodorou's model, structural and thermodynamic parameters were examined with respect to chain length (r) and relative surface-adsorption affinity of the system components (χ_s). The model describes the surface-adsorption behavior of linear polymers of the structure AB_{r-1} in which the A segments are surface-active and $r_A = 1$; this means that the surface interaction parameter is positive ($\chi_s > 0$).

Our SAP:E-1 system could be described accurately by this model and our experimental results actually bear out Theodorou's predictions. The model predicts that surface-adsorption by the surface-active moiety causes a surface excess that becomes more pronounced with increasing surface-active chain length and that this enriched surface layer would be followed by a depletion layer because of chain connectivity. In our experiments, we have observed a surface excess of fluorine that increases with the molecular weight of the polystyrene tail on the SAP:E-1 polymers. Examination of the data indicates that the surface excess observed for the 100 K SAP:E-1 films is approximately four times greater than that observed for the 10 K samples. The discrepancy between the 15° and 75° takeoff angle XPS data obtained for these samples indicates that the outermost layers of the surfaces are highly concentrated in fluorine and that a depletion layer containing very little fluorine is beneath. The XPS data indicate that the

F/C values obtained at 75° for the 10 K samples are almost 40% of the 15° takeoff angle values (in plateau region), but the 100 K 75° data are only ~33% of the values obtained at the 15° angle. This suggests that the extent of depletion in the subsurface region is greater in the 100 K case, as would be expected because of the larger chain size.

Comparison of our calculated "unperturbed chain" dimensions with those determined from XPS data obtained for the reconstructed surfaces confirms the validity of Theodorou's prediction that the migration of surface-active chains to an interface would perturb their natural conformation. Our data indicate a considerable amount of chain stretching for the SAP:E-1 chains and this increases with molecular weight. Our calculations indicate that the chains extend downward (perpendicular to the plane of the surface) for a depth that far exceeds the amount of surface area they occupy. It is possible that the shape of the isotherms obtained for the SAPE:-1 samples may be controlled by chain-packing or surface-crowding, especially at the higher molecular weights.

Diffusion Constant. A diffusion constant was sought for polystyrene in an effort to understand how surface-active polymers migrate through the bulk and why they segregate to the surface of a film. Comparison between calculated diffusion constants for polystyrene and the experimentally observed rates of reconstruction was expected to provide information about whether the surface-active groups arrive at the surface by chance as chains in the bulk relax, or whether a "field" exists in the material resulting in an attractive surface force. In the scenario where fluorine surface enrichment

occurs by chance, we would expect that if a perfluoroalkyl group happened to diffuse by the surface (such as when an endcapped chain turned over) it would remain there because of the reduction in surface energy it provided. In the case of a field in the material, the chains would be driven to the surface from a certain depth in a concerted fashion (although diffusion would still be the means of transport). The diffusion constant for polystyrene found in the literature[16] is $1.6 \pm 0.5 * 10^{-10}$ cm^2/sec, measured for 80 K radioactively labelled polystyrene at 237 °C. This is much higher than our use temperature and therefore not considered an appropriate value. The researchers who measured this diffusion constant also tried to obtain a value for diffusion of 100 K polystyrene at 150 °C but found diffusion so slow that no significant diffusion occurred over weeks.[17] These results indicate a strong temperature dependence for the diffusion constant.

In another set of experiments,[18] a diffusion coefficient was measured at 150 °C for a polystyrene-poly(*o*-chlorostyrene) system using energy dispersive analysis of X-ray fluorescence (EDS), and the results of these experiments indicate a diffusion coefficient of $2.32 * 10^{-14}$ cm^2/sec. In the polystyrene-poly(*o*-chlorostyrene) system, the polystyrene sample was monodisperse and had a molecular weight of 20 K, and the poly(*o*-chlorostyrene) sample had a polydispersity of 2.1 and a molecular weight of 160 K. The 150 °C annealing temperature is 25° above the glass transition temperature for poly(*o*-chlorostyrene) and a little more than 50° above that for polystyrene. The physics of polymer-polymer diffusion are fairly complicated because of the influence of many factors, including molecular weight, Tg, polydispersity, chemical nature of the polymer

chains and interactions between diffusing species. In our own SAP:E-1 system, we have blended 1, 5, 10, 40 or 100 K perfluoroalkyl group-endcapped polymer into matrix polymer (Mn = 10 K) and heated at 110 °C which is ~25° above Tg for 10 K polystyrene (at equilibrium). This temperature is considerably higher than Tg for the lower molecular weight SAP polymers, although the difference for the 100 K polymer is only about 10°. In the SAP:E-1 system, as in the polystyrene-poly(*o*-chlorostyrene) system, the halogen-modified polymer is diffusing through a polystyrene matrix and the temperatures chosen (for the two types of experiments) are different in terms of the actual values, but similar with respect to providing mobility to the system. Because of the similarities between these systems, we have used $2.32 * 10^{-14}$ cm^2/sec as a ballpark figure to represent diffusion in our SAP polymer samples.

One model in polymer physics that describes the motion of chains through the bulk is reptation.[19,20] This model suggests that in the bulk free diffusion of polymeric species is not possible due to entanglements with other chains. These entanglements act as fixed obstacles that impede chain motion, as if confining a polymer in a tube. In order to diffuse through the bulk, a chain must wriggle along its tube as the material relaxes. In the simplest form, this model indicates that diffusion varies as

$$D \sim M^{-2} \tag{6.3}$$

and the time for complete conformational change of the chain is[20]

$$\tau \sim M^{3}. \tag{6.4}$$

De Gennes[19] has developed a method for calculating relaxation times (τ_{max}) and diffusion times (D_{rep}) which relate to the time required for a chain to diffuse out of the (original) confining tube (termed tube renewal time). Because the contour of the tube would be affected by external stresses, the velocity (v) of a polymer traveling through a tube depends on the applied force f and the mobility of the molecule in the tube μ_{tube} as[3,19]

$$v = \mu_{tube} f. \tag{6.5}$$

The force felt on the tube would relate to the length of the polymer, n, which means the mobility of the polymer also relates to n as

$$\mu_{tube} = \frac{v}{n} = \frac{\mu_1}{n} \tag{6.6}$$

which makes μ_1 independent of chain length. With this molecular mobility, the diffusion constant for the tube can be calculated from the Nerst-Einstein equation:[3]

$$D_{tube} = kT\mu_{tube} = \frac{kT\mu_1}{n} = \frac{D_1}{n} \tag{6.7}$$

where k is Boltzmann's constant and D_1 is essentially a "prefactor" and does not depend on chain length. Small molecule diffusion indicates that diffusion relates to the average distance (in terms of a random walk) that a molecular species would travel through a medium of diffusion constant D in time t as[21]

$$D = \frac{x^2}{2t} \quad \text{or, solving for time } t = \frac{x^2}{2D}. \tag{6.8}$$

In terms of the reptation model, this can be written in terms of the end-to-end distance of the polymer (R_o) and relaxation time (τ) as[19]

$$D_{rep} \sim \frac{R_o^2}{\tau} \sim \frac{D_1}{n^2} \tag{6.9}$$

which means that knowledge of the prefactor value, molecular weight and either distance traveled or time of travel will lead to the reptation diffusion constant. The rate of diffusion of a polymer through a tube is associated with a maximum relaxation time and the distance it diffuses is tube length (L) (it escapes from its tube). The small molecule diffusion equation indicates that maximum relaxation time must be proportional to the size of the tube (i.e. size of the chain) and combining this with the other equations

$$\tau_{max} \sim \frac{L^2}{D_{tube}} \sim \frac{L^2 n}{D_1} \sim n^3 \tag{6.10}$$

indicates that the maximum relaxation time scales with polymer molecular weight to the third power.

Using de Gennes' reptation model[19] and Gilmore's diffusion coefficient,[18] we have performed rough calculations to determine how surface reconstruction in our system compares to regular diffusion through bulk polystyrene. We normalized Gilmore's coefficient with respect to the average molecular weights of the polymers in his system to obtain a D_1

value equal to $1.88 * 10^{-8}$ cm^2/sec. We divided this value by n^2 (n is meant to represent kuhn segments but in lieu of this value we used DP, degree of polymerization) to obtain diffusion constants for 10 K and 100 K polystyrene. From the diffusion constants we have calculated the length of time (τ) (a tube renewal time) for 10 and 100 K polystyrenes to travel R_o, end-to-end distances which equal 78 Å and 247 Å, respectively. In the 10 K case, τ is on the order of a second and, in the 100 k case, it is on the order of 5 - 6 minutes. Compared to the rates of diffusion for small molecules, these values are exceedingly slow, but in terms of surface reconstruction they are fast. These values of τ have very important implications: they indicate that the surface reconstruction observed in our SAP:E-1 system does not occur merely by chains in the surface region turning over, but rather involves adsorption of chains from deeper in the material. We have observed continued reconstruction up to 72 h for the 10 K samples and 120 h for the 100 K ones. If reconstruction was due soley to chain reorientation at the surface, it would cease after very short times, on the order of τ.

Examination of surface excess values for the 10 and 100 K SAP:E-1 samples series should give an indication of the depth from which surface-segregated SAP polymers originate. For the 10 K SAP:E-1 system, XPS analysis indicates a maximum surface excess range of 9.5 times the bulk F/C value. Using a mass balance equation of the sort $C_1V_1 = C_2V_2$, we can use F/C values (X) to determine a thickness (h) for SAP migration

$$X_{bulk}\ (h) = X_{surface}\ (11\ Å) \qquad (6.11)$$

although 11 Å is not perfectly accurate as a measure of surface thickness because the XPS data is biased high by species concentrated in the outermost surface layers. In the 10 K case, h ranges from 105 Å at the beginning of the plateau, to 44 Å at the end. These values are on the order of 3.3 Rg and 1.4 Rg, respectively, perpendicular to the plane of the surface. These calculations support our postulate that surface reconstruction in these samples occurs via SAP chain migration from the bulk and not (merely) surface reorganization. Considering that diffusion is not "directed" and that distance traveled by a chain end varies with the square root of time (because of the convoluted path), diffusion to the surface should take very long times (days), as we observed in our surface reconstruction systems. For molecular weight comparisons, the 100 K samples exhibited a maximum surface excess value of 36.6. In terms of migration depths, at the begining of the plateau, h is 402 Å, equal to ~3.9 Rg and at the end, h is 286 Å or ~2.8 Rg. These findings are in keeping with Theodorou's prediction[15] that samples of larger surface-active polymers feel perturbations at greater depths than samples containing shorter SAPs. (It is interesting to see that perturbation (or migration) depths are similar when compared on the basis of number of coils affected (i.e. Rg), rather than the laboratory-imposed measurement in terms of Å.) Diffusion of the 100 K polymers would take even longer than for the 10 K ones, and we observed significant differences in the time required for surface reconstruction between samples of these molecular weights. Analysis of the possible rates of SAP polymer diffusion in comparison with the observed rates of surface reconstruction does not imply a concerted transport process (in other words, migration has to rely on diffusional processes). All of the SAP:E-1 samples exhibit large fluorine surface

excesses, in combination with (varied) extents of chain stretching. This indicates that surface-active molecules within a certain depth of the surface adsorb (due to an incompatibility or instability in the bulk polymer) and cause chain crowding in the surface region.

SAP:E-2 Polymer

In the second section of this work, films containing 10 K surface-active polymers functionalized with two perfluoroalkyl endgroups were prepared for comparison with the 10 K SAP:E-1 films. The purpose of these experiments was to shed light on what effect controls the shape of the F/C isotherm at 10 K (i.e. chain packing or surface energy minimization) and to observe the effect of doubling the headgroup size on the surfactant. The expectations were that if surface energy minimization were the major controlling factor, then the SAP:E-2 samples would continue to reconstruct until migration of the SAP chains to the surface became too energetically expensive (i.e. energy tradeoff is no longer favorable). If chain-packing at the surface were the main limiting factor, then the F/C value would double in the SAP:E-2 case because each chain contains twice as much fluorine.

Characterization. SAP:E-2 polymers were prepared by reacting polystyryllithium with epoxypropyltetrahydropyranyl ether (protected glycidol) and subsequent cleavage of the THP group to produce the diol endgroup. Figure 6.17 shows the IR and NMR spectra confirming the structure of the protected glycidol. The PS-2(OH) polymer was reacted with two equiv. perfluorodecanoyl chloride to produce the final polymer (eq. **2** - **3**).

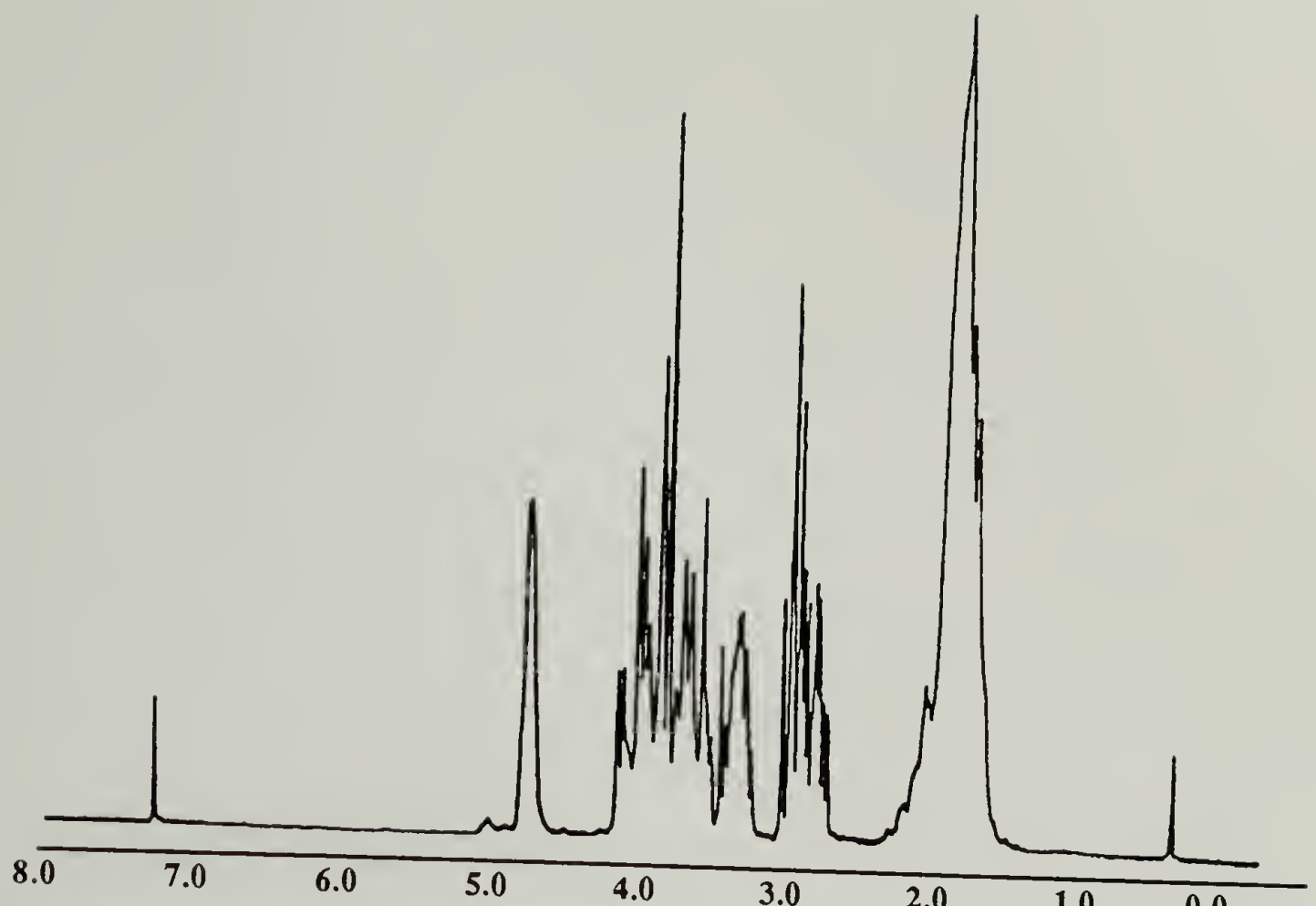

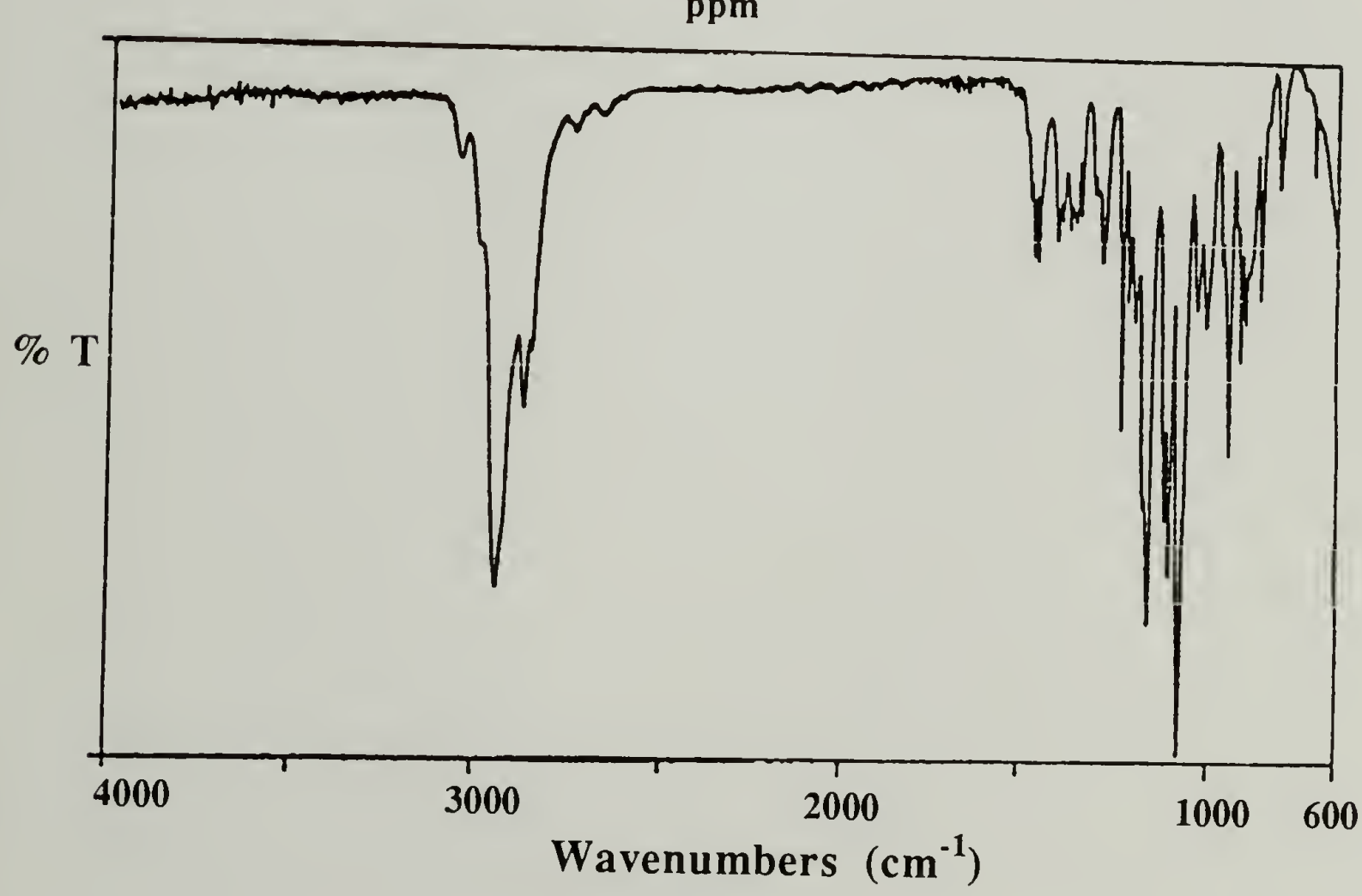

Figure 6.17. IR and NMR Spectra of Epoxypropyltetrahydropyranyl Ether.

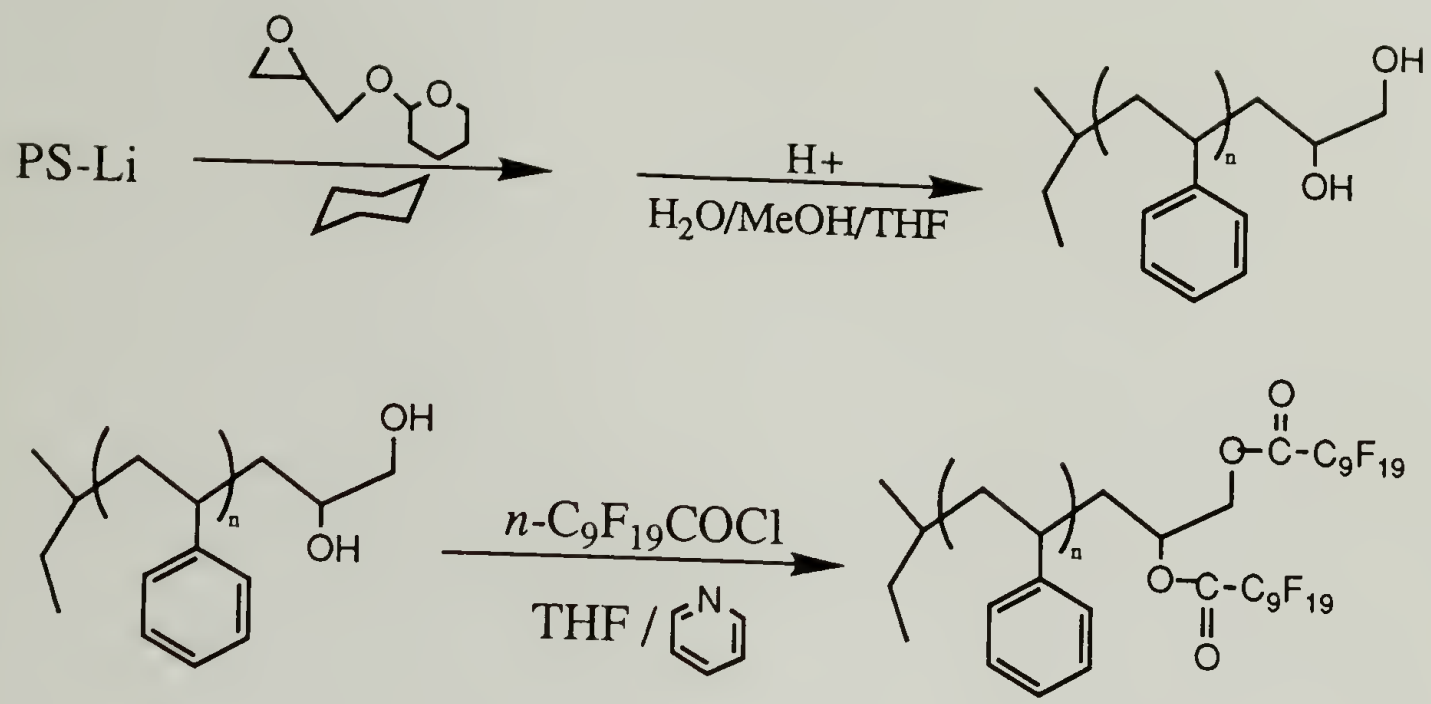

(2)

(3)

SAP:E-2

A 1 K polymer was prepared parallel to the 10 K polymer for characterization purposes. The IR spectra for PS-2(OH) and SAP:E-2 are shown in Figure 6.18. Features in the PS-2(OH) spectrum include a large hydroxyl stretching absorbance, comprised of a broad peak at 3500 cm^{-1} and a shoulder at 3650 cm^{-1}, as well as a C-O stretching band at 1050 cm^{-1}. The spectrum of the SAP:E-2 polymer has no hydroxyl stretching, but has a large peak at 1790 cm^{-1} due to the carbonyl group on each fluorinated ester, and strong absorbances in the 1150 - 1350 cm^{-1} region, indicative of C-F stretching. The NMR spectra for PS-2(OH) and SAP:E-2 are in Figure 6.19. The PS-2(OH) spectrum has peaks at 3.7 and 3.2 ppm due to methine and methylene protons, respectively, on each carbon immediately adjacent to the two alcohol groups. These two peaks shift to 4.7 and 4.0 ppm upon conversion of the alcohol groups to the fluorinated esters in SAP:E-2.

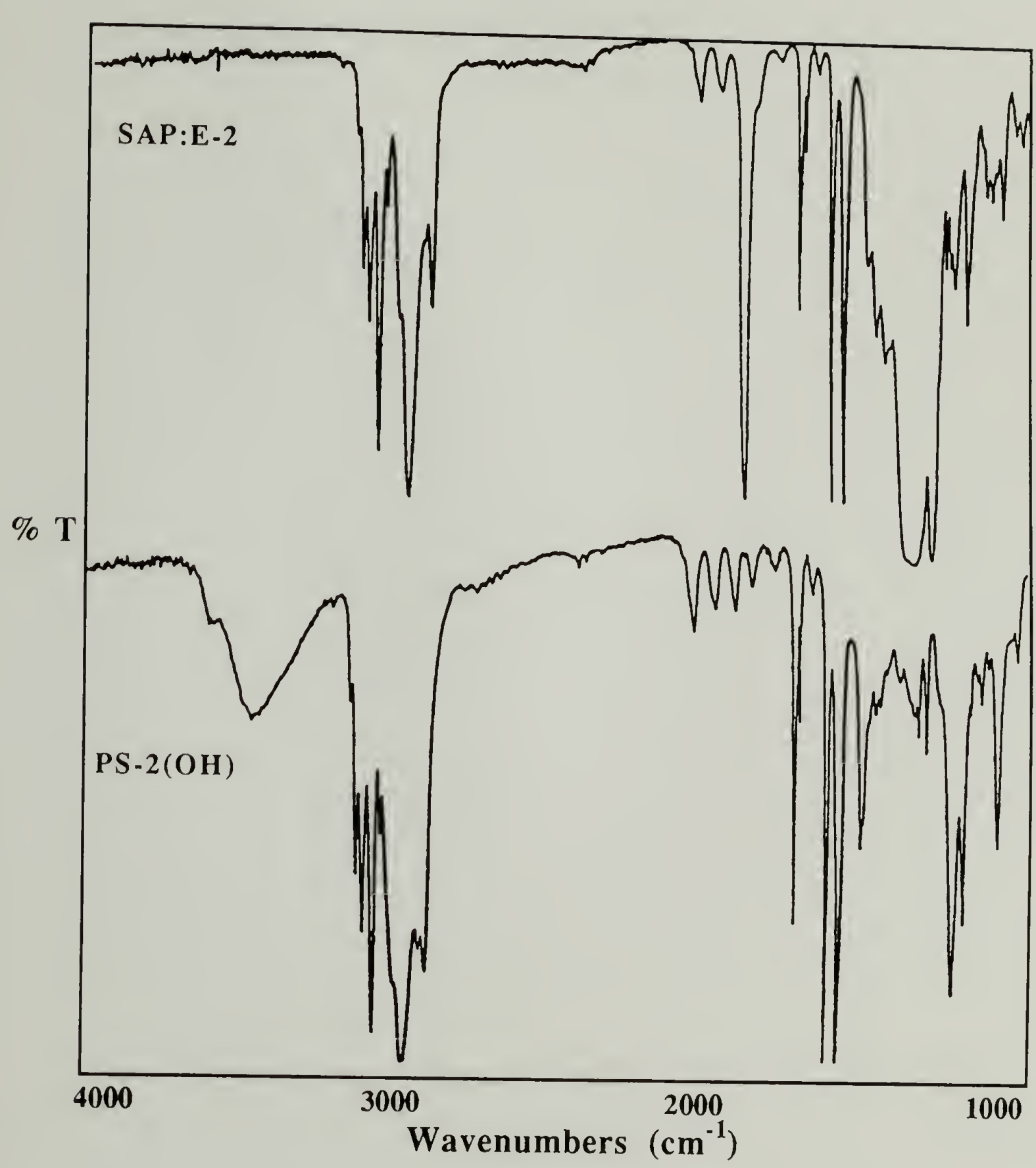

Figure 6.18. IR Spectra of PS-2(OH) and SAP:E-2 Polymers (Mn = 1 K).

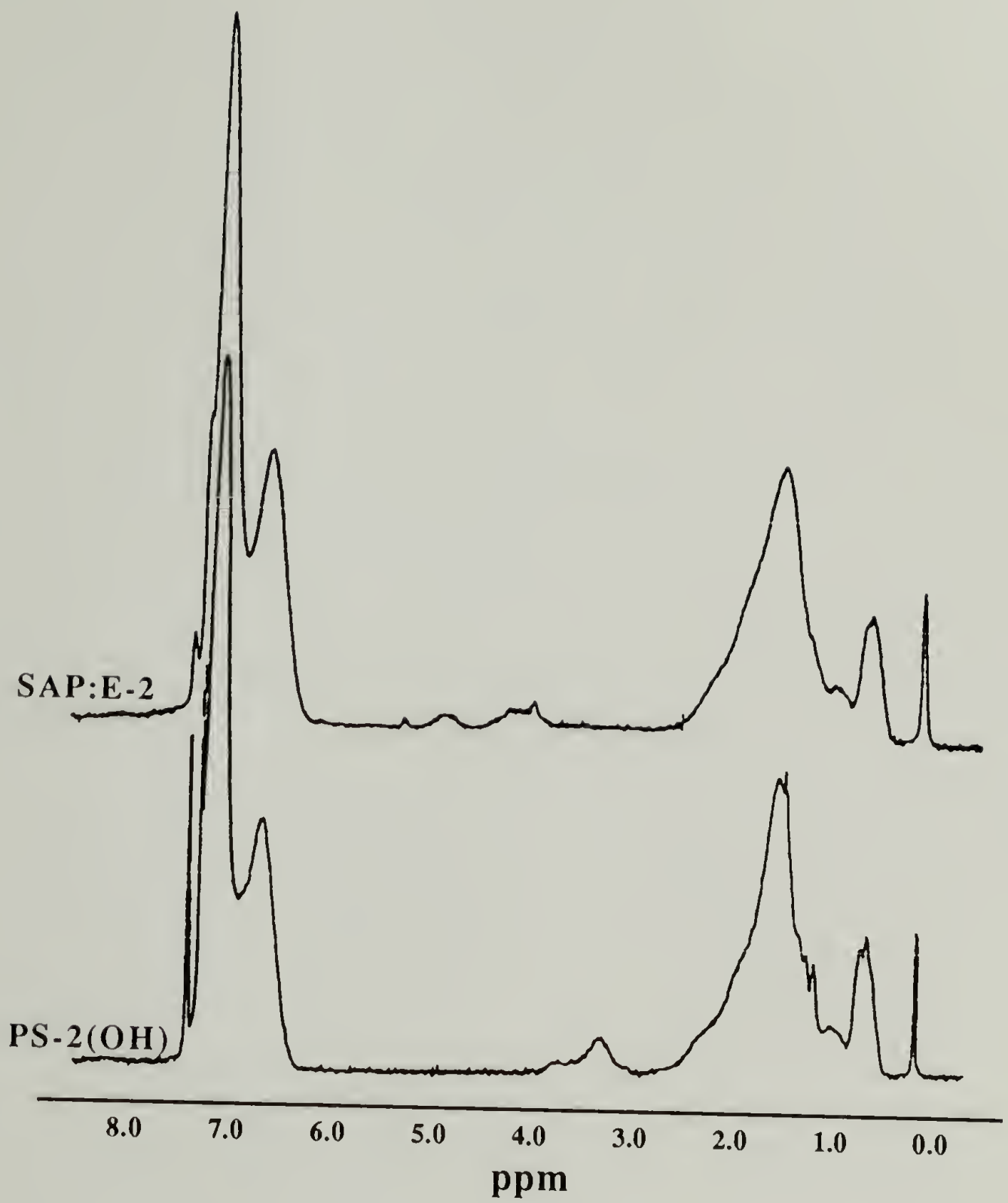

Figure 6.19. NMR Spectra of PS-2(OH) and SAP:E-2 Polymers (Mn = 1 K).

An overlay of the GPC data for the PS-2(OH) and SAP:E-2 polymers for 10 K and 1 K molecular weights has been provided in Figure 6.20 to display the shift in peak position upon conversion to the diester. The shift is more obvious at 1 K because the molecular weight doubles. In the 1 K chromatogram, a bump can be seen on the low molecular weight side of the peak due to monofunctionalized polymer which could also be detected by TLC. In the case of the 10 K polymer, an attempt was made to fractionally precipitate the monofunctionalized polymer out of the sample. The TLC data for these polymers indicated that the 1 K PS-2(OH) did not elute and the 10 K PS-2(OH) spot grew slightly longer but did not elute any distance. The 1 K and 10 K SAP:E-2 polymers eluted a slightly greater distance than polystyrene of corresponding molecular weight and the spots were tear-drop shaped with the point directed at the solvent front. A sketch of the TLC data has been included in Figure 6.21. Table 24 (page 187) contains molecular weight, polydispersity, TLC and elemental analysis data for these polymers.

SAP:E-2 Film Samples. The film samples containing the 10 K SAP:E-2 polymers were prepared in the same fashion and with the same concentrations as the monofunctional SAP:E-1 polymer samples. Kinetics data were not obtained, although slightly longer heating times were investigated briefly to make sure that no further reconstruction would occur beyond 72 h.

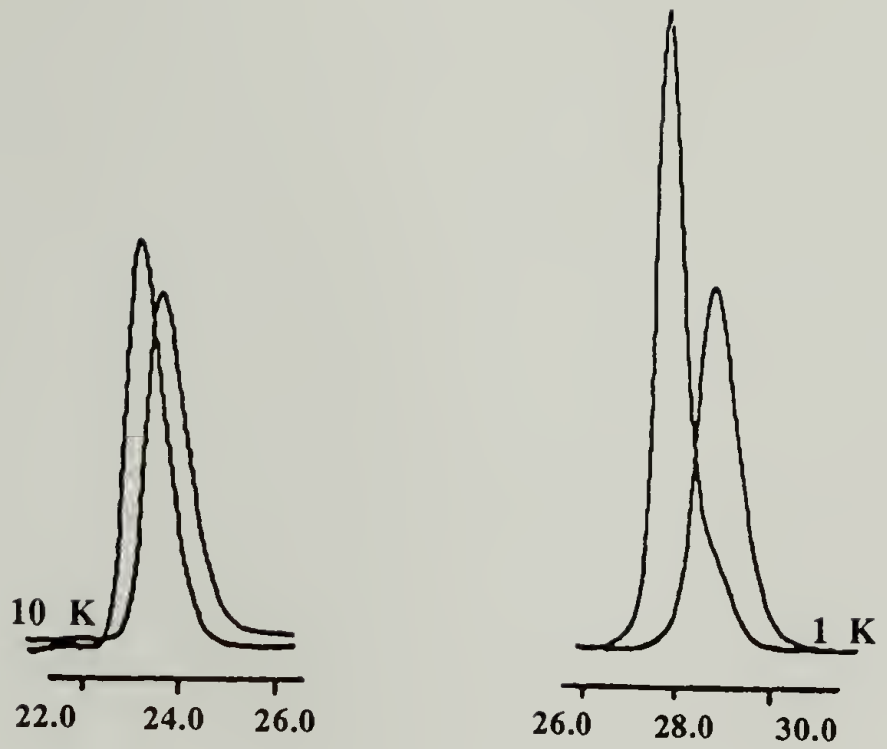

Figure 6.20. Overlaid GPC Data for 10 K and 1 K PS-2(OH) and SAP:E-2 Polymers.

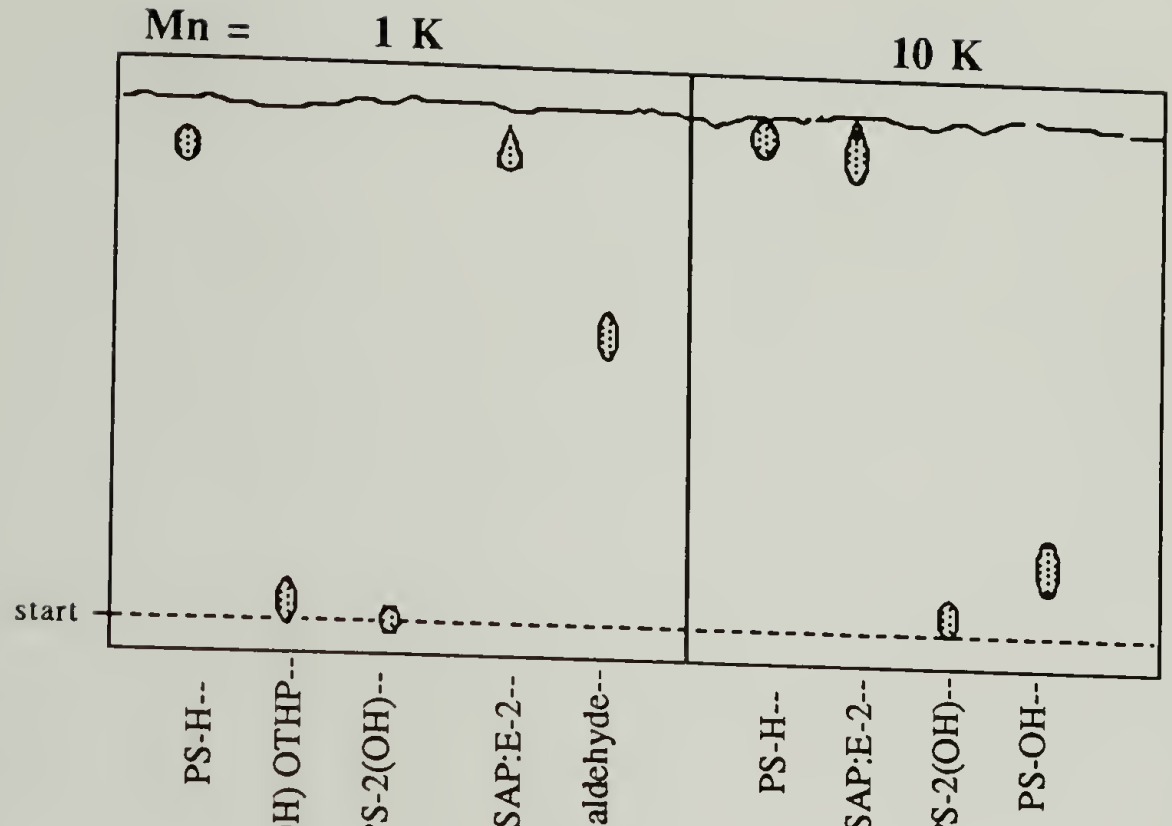

eluent: toluene
plate: glass-backed silica

Figure 6.21. TLC Data for PS-H, PS-2(OH) and SAP:E-2 Polymers with Mn = 1 and 10 K.

Table 24. Molecular Weight (Mn), Polydispersity, Rf and Elemental Analysis Data for SAP:E-2 and SAP:M-1 Polymers.

Polymer	Mn	PDI	Rf	Elemental Analysis (%) C	H	O	F	Empirical Formula
SAP:E-2								
PS(OH)-OTHP	1245	*	.04					
	8485	*	.12					
PS-2(OH)	1245	1.127	00					
	8485	1.035	.08					
PS-2(OF)	3435	1.096	.95					
	9730	1.026	1.0					
Theoretical {PS-2(OF)}				85.15	6.96	.64	7.25	$C_{707}H_{694}O_4F_{38}$
Experimental {PS-2OF)}				84.68	6.92	1.18	7.22	$C_{706}H_{692}O_7F_{38}$
SAP:M-1								
PS-OH	3600	1.054	.15					
PS-OFO-PS	7910	1.033	.97					
Theoretical {PS-OFO-PS}				88.11	7.39	.78	3.73	$C_{598}H_{602}O_4F_{16}$
Experimental {PS-OFO-PS}				87.92	7.68	.86	3.54	$C_{628}H_{659}O_{4.5}F_{16}$

*no gpc data taken

Surface Reconstruction Data for 10 K SAP:E-2 Samples. Data obtained for samples containing varied concentrations of 10 K SAP:E-2 polymer indicate that the size of the surface-active group on a SAP chain does affect surface reconstruction. XPS data was used to construct an isotherm for this sample series; the isotherm is shown in Figure 6.22. Similar to the SAP:E-1 isotherms, the data show increasing F/C with concentration up to a point and then no further reconstruction. The surface F/C plateau value for this plot is ~.125, only slightly higher

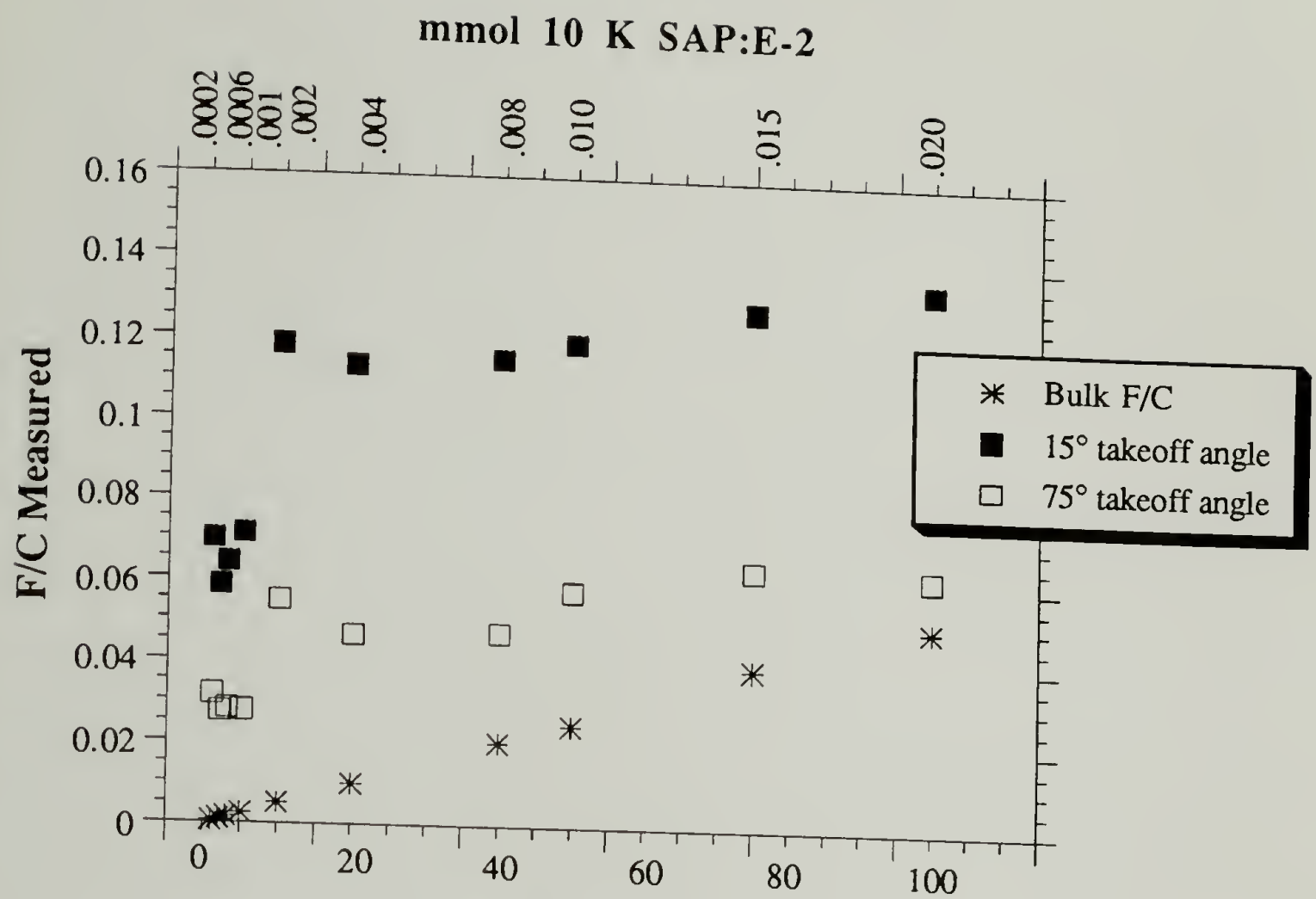

Figure 6.22. Changes in F/C with Concentration for 10 K SAP:E-2 Samples Heated at 110 °C for 72 Hours.

than that for the SAP:E-1 10 K plot, and the knee occurs at ~10% SAP (0.002 mmol) chain concentration. The isotherm for the SAP:E-2 samples is higher affinity than the SAP:E-1 plot, meaning that it rises faster and stops changing at lower concentration. This implies that the two surface-active groups cause the SAP chains to be more surface-active at lower concentration than the monofunctional chains and that SAP:E-2 samples reach a surface-energy minimum at lower concentration. The maximum surface excess observed for the SAP:E-2 samples is 25.1 times the bulk F/C value.

At first glance, the data imply that SAP:E-2 samples have fewer surface-active chains in the surface region than SAP:E-1 samples because the F/C plateau values are comparable although the SAP:E-2 polymers contain twice as much fluorine. However, it may not be possible to draw simple comparisons between these samples because the distribution of fluorine in the surface layers might be different. For example, the discrepancy between 15° and 75° takeoff angle data shown in the SAP:E-2 isotherm is smaller than that observed for 10 K SAP:E-1 samples. The 75° SAP:E-2 F/C value is roughly 50 % of the 15° value, whereas the 75° SAP:E-1 value is only ~40 %. These data indicate that the outer 11 Å of the SAP:E-2 samples is somewhat more homogeneous in fluorine concentration than the SAP:E-1 samples. One explanation for these data is that both perfluoroalkyl groups on each SAP may not be positioned at the very surface of the film; for some chains one fluorinated group could be at the surface and the other just below. In this scenario, there may be the same number of SAP chains in the surface region for the SAP:E-2 samples as for the SAP:E-1 films, but the different distribution of perfluoroalkyl

groups causes the 15° takeoff angle data not to reflect this (i.e. F/C is not twice as large in SAP:E-2 case). (In truth, the 75° data do not support this because the F/C values are too low). A second (and much better) explanation is that there are fewer SAP chains in the surface region in the SAP:E-2 samples (compared to the SAP:E-1 samples), some of these with two perfluoroalkyl groups at the surface and others with only one, and a greater concentration of SAP chains in the region immediately below the surface. In either case, the controlling factor for surface reconstruction in these films seems to be surface energy reduction more than chain-packing at the surface. The driving force for putting perfluoroalkyl groups at the surface does not draw the same number of chains (assuming that each chain has both endgroups in the surface region) as were at the surface in the SAP:E-1 samples, but rather draws almost the same amount of fluorine (in terms of F/C ratio). This suggests a surface energy minimum is attained (with respect to the thermodynamics of the system). At this point, it may be important to emphasize that the controlling influence in 10 K SAP film reconstruction may not be the most important factor in films containing different molecular weight polymers; generalizations may not be accurate.

The contact angles measured for the SAP:E-2 films were higher than the values measured for any other reconstructed surface, even those with higher F/C plateau values. Water contact angles are $\theta_A/\theta_R = 103°/82°$ and with hexadecane, $\theta_A/\theta_R = 54°/46°$. For comparison, the contact angles for the 1 K SAP:E-1 samples with F/C = .329 are water: $\theta_A/\theta_R = 101°/79°$ and hexadecane: $\theta_A/\theta_R = 47°/35°$, and for teflon (F/C = 2), water and hexadecane contact angles are $\theta_A/\theta_R = 120°/89°$ and $\theta_A/\theta_R = 52°/45°$, respectively. The contact angle measurements for the SAP:E-2 films

suggest that at least some of the fluorine in the sample must be concentrated in the very outer surface layers to give such high contact angles. In cases cited in the literature,[4] researchers have discovered exceptionally high contact angle values for surfaces in which packing of CF_3 groups can occur, for example, the critical surface tension measured for close-packed monolayers of CF_3 groups is 6 dyn/cm.[8] Packing of CF_3 groups is unlikely for these samples, due to dilution by polystyrene. The best explanation for these data is that CF_3 endgroups comprise a greater percentage of the fluorinated species on the surface relative to the other samples examined, and the net effect is a significant increase in contact angles.[22] Figure 6.23 shows advancing contact angle data for all three 10 K SAP polymers (including SAP:M-1 which is discussed below) using water as the probe fluid and Figure 6.24 shows the data obtained using hexadecane as the probe fluid. Note that these data are plotted as mmol surface-active polymer which means that at each data point, SAP:E-2 polymer samples contain twice as much fluorine in the bulk than the other samples.

SAP:M-1 Polymer

In the last section of this work, films containing 10 K surface-active polymers middle-functionalized with a perfluorosebacate group were prepared for comparison with the 10 K SAP:E-1 and SAP:E-2 films. The purpose of these experiments was to examine the effect of perfluoroalkyl group position on its effectiveness as a surface-active moiety. From data obtained and information in the literature, it is apparent that endgroups are an important influence controlling the surface tension of a polymer sample. Chain ends concentrate at the polymer-air interface to reduce surface

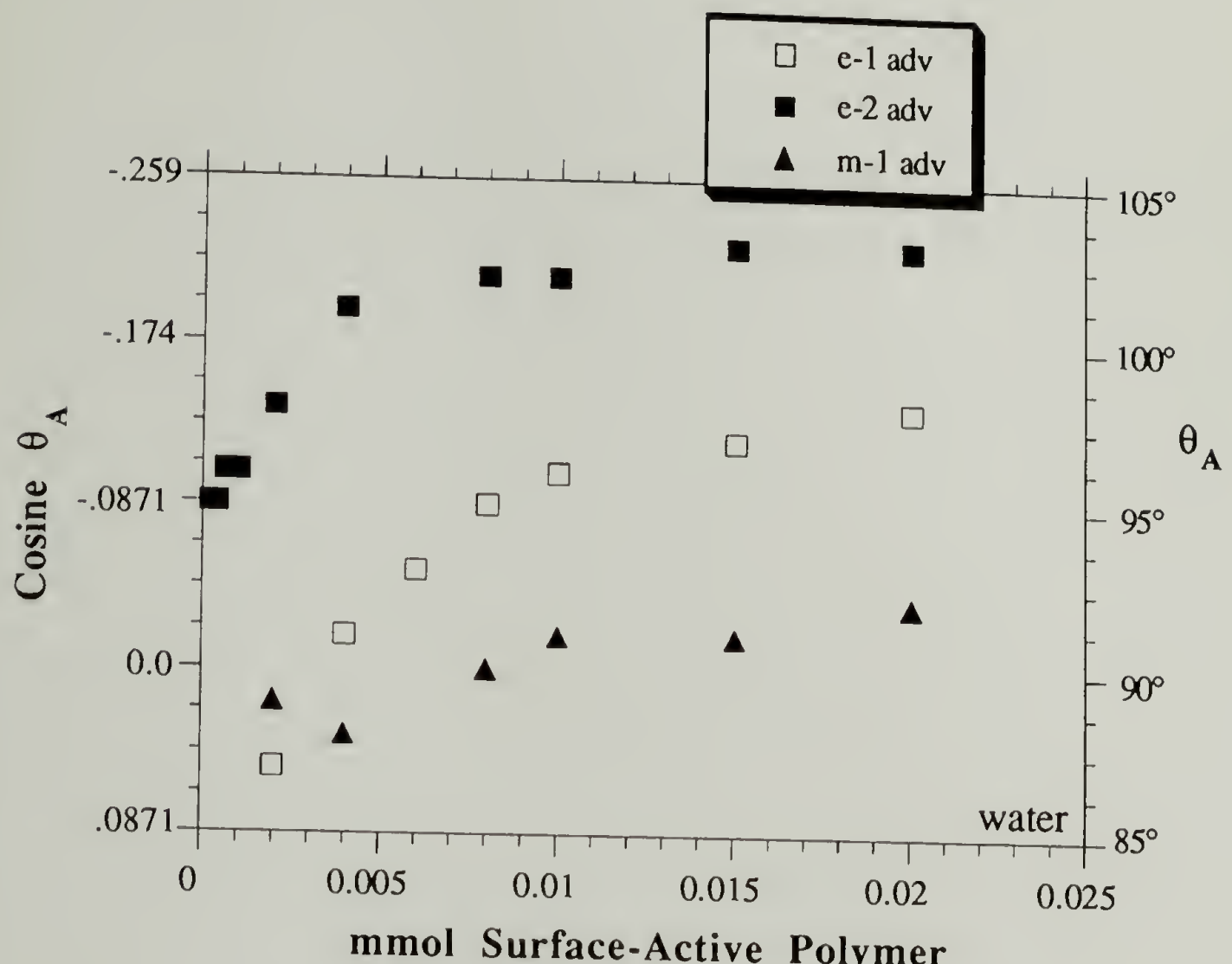

Figure 6.23. Comparison of Advancing Contact Angle Data for 10 K SAP:E-1, SAP:E-2 and SAP:M-1 Polymers Using Water as the Probe Fluid.

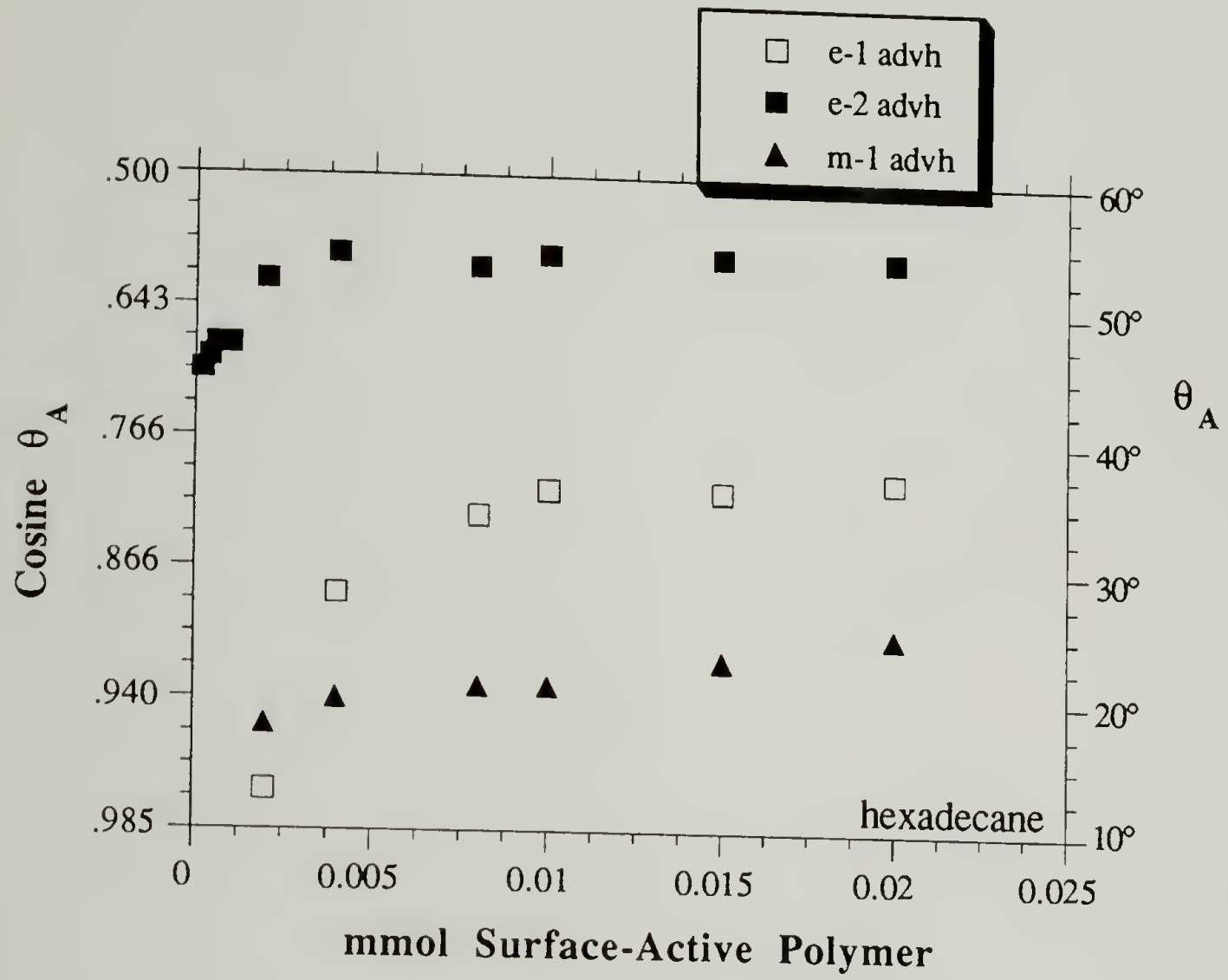

Figure 6.24. Comparison of Advancing Contact Angle Data for 10 K SAP:E-1, SAP:E-2 and SAP:M-1 Polymers Using Hexadecane as the Probe Fluid.

tension, so positioning a perfluoroalkyl group at the end of a chain (as in the SAP:E samples) might facilitate this effect. In order to separate the chain-end effect from the surface-activity effect of the fluorinated species, the perfluoralkyl group was put in the middle of the chain and surface reconstruction was monitored under the same conditions used for the 10 K SAP:E-1 and SAP:E-2 samples. Slightly longer times were also examined to make sure that no further reconstruction would occur for these samples. The expectation was that these middle functionalized SAPs would not be as surface-active as the other polymers used because chain middles have less mobility than chain ends. Further, entropic considerations make constraint of the middle of the SAP:M-1 polymer less favorable and therefore less likely.

Characterization. The SAP:M-1 polymers were prepared by coupling two alcohol-terminated polystyrenes with perfluorosebacoyl chloride and the 10 K polymer prepared for film sample experiments was

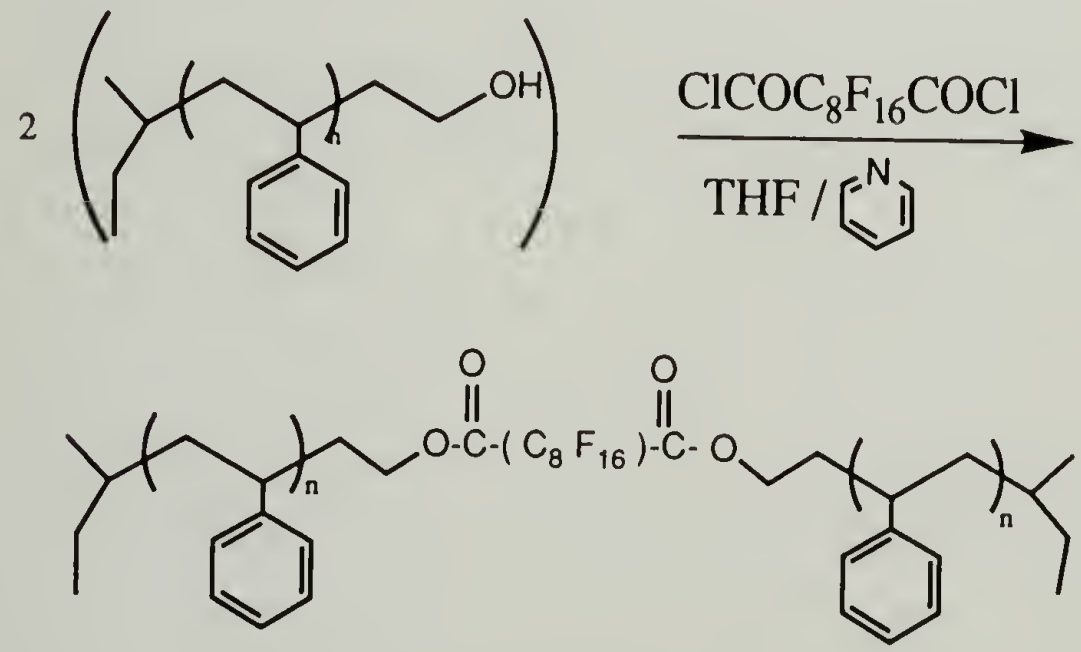

(4)

SAP:M-1

also used for spectroscopic characterization. The IR and NMR spectra for the SAP:M-1 polymer are in Figure 6.25. The IR has a fairly large peak at 1787 cm^{-1} due to the two carbonyl groups on each end of the perfluorosebacate group, and strong absorbances in the 1150 - 1350 cm^{-1} region, indicative of C-F stretching. The NMR spectrum has a broad peak at ~3.8 ppm due to the sets of methylene protons immediately adjacent to the fluorinated ester groups. These features are smaller than those observed in the spectra for the SAP:E polymers analyzed because of the difference in molecular weight.

The SAP:M-1 polymers were prepared using a slight excess of alcohol-terminated polystyrene and some of the low molecular weight homopolymer remained in the sample after the coupling reaction despite efforts to fractionally precipitate out these chains. The GPC data indicate a low molecular weight tail for the coupled polymer and the TLC data show a light spot that elutes from the start up to the same distance that PS-OH would travel. This light spot, due to unreacted PS-OH and half-reacted PS-OF-(acid), grew lighter with fractional precipitation.The GPC trace and a sketch of the TLC data are included in Figure 6.26. An interesting feature of the TLC data is that the SAP:M-1 polymer elutes about the same distace as polystyrene of the same molecular weight, but the spot is longer and narrower. Elemental analysis indicates roughly 95% of sample is SAP:M-1 polymer. Molecular weight, polydispersity, elemental analysis and TLC data for these polymers have been summarized in Table 24 (page 187).

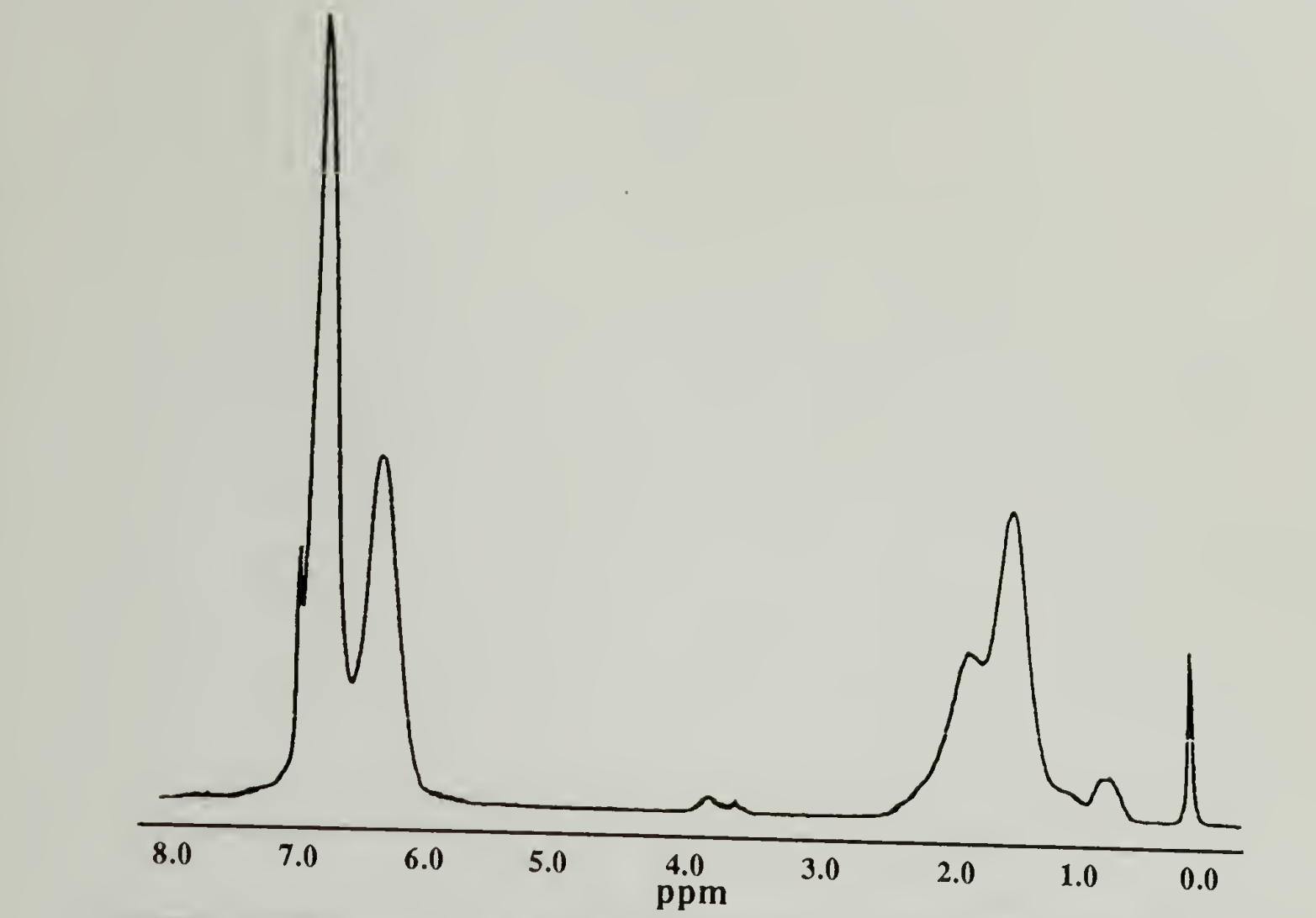

Figure 6.25. IR and NMR Spectra of SAP:M-1 Polymer (Mn = 10 K).

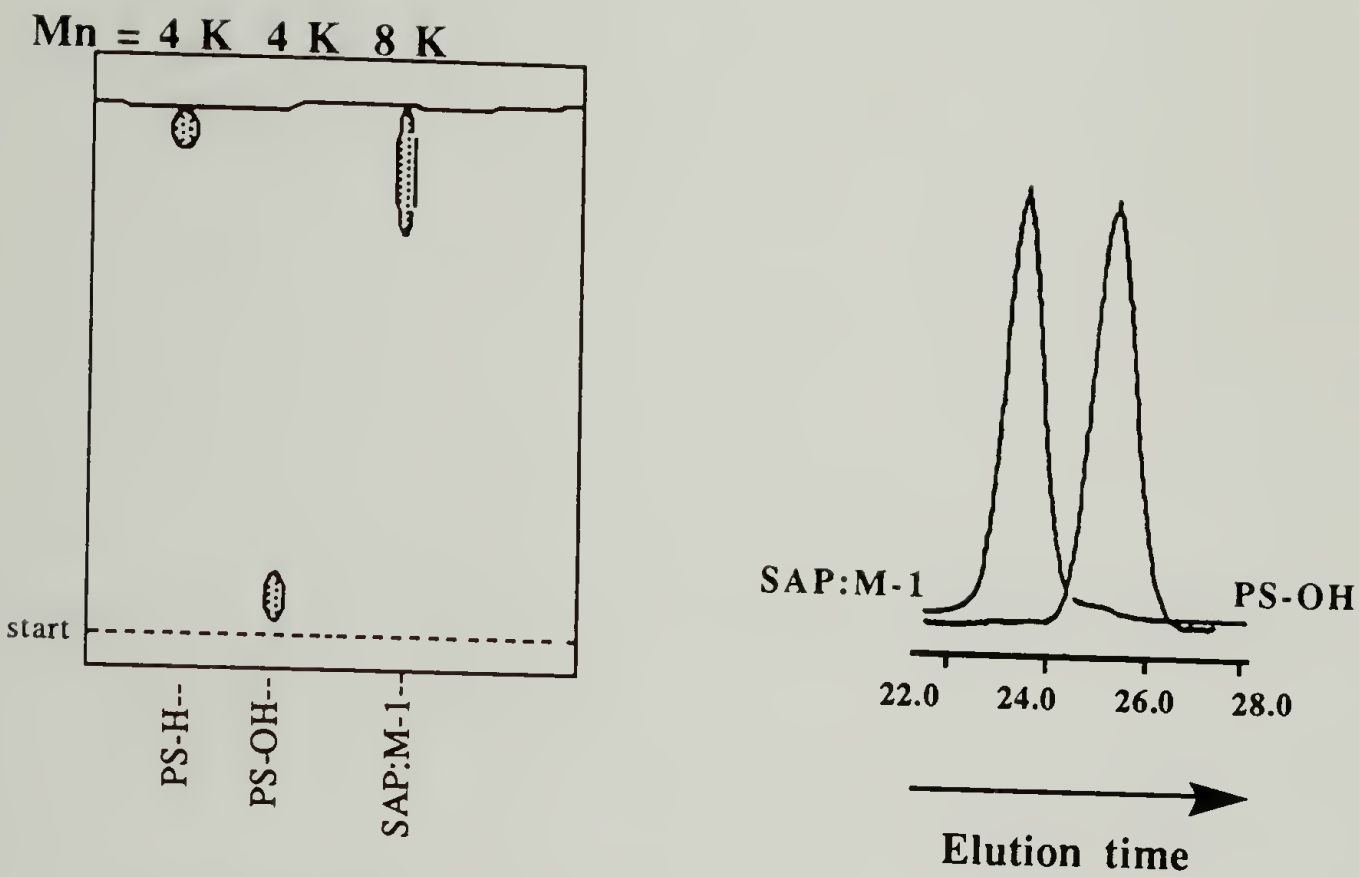

eluent: toluene
plate: glass-backed silica

Figure 6.26. TLC and Overlaid GPC Data for PS-OH and SAP:M-1 Polymers.

SAP:M-1 Film Samples. The film samples containing the 10 K SAP:M-1 polymers were prepared in the same fashion and concentrations as the mono- and di- functional SAP:E samples. Kinetics data were not obtained, although slightly longer heating times were investigated briefly to make sure that further reconstruction would not occur beyond the 72 h time interval.

Surface Reconstruction Data for 10 K SAP:M-1 Samples. The XPS and contact angle data indicate that some (limited) reconstruction does occur with the SAP:M-1 samples. XPS data was used to construct an isotherm for this sample series; the isotherm is shown in Figure 6.27. The isotherm for these samples shows a small increase in F/C with concentration, but not nearly as much as seen in the data for the end-functionalized SAP samples. The surface F/C plateau value for this plot is ~0.033 and begins at ~30% SAP chains (0.006 mmol), and the maximum surface excess is 3.9 times the bulk F/C value. The 75° takeoff angle data indicate that at lower concentrations the F/C ratio exceeds the bulk value slightly, but not at the higher concentration end. Water contact angles for the plateau region are θ_A/θ_R = 92°/79° and for hexadecane, θ_A/θ_R = 25°/19°. These contact angle values are higher than those obtained for polystyrene film samples, but are the lowest obtained for any of the reconstructed surfaces; this was the expected result, based on the low F/C ratio observed. (Plots of the contact angle data are shown in Figures 6.23 and 6.24, pp. 192-193, in comparison to the 10 K SAP:E-1 and SAP:E-2 data.)

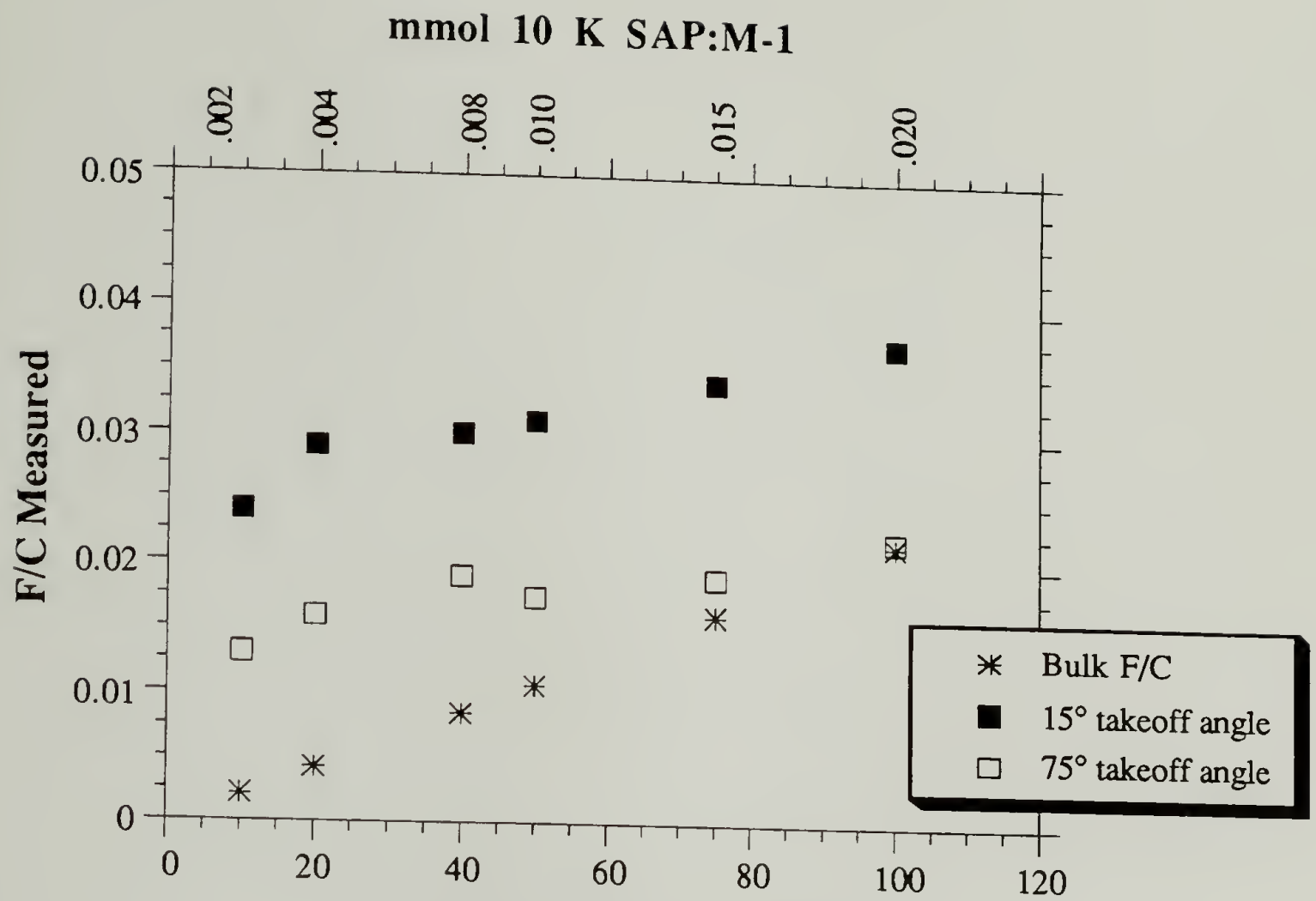

Figure 6.27. Changes in F/C with Concentration for 10 K SAP:M-1 Samples Heated at 110 °C for 72 Hours.

We can determine (roughly) the depth from which SAP:M-1 chains migrate to the surface using the mass balance equation 6.11. From the F/C data at the point of maximum surface excess, we determine that the SAP:M-1 chains move from a depth of only ~43 Å which is comparable to 1 Rg for a 10 K (polystyrene) chain. This result indicates that these chains, unlike the SAP:E-1 case, are not migrating to the surface from the bulk, but rather that chains in the top layer of the surface region are "turning over". The reduction in surface energy attained in putting perfluoroalkyl groups at the surface may cause chains in the surface region to maintain this arrangement. As successive chains turn over (and stay), the net effect is a slight (~4X) excess of perfluoroalkyl groups at the surface.

The limited fluorine surface-enrichment observed for these samples relative to the end-functionalized polymers can be attributed to the position of the surface-active group, and can be rationalized to a certain extent with entropic considerations. To maximize the amount of fluorine at the surface the SAP:M-1 chain would have to be pinned in the middle (shaped like a staple). The entropy of a chain is reduced further by a middle constraint than an end constraint because of chain connectivity. The middle-constrained chain would have twice as many next-neighbor segments that are also constrained, compared to the end-constrained chain. Because adsorption at a surface is governed by thermodynamics, entropic unfavorability can overcome enthalpic gains. The limited increase in surface F/C values measured for SAP:M-1 samples could result from the position of the perfluoroalkyl group relative to the chain ends. Using the reptation model to describe the motion of polymer chains through the bulk, the chains are considered to be confined in a tube through which they move

(reptate) from their ends.[18,19] Travel by an endgroup would be facilitated by the greater free volume associated with it and its progress would be detected sooner because it leads the chain through the tube. If the surface-active moiety is less effective (compared to the SAP:E-1 or SAP:E-2 samples) surface reconstruction may require much longer times; it is possible that the time required to achieve an actual surface energy minimization for these samples is longer than practicality would permit.

Comparisons Among 10 K SAP Samples

XPS and contact angle data obtained for 10 K SAP:E-1, SAP:E-2 and SAP:M-1 samples indicate that surface-active group size and SAP chain architecture both influence surface reconstruction. A comparison of XPS survey spectra for 100% SAP chain samples of each type is provided in Figure 6.28 to show the relative carbon, fluorine and oxygen peak sizes; the SAP:M-1 spectrum contains the greatest concentration of oxygen because there are two ester groups (four oxygens) per surface-active group (eight CF_2). Figure 6.29 compares the F/C values for the 10 K SAP polymers on a percent chain basis (no bulk F/C data is provided). Comparison of the data shows that the increase in F/C with concentration for the SAP:M-1 samples is much less than for the end-functionalized polymers, and the surface excess for these samples is lower, as well. Figure 6.29 indicates that the F/C values for the SAP:E-2 samples are higher than those for the SAP:E-1 films. At low concentrations (~10% SAP chains), the F/C value for the SAP:E-2 samples is twice that observed for SAP:E-1 films (0.06 vs. .12). After this point, the F/C data for the SAP:E-1 samples rise faster than those for SAP:E-2 films, and at high

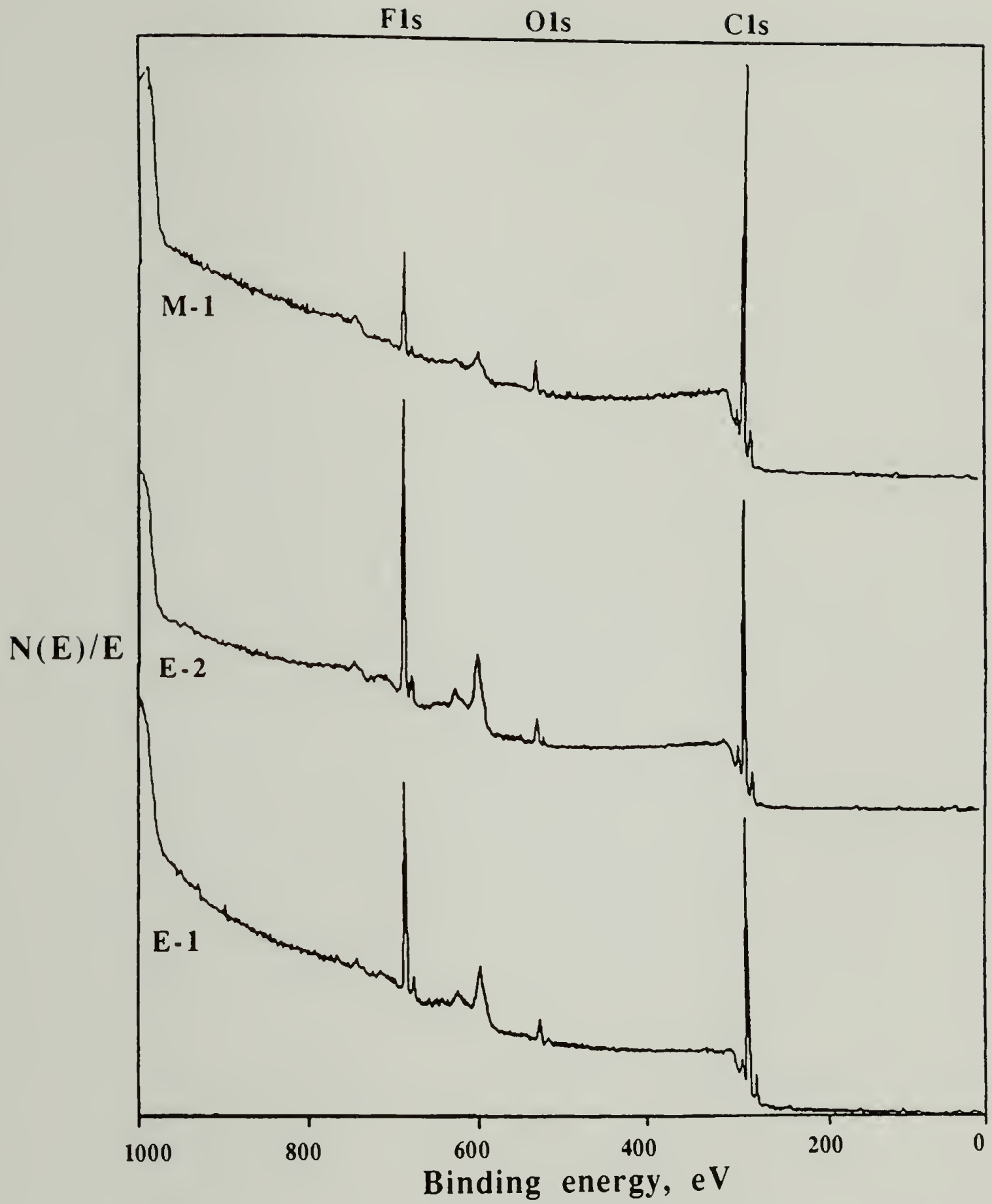

Figure 6.28. Comparison of XPS Survey Spectra Among 10 K SAP:E-1, SAP:E-2 and SAP:M-1 Samples at 100% Concentration.

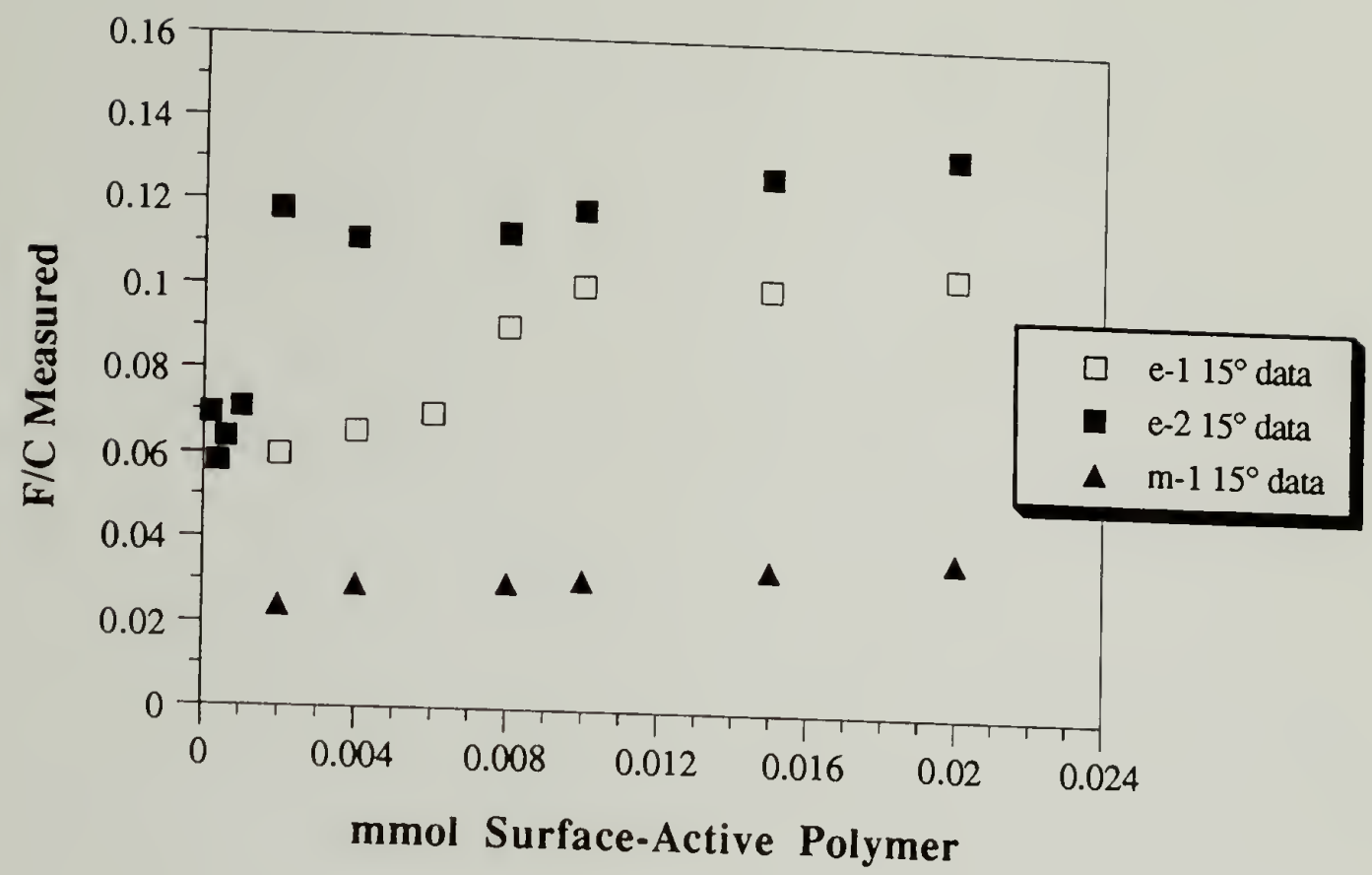

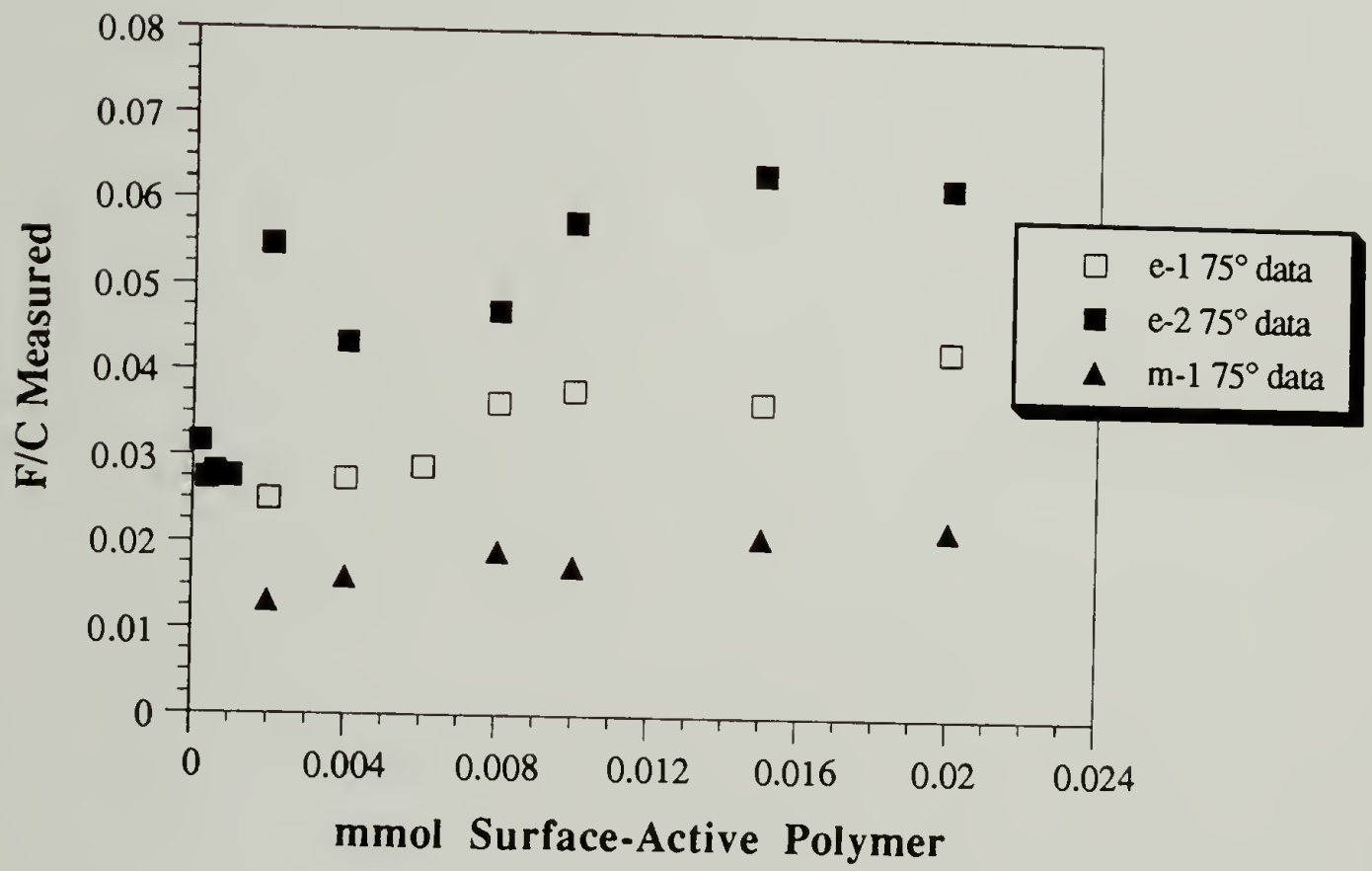

Figure 6.29. Comparison of Changes in F/C with Concentration Among 10 K SAP:E-1, SAP:E-2 and SAP:M-1 Polymers.

concentration, the difference is much smaller (.105 vs. .123). The surface excess values for these two SAPs are comparable, although the plateau occurs sooner for the SAP:E-2 films which makes the surface excess range considerably wider.

Comparison of Surface Reconstruction for All SAPs

A comparison of the data obtained for each SAP polymer was made to shed light on how molecular weight, chain architecture and surface-active group size would influence F/C values at the plateau. A plot comparing these data is shown in Figure 6.30. These data indicate that lower molecular weight SAP:E-1 samples achieve higher F/C values at the plateau than any other SAP. This is partly due to the fact that these samples contain more fluorine originally. The plateau F/C values decrease with increasing molecular weight although 40 K and 100 K SAP:E-1 samples have roughly the same plateau value. The contact angle data for these (SAP:E-1) films (refer to Figures 6.15 and 6.16) indicate a similar pattern. The 1 K SAP:E-1 samples have the highest contact angles, and the higher molecular weight samples have the lowest. It is interesting that the 100 K samples have slightly higher contact angles than the 40 K samples (although these values are fairly close) and that the 10 K samples have the same contact angles as the 5 K samples, despite differences in 15° takeoff angle XPS data. These data suggest that greater extents of chain stretching are observed for the surface-active polymers in the surface region (sampled by XPS) of the higher molecular weight SAP:E-1 sample of each pair (5 and 10 K, 40 and 100 K). The F/C values for SAP:M-1 samples at the plateau are considerably lower than the values for other SAP samples,

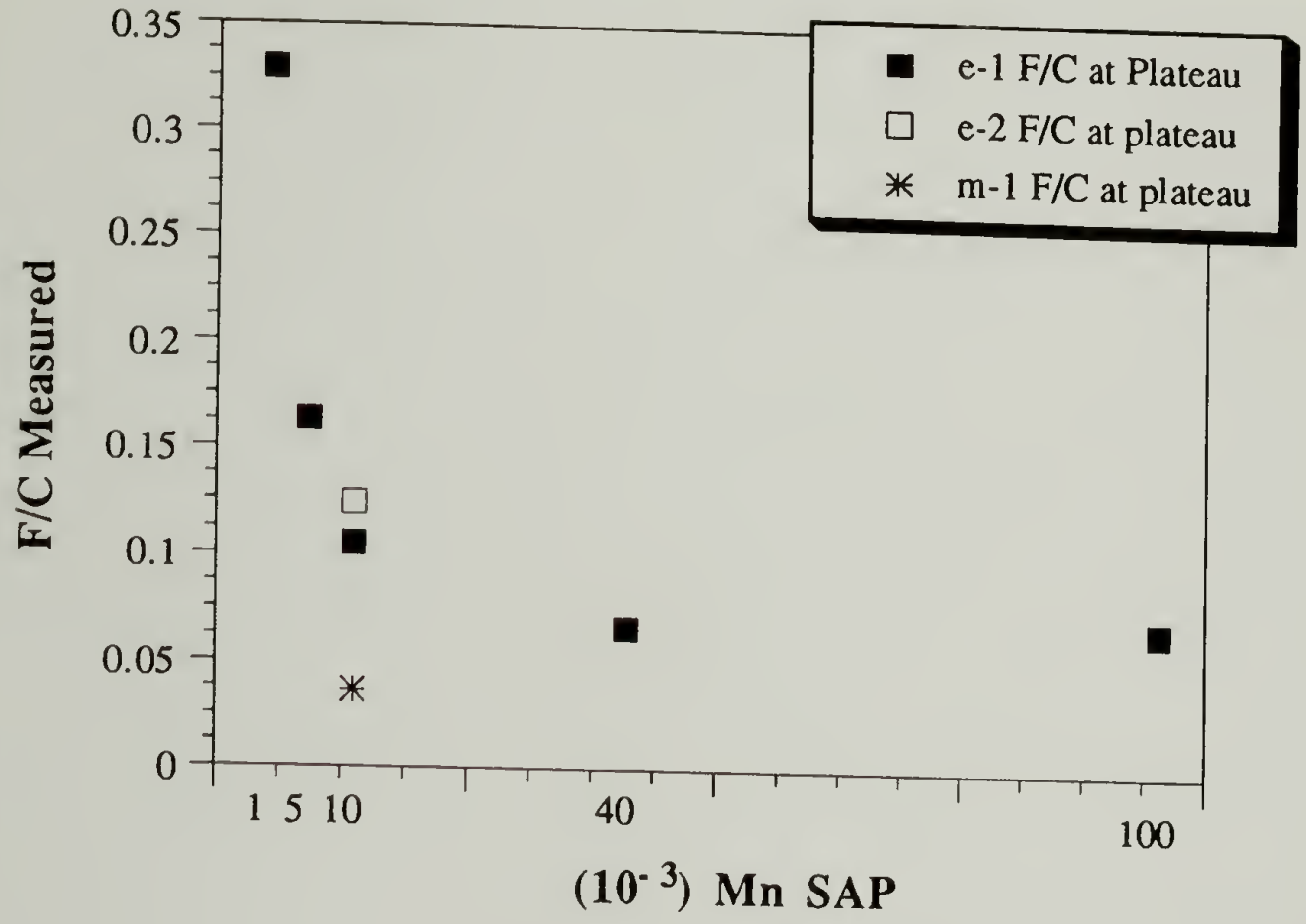

Figure 6.30. Comparison of F/C Values at Plateau for SAP Polymers.

as are the contact angle values. The F/C value for SAP:E-2 samples at the plateau value is somewhat higher than that observed for 10 K SAP:E-1 samples, and the contact angles indicate low wettability for this surface. The high contact angles have been attributed to the number of CF_3 groups in the surface region.

Conclusion

Surface reconstruction was observed for heat-treated films containing varied concentrations of polystyrene molecules functionalized with perfluoroalkyl groups. The driving force for this reconstruction is surface energy minimization, and certain molecular and environmental parameters affect surface-segregation of the functionalized polymers. For example, increasing the molecular weight of the polystyrene tail increases the amount of time needed for reconstruction and this reconstruction ceases at lower SAP chain concentration. On a simple level, surface-migration observed for the surface-active polymers in this system occurs on roughly the same time scale predicted by diffusion coefficients obtained from the literature or estimated from the reptation model. However, the data calculated to determine the dimensions of chains at the surfaces of SAP:E-1 films indicate that chains are fairly stretched and oriented. This suggests that, although surface reconstruction depends on diffusion, another effect, such as a field effect which actually attracts the surface active species to the surface, must also be important. A controlling factor limiting migration of surface-active chains could be chain packing at the surface, especially at higher molecular weights. Chain architecture is an important influence controlling surface-migration. The data obtained indicate that a surface-

active endgroup is more effective than a surface-active chain middle, at least on the time scale of these measurements. Further, the data indicate that doubling the surface-active endgroup increases surface activity at lower SAP concentrations but does not double the maximum fluorine surface-enrichment.

References

1. Iyengar, D.R.; McCarthy, T.J. *Macromolecules* **1990**, *23*, 4344.
2. Fox, T.G., Jr.; Flory, P.J. *J. Appl. Phys.* **1950**, *21*, 581.
3. Aklonis, J.J.; MacKnight, W.J. *Introduction to Polymer Viscoelasticity*, 2nd ed. Wiley Interscience, New York, 1983, p. 41.
4. Höpken, J.; Möller, M. *Macromolecules* **1992**, *25*, 1461.
5. Fox, R.B.; Price, T.R.; Cain, D.S. *Adv. Chem. Ser.* **1968**, *87*, 72.
6. Fox, R.B.; Price, T.R. *Adv. Chem. Ser.* **1968**, *87*, 96.
7. Costello, C.A.; McCarthy, T.J. *Macromolecules* **1987**, *20*, 2819.
8. Zisman, W.A. *Adv. Chem. Ser.* **1964**, *43*, 1.
9. Billmeyer, F.W. *Textbook of Polymer Science*, 3rd ed. Wiley Interscience, New York, 1984, p. 153.
10. Billmeyer, F.W., in Reference 9, p. 176.
11. Andrade, J.D.; Gregonis, D.E.; Smith, L.M. In *Surface and Interfacial Aspects of Biomedical Polymers*; Andrade, J.D. ed. Plenum: New York, **1986**, Vol. , Ch. 2.
12. Brandup, J.; Immergut, E.H., eds. *Polymer Handbook*, 2nd ed.Wiley Interscience, New York, **1975**, p. V-59.
13. Flory, J.P. *Principles of Polymer Chemistry*, Cornell University Press: New York, 1953, Ch. X.
14. Reference 12, p. IV-39.
15. Theodorou, D.N. *Macromolecules* **1988**, *21*, 1422.
16. Bueche, F. *J. Chem. Phys.* **1968**, *48*, 1410.
17. Bueche, F.; Cashin, W.M.; Debye, P. *J. Chem. Phys.* **1952**, *20*, 1956.
18. Gilmore, P.T. Ph. D. Thesis, Univ. of Mass., 1978.
19. de Gennes, P.G. *Scaling Concepts in Polymer Physics,* Cornell University Press, New York, **1979**.
20. Graessley, W.W. In *Advances in Polymer Science*; Springer-Verlag, NewYork, **1982**, p. 67.

21. Eisenberg, D.; Crothers, D. *Physical Chemistry*, Benjamin/Cummings Publishing, London, 1979, Ch. 15.

22. Reardon, J.P.; Zisman, W.A. *Macromolecules* **1974**, *7*, 920.

APPENDIX A

MISCELLANEOUS SAP EXPERIMENTS

In a few cases, several secondary experiments were run to learn more about the parameters influencing surface reconstruction in the SAP:E-1 polymer system. For the most part, the data obtained are interesting, but do not necessarily lead to a conclusion and so are discussed only briefly.

Surface Reconstruction for 1 K Samples at 60 °C

A few experiments were carried out to observed what effect heating the 1 K SAP:E-1 samples at a temperature lower than the Tg of the film would have on surface reconstruction. Three concentrations of 1 K SAP film were prepared and heated at 60 °C for 24, 48 and 72 h, and the samples were analyzed by XPS and contact angles. One interesting effect noticed with these films is that the lowest concentration sample (10% SAP chains) had a smooth surface after heating under vacuum, but the 52 and 71% SAP chain samples foamed and the tiny bubbles remained even after heat treatment. Compared to other SAP samples the foaming behavior is not unusual. Samples containing more (or better) surfactants tended to foam and samples with fewer (or less) surface-active moieties would have large bubbles. However, bubbles usually were gone by the time of analysis. The samples containing lower SAP concentrations heated to 60 °C for 72 h show slightly more surface reconstruction than the 110 °C

samples, but the higher concentration samples are about the same. One interpretation of this result is that at the lower concentrations the driving force for reconstruction is reduced at the higher temperature (surface tension decreases with increasing temperature), but the highest concentration is not affected because a surface energy minimum has been attained. Reports in the literature indicate that surface tension decreases with increasing temperature[1] and that the chemical potential that favors having the lowest energy component at the surface also decreases with rising temperature.[2] Other interpretations of these results are possible, but the data is insufficient for a conclusion.

Backside and Glass Surfaces of 1 and 10 K Films

The backsides of 1 K and 10 K SAP:E-1 films were analyzed to learn what effect the glass substrate had on the SAPs in the adjacent polymer layer, and the opposite glass surfaces were analyzed, as well. It was expected that the adjacent layer would contain much less fluorine than the polymer-air interface and even less than the bulk F/C value because of the incompatibility between the low energy fluorine phase and the high energy glass phase. These analyses were made by removing films samples from the glass by a piece of double stick tape so the bottom surface would not be touched during removal. For the highest concentration samples, XPS analyses indicate that the backside of 1 and 10 K films had F/C values that far exceeded the values obtained for each respective polymer-air interface, and the F/C data obtained for the glass surfaces were even higher. At lower concentrations, the F/C values for the backs of the films did not exceed the values observed for the polymer-air interface. However, the

data obtained for the glass surfaces from the 10 K samples were comparable to the data for the polymer-air interface, and the 1 K glass surface data were much higher (than those for the air interface). The atomic composition data for these samples are in Tables 33 (1 K) and 45 (10 K) in Appendix B.

One interpretation of the 10 K results is that in the highest concentration case, all of the polymers in the sample are functionalized with a perfluoroalkyl group so to avoid putting this group against the glass, the polystyrene segment acts like a sticky foot and forms a hydrocarbon monolayer on the glass. This monolayer forces the formation of a domain rich in fluorine above it. When the samples are pulled off the glass, the film fails in this fluorine-rich domain providing two surfaces with high fluorine concentrations for XPS analysis. This same phenomenon occurs in the samples containing lower SAP concentrations, but to a lesser extent. The SAP molecules near the glass surface are oriented with the fluorinated group away from the glass creating a somewhat fluorine-rich domain which is where the films fail, so the XPS data is biased high in fluorine. Another interpretation of the lower concentration data is that the surface-active chains are not near the glass at all, but that the films fail in phase-segregated zones in the bulk. We know that polystyrene adheres to glass fairly well because regular polystyrene films cannot be pulled off glass substrates as a whole entity; removal of SAP films from glass depends on having domains of fluorine. The graphics below depict a reconstructed film sample with SAP polymers lining the polymer-glass surface and the zone of failure is marked. The adjacent picture shows the glass surface

sitting on an XPS sample holder; analysis of this surface would indicate tremendous amounts of fluorine.

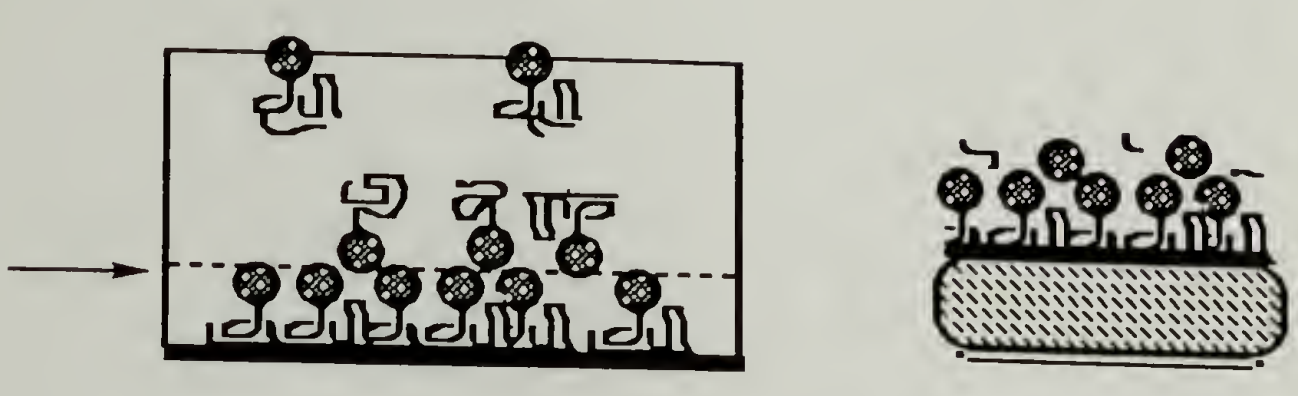

It is interesting to compare the difference in extent of film reconstruction that occurs at the polymer-air interface relative to the polymer-glass interface; reconstruction is much more extensive at the glass interface. One explanation is that the glass substrate has a stronger influence on film reconstruction because the difference in surface energy between glass and the fluorinated species is so much greater than that between polystyrene and air.

Depth Profiling

In an effort to understand how fluorine concentration changes with depth, XPS data was obtained for a 1 K sample containing 71% SAP chains at several angles to probe different depths. In the case of vertically homogeneous materials, the relative intensities of photoelectrons detected do not vary with takeoff angle. However, the XPS data for these samples indicate that the concentration drops off exponentially from 3 Å to 42 Å, and the F/C values range from .551 at 5° to .100 at 85°. Figure A.1. shows

the F/C data as a function of depth. (These data are tabulated in Table 32, Appendix B.) Unfortunately, certain problems inherent to variable angle XPS undermine these analyses. For example, at low angles (very shallow depths) the atomic concentration can be strongly influenced by surface roughness[3] (even on a molecular level) which means that a true analysis of the very outermost surface often is not possible.

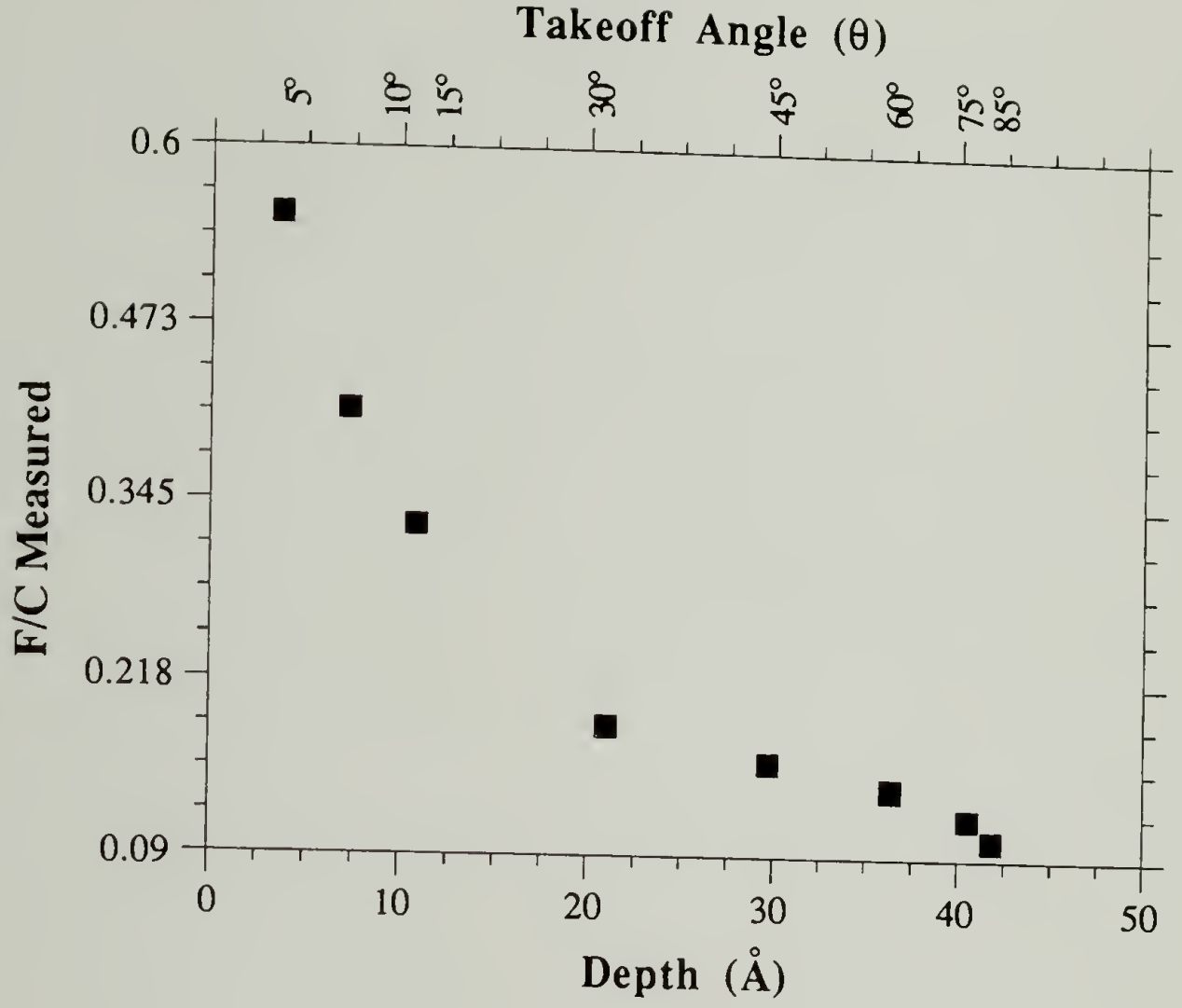

Figure A.1. F/C Depth Profiling for 71% 1 K SAP:E-1 Samples.

References

1. Anastasiadis, S.H.; Gancarz, I.; Koberstein, J.T. *Macromolecules* **1988**, *21*, 2980.

2. Green, P.F.; Cristensen, T.M.; Russell, T.P. *Macromolecules* **1991**, *24*, 252.

3 Yoon, S.C.; Ratner, B.D. *Macromolecules* **1986**, *19*, 1068.

APPENDIX B

SAP DATA TABLES

The following section contains tables of data from Part II of this dissertation. The tables have been referred to in appropriate places in the text and are numbered consecutively. For the most part the tables contain representative XPS and contact angle data.

Table 25. XPS Data and F/C Values for SAP:E-1 Samples (Mn = 1 K) Heated at 150 °C (24 and 72 Hours) and 180 °C.

% chains	time h	T °C	XPS Atomic Composition 15°/75° C	π–π* C	O	F	Si	F/C expt.	F/C avg.	F/C bulk
9.5	24	150	89.2	6.2	1.9	2.7	--	.0283	.0309	.00248
			91.0	5.0	2.0	2.0	--	.0208	.0239	
			88.9	6.3	1.6	3.2	--	.0336		
			91.6	4.2	1.6	2.6	--	.0271		
71	24	150	all samples flowed off glass substrates: no data							.0539
9.5	72	150	89.1	5.8	2.1	2.9	--	.0306	.0317	.00248
			90.5	5.1	2.8	1.6	--	.0167	.0181	
			88.0	6.4	2.5	3.1	--	.0328		
			93.1	4.0	1.0	1.9	--	.0196		
71	72	150	all samples flowed off glass substrates: no data							.0539
9.5	24	180	all samples flowed off glass substrates: no data							.00248
71	24	180								.0539

Table 26. Water Contact Angle Data for SAP:E-1 Samples (Mn = 1 K) Heated at 150 °C (24 and 72 Hours) and 180 °C.

% chains	time h	T °C	θ_A/θ_R water	avg.	cos
9.5	24	150	91/72, 90/71 92/72, 91/70	91/72	-.0174 .309
71	24	150	no data		
9.5	72	150	93/72, 90/71 92/71, 92/72	92/72	-.0349 .309
71	72	150	no data		
9.5	24	180			
71	24	180	no data		

Table 27. XPS Data and F/C Values for SAP:E-1 Samples (Mn = 1 K) Heated at 110 °C for 24, 48, 72, 96 and 120 Hours.

% chains	time h	T °C	XPS Atomic Composition 15°/75° C	π–π* C	O	F	Si	F/C expt.	F/C avg.	F/C bulk
9.5	24	110	83.8	8.5	1.6	5.7	.4	.0617	.0626	.00248
			89.6	6.6	1.2	2.4	.1	.0249	.0232	
			83.7	8.2	1.8	5.7	.6	.0620		
			90.7	5.8	1.2	2.1	.2	.0218		
			83.6	8.3	1.5	5.9	.7	.0642		
			89.7	6.3	1.3	2.2	.4	.0229		
71	24	110	61.5	13.9	2.6	21.6	.4	.286	.271	.0539
			76.9	9.7	1.9	11.3	.2	.130	.142	
			63.2	14.8	1.4	20.6	0	.264		
			77.8	9.5	1.1	11.5	.1	.132		
			65.6	10.8	2.7	20.1	.8	.263		
			74.4	9.8	1.5	13.8	.5	.163		
9.5	48	110	82.3	8.8	1.9	6.3	.6	.0691	.0706	.00248
			88.6	6.3	2.1	2.8	.2	.0295	.0234	
			80.9	9.4	2.4	6.6	.6	.0731		
			88.6	6.5	2.1	2.4	.4	.0252		
			83.5	8.4	1.6	6.4	.1	.0696		
			89.6	6.8	1.7	1.5	.4	.0156		
71	48	110	59.1	13.6	3.3	23.1	.8	.318	.307	.0539
			72.7	8.8	3.2	14.7	.5	.180	.177	
			59.4	14.3	2.8	22.9	.6	.311		
			71.7	9.9	2.6	14.8	.5	.181		
			60.5	13.7	3.7	21.6	.5	.291		
			72.6	10.7	2.0	14.1	.5	.169		
9.5	72	110	82.5	8.0	2.3	6.8	.4	.0751	.0752	.00248
			89.4	6.2	1.6	2.5	.4	.0261	.0242	
			82.6	8.0	1.9	7.1	.4	.0783		
			89.4	7.1	1.2	2.2	0	.0228		
			83.1	8.3	1.6	6.6	.4	.0722		
			88.9	7.6	1.1	2.3	.1	.0238		
71	72	110	58.3	14.0	2.5	24.9	.3	.344	.329	.0539
			75.7	9.1	2.0	12.8	.4	.151	.140	
			59.0	15.0	2.6	23.3	.1	.314		
			78.0	9.1	1.9	11.0	0	.126		
			62.1	14.7	2.6	20.4	.3	.266		
			79.2	8.1	2.4	10.1	.3	.116		

continued next page

Table 27. cont.,

71	96	110	61.5	13.7	2.1	22.2	.5	.295	.278	.0539
			75.9	10.7	1.9	11.5	0	.133	.125	
			67.3	10.2	2.1	20.3	0	.262		
			79.1	9.1	1.5	10.3	0	.117		
71	120	110	61.0	14.1	2.5	23.1	.3	.308	.321	.0539
			78.1	9.1	1.8	11.0	0	.126	.138	
			58.9	14.0	2.4	24.4	.3	.335		
			75.0	9.8	2.1	12.9	.2	.150		

Table 28. Water and Hexadecane Contact Angle Data for SAP:E-1 Samples (Mn = 1 K) Heated at 110 °C for 24, 48, 72, 96 and 120 Hours.

% chains	time h	T °C	θ_A/θ_R water	avg.	cos	θ_A/θ_R hexadecane	avg.	cos
71	24	110	98/76, 98/79	98/78	-.139	45/31, 44/32	45/31	.707
			99/78, 97/78		.208	46/32, 46/31		.857
71	48	110	101/80	100/79	-.174	46/32, 45/33	46/33	.695
			100/79, 100/80		.191	46/33, 46/34		.839
			98/79, 100/79			47/34		
71	72	110	100/76	101/79	-.191	47/36, 48/34	47/35	.682
			102/82, 101/78		.191	47/33, 46/36		.819
			101/80, 100/79			45/34		
71	96	110	100/76	100/79	-.174	47/35, 46/35	47/35	.682
			100/81, 101/79		.191	47/34, 46/36		.819
			98/79			48/36		
71	120	110	101/78	100/79	-.174	46/34, 47/36	46/35	.682
			100/79, 102/79		.191	46/36, 46/35		.819
			99/80			48/34		

Table 29. XPS Data and F/C Values for SAP:E-1 Samples (Mn = 1 K) Heated at 110 °C for 72 Hours.

% chains	time h	T °C	XPS Atomic Composition 15°/75° C	π–π* C	O	F	Si	F/C expt.	F/C avg.	F/C bulk
9.5	72	110	82.5	8.0	2.3	6.8	.4	.0751	.0752	.00248
			89.4	6.2	1.6	2.5	.4	.0261	.0242	
			82.6	8.0	1.9	7.1	.4	.0783		
			89.4	7.1	1.2	2.2	0	.0228		
			83.1	8.3	1.6	6.6	.4	.0722		
			88.9	7.6	1.1	2.3	.1	.0238		
17	72	110	81.7	8.1	2.7	6.9	.6	.0768	.0955	.00498
			87.3	6.7	2.3	3.2	.5	.0340	.0386	
			80.5	9.5	1.5	7.8	.7	.0867		
			88.8	6.2	1.6	3.3	0	.0347		
			79.6	9.4	1.5	8.9	.6	.0937		
			88.5	6.5	1.1	3.8	.1	.0400		
			79.1	9.3	1.8	9.4	.4	.106		
			88.0	6.9	1.0	3.9	.2	.0411		
29	72	110	76.0	9.5	2.1	12.3	.1	.144	.135	.0100
			86.5	6.9	2.0	4.5	.1	.0482	.0515	
			76.8	9.8	1.8	10.9	.6	.126		
			87.1	5.8	1.7	5.1	.3	.549		
			78.0	9.5	2.1	10.3	.1	.118		
			86.9	6.7	2.1	4.2	.1	.0449		
34	72	110	70.9	11.8	2.0	14.8	.4	.179	.184	.0126
			85.7	7.4	1.4	5.4	0	.0580	.0588	
			69.8	12.2	2.3	15.5	.1	.189		
			84.9	7.4	2.3	5.5	0	.0596		
52	72	110	65.9	13.2	2.4	17.9	.6	.226	.236	.0258
			82.8	8.0	1.8	7.3	.1	.0804	.0851	
			65.3	12.7	2.5	19.2	.3	.246		
			81.5	8.7	1.7	8.1	0	.0898		
			64.9	12.3	3.0	19.3	.5	.249		
			75.6	8.5	2.8	12.9	.2	.153		
63	72	110	61.3	13.7	2.7	21.7	.6	.289	.308	.0395
			76.6	8.6	1.1	13.5	.2	.158	.146	
			59.7	13.8	2.1	23.8	.6	.323		
			78.0	9.2	1.8	11.0	0	.126		
			60.5	13.5	2.4	23.2	.5	.313		
			77.0	8.6	1.1	13.1	.2	.153		

continued next page

Table 29. cont.,

71	72	110	58.3	14.0	2.5	24.9	.3	.344	.329	.0539
			75.7	9.1	2.0	12.8	.4	.151	.140	
			59.0	15.0	2.6	23.3	.1	.314		
			78.0	9.1	1.9	11.0	0	.126		
			62.1	14.7	2.6	20.4	.3	.266		
			79.2	8.1	2.4	10.1	.3	.116		
			55.5	15.0	3.2	25.4	.5	.358		
			75.2	9.7	2.5	12.4	.2	.146		

Table 30. Water and Hexadecane Contact Angle Data for SAP:E-1 Samples (Mn = 1 K) Heated at 110 °C for 72 Hours.

% chains	time h	T °C	θ_A/θ_R water	avg.	cos	θ_A/θ_R hexadecane	avg.	cos
9.5	72	110	90/75, 91/73 90/74, 92/75 91/76, 91/75	91/75	-.0174 .259	32/25, 29/22 29/23, 29/23 32/26, 30/23	30/24	.866 .913
17	72	110	93/75, 95/76 95/75, 94/76 95/75, 96/74	94/75	-.0697 .259	37/30, 35/31 36/34, 37/33 35/32, 35/30	36/31	.809 .857
29	72	110	95/76, 96/76 97/77, 96/74 96/78, 96/76	96/76	-.104 .242	40/32, 42/30 39/32, 40/34 38/33	40/32	.766 .848
34	72	110	97/80, 98/80 99/83, 97/78 96/80, 99/82	98/80	-.139 .174	46/32, 44/31 45/32, 44/31 45/30	45/31	.707 .857
52	72	110	100/81 98/79, 99/81 99/82	99/81	-.156 .156	47/33, 45/33 46/31, 46/30	46/32	.695 .848
63	72	110	100/81 102/81, 101/81 101/80, 102/79	101/81	-.191 .156	47/33, 46/32 47/34, 46/33 45/33	46/33	.695 .839
71	72	110	100/76 102/82, 101/78 101/80, 100/79	101/79	-.191 .191	47/36, 48/34 47/33, 46/36 45/34	47/35	.682 .819

Table 31. XPS Data and F/C Values for SAP:E-1 Samples (Mn = 1 K) Heated at 60 °C for 24, 48 and 72 Hours.

% chains	time h	T °C	XPS Atomic Composition 15°/75° C	π–π* C	O	F	Si	F/C expt.	avg.	F/C bulk
9.5 flat	24	60	84.8	8.4	1.4	5.2	.2	.0558	.0522	.00248
			89.8	6.7	1.2	2.1	.1	.0218	.0193	
			86.7	7.6	1.0	4.5	.1	.0477		
			92.1	5.8	.6	1.5	.1	.0153		
			85.4	8.2	1.6	4.2	.6	.0453		
			89.5	7.1	1.0	2.0	.4	.0207		
52 foamed	24	60	81.6	8.3	1.3	8.7	.1	.0968	.109	.0258
			84.6	5.1	.8	4.6	0	.0486	.0682	
			77.2	9.3	2.6	10.5	.4	.121		
			83.3	7.7	1.0	8.0	0	.0879		
71 foamed	24	60	68.3	11.4	2.8	17.0	.6	.213	.227	.0539
			80.0	8.4	2.3	8.7	.6	.0984	.0971	
			67.7	10.7	2.2	19.0	.6	.242		
			81.6	8.2	1.4	8.6	.3	.0958		
9.5 flat	48	60	82.5	8.2	1.5	7.5	.2	.0827	.0716	.00248
			89.9	6.0	1.0	3.0	0	.0313	.0244	
			84.2	8.7	1.3	5.6	.2	.0603		
			90.0	7.6	.6	1.7	.1	.0174		
52 foamed	48	60	73.5	9.6	1.8	14.5	.6	.174	.136	.0258
			83.0	7.1	2.2	7.7	0	.0855	.0677	
			81.5	8.0	1.4	8.7	.3	.0972		
			85.5	7.5	1.9	4.7	.3	.0505		
71 foamed	48	60	67.9	11.0	2.5	18.2	.4	.230	.252	.0539
			76.1	7.6	2.2	13.9	.2	.166	.152	
			64.4	12.2	1.7	21.1	.4	.275		
			78.6	7.4	1.2	11.9	.9	.138		
9.5 flat	72	60	80.1	9.0	1.6	9.0	.3	.101	.115	.00248
			89.3	5.5	2.0	3.1	.1	.0327	.0388	
			76.7	9.3	2.2	10.9	.8	.127		
			86.9	5.1	3.1	3.9	.8	.0424		
			76.6	9.6	2.3	10.6	.8	.122		
			87.9	7.3	.9	3.9	.1	.0410		
			78.8	9.7	1.4	9.7	.2	.110		
			88.2	6.6	1.3	3.7	.2	.0393		

continued next page

Table 31. cont.,

52 foamed	72	60	70.3	9.3	3.1	16.7	.4	.210	.250	.0258
			72.9	8.3	4.8	13.0	1.0	.160	.130	
			66.1	9.7	4.0	19.1	1.0	.252		
			76.6	6.5	3.8	12.4	.6	.149		
			62.2	14.2	2.5	20.8	.2	.272		
			80.3	7.4	1.8	9.9	.6	.113		
			64.9	12.5	1.8	20.7	.1	.267		
			81.6	7.9	1.4	9.0	.1	.100		
71 foamed	72	60	64.9	10.5	2.5	21.4	.4	.284	.310	.0539
			75.9	8.2	2.5	13.0	.4	.154	.162	
			65.0	10.3	2.5	21.4	.7	.285		
			71.3	9.3	3.1	15.8	.5	.196		
			57.4	14.3	3.1	23.8	1.4	.332		
			77.0	8.3	2.7	11.2	.8	.131		
			56.3	14.7	3.8	24.1	1.2	.340		
			72.4	9.9	2.7	13.9	1.1	.169		

Table 32. Water and Hexadecane Contact Angle Data for SAP:E-1 Samples (Mn = 1 K) Heated at 60 °C for 24, 48 and 72 Hours.

% chains	time h	T °C	θ_A/θ_R water	avg.	cos	θ_A/θ_R hexadecane	avg.	cos
9.5	72	60	94/75, 96/76	95/75	-.0871	35/21, 33/23	33/24	.839
			96/74, 95/76		.259	33/24, 33/23		.913
			95/76, 95/75			34/26, 33/25		
52	72	60	98/83, 96/83	97/82	-.122	36/29, 37/27	37/28	.799
			98/81 97/80		.139	39/30, 38/28		.883
			98/82, 96/82			36/28, 38/29		
71	72	60	99/83, 100/80	101/82	-.191	43/36, 40/35	42/36	.743
			101/82, 101/83		.139	41/37, 43/36		.809
			103/83, 102/81			42/36, 42/37		

Table 33. XPS Data and F/C Values for Depth Profiling for SAP:E-1 Samples (Mn = 1 K) Heated at 110 °C for 72 Hours.

θ	Depth Å		XPS Atomic Composition 15°/75° C	π–π* C	O	F	Si	F/C expt.	avg.	F/C bulk
5°	3.66	**1.**	47.8	14.4	3.5	34.3	.2	.551	.552	.0539
		2.	46.7	15.4	3.4	34.5	0	.554		
10°	7.29	**1.**	50.4	17.2	3.2	29.1	.1	.431	.411	.0539
		2.	52.4	17.1	3.0	27.2	.3	.391		
15°	10.87	**1.**	58.5	13.0	3.1	24.5	.8	.343	.328	.0539
		2.	59.0	15.0	2.6	23.3	.1	.314		
30°	21.00	**1.**	71.9	9.2	2.8	15.8	.3	.195	.184	.0539
		2.	73.5	9.8	1.8	14.5	.3	.174		
45°	29.70	**1.**	76.8	7.9	2.1	12.9	.3	.152	.158	.0539
		2.	74.8	8.3	2.5	13.6	.8	.164		
60°	36.37	**1.**	78.8	7.7	1.8	11.5	.2	.133	.140	.0539
		2.	76.0	10.0	1.3	12.7	0	.148		
75°	40.57	**1.**	81.7	7.2	1.0	10.1	.1	.114	.120	.0539
		2.	76.4	10.3	1.2	10.9	.2	.126		
85°	41.84	**1.**	82.0	7.5	1.0	9.0	0	.100	.104	.0539
		2.	80.5	7.8	2.1	9.5	0	.108		

Table 34. XPS Data and F/C Values for Backside of SAP:E-1 Samples (Mn = 1 K) Pulled Off Glass.

% chains	surface	XPS Atomic Composition 15°/75° C	π–π* C	O	F	Si	F/C expt.	F/C avg.	F/C bulk
9.5	back	89.2	8.2	1.1	1.4	0	.0144	.0180	.00248
		91.0	7.0	1.3	1.0	0	.0102	.0106	
		87.8	8.9	1.1	2.1	0	.0217		
		90.5	7.3	1.0	1.1	0	.0112		
9.5	glass	73.3	6.8	9.3	8.1	2.5	.101	.140	.00248
		51.9	2.5	30.3	4.1	11.1	.0753	.0941	
		65.8	6.8	11.8	11.9	3.7	.179		
		49.3	---	33.0	5.6	12.0	.113		
30	back	80.3	6.6	4.4	8.8	.2	.0978	.102	.0126
		82.7	5.4	7.3	2.9	.6	.0224	.0329	
		77.8	11.0	1.6	9.5	.1	.107		
		87.0	7.2	1.7	4.1	0	.0435		
30	glass	48.6	9.7	17.1	18.2	6.8	.312	.314	.0126
		44.0	---	33.0	10.0	13.1	.227	.217	
		51.7	11.0	13.1	19.9	4.3	.317		
		44.4	---	34.1	9.1	12.3	.207		
71	back	59.6	14.7	2.4	23.3	0	.313	.377	.0539
		68.0	9.7	3.0	18.7	.6	.241	.231	
		57.2	14.6	2.8	25.3	0	.351		
		68.7	9.8	3.0	17.9	.6	.228		
71	glass	26.3	20.4	12.8	37.4	3.1	.801	.834	.0539
		35.4	---	31.0	22.6	11.7	.655	.676	
		35.8	14.7	10.6	36.0	2.8	.725		
		34.9	8.6	27.0	18.7	10.8	.430		

Table 35. XPS Data and F/C Values for SAP:E-1 Samples (Mn = 5 K) Heated at 150 °C (24 and 72 Hours) and 180 °C.

% chains	time h	T °C	XPS Atomic Composition 15°/75° C	π–π* C	O	F	Si	F/C expt.	F/C avg.	F/C bulk
9.5	24	150	82.5	6.8	5.0	5.7	--	.0624	.0658	.00248
			88.6	6.5	2.3	2.6	--	.0273	.0312	
			81.5	6.5	5.9	6.1	--	.0693		
			87.9	6.1	2.7	3.3	--	.0351		
100	24	150	81.5	6.0	4.6	7.9	--	.0903	.0903	.0539
			87.1	6.1	3.0	3.8	--	.0408	.0364	
			80.7	6.6	4.8	7.9	--	.0904		
			85.4	8.0	3.6	3.0	--	.0321		
9.5	72	150	78.6	1.2	13.5	6.7	--	.0840	.0852	.00248
			90.6	6.6	1.2	1.6	--	.0164	.0325	
			80.9	7.0	4.5	7.6	--	.0865		
			87.3	5.2	3.0	4.5	--	.0486		
100	72	150	82.9	7.5	1.7	7.8	--	.0863	.0896	.0539
			91.5	5.4	.8	2.2	--	.0227	.0281	
			80.8	4.1	7.2	7.9	--	.0930		
			89.1	6.4	1.4	3.2	--	.0335		
9.5	24	180	all samples flowed off glass substrates:							
100	24	180	no data							

Table 36. Water and Hexadecane Contact Angle Data for SAP:E-1 Samples (Mn = 5 K) Heated at 150 °C (24 and 72 Hours) and 180 °C.

% chains	time h	T °C	θ_A/θ_R water	avg.	cos	θ_A/θ_R hexadecane	avg.	cos
9.5	24	150	91/71, 91/71 92/73, 91/70	91/70	-.0174 .342	20/15, 21/18 21/17, 20/17	20/17	.940 .956
100	24	150	93/72, 93/74 91/70, 92/72	92/72	-.0350 .309	25/19, 26/18 25/20, 27/21	26/20	.899 .940
9.5	72	150	92/71, 93/71 91/72, 91/73	92/72	-.0349 .309	20/18, 21/17 20/18, 22/17	21/17	.933 .956
100	72	150	94/75, 92/71 94/74, 93/71	93/72	-.0523 .309	23/21, 26/21 25/20, 25/20	25/20	.906 .940
9.5	24	180	all samples flowed off			glass substrates		
75	24	180	no data					

Table 37. XPS Data and F/C Values for SAP:E-1 Samples (Mn = 5 K) Heated at 110 °C for 48, 72, 96,120 and 144 Hours.

% chains	time h	T °C	XPS Atomic Composition 15°/75° C	π–π* C	O	F	Si	F/C expt.	F/C avg.	F/C bulk
100	48	110	71.3	13.1	1.4	13.9	.3	.164	.166	.0539
			84.0	8.0	1.2	6.8	0	.0739	.0750	
			72.0	12.4	1.1	14.2	.2	.168		
			84.3	7.6	.9	7.0	.2	.0762		
100	72	110	71.0	13.3	1.5	14.0	.2	.167	.169	.0539
			83.6	8.1	1.6	6.7	0	.0731	.0723	
			70.7	13.0	2.1	14.1	0	.169		
			84.1	7.9	1.2	6.7	0	.0728		
			70.9	12.0	1.7	14.3	0	.0170		
			82.8	8.7	1.8	6.5	.1	.0710		
100	96	110	72.0	13.1	1.6	13.2	.1	.155	.161	.0539
			84.3	8.0	1.1	6.5	0	.0704	.0706	
			70.7	12.5	2.5	14.0	.3	.168		
			83.0	7.8	1.4	6.5	.3	.0709		
100	120	110	72.6	11.8	1.5	14.1	.1	.1647	.165	.0539
			85.4	6.9	1.3	6.4	0	.0693	.0668	
			73.5	11.0	1.3	13.9	.3	.164		
			85.8	7.4	.8	6.0	0	.0643		
100	144	110	71.6	12.6	1.6	14.2	.1	.168	.163	.0539
			84.2	8.0	1.1	6.7	0	.0727	.0749	
			72.0	12.5	1.9	13.4	.2	.158		
			84.0	8.1	.8	7.1	0	.0771		

Table 38. XPS Data and F/C Values for SAP:E-1 Samples (Mn = 5 K) Heated at 110 °C for 72 Hours.

% chains	time h	T °C	XPS Atomic Composition 15°/75° C	π–π* C	O	F	Si	F/C expt.	F/C avg.	F/C bulk
9.5	72	110	85.3	6.9	2.1	5.3	.4	.0575	.0631	.00248
			90.9	6.0	1.2	1.9	0	.0196	.0249	
			83.6	7.5	2.1	6.3	.5	.0691		
			89.6	6.3	.8	3.2	.1	.0321		
			82.5	9.7	1.9	5.8	0	.0629		
			89.1	6.4	2.3	2.2	0	.0230		
31	72	110	76.8	10.6	2.5	9.7	.3	.111	.102	.00941
			86.2	7.8	1.7	4.2	.1	.0447	.0425	
			79.0	9.6	2.3	8.5	.6	.0959		
			86.1	7.7	2.5	3.6	0	.0384		
			79.9	9.1	1.9	9.0	0	.101		
			87.4	6.5	2.1	3.9	.2	.0444		
			83.0	7.6	2.3	6.6	.3	.0730		
			88.8	6.6	1.6	2.8	.2	.0294		
40	72	110	77.1	10.6	1.6	10.7	0	.122	.123	.0126
			86.5	7.4	1.9	4.0	.1	.0426	.0493	
			75.4	10.7	2.7	11.0	.2	.128		
			85.0	7.9	1.8	5.3	0	.0570		
			77.6	9.9	1.9	10.5	.2	.120		
			86.1	7.3	1.8	4.5	.2	.0482		
			79.9	9.1	1.9	9.0	0	.101		
			87.4	6.5	2.1	3.9	.2	.0444		
61	72	110	73.6	11.7	2.2	12.5	0	.146	.163	.0224
			84.6	8.2	1.2	6.0	0	.0646	.0654	
			70.7	10.7	2.7	14.1	0	.169		
			84.1	13.0	2.1	6.7	0	.0728		
			74.5	10.7	1.6	12.8	.2	.150		
			85.1	7.1	2.1	5.7	0	.0618		
			71.8	11.8	1.9	14.2	.4	.170		
			84.8	7.7	1.4	5.7	.2	.0610		
100	72	110	73.6	11.7	2.0	12.8	0	.150	.163	.0539
			84.6	8.2	1.2	6.0	0	.0646	.0704	
			71.0	12.3	2.0	14.3	0	.171		
			83.4	7.8	2.0	6.7	.1	.0735		
			71.0	13.3	1.5	14.0	.2	.167		
			83.6	8.1	1.6	6.7	0	.0731		

Table 39. Water and Hexadecane Contact Angle Data for SAP:E-1 Samples (Mn = 5 K) Heated at 110 °C for 72 Hours.

% chains	time h	T °C	θ_A/θ_R water	avg.	cos	θ_A/θ_R hexadecane	avg.	cos
9.5	72	110	90/72, 89/69 90/71, 90/72 92/71, 89/73	90/71	.00 .325	28/22, 27/19 26/20, 28/18 27/17, 27/16	27/18	.891 .951
30	72	110	92/73, 94/74 94/76, 93/74	93/74	-.0523 .276	32/26, 31/24 32/25, 32/25	32/25	.848 .906
40	72	110	96/76, 96/75 96/77, 94/74 95/74, 94/75	95/75	-.0871 .259	34/27, 34/25 35/26, 34/25 32/23, 32/24	33/25	.839 .906
60	72	110	97/81, 96/81 97/79, 98/76 97/76, 97/80	97/79	-.122 .191	34/27, 34/25 35/26, 34/25 32/23, 32/24	35/24	.819 .913
100	72	110	97/80, 98/79 96/79, 98/77 97/79, 100/77	98/78	-.142 .208	36/26, 37/25 36/28, 36/25 36/26, 37/23	36/26	.809 .899

Table 40. XPS Data and F/C Values for SAP:E-1 Samples (Mn = 10 K) at RT (72 Hours) and Heated at 150 °C (24 and 72 Hours) and 180 °C.

% chains	time h	T °C	XPS Atomic Composition 15°/75° C	π–π* C	O	F	Si	F/C expt.	avg.	F/C bulk
0	72	RT	94.1	5.7	.2	0	--	0	0	0
			94.2	5.6	.2	0	--	0		
10	72	RT	92.5	5.0	.5	2.0	--	.0205	.0195	.00248
			95.0	3.7	.7	.6	--	.00608	.00506	
			92.1	5.3	.8	1.8	--	.0185		
			94.8	4.2	.6	.4	--	.00404		
75	72	RT	90.0	4.7	1.8	2.0	--	.0369	.0345	.0191
			94.0	2.2	2.0	1.8	--	.0187	.0185	
			90.1	6.1	.7	3.1	--	.0322		
			94.7	3.0	.5	1.8	--	.0184		
0	24	150	91.5	5.1	3.4	0	--	0	0	0
			92.2	5.5	2.3	0	--	0		
10	24	150	85.5	5.9	3.9	4.6	--	.0503	.0573	.00248
			84.0	5.7	4.8	5.3	--	.0590	.0549	
			83.9	6.1	4.2	5.8	--	.0644		
			86.9	5.5	2.9	4.7	--	.0508		
75	24	150	83.1	5.6	5.1	6.1	--	.0699	.0677	.0191
			88.9	3.7	4.4	3.0	--	.0324	.0358	
			84.2	5.9	4.0	5.9	--	.0655		
			89.0	5.0	2.3	3.7	--	.0393		
0	72	150	90.3	5.4	4.3	0	--	0	0	0
			91.9	4.5	3.6	0	--	0		
10	72	150	86.3	5.5	3.6	5.2	--	.0540	.0540	.00248
			90.4	5.0	2.1	2.5	--	.0262	.0262	
75	72	150	84.7	6.0	3.6	5.7	--	.0628	.0640	.0191
			91.2	5.1	2.0	1.7	--	.0176	.0266	
			83.8	6.5	3.8	5.9	--	.0653		
			88.7	4.9	3.0	3.4	--	.0363		
0	24	180								
10	24	180	all samples flowed off glass substrates:							
75	24	180	no data							

Table 41. Water and Hexadecane Contact Angle Data for SAP:E-1 Samples (Mn = 10 K) at RT (72 Hours) and Heated at 150 °C (24 and 72 Hours) and 180 °C.

% chains	time h	T °C	θ_A/θ_R water	avg.	cos	θ_A/θ_R hexadecane	avg.	cos
0	72	RT	85/70, 85/65 86/68, 87/67	86/67	.0697 .391	7/0, 10/5 10/7, 11/8	9/5	.988 .996
10	72	RT	88/70, 88/65 87/68, 87/67	87/68	.0532 .375	16/7, 18/7 19/10, 20/8	18/8	.951 .990
75	72	RT	91/72, 90/70 92/70, 91/72	91/71	-.0174 .325	21/10, 20/15 21/12, 22/13	21/12	.933 .978
0	24	150	87/72, 85/69 88/73, 88/67	87/70	.0532 .342	12/8, 11/5 14/9, 11/8	12/8	.978 .990
10	24	150	92/73, 91/71 93/73, 91/70	92/72	-.0349 .309	20/15, 23/16 24/16, 20/17	22/16	.920 .956
75	24	150	94/75, 93/71 94/72, 94/73	94/73	-.0697 .292	25/17, 25/20 23/18, 24/18	25/18	.906 .951
0	72	150	85/72, 86/67 88/71, 89/69	87/70	.0532 .342	11/6, 9/5 13/8, 11/8	11/7	.982 .992
10	72	150	93/71, 92/72 91/72, 92/73	92/72	-.0349 .309	22/18, 23/16 23/16, 24/18	23/17	.920 .956
75	72	150	95/75, 94/74 94/74, 95/73	94/75	-.0697 .259	25/21, 26/21 25/20, 25/20	25/20	.906 .940
0	24	180	all samples flowed off glass substrates					
10	24	180	no data					
75	24	180						

Table 42. XPS Data and F/C Values for SAP:E-1 Samples (Mn = 10 K) Heated at 110 °C for 24, 48, 72, 96, 120, 144, 168 and 192 Hours and Two Weeks.

% chains	time h	T °C	XPS Atomic Composition 15°/75° C	π–π* C	O	F	Si	F/C expt.	F/C avg.	F/C bulk
10	24	110	91.7	3.2	2.2	2.0	.8	.0211	.0240	.00248
			91.3	5.8	1.3	1.0	.5	.0103	.00920	
			88.9	7.6	.6	2.6	.3	.0269		
			91.8	7.0	.5	.8	0	.00810		
75	24	110	84.5	7.8	1.0	6.0	0	.0712	.0725	.0191
			89.0	6.5	1.8	2.2	.1	.0230	.0314	
			84.2	8.0	1.0	6.8	0	.0737		
			87.8	7.4	1.0	3.8	0	.0399		
10	48	110	87.2	8.4	1.3	2.7	.4	.0282	.0301	.00248
			90.6	7.3	1.4	.7	0	.0071	.00815	
			85.6	8.1	2.0	3.0	1.3	.0321		
			91.0	7.0	1.1	.9	0	.00921		
75	48	110	82.5	9.1	1.0	7.1	.3	.0775	.0810	.0191
			88.8	6.8	1.1	3.0	.3	.0314	.0292	
			81.7	9.3	1.2	7.7	.1	.0846		
			88.2	8.1	.7	2.6	.3	.0270		
10	72	110	85.5	6.9	2.2	5.0	.4	.0541	.0545	.00248
			90.9	6.0	1.5	1.6	0	.0165	.0207	
			83.9	8.8	1.7	5.1	.4	.0550		
			89.3	6.6	1.7	2.4	0	.0250		
75	72	110	79.0	8.5	2.7	9.1	.7	.104	.102	.0191
			89.1	6.3	1.4	3.2	0	.0335	.0321	
			80.2	8.5	2.0	8.9	.4	.100		
			87.9	6.6	2.3	2.9	.2	.0307		
100	96	110	79.7	10.2	1.5	8.5	0	.0950	.102	.0258
			87.4	7.1	1.4	4.1	0	.0434	.0422	
			78.1	10.1	2.0	9.7	.2	.110		
			87.4	7.4	1.2	3.9	0	.0411		
100	120	110	78.6	10.4	1.3	9.7	0	.109	.109	.0258
			88.2	6.8	1.3	3.6	.1	.0379	.0418	
			78.9	9.9	1.4	9.8	0	.110		
			87.0	7.2	1.3	4.5	0	.0457		

continued next page

Table 42. cont.,

100	144	110	79.5	10.1	1.6	8.7	0	.0971	.106	.0258
			87.0	7.3	1.1	4.6	0	.0488	.0476	
			78.6	9.6	1.6	10.2	0	.116		
			87.3	7.4	1.0	4.4	0	.0465		
100	168	110	80.8	9.7	1.6	7.9	0	.0872	.0956	.0258
			88.6	7.4	1.2	2.8	0	.0292	.0341	
			80.1	8.7	1.7	9.2	.3	.104		
			87.8	6.9	1.5	3.7	.1	.0391		
100	192	110	81.0	9.9	1.7	7.2	.1	.0792	.0863	.0258
			87.2	7.9	1.3	3.4	.1	.0357	.0341	
			80.2	9.6	1.7	8.4	.1	.0935		
			87.9	7.5	1.5	3.1	0	.0325		
75	2wks*	110	83.2	6.8	4.2	5.7	--	.0633	.0617	.0258
			86.6	6.5	3.5	3.4	--	.0365	.0330	
			84.2	7.3	3.0	5.5	--	.0601		
			89.1	5.8	2.3	2.8	--	.0295		

*data measured on different XPS.

Table 43. Water and Hexadecane Contact Angle Data for SAP:E-1 Samples (Mn = 10 K) Heated at 110 °C for 24, 48, 72, 96, 120, 144, 168 and 192 Hours and Two Weeks.

% chains	time h	T °C	θ_A/θ_R water	avg.	cos	θ_A/θ_R hexadecane	avg.	cos
10	24	110	88/78, 89/77 89/79, 92/81	89/79	.0174 .191	28/25, 27/23 28/23, 28/24	28/24	.883 .913
75	24	110	94/75, 94/74 95/75, 95/76	95/75	-.0871 .259	32/25, 34/26 34/27, 33/23	34/25	.829 .906
10	48	110	93/75, 91/76 93/78, 90/77	92/76	-.0349 .242	30/26, 31/25 31/26, 32/26	31/26	.857 .899
75	48	110	95/76, 96/78 97/79, 96/82	96/79	-.104 .191	35/28, 36/27 35/27, 36/30	35/28	.819 .883
10	72	110	90/77, 91/78 92/78, 91/79	91/78	-.0174 .208	30/24, 33/25 30/26, 32/28	31/26	.857 .899
75	72	110	98/80, 97/82 97/81, 96/82	97/81	-.123 .156	37/29, 36/28 37/29, 36/30	36/29	.809 .875
100	72	110	98/82, 97/83 98/83, 98/83	98/83	-.139 .122	38/31, 37/29 38/30, 38/29	38/30	.788 .866
100	96	110	97/82, 98/81 97/82, 97/84	97/82	-.123 .139	37/30, 36/28 37/28, 36/29	36/29	.809 .875
100	120	110	97/83, 96/84 96/82, 98/80	97/83	-.123 .122	38/31, 37/31 36/30, 37/29	37/30	.799 .866
100	144	110	99/80, 97/83 98/83, 97/82	98/82	-.139 .139	38/29, 37/29 38/30, 38/29	38/29	.788 .875
100	168	110						
100	192	110	97/81, 98/82 97/82, 96/81	97/81	-.123 .156	37/26, 38/29 37/28, 36/29	37/28	.799 .883
75	2wks	110	95/81, 94/81 96/80, 96/81	95/81	-.0871 .156	36/28, 35/27 37/31, 37/30	36/29	.809 .875

Table 44. XPS Data and F/C Values for SAP:E-1 Samples (Mn = 10 K) Heated at 110 °C for 72 Hours.

% chains	time h	T °C	XPS Atomic Composition 15°/75° C	π–π* C	O	F	Si	F/C expt.	F/C avg.	F/C bulk
0	72	110	93.4	6.0	.4	0	.2	0	0	0
			93.7	6.1	.2	0	0	0		
10	72	110	82.7	9.7	1.7	5.8	.1	.0628	.0606	.00248
			88.4	8.1	1.1	2.2	.1	.0228	.0250	
			83.9	8.5	1.7	5.4	.4	.0584		
			89.3	6.4	1.7	2.6	0	.0272		
			82.9	9.5	1.8	5.6	.2	.0605		
			88.0	8.3	1.2	2.4	.1	.0249		
20	72	110	85.0	7.8	1.2	5.7	.3	.0614	.0625	.00498
			89.9	6.4	1.3	2.4	0	.0250	.0275	
			86.7	6.5	1.1	5.6	.1	.0600		
			88.7	6.9	1.5	2.8	.1	.0293		
			84.6	6.9	1.9	6.1	.5	.0667		
			89.5	5.9	1.7	2.7	.2	.0283		
30	72	110	82.9	8.5	2.1	6.3	.2	.0689	.0688	.00710
			89.5	6.3	.9	3.2	.1	.0334	.0288	
			82.2	7.8	2.8	6.5	.6	.0722		
			89.3	6.3	1.4	2.7	.3	.0282		
			84.5	7.2	1.8	6.0	.5	.0654		
			90.1	6.3	1.0	2.4	.2	.0249		
40	72	110	80.5	9.8	1.3	7.6	.2	.0908	.0907	.0100
			88.3	7.4	.7	3.6	0	.0377	.0343	
			79.9	8.4	2.7	7.5	1.4	.0861		
			88.7	6.4	.8	2.9	.4	.0376		
			82.2	7.9	1.9	8.7	.4	.0832		
			89.0	6.8	1.1	3.6	.2	.0303		
			80.5	9.6	1.1	8.7	.1	.0965		
			88.0	7.4	1.0	3.6	0	.0317		
50	72	110	79.7	8.3	2.0	9.2	.6	.104	.101	.0126
			87.9	6.4	2.3	2.9	.4	.0310	.0360	
			78.8	9.6	2.2	8.9	.4	.101		
			88.1	6.9	1.5	3.4	.1	.0358		
			80.8	8.3	2.1	8.8	0	.0988		
			88.2	6.4	1.5	3.9	0	.0412		
			82.2	7.9	1.9	7.5	.4	.0832		
			89.0	6.8	1.1	2.9	.2	.0303		

continued next page

Table 44. cont.,

75	72	110	80.2	8.3	2.0	8.7	.8	.0981	.100	.0191
			87.9	6.4	2.3	2.9	.4	.0310	.0364	
			79.8	8.8	2.0	8.9	.5	.100		
			89.1	6.3	1.4	3.2	0	.0335		
			78.5	9.2	2.5	9.7	.1	.111		
			87.9	6.7	1.8	3.6	0	.0380		
			80.8	9.9	1.1	8.1	.1	.0893		
			88.0	7.5	1.0	3.6	0	.0377		
100	72	110	79.1	9.2	2.7	8.5	.5	.0962	.105	.0258
			87.5	6.7	1.6	3.9	.3	.0413	.0431	
			77.6	10.5	2.2	9.5	.3	.108		
			86.3	7.9	1.6	4.1	.1	.0435		
			79.0	8.9	2.0	9.7	.4	.110		
			88.4	5.8	1.5	4.1	.2	.0435		
			79.1	9.8	2.1	8.7	.3	.0979		
			87.5	6.9	1.4	4.0	.2	.0424		

Table 45. Water and Hexadecane Contact Angle Data for SAP:E-1 Samples (Mn = 10 K) Heated at 110 °C for 72 Hours.

% chains	time h	T °C	θ_A/θ_R water	avg.	cos	θ_A/θ_R hexadecane	avg.	cos
0	72	110	87/73, 89/74 87/75, 86/75	87/74	.0523 .276	15/10, 13/7 12/8, 13/8	13/8	.974 .990
10	72	110	90/75, 94/75 92/76, 92/75 91/75	91/75	-.0174 .259	27/18, 28/22 27/19, 29/23 29/23	28/21	.883 .933
20	72	110	92/75, 94/75 92/73, 92/74 94/74	93/74	-.0523 .276			
40	72	110	94/76, 94/73 95/75, 95/75 96/74	95/75	-.0871 .259	33/25, 34/27 34/27, 33/26 35/28	34/27	.829 .891
50	72	110	96/77, 96/76 97/77, 97/75 96/76, 96/74	96/76	-.104 .242	35/28, 36/28 35/28, 37/28 37/27, 35/26	36/28	.809 .883
75	72	110	98/80, 96/80 97/82, 97/81 97/82, 97/82	97/81	-.122 .156	36/30, 36/28 37/31, 36/29 35/28	36/29	.809 .875
100	72	110	98/82, 97/80 99/80, 97/83 98/83, 98/81	98/81	-.139 .156	38/31, 37/29 38/30, 38/29 37/30, 36/28	37/29	.799 .875

Table 46. XPS Data and F/C Values for Backside of SAP:E-1 Samples (Mn = 10 K) Pulled Off Glass.

% chains	surface	XPS Atomic Composition 15°/75° C	π–π* C	O	F	Si	F/C expt.	F/C avg.	F/C bulk
10	back	85.9	8.7	1.9	3.1	.3	.0328	.0264	.00248
		87.9	7.0	2.1	2.7	.3	.0284	.0221	
		87.4	8.1	2.1	1.9	.5	.0200		
		88.5	5.9	3.6	1.5	.5	.0159		
10	glass	81.8	7.7	3.1	6.1	1.2	.0670	.0487	.00248
		64.6	---	21.5	4.7	9.2	.0727	.0493	
		87.1	8.0	1.6	2.9	.5	.0305		
		88.2	6.0	11.9	2.1	5.1	.0259		
50	back	86.5	8.6	1.7	3.2	0	.0336	.0406	.0126
		89.5	7.1	1.6	1.8	0	.0186	.0262	
		85.4	9.0	.9	4.5	.1	.0477		
		88.3	6.4	1.8	3.2	.3	.0338		
50	glass	83.4	9.6	1.5	5.2	.2	.03559	.0559	.0126
		76.6	7.4	8.1	4.3	3.5	.0512	.0512	
75	back	82.4	8.5	2.0	7.1	.1	.0780	.0654	.0191
		83.1	7.7	2.7	6.4	.2	.0705	.0530	
		83.4	9.4	1.9	4.9	0	.0528		
		82.3	7.6	4.9	3.2	0	.0356		
75	glass	78.0	9.6	2.7	8.9	.7	.101	.110	.0191
		62.7	5.4	17.3	7.4	7.1	.108	.116	
		75.3	9.5	3.5	10.2	1.5	.120		
		57.7	5.6	20.3	7.9	8.4	.125		
100	back	32.8	23.8	5.6	36.8	.9	.650	.580	.0258
		45.6	16.7	4.5	32.4	.7	.520	.463	
		43.0	19.7	4.2	32.5	.7	.520		
		54.4	13.5	4.4	27.6	.2	.406		
100	glass	46.4	11.0	12.1	26.7	3.9	.465	.459	.0258
		46.2	5.3	24.4	15.6	8.5	.303	.369	
		48.8	13.0	7.3	28.0	2.9	.453		
		40.4	5.6	24.1	20.0	9.9	.435		

Table 47. XPS Data and F/C Values for SAP:E-1 Samples (Mn = 40 K) Heated at 110 °C for 120 Hours.

% chains	time h	T °C	XPS Atomic Composition 15°/75° C	π–π* C	O	F	Si	F/C expt.	F/C avg.	F/C bulk
6	120	110	88.4	8.0	.7	3.0	0	.0311	.0381	.00124
			92.4	6.0	.6	1.1	0	.0111	.0164	
			86.0	8.6	1.3	4.0	.1	.0422		
			89.4	7.2	1.5	1.9	0	.0197		
			86.3	8.4	1.3	3.8	.2	.0401		
			89.2	7.4	1.6	1.6	.2	.0166		
			85.0	9.8	1.4	3.7	0	.0390		
			90.3	7.7	.2	1.8	0	.0184		
14	120	110	84.5	9.6	1.2	4.7	.1	.0490	.0486	.00248
			89.3	7.5	1.3	1.9	0	.0197	.0200	
			84.1	9.9	1.3	4.7	0	.0500		
			89.5	7.4	1.0	2.0	0	.0206		
			85.5	8.2	1.6	4.4	.2	.0469		
			89.9	6.7	1.5	1.9	0	.0197		
27	120	110	84.3	8.8	1.6	5.0	.2	.0530	.0550	.00367
			89.5	7.5	1.0	2.1	0	.0216	.0221	
			84.6	8.8	1.4	5.1	0	.0546		
			88.0	7.7	1.6	2.5	.2	.0261		
			86.4	7.0	1.2	5.0	.3	.0535		
			90.9	5.3	1.6	1.8	.3	.0187		
			85.0	8.0	1.5	5.3	0	.0570		
			90.3	6.8	.7	2.1	0	.0216		
37	120	110	82.6	9.8	1.8	5.7	.1	.0617	.0653	.00420
			89.6	7.2	.8	2.7	0	.0279	.0270	
			82.8	9.6	1.4	6.1	.1	.0660		
			89.0	7.4	.9	2.7	0	.020		
			83.2	9.1	1.3	6.3	.1	.0682		
			89.2	6.9	1.3	2.4	.1	.0250		
50	120	110	83.4	8.7	2.2	5.5	.1	.0597	.0661	.00498
			91.9	6.3	1.6	1.8	.3	.0187	.0288	
			86.0	9.6	2.5	5.9	.9	.0645		
			89.4	7.1	1.6	3.1	0	.0325		
			86.3	9.1	1.5	6.4	.1	.0695		
			89.2	7.5	1.0	2.5	0	.0259		
			85.0	9.7	.7	6.0	0	.0643		
			90.3	6.5	1.3	2.7	0	.0281		

continued next page

Table 47. cont.,

100	120	110	85.3	8.2	2.0	4.4	.1	.0470	.0644	.00624
			89.5	6.2	2.0	2.1	.1	.0219	.0276	
			82.7	9.7	1.5	5.8	.3	.0627		
			89.7	7.0	.8	2.7	0	.0279		
			82.9	10.4	1.0	5.7	0	.0611		
			89.1	7.4	.9	2.6	0	.0289		
			82.8	9.4	1.2	6.4	.2	.0694		
			89.2	6.8	1.2	2.5	0	.0260		

Table 48. Water and Hexadecane Contact Angle Data for SAP:E-1 Samples (Mn = 40 K) Heated at 110 °C for 120 Hours.

% chains	time h	T °C	θ_A/θ_R water	avg.	cos	θ_A/θ_R hexadecane	avg.	cos
6	120	110	92/74, 91/75 92/73, 93/73 91/72, 92/71	92/73	-.0349 .292	25/19, 24/19 24/20, 26/18 23/19, 25/19	24/19	.913 .945
14	120	110	92/76, 94/75 92/73, 93/73 94/74, 95/73	93/74	-.0523 .276	25/21, 27/23 26/20, 26/21 27/20, 25/20	26/20	.899 .940
27	120	110	94/76, 94/78 95/78, 95/77 95/74, 95/73	94/75	-.0697 .259	29/21, 27/21 30/24, 29/24 27/20, 25/20	28/21	.883 .933
37	120	110	95/75, 96/74 94/74, 95/76 93/75, 95/73	95/75	-.0871 .259	28/21, 29/22 28/23, 29/22 27/23, 27/23	28/23	.883 .920
50	120	110	93/77, 93/74 94/77, 95/76 94/76, 95/77	94/77	-.0697 .225	29/23, 30/26 28/23, 29/22 27/22, 28/23	28/23	.883 .920
100	120	110	93/77, 94/80 95/75, 95/79 95/76, 95/77	95/77	-.0871 .225	29/24, 30/25 28/25, 28/24 30/25, 28/24	28/24	.883 .913

Table 49. XPS Data and F/C Values for SAP:E-1 Samples (Mn = 100 K) Heated at 110 °C for 24, 48, 72, 96, 120, 144, 168 and 192 Hours.

% chains	time h	T °C	XPS Atomic Composition 15°/75° C	π–π* C	O	F	Si	F/C expt.	avg.	F/C bulk
100	24	110	86.1	7.4	2.2	3.8	.4	.0406	.0447	.00248
			91.1	6.2	1.0	1.4	.2	.0143	.0148	
			87.5	6.5	1.3	4.6	0	.0489		
			90.8	6.3	1.4	1.5	0	.0154		
100	48	110	84.9	6.4	2.4	5.3	1.0	.0574	.0542	.00248
			90.4	6.1	1.2	1.9	.3	.0197	.0193	
			85.1	7.3	1.9	4.7	.9	.0509		
			91.1	5.4	1.6	1.9	0	.0197		
			85.4	6.6	2.3	5.0	.7	.0543		
			90.6	6.1	1.2	1.8	.2	.0186		
100	72	110	84.5	7.5	2.7	5.1	.2	.0554	.0602	.00248
			90.6	6.2	.9	2.3	0	.0238	.0208	
			83.9	7.8	1.9	5.9	.5	.0643		
			91.5	5.8	.9	1.8	0	.0185		
			84.0	8.8	1.3	5.6	.4	.0603		
			90.5	5.9	.8	2.7	.1	.0280		
100	96	110	82.4	9.6	1.8	6.2	0	.0674	.0689	.00248
			89.4	6.7	1.1	2.7	.1	.0281	.0293	
			82.0	9.8	1.6	6.5	.1	.0708		
			88.4	6.5	1.8	3.1	.1	.0327		
			82.6	9.2	1.9	6.3	0	.0686		
			89.7	6.4	1.3	2.6	0	.0270		
100	120	110	82.5	9.9	.8	6.6	.2	.0714	.0717	.00248
			90.0	6.5	.8	2.7	0	.0280	.0266	
			82.3	9.2	1.6	6.9	0	.0754		
			89.9	6.4	1.0	2.7	0	.0280		
			83.1	9.3	1.3	6.3	0	.0682		
			89.7	7.0	1.0	2.3	0	.0238		
100	144	110	82.3	10.3	1.0	6.4	0	.0693	.0711	.00248
			90.3	6.2	.8	2.6	.1	.0269	.0261	
			82.0	9.9	1.3	6.7	0	.0729		
			90.2	6.8	.6	2.3	0	.0253		
100	168	110	84.7	8.5	1.2	5.5	.1	.0590	.0623	.00248
			90.8	6.6	.9	1.7	0	.0171	.0222	
			82.5	10.4	1.0	6.1	0	.0657		
			90.3	6.0	1.0	2.6	0	.0270		

continued next page

Table 49. cont.,

100	192	110	83.4	10.0	.9	5.7	0	.0610	.0662	.00248
			90.0	7.2	1.3	1.4	0	.0144	.0191	
			82.6	9.8	1.0	6.6	0	.0714		
			90.3	6.4	.9	2.3	0	.0238		

Table 50. Water and Hexadecane Contact Angle Data for SAP:E-1 Samples (Mn = 100 K) Heated at 110 °C for 24, 48, 72, 96, 120, 144, 168 and 192 Hours.

% chains	time h	T °C	θ_A/θ_R water	avg.	cos	θ_A/θ_R hexadecane	avg.	cos
100	24	110	90/72, 90/73	91/73	-.0174	22/18, 20/18	20/17	.940
			91/73, 92/74		.292	20/17, 20/17		.956
100	48	110	92/74, 93/76	92/75	-.0349	23/18, 24/18	24/17	.913
			92/75, 93/74		.292	24/17, 24/16		.956
100	72	110	95/79, 97/82	95/82	-.0871	29/27, 30/24	28/25	.883
			95/83, 95/84		.139	27/25, 27/24		.906
100	96	110	97/81, 95/83	95/81	-.0871	29/25, 28/23	28/24	.883
			93/80, 95/81		.156	28/25, 28/24		.913
100	120	110	96/80, 95/82	95/81	-.0871	29/23, 28/24	28/23	.883
			95/81, 97/81		.156	27/24, 28/23		.920
100	144	110	95/81, 96/80	95/80	-.0871	29/24, 29/23	29/23	.875
			95/80, 97/81		.174	30/24, 28/21		.920
100	168	110	95/80, 94/82	95/81	-.0871	28/23, 27/24	28/24	.875
			95/81, 97/82		.156	29/24, 29/24		.913
100	192	110	96/80, 95/80	95/80	-.0871	29/25, 28/23	28/24	.875
			95/80, 96/81		.174	27/25, 29/23		.913

Table 51. XPS Data and F/C Values for SAP:E-1 Samples (Mn = 100 K) Heated at 110 °C for 120 Hours.

% chains	time h	T °C	XPS Atomic Composition 15°/75° C	π–π* C	O	F	Si	F/C expt.	avg.	F/C bulk
2.5	120	110	87.4	7.7	1.6	3.2	.2	.0336	.0360	.000494
			90.6	7.5	.9	1.0	0	.0102	.0131	
			87.4	6.5	1.9	4.1	0	.0437		
			89.4	6.6	2.3	1.7	0	.0177		
			86.9	7.8	2.2	2.2	.1	.0306		
			89.8	6.8	2.2	1.1	.1	.0114		
			86.6	8.1	1.1	3.3	.8	.0348		
			90.1	7.0	1.6	1.2	0	.0123		
5	120	110	84.9	8.5	2.0	4.2	.3	.0450	.0453	.000866
			90.8	6.8	1.0	1.4	0	.0143	.0148	
			85.5	8.6	1.3	4.3	.2	.0457		
			89.8	7.7	1.0	1.5	0	.0153		
13	120	110	83.5	8.3	2.1	5.4	.6	.0588	.0630	.00149
			91.1	5.2	1.8	1.9	0	.0197	.0240	
			86.1	6.7	1.8	5.2	.1	.0560		
			92.2	5.1	.7	2.0	0	.0205		
			83.6	9.7	.7	6.0	0	.0643		
			89.4	6.5	1.3	2.7	0	.0281		
			82.2	9.5	1.6	6.7	0	.0731		
			89.6	7.0	.7	2.7	0	.0279		
23	120	110	83.7	8.2	1.9	5.6	.6	.0609	.0678	.00186
			91.2	5.1	1.3	2.0	.2	.0208	.0244	
			83.2	9.3	1.1	6.3	.1	.0681		
			89.2	6.9	1.3	2.4	.1	.0250		
			82.3	10.0	1.1	6.5	0	.0704		
			88.7	7.8	1.2	2.4	0	.0249		
			81.8	10.0	1.4	6.5	.2	.0719		
			88.8	7.6	1.0	2.6	0	.0270		
35	120	110	82.3	9.5	2.1	5.7	.4	.0621	.0679	.00209
			89.7	6.8	1.0	2.2	.3	.0198	.0243	
			81.8	10.3	1.2	6.5	.2	.0706		
			89.6	7.4	.7	2.3	0	.0237		
			81.9	8.1	2.5	6.4	1.1	.0711		
			87.7	6.5	2.2	2.5	1.0	.0265		

continued next page

Table 51. cont.,

55	120	110	85.9	7.5	1.1	5.5	.1	.0600	.0678	.00229
			89.4	6.7	1.9	1.9	0	.0198	.0243	
			83.5	9.2	.8	6.5	.1	.0701		
			89.8	7.1	.4	2.7	0	.0279		
			82.0	9.9	1.3	6.7	0	.0729		
			90.2	6.8	.6	2.3	0	.0253		
80	120	110	82.0	9.4	2.1	5.9	.6	.0645	.0675	.00241
			90.1	6.1	1.2	1.9	.3	.0197	.0235	
			82.1	9.7	1.6	6.4	.2	.0697		
			90.3	6.3	.7	2.6	.1	.0269		
			83.1	9.3	1.3	6.3	0	.0682		
			89.7	7.0	1.0	2.3	0	.0238		
100	120	110	82.4	9.7	1.0	6.7	.2	.0725	.0678	.00248
			90.4	6.1	1.0	2.5	0	.0259	.0243	
			82.5	9.9	.8	6.6	.2	.0714		
			90.0	6.5	.8	2.7	0	.0280		
			82.3	9.2	1.6	6.9	.3	.0754		
			89.9	6.4	1.0	2.7	0	.0280		

Table 52. Water and Hexadecane Contact Angle Data for SAP:E-1 Samples (Mn = 100 K) Heated at 110 °C for 120 Hours.

% chains	time h	T °C	θ_A/θ_R water	avg.	cos	θ_A/θ_R hexadecane	avg.	cos
2.5	120	110	90/72, 91/72 92/71, 90/73 91/74, 90/72	90/72	.00 .309	20/15, 18/14 21/16, 26/18 19/15, 19/14	19/15	.945 .966
5	120	110	92/74, 93/76 92/75, 90/74 92/73, 91/74	92/74	-.0349 .276	23/18, 24/17 23/16, 24/18 24/17, 25/17	24/17	.913 .956
13	120	110	95/75, 95/75 95/76, 94/73 94/74, 95/73	95/74	-.0871 .276	25/19, 25/17 23/17, 24/18 24/18, 24/18	24/18	.913 .950
23	120	110	95/74, 96/75 95/75, 96/73 96/75, 96/75	96/75	-.104 .259	25/21, 24/19 26/20, 22/17 25/19, 26/21	25/20	.906 .940
35	120	110	95/76, 96/76 97/77, 95/77 96/75, 95/77	95/77	-.0871 .225	24/17, 25/19 26/20, 25/20 27/23, 26/21	26/20	.899 .940
55	120	110	96/78, 96/75 95/77, 95/78 96/76, 96/78	96/78	-.104 .208	23/20, 27/21 26/20, 27/22 27/21, 26/22	27/21	.891 .933
80	120	110	96/78, 96/79 95/79, 97/82 96/83, 96/80	96/80	-.104 .174	26/21, 29/23 28/23, 29/25 28/23, 28/24	28/23	.883 .920
100	120	110	96/78, 96/79 95/79, 97/82 96/83, 96/80	96/81	-.104 .174	27/21, 29/23 30/24, 29/25 30/26, 28/24	29/23	.883 .920

Table 53. XPS Data and F/C Values for SAP:E-2 Samples (Mn = 10 K) Heated at 110 °C for 72 Hours.

% chains	time h	T °C	XPS Atomic Composition 15°/75° C	π–π* C	O	F	Si	F/C expt.	F/C avg.	F/C bulk
1	72	110	82.0	8.4	1.9	7.1	.6	.0785	.0695	.000494
			88.3	6.8	1.4	3.4	.1	.0357	.0316	
			81.9	8.2	2.3	7.0	.5	.0777		
			89.9	6.7	.5	2.9	0	.0300		
			84.3	9.0	1.5	4.9	.2	.0525		
			88.5	7.4	1.3	2.8	0	.0292		
2	72	110	83.7	8.6	2.0	5.6	0	.0606	.0582	.000990
			89.2	6.8	1.2	2.7	0	.0281	.0274	
			84.1	9.1	1.5	5.2	.1	.0558		
			89.8	7.1	.5	2.6	0	.0268		
3	72	110	83.9	8.9	.9	6.3	.1	.0679	.0639	.00148
			88.9	6.7	1.6	2.8	0	.0293	.0281	
			83.1	9.0	1.9	5.6	.3	.0586		
			88.6	7.3	1.1	2.8	.1	.0292		
			83.6	8.5	1.5	6.0	.4	.0651		
			90.7	6.3	.5	2.5	0	.0258		
5	72	110	81.4	9.2	2.1	6.8	.4	.0750	.0710	.00248
			87.8	8.1	1.3	2.9	0	.0302	.0276	
			82.5	8.9	2.2	6.0	.3	.0656		
			89.3	7.2	.9	2.6	0	.0269		
			81.5	9.7	2.0	6.6	.4	.0724		
			90.4	6.7	.5	2.5	0	.0257		
10	72	110	76.5	10.0	3.0	9.5	1.0	.110	.118	.00498
			87.2	7.7	1.1	3.9	.1	.0411	.0547	
			74.4	10.4	3.2	10.0	.9	.118		
			84.5	7.9	2.7	4.7	.1	.0509		
			73.7	10.7	3.4	12.1	.2	.143		
			83.8	8.5	1.8	5.9	0	.0639		
			75.5	10.0	2.1	10.3	.1	.120		
			81.3	7.8	4.4	5.6	1.0	.0628		
20	72	110	76.9	10.2	2.4	9.3	1.0	.107	.111	.00990
			86.9	7.3	1.7	3.7	.3	.0393	.0434	
			74.0	10.3	3.8	11.0	.9	.130		
			84.2	7.0	2.9	5.7	.2	.0625		
			79.8	8.0	2.4	8.6	1.2	.0980		
			87.9	7.3	1.8	2.7	.3	.0284		

continued next page

Table 53. cont.,

40	72	110	73.3	10.6	2.6	11.8	1.5	.141	.113	.0204
			85.3	7.4	1.5	5.8	0	.0625	.0472	
			78.1	9.9	2.5	8.0	1.5	.0910		
			86.3	7.6	1.7	3.8	.5	.0405		
			77.7	9.6	2.3	9.4	1.0	.108		
			87.5	7.8	1.6	3.1	0	.0352		
			74.6	10.3	3.0	11.5	.5	.135		
			86.2	7.1	1.9	4.7	.1	.0504		
50	72	110	75.2	11.0	2.2	11.0	.5	.128	.119	.0248
			82.9	5.6	2.0	6.5	0	.0734	.0577	
			75.8	10.0	2.5	11.2	.5	.130		
			85.0	7.3	1.7	5.5	.4	.0596		
			75.5	10.3	3.1	10.5	.5	.122		
			85.3	8.1	1.0	5.4	.1	.0578		
			79.0	9.4	2.4	8.5	.8	.0961		
			87.3	7.6	1.1	3.8	.2	.0400		
75	72	110	76.0	10.1	2.8	10.6	.5	.123	.128	.0393
			84.1	8.5	2.1	5.4	0	.0584	.0636	
			74.8	10.5	2.8	10.8	1.0	.127		
			85.2	7.9	1.6	5.3	0	.0569		
			75.8	9.2	3.7	10.3	1.0	.121		
			81.9	7.5	3.5	6.9	.2	.0772		
			75.1	10.3	2.5	12.0	.2	.140		
			83.4	8.6	2.3	5.7	0	.0619		
100	72	110	75.0	10.2	2.8	11.7	.2	.137	.134	.0498
			84.4	8.1	1.4	6.1	0	.0659	.0625	
			74.4	11.2	2.5	11.7	.1	.137		
			83.9	8.4	1.7	6.0	.1	.0650		
			75.8	10.6	2.1	11.2	.1	.130		
			84.9	8.5	1.2	5.3	.1	.0567		
100	96	110	75.2	11.1	2.0	11.4	.3	.132	.132	.0498
			83.1	8.6	1.9	6.3	.1	.0687	.0687	
100	120	110	74.9	10.7	2.6	11.0	.8	.132	.129	.0498
			84.1	8.2	2.1	5.3	.3	.0687	.0574	

Table 54. Water and Hexadecane Contact Angle Data for SAP:E-2 Samples (Mn = 10 K) Heated at 110 °C for 72 Hours.

% chains	time h	T °C	θ_A/θ_R water	avg.	cos	θ_A/θ_R hexadecane	avg.	cos
1	72	110	95/77, 95/75 96/76	95/76	-.0871 .242	45/38, 45/37 45/34, 45/34	45/36	.707 .809
2	72	110	96/80, 94/78 96/78	95/79	-.0871 .191	46/43, 47/44 46/44,	46/44	.695 .719
3	72	110	95/78, 94/78 98/80	96/79	-.104 .191	47/42, 46/43 47/44, 47/43	47/43	.682 .731
5	72	110	98/80, 99/81 95/81, 95/80 96/81, 96/80	96/80	-.104 .174	46/44, 49/45 46/44, 46/43 47/41, 47/44, 49/45	47/43	.682 .731
10	72	110	96/80, 98/79 96/80, 100/80 100/81, 96/83, 98/83	98/81	-.139 .156	52/43, 53/47 52/47, 52/44 51/46, 52/43, 51/44	52/45	.616 .707
20	72	110	100/80 99/82, 102/80 102/82, 101/82	101/81	-.191 .156	56/46, 53/45 53/45, 56/45 52/46, 53/46, 51/44	54/45	.588 .707
40	72	110	105/80 102/82, 102/82 103/79, 104/83	102/81	-.208 .156	51/43, 53/45 54/45, 55/48 55/47, 51/43, 54/45	53/45	.602 .707
50	72	110	103/85 101/83, 100/83 103/84, 104/83	102/82	-.208 .139	52/47, 55/46 53/46, 55/48 53/47, 55/47, 53/47	54/47	.588 .682
75	72	110	103/82 104/83, 102/83 102/82, 104/83	103/82	-.225 .139	53/47, 52/45 54/46, 55/48 55/46, 53/47, 55/46	54/46	.588 .695
100	72	110	105/82 101/82, 103/80 102/82, 104/83	103/82	-.225 .139	52/46, 53/44 55/48, 53/44 55/46, 54/46, 55/46	54/46	.588 .695
100	96	110	103/81 102/82, 103/80	103/82	-.225 .139	53/46, 55/46 54/48, 51/44	54/47	.588 .682
100	120	110	103/80 102/83, 103/81	103/81	-.225 .156	55/46, 53/43 54/44, 51/45	54/46	.588 .695

Table 55. XPS Data and F/C Values for SAP:M-1 Samples (Mn = 10 K) Heated at 110 °C for 72 Hours.

% chains	time h	T °C	XPS Atomic Composition 15°/75° C	π–π* C	O	F	Si	F/C expt.	F/C avg.	F/C bulk
10	72	110	86.1	7.6	3.2	2.2	.9	.0235	.0240	.00209
			88.5	6.7	3.0	1.6	.1	.0168	.0130	
			87.4	7.8	2.1	2.3	.4	.0241		
			90.7	6.9	1.4	1.0	.1	.0102		
			88.2	8.1	2.0	1.7	.1	.0176		
			90.9	6.5	2.2	.4	0	.00410		
			86.3	7.5	3.0	2.9	.1	.0309		
			88.7	6.7	2.5	2.0	0	.0210		
20	72	110	85.8	8.4	2.1	3.5	.3	.0371	.0290	.00419
			89.0	7.2	1.2	2.2	.2	.0229	.0159	
			87.8	6.8	1.4	3.4	.5	.0359		
			90.0	6.3	1.6	2.0	0	.0208		
			89.6	7.5	.7	1.5	.6	.0154		
			93.3	4.8	.9	.6	.4	.00410		
40	72	110	87.9	8.5	1.5	2.0	0	.00207	.0300	.00842
			92.3	6.4	.2	1.0	.1	.0101	.0190	
			86.3	7.4	2.3	3.5	.4	.0373		
			89.5	6.8	1.5	2.1	0	.0218		
			86.5	8.5	1.7	3.0	.2	.0316		
			88.7	6.7	1.6	2.4	.3	.0251		
50	72	110	89.4	5.8	3.1	3.3	1.4	.0347	.0310	.0106
			88.8	5.7	2.8	2.3	.4	.0243	.0174	
			86.8	7.0	2.5	2.5	1.2	.0266		
			91.3	5.7	1.4	1.0	.5	.0103		
			87.3	7.5	1.7	3.0	.4	.0316		
			90.4	6.7	1.0	1.7	.2	.0175		
75	72	110	86.6	7.1	2.5	3.2	.6	.0344	.0341	.0161
			89.9	6.0	2.3	1.7	.1	.0167	.0190	
			86.2	8.0	2.2	3.2	.3	.0340		
			89.7	6.4	1.9	1.8	.2	.0187		
			86.5	7.0	2.9	3.3	.2	.0353		
			90.7	5.5	1.9	1.8	.2	.0187		
			86.5	7.7	2.5	3.1	.2	.0329		
			88.5	7.2	2.0	2.1	.2	.0219		

continued next page

Table 55. cont.,

100	72	110	85.1	6.5	3.1	3.7	1.5	.0404	.0372	.0217
			89.6	6.3	2.0	1.9	.1	.0198	.0221	
			84.7	8.5	2.8	3.5	.5	.0375		
			89.6	6.3	1.5	2.1	.4	.0219		
			86.8	7.5	2.2	3.5	.4	.0373		
			88.7	6.6	1.9	2.4	.4	.0251		
			88.3	7.2	1.2	3.2	.2	.0335		
			88.7	7.6	1.4	2.1	.1	.0218		
100	96	110	85.8	6.4	3.4	3.4	1.0	.0369	.0369	.0217
			88.9	6.3	2.1	2.4	.3	.0252	.0252	
100	120	110	86.2	7.5	2.3	3.3	.7	.0352	.0352	.0217
			89.1	6.6	2.2	1.9	.2	.0198	.0198	

Table 56. Water and Hexadecane Contact Angle Data for SAP:M-1 Samples (Mn = 10 K) Heated at 110 °C for 72 Hours.

% chains	time h	T °C	θ_A/θ_R water	avg.	cos	θ_A/θ_R hexadecane	avg.	cos
10	72	110	89/72, 89/72 89/73, 88/73 89/72, 88/70	89/72	.0174 .309	18/14, 19/14 18/16, 19/15 18/13, 19/15	18/14	.951 .970
20	72	110	89/77, 87/72 89/73, 88/74 89/73, 87/75	88/74	.0349 .276	20/14, 21/16 18/16, 21/15 20/17, 19/15	20/16	.951 .961
40	72	110	90/80, 90/79 90/77, 91/77 91/74, 89/74	90/76	.00 .242	21/17, 23/17 20/15, 22/17 21/17, 22/16	21/16	.933 .961
50	72	110	91/79, 90/78 90/77, 91/78 91/74, 91/73	91/76	-.0174 .242	21/17, 20/17 20/18, 22/17 21/17, 22/16	21/17	.933 .956
75	72	110	92/80, 91/81 90/79, 90/77 91/78, 91/79	91/79	-.0174 .191	23/17, 24/17 24/19, 23/17 23/18, 22/16	23/17	.920 .956
100	72	110	92/80, 92/81 93/79, 92/79 92/79, 91/79	92/79	-.0349 .191	25/21, 24/19 24/18, 25/18 25/18, 25/19	25/19	.906 .945
100	96	110	91/81, 92/80 93/79, 92/79 91/79	92/79	-.0349 .191	24/21, 25/20 26/19, 25/18 25/19	25/19	.906 .945
100	120	110	93/79, 91/80 92/77, 93/78 92/78	92/78	-.0349 .208	22/21, 26/19 24/20, 25/21 26/21	25/20	.906 .940

Table 57. Comparison of Plateau F/C Ratios, Contact Angles and Surface Excess Values Among all SAPs at 100% Concentration.

Polymer	Mn	F/C plateau	F/C bulk	Surface Excess	θ_A/θ_R water	θ_A/θ_R hexadec.
SAP:E-1	1K	.329	.0400	8.2	101/79	47/35
SAP:E-1	5K	.163	.0150	10.9	98/78	36/26
SAP:E-1	10K	.105	.0110	9.5	98/81	37/29
SAP:E-1	40K	.0661	.00420	15.7	95/77	28/24
SAP:E-1	100K	.0678	.00185	36.6	96/81	29/23
SAP:E-2	10K	.125	.00498	25.1	103/82	54/46
SAP:M-1	10K	.0330	.00842	3.9	92/79	25/19

BIBLIOGRAPHY

Aklonis, J.J.; MacKnight, W.J. *Introduction to Polymer Viscoelasticity,* 2nd ed. Wiley Interscience, New York, 1983, p. 41.

Allmér, K.; Hult, A.; Rånby, B. "Surface Modification of Polymers. II. Grafting with Glycidyl Acrylates and the Reactions of the Grafted Surfaces with Amines" *J. Polym. Sci. Polym. Chem.* **1989**, *27*, 1641.

Anastasiadis, S.H.; Gancarz, I.; Koberstein, J.T. "Interfacial Tension of Immiscible Polymer Blends: Temperature and Molecular Weight Dependence" *Macromolecules* **1988**, *21*, 2980.

Andrade, J.D.; Gregonis, D.E.; Smith, L.M. In *Surface and Interfacial Aspects of Biomedical Polymers;* Andrade, J.D. ed. Plenum: New York, 1986, Vol. 1, Ch. 2, 5, 7.

Andrade, J.D. *Polymer Surface Dynamics*, Plenum, New York, 1988.

Andrade, J.D. "Probing Surface and Interface Dynamics" *Surf. Interf. Anal.* **1986**, *8*, 253.

Attwood, T.E.; Dawson, P.C.; Freeman, J.L.; Hoy, L.R.J.; Rose, J.B.; Staniland, P.A. "Synthesis and Properties of Polyaryletherketones *Polymer* **1981**, *22*, 1006.

Azrak, R.G. "Surface Property Variations in Melt-Formed Thermoplastics" *J. Coll. and Interf. Sci.* **1974**, *47*, 779.

Barker, D.J.; Brewis, D.M.; Dahm, R.H. "Study of Intercalated Carbon Formed by Electrochemical Reduction of Poly(tetrafluoroethylene) *Polymer* **1978**, *19*, 856.

Baszkin, A.; Ter-Minassian-Saraga, L. "Chemical Structures of Surface-Oxidized and Grafted Polyethylene: Adsorption and Wetting Studies" *J. Polym. Sci., Part. C.* **1971**, *34*, 243.

Bates, F.S. "Polymer-Polymer Phase Behavior" *Science* **1991**, *251,* 898.

Batich, C.D.; Wendt, R.C. In *Photon, Electron, and Ion Probes of Polymer Structure and Properties,* Dwight, D.W.; Fabishi, T.J.; Thomas,H.R., eds. *ACS Symp. Ser.*, 1981, *162*, Ch. 15.

Bee, T.G.; McCarthy, T.J. "Surface Modification of Poly(chlorotrifluoroethylene): Introduction of Reactive Carboxylic Acid Functionality" *Macromolecules* **1992**, *25*, 2093.

Bening, R.C.; McCarthy, T.J. "Surface Modification of Poly(tetrafluoroethylene-*co*-hexafluoropropylene). Introduction of Alcohol Functionality" *Macromolecules* **1990**, *23*, 2648.

Bergbreiter, D.E.; Hu, H.-P.; Hein, M.D. "Control of Surface Functionalization of Polyethylene Powders Prepared by Coprecipitation of Functionalized Oligomers and Polyethylene" *Macromolecules* **1989**, *22*, 654.

Bergbreiter, D.E.; Chen, Z.; Hu, H.-P. "Entrapment of Functionalized Ethylene Oligomers in Polyethylene" *Macromolecules* **1984**, *17*, 2111.

Billmeyer, F.W. *Textbook of Polymer Science*, 3rd ed. Wiley Interscience, New York, **1984**, p. 153, 176.

Bishop, M.T.; Karasz, F.E.; Russo, P.S.; Langley, K.H. "Solubility and Properties of a Poly(aryl ether ketone) in Strong Acids" *Macromolecules* **1985**, *18*, 86.

Blundell, D.J.; Osborn, B.N. "The Morphology of Poly(aryl ether ether ketone)" *Polymer* **1983**, *24*, 953.

Bonafini, J. "Polymer Surface Modification by Reaction of Hydroxyl Functionality" Master of Science Thesis, Univ. of Mass., 1985.

Bozarth, M.J.; Gillespie, J.W., Jr.; McCullough, R.L. "Fiber Orientation and Its Effect Upon Thermoelastic Properties of Short Carbon Fiber Reinforced Poly(ether ether ketone) (PEEK)" *Polymer Composites* **1987**, *8*, 74.

Brandup, J.; Immergut, E.H. eds. *Polymer Handbook*, 2nd ed. Wiley Interscience, New York, 1975, pp. IV-39, V-59.

Brauman, S.K.; Pronko, J.G. "Chemiluminescence Studies of the Thermooxidation of PEEK" *J. Polym. Sci. Part B* **1988**, *26*, 1205.

Brennan, J.V.; McCarthy, T.J. "The Introduction of Specific Functionality onto Poly(vinylidene fluoride)" *Polym. Prepr. (Am. Chem. Soc., Div. Polym. Chem.)* **1988**, *29(2)*, 338.

Brennan, J.V.; McCarthy, T.J. "Surface Modification of Poly(vinylidene fluoride): Introduction of Reactive Handles" *Polym. Prepr. (Am. Chem. Soc., Div. Polym. Chem.)* **1989**, *30(2)*, 152.

Brewis, D.M.; Briggs, D. "Adhesion ot Polyethylene and Polypropylene" *Polymer* **1981**, *22*, 7 and references therein.

Broseta, D.: Fredrickson, G.H.; Helfand, E.; Leibler, L. "Molecular Weight and Polydispersity Effects at Polymer-Polymer Interfaces"*Macromolecules* **1990**, *23*, 132.

Bueche, F. "Diffusion of Polystyrene in Polystyrene: Effect of Matrix Molecular Weight" *J. Chem. Phys.* **1968**, *48*, 1410.

Bueche, F.; Cashin, W.M.; Debye, P. "The Measurement of Self-Diffusion in Solid Polymers" *J.Chem. Phys.* **1952**, *20*, 1956.

Campbell, T.W.; Lyman, D.J. "Chlorinated Isotactic Polyhydrocarbons" *J. Polm. Sci.* **1961**, *55*, 169.

Capka, M.; Chvalovsky, V.; Kochloefl, K.; Kraus, M. "Properties of Sodium Bis-(2-methoxyethoxy)aluminum Hydride. II. Reduction of Aldehydes and Ketones" *Coll. Czech. Chem. Comm.* **1969**, *34*, 118.

Carey, F.A.; Sundberg, R.J. *Advanced Organic Chemistry Part B: Reactions and Synthesis*, Plenum Press: New York, 1983.

Chalmers, J.M.; Gaskin, W.F.; Mackenzie, M.W. "Crystallinity in Poly(aryl ether ketone) Plaques Studied by Multiple Internal Reflection Spectroscopy" *Polymer Bulletin* **1984**, *11*, 433.

Clark, D.T.; Feast, E.J.; Musgrave, W.K.R.; Ritchie, I. "Applications of ESCA to Polymer Chemistry. Part IV. Surface Fluorination of Polyethylene." *J. Polm. Sci. Polym. Chem.* **1975**, *13*, 857.

Clark, D.T.; Peeling, J.; O'Malley, J.M. "Applications of ESCA to Polymer Chemistry. VIII. Surface Structure of AB Block Copolymers of Polydimethylsiloxane and Polystyrene" *J. Polym. Sci., Polym. Chem.* **1976**, *14*, 543.

Clark, D.T.; Thomas, H.R. "Application of ESCA for Polymer Chemistry. XVI. Electron Mean Free Paths as a Function of Kinetic Energy in Polymeric Films Determined by Means of ESCA" *J. Polym. Sci., Polym. Chem. Ed.* **1977**, *15*, 2843.

Clark, M.B., Jr.; Burkhardt, C.A.; Gardella, J.A., Jr. "Surface Studies of Polymer Blends. 3. An ESCA, IR, and DSC Study of Poly(ε-caprolactone)/Poly(vinyl chloride) Homopolyer Blends" *Macromolecules* **1989**, *22*, 4495.

Clark, M.B., Jr.; Burkhardt, C.A.; Gardella, J.A., Jr. "Surface Studies of Polymer Blends. 4. An ESCA, IR, and DSC Study of the Effect of Homopolymer Molecular Weight on Crystallinity and Miscibility of Poly(ε-caprolactone)/Poly(vinyl chloride) Homopolymer Blends" *Macromolecules* **1991**, *24*, 799.

Clendinning, R.A.; Farnham, A.G.; Johnson, R.N. "The Development of Polysulphone and Other Polyarylethers" *Polym. Prepr. (Am. Chem. Soc., Div. Polym. Chem.)* **1986**, *27(1)*, 478.

Coopes, I.H.; Gifkins, K.J. "Gas Plasma Treatment of Polymer Surfaces" *J. Macromol. Sci.-Chem.* **1982**, *A17*, 217.

Corbin, G.A.; Cohen, R.E.; Baddour, R.F. "Surface Fluorination of Polymers in a Glow Discharge Plasma: Photochemistry" *Macromolecules* **1985**, *18*, 98.

Corey, E.J.; Chaykovsky, M. "Dimethyloxosulfonium Methylide and Dimethylsulfonium Methylide. Formation and Application to Organic Synthesis" *J. Am. Chem. Soc.* **1965**, *87*, 1353.

Corey, E.J.; Chaykovsky, M. "Methylsulfinylcarbanion" *J. Am. Chem. Soc.* **1962**, *84*, 866.

Costello, C.A.; McCarthy, T.J. "Surface-Selective Introduction of Specific Functionalities onto Poly(tetrafluoroethylene)" *Macromolecules* **1987**, *20*, 2819.

Costello, C.A.; McCarthy, T.J. "Surface Modification of Poly(tetrafluoro-ethylene) with Benzoin Dianion" *Macromolecules* **1984**, *17*, 2940.

Creton, C.; Kramer, E.J.; Hadziioannou, G. "Critical Molecular Weight for Block Copolymer Reinforcement of Interfaces in a Two-Phase Polymer Blend" *Macromolecules* **1991**, *24*, 1846.

Cross, E.M.; McCarthy, T.J. "Controlled Chlorination of Polyethylene Surfaces" *Polym. Prepr. (Am. Chem. Soc., Div. Polym. Chem.)* **1989**, *30(1)*, 422.

Cross, E.M.; McCarthy, T.J."Surface Reorganizations in Functionalized Poly(chlorotrifluoroethylene)" *Macromolecules* **1990**, *23*, 3921.

Dawson, P.C.; Blundell, D.J. "X-Ray Data for Poly(aryl ether ketones)" *Polymer* **1980**, *21*, 577.

de Gennes, P.G. *Scaling Concepts in Polymer Physics*, Cornell University Press, New York, 1979.

Dias, A.J.; McCarthy, T.J. "Synthesis of a Two-Dimensional Array of Organic Functional Groups: Surface-Selective Modification of Poly(vinylidene fluoride)" *Macromolecules* **1984**, *17*, 2529.

Dias, A.J.; McCarthy, T.J. "Surface Modification of Poly(chlorotrifluoro ethylene) with Methyllithium" *Macromolecules* **1985**, *18*, 1826.

Dias, A.J.; McCarthy, T.J. "Introduction of Carboxylic Acid, Aldehyde, and Alcohol Functional Groups onto the Surface of Poly(chloro-trifluoroethylene)" *Macromolecules* **1987**, *20*, 2068.

Eisenberg, D.; Crothers, D. *Physical Chemistry,* Benjamin/Cummings Publishing, London, 1979, Ch. 15.

Evans, D.A.; Truesdale, L.K.; Carroll, G.L. "Cyanosilylation of Aldehydes and Ketones" *Chem. Commun.* **1973**, 55.

Everhart, D.S.; Reilley, C.N. "Chemical Derivatization in Electron Spectroscopy for Chemical Analysis of Surface Functional Groups Introduced in Low-Density Polyethylene Film" *Anal. Chem.* **1981**, *53*, 665.

Foster, K.L.; Wool, R.P. "Strength of Polystyrene-Poly(methyl methacrylate) Interfaces" *Macromolecules* **1991**, *24*, 1397.

Fox, R.B.; Price, T.R.; Cain, D.S. "Wettability and Constitution of Photooxidized Polystyrene and Other Amorphous Polymers" *Adv. Chem. Ser.* **1968**, *87*, 72.

Fox, R.B.; Price, T.R. "Photoyellowing of Polystyrene and Poly(styrene-*alt*-methyl methacrylate)" *Adv. Chem. Ser.* **1968**, *87*, 96.

Fox, T.G., Jr.; Flory, P.J. "Second-Order Transition Temperatures and Related Properties of Polystyrene. I. Influence of Molecular Weight" *J. Appl. Phys.* **1950**, *21*, 581.

Franchina, N.L.; McCarthy, T.J. "Surface Modifications of Poly(ether ether ketone)" *Macromolecules* **1991**, *24*, 3045.

Franchina, N.L.; McCarthy, T.J. "Poly(ether ether ketone) Surface Chemistry" In *Chemically Modified Surfaces,* Mottola, H.A.; Steinmetz, J.R. eds., Elsevier Science Publishers: New York, 1991, 173.

Fredrickson, G.H. "Surface Ordering Phenomena in Block Copolymer Melts" *Macromolecules* **1987**, *20*, 2535.

Gagnon, D.R.; McCarthy, T.J. "Polymer Surface Reconstruction by Diffusion of Organic Functional Groups From and To the Surface" *J. Appl. Polym. Sci.* **1984**, *29*, 4335.

Gaines, G.L., Jr.; Bender, G.W. "Surface Concentration of Styrene-Dimethylsiloxane Block Copolymer in Mixtures with Polystyrene" *Macromolecules* **1972**, *5*, 82.

Gaines, G.L., Jr. "Surface Activity of Semifluorinated Alkanes" *Langmuir* **1991**, *7*, 3054.

Gaines, G.L., Jr. "Diffusion and Surface Activity of Block Copolymers in Melts: Effects of Copolymer Molecular Weight and Morphology" *Macromolecules* **1979**, *12*, 1011.

Gibson, H.W.; Bailey, F.C. "Chemical Modification of Polymers. 13. Sulfonation of Polystyrene Surfaces" *Macromolecules* **1980**, *13*, 34.

Gilmore, P.T. "Macromolecular Diffusion in Polymer Melts" Ph.D. Thesis, Univ. of Mass., 1978.

Graessley, W.W. "Entangled, Linear, Branched and Network Polymer Systems-Molecular Theories" In *Advances in Polymer Science*; Springer-Verlag, NewYork, **1982**, p. 67.

Green, P.F.; Christensen, T.M.; Russell, T.P.; Jérôme, R. "Surface Interaction in Solvent-Cast Polystyrene/Poly(methyl methacrylate) Diblock Copolymers" *Macromolecules* **1989**, *22*, 2189.

Green, P.F.; Christensen, T.M.; Russell, T.P. "Ordering at Diblock Copolymer Surfaces" *Macromolecules* **1991**, *24*, 252.

Green, P.F.; Russell, T.P. "Segregation of Low Molecular Weight Symmetric Diblock Copolymers at the Interface of High Molecular Weight Homopolymers" *Macromolecules* **1991**, *24,* 2931.

Hariharan, A.; Kumar, S.K.; Russell, T.P. "A Lattice Model for the Surface Segregation of Polymer Chains Due to Molecular Weight Effects" *Macromolecules* **1990**, *23*, 3584.

Hariharan, A.; Kumar, S.K.; Russell, T.P. "Surface Segregation in Binary Polymer Mixtures: A Lattice Model" *Macromolecules* **1991**, *24*, 4909.

Höpken, J.; Möller, M. "Low Surface Energy Polystyrene" *Macromolecules* **1992**, *25*, 1461.

Hsieh, Y.-L,; Timm, D.A.; Wu, M. "Solvent- and Glow-Discharge-Induced Surface Wetting and Morphological Changes of Poly(ethylene terephthalate) (PET)" *J. Appl. Polym. Sci.* **1989**, *38*, 1719.

Huh, C.; Mason, S.G. "Effects of Surface Roughness on Wetting" *J. Coll. and Interf. Sci.* **1977**, *60*, 11.

Iyengar, D.R.; McCarthy, T.J. "Trends in Adsorption of End-Functionalized Polystyrenes by Thin layer Chromatography" *Macromolecules* **1990**, *23*, 4344.

Jarvis, N.L.; Fox, R.B.; Zisman, W.A. "Surface Activity at Organic Liquid-Air Interfaces" *Adv. Chem. Ser.* **1964**, *43*, 317.

Johnson, R.E.; Dettre, R.H. "Contact Angle Hysteresis. III. A Study of Idealized Heterogeneous Surfaces" *J. Phys. Chem.* **1964**, *68*, 1744.

Kemmish, D.J.; Hay, J.N. "The Effect of Physical Aging on the Properties of Amorphous PEEK" *Polymer*, **1985**, *26*, 905.

Kemp, D.S.; Vellacio, F. *Organic Chemistry*, Worth Publishers, New York, 1980, Ch. 6.

Koberstein, J.T. In *Encyclopedia of Polymer Science and Engineering*, 2nd ed.; Mark, H.F.; Bikales, N.M.; Overberger, C.G.; Menges, G.; Kroschwitz, J.I., eds.; John Wiley and Sons: New York, 1989; Vol. 8, p. 237.

Kogoma, M.; Kasai, H.; Takahashi, K.; Moriwaki, T.; Okazaki, S. "Wettability Control of a Plastic Surface by CF_4-O_2 Plasma and Its Etching Effect" *J. Phys. D: Appl. Phys.* **1987**, *20*, 147.

Kumar, S.K.; Vacatello, M.; Yoon, D.Y. "Off-Lattice Monte Carlo Simulations of Polymer Melts Confined between Two Plates. 2. Effects of Chain Length and Plate Separation" *Macromolecules* **1990**, *23*, 2189.

Kumar, S.K.; Russell, T.P. "Behavior of Isotopic, Binary Polymer Blends in the Vicinity of Neutral Surfacces: The Effects of Chain Length Disparity" *Macromolecules* **1991**, *24*, 3816.

Lachman, A. In *Organic Syntheses;* Blatt, A. H., ed., John Wiley & Sons: New York, 1943, Collect. Vol. II, p. 70.

Lee, K.-W.; McCarthy, T.J. "Surface-Selective Hydroxylation of Polypropylene" *Polym. Prepr. (Am. Chem. Soc., Div. Polym. Chem.)* **1987**, *28*, 250.

Lee, K.-W.; McCarthy, T.J. "Chemistry of Surface-Hydroxylated Poly(chlorotrifluoroethylene)" *Macromolecules* **1988**, *21*, 2318.

Lee, K.-W.; McCarthy, T.J. "Synthesis of a Polymer Surface Containing Covalently Attached Triethoxysilane Functionality: Adhesion to Glass: *Macromolecules* **1988**, *21*, 3353.

LeGrand D.G.; Gaines, G.L., Jr. "The Molecular Weight Dependence of Polymer Surface Tension" *J. Coll. and Interf.* **1969**, *31*, 162.

LeGrand, D.G.; Gaines, G.L., Jr. "Surface Activity of Block Copolymers of Dimethylsiloxane and Bisphenol A Carbonate in Polycarbonate" *Polym. Prepr. (Am. Chem. Soc., Div Polym. Chem.)* **1970**, *11*, 442.

Lovinger, A.J.; Davis, D.D. "Solution Crystallization of Poly(ether ether ketone)" *Macromolecules* **1986**, *19*, 1861.

March, J. *Advanced Organic Chemistry*, 3rd ed. Wiley-Interscience: New York, 1985.

Matsuda, T.; Litt, M.H. "Modification and Characterization of Polystyrene Surfaces Used for Cell Culture" *J. Polym. Sci. Polym. Chem.* **1974**, *12*, 489.

Matsunaga, T. Tamai, Y."Surface Free Energy Analysis of Ethylene-Vinyl Acetate Copolymers" *J. Appl. Polym. Sci.* **1978**, *22*, 3525.

Matthews, C.N.; Ludicky, R. "The Dark Nucleus of Halley's Comet: Hydrogen Cyanide Polymers" *Polym. Prepr. (Am. Chem. Soc., Div. Polym. Chem.)* **1987**, *28 (2)*, 104.

May, R. In *Encyclopedia of Polymer Science and Engineering*, 2nd ed.; Mark, H.F.; Bikales, N.M.; Overberger, C.G.; Menges, G.; Kroschwitz, J.I., eds., John Wiley and Sons: New York, 1989; Vol. 12 , p. 313.

McFarland, J.W.; Howard, J.B. "The Chemistry of Benzenesulfonyl Isocyanate" *J. Org. Chem.* **1965**, *30*, 957.

Miyashita, N.; Yoshikoshi, A.; Grieco, P.A. "Pyridinium *p*-Toluenesulfonate. A Mild and Efficient Catalyst for the Tetrahydropyranylation of Alcohols" *J. Org. Chem* **1977**, *42*, 3772.

Morra, M.; Occhiello, E.; Garbassi, F. "Contact Angle Hysteresis in Oxygen Plasma Treated Poly(tetrafluoroethylene)" *Langmuir*, **1989**, *5*, 872.

Muilenberg, G.E. *Handbook of X-Ray Photoelectron Spectroscopy*, Perkin-Elmer Corp., 1979.

Munro, H.S.; Clark, D.T.; Recca, A. "Surface Photo-Oxidation of Phenoxy Resin and Poly(ether ether ketone)" *Polymer Degradation and Stability* **1987**, *19*, 353.

Nambu, K. "Studies on Chlorinated Polyethylenes. 1. Infrared Spectra of Chlorinated Polyethylenes" *J. Appl. Polm. Sci.* **1960**, *4*, 69.

Nguyen, H.X; Ishida, H. "Poly(aryl ether ether ketone) and its Advanced Composites: A Review" *Polymer Composites* **1987**, *8*, 57.

Noolandi, J.; Hong, K.M. "Interfacial Properties of Immiscible Homopolymer Blends in the Presence of Block Copolymers" *Macromolecules* **1982**, *15*, 482.

Olley, R.H.; Bassett, D.C.; Blundell, D.J. "Permanganate Etching of PEEK" *Polymer* **1986**, *27*, 343.

O'Malley, J.J.; Thomas, H.R.; Lee, G.M. "Surface Studies on Multicomponent Polymer Systems by X-ray Photoelectron Spectroscopy. Polystyrene/Poly(ethylene oxide) Triblock Copolymers" *Macromolecules* **1979**, *12*, 996.

Oster G.; Oster, G.K.; Moroson, H. "Ultraviolet Induced Crosslinking and Grafting of Solid High Polymers" *J. Polm. Sci.* **1959**, *34*, 671.

Pao, P.S.; Grayson, M.A.; Wolf, C.J. "Effect of Methylene Chloride Sorption on the Mechanical Properties of Poly(aryl ether ether ketone) (PEEK)" *J. Polym. Sci.* **1988**, *35*, 727.

Peeling, J.; Clark, D.T. "Surface Ozonation and Photooxidation of Polyethylene Film" *J. Polm. Sci. Polym. Chem.* **1983**, *21*, 2047.

Pennings, J.F.M.; Bosman, B. "Relaxation of the Surface Energy of Solid Polymers" *Coll. and Polym. Sci.* **1979**, *257*, 720.

Pennings, J.F.M. "Adsorption at the Interface of a Polymer Melt and a Substrate" *Coll. and Polym. Sci.* **1978**, *256*, 78.

Phillips, R.W.; Dettre, R.H. "Application of ESCA and Contact Angle Measurements to Studies of Surface Activity in a Fluoropolymer Mixture" *J. Coll. and Interf. Sci.* **1976**, *56*, 251.

Pizey, S.S. *Synthetic Reagents*, John Wiley & Sons: New York, 1974, Vol. 1, Ch. 4.

Plueddemann, E.P. *Silane Coupling Agents*; Plenum: New York, 1982.

Quirk, R.P.; Seung, N.S. In *Ring Opening Polymerization*; McGrath, J.E. ed. Plenum: New York, 1986, Vol. 1, Ch. 2.

Rabolt, J.F.; Russell, T.P.; Twieg, R.J. "Structural Studies of Semifluorinated *n*-Alkanes" *Macromolecules* **1984**, *17*, 2786.

Rasmussen, J.R.; Stredonsky, E.R.; Whitesides, G.M. "Introduction, Modification, and Characterization of Functional Groups on the Surface of Low Density Polyethylene Film" *J. Am. Chem. Soc.* **1977**, *99*, 4736.

Rastogi A.K.; St. Pierre L.E. "Interfacial Phenomena in Macromolecular Systems III. The Surface Free-Energies of Polyethers" *J. Coll. and Interf. Sci.* **1969**, *31*, 169.

Reardon, J.P.; Zisman, W.A. "Critical Surface Tensions of Tetrafluoroethylene-Perfluoro(propyl vinyl ether) Copolymers" *Macromolecules* **1974**, *7*, 920.

Reilley, C.N.; Everhart, D.S.; Ho, F.F.L. In *Applied Electron Spectroscopy for Chemical Analysis*; Windawi, H., Ho, F.F.L., eds.; John Wiley & Sons: New York, 1982, Chapter 6.

Rose, J.B. "Discovery and Development of the "Victrex" Polyarylethersulphone, PES, and Polyaryletherketone, PEEK" *Polym. Prepr. (Am. Chem. Soc., Div. Polym. Chem.)* **1986**, *27(1)*, 480.

Rosen, M.J. *Surfactants and Interfacial Phenomena*, John Wiley & Sons, NY, **1978**, Ch. 2.

Ruckenstein, E.; Gourisankar, S.V. "Environmentally Induced Restructuring of Polymer Surfaces and Its Influence on Their Wetting Characteristics in an Aqueous Environment: *J. Coll. and Interf. Sci.* **1985**, *107*, 488.

Ruckenstein, E.; Gourisankar, S.V. "Surface Restructuring of Polymeric Solids and Its Effect on the Stability of the Polymer-Water Interface" *J. Coll. and Interf. Sci.* **1986**, *109*, 557.

Russell, T.P.; Anastasiadis, S.H.; Menelle, A.; Felcher, G.P.; Satija, S.K. "Segment Density Distribution of Symmetric Diblock Copolymers at the Interface between Two Homopolymers As Revealed by Neutron Reflectivity" *Macromolecules* **1991**, *24*, 1575.

Sauer, B.B.; Dee, G.T. "Molecular Weight and Temperature Dependence of Polymer Surface Tension: Comparison of Experiment with Theory" *Macromolecules* **1991**, *24*, 2124.

Scheutjens, J.M.H.M.; Fleer, G.J. "Statistical Theory of the Adsorption of Interacting Chain Molecules. 1. Partition Function, Segment Density Distribution and Adsorption Isotherms" *J. Phys. Chem.* **1979**, *83*, 1619.

Scheutjens, J.M.H.M.; Fleer, G.J. "Statistical Theory of the Adsorption of Interacting Chain Molecules. 2. Trains, Loops and Tail Size Distribution." *J. Phys. Chem.* **1980**, *84*, 178.

Scheutjens, J.M.H.M.; Fleer, G.J. "Interaction between Two Adsorbed Polymer Layers" *Macromolecules* **1985**,*18*, 1882.

Schmidt, J.J.; Gardella, J.A., Jr.; Salvati, L., Jr. "Surface Studies of Polymer Blends. 2. An ESCA and IR Study of Poly(methyl methacrylate)/Poly(vinyl chloride) Homopolymer Blends" *Macromolecules* **1989**, *22*, 4489.

Schmitt, R.L.; Gardella, J.A., Jr.; Magill, J.H.; Salvati, L., Jr.; Chin, R.L. "Study of Surface Composition and Morphology of Block Copolymers of Bisphenol A Polycarbonate and Poly(dimethylsiloxane) by XPS and ISS" *Macromolecules* **1985**, *18*, 2675.

Schmitt, R.L.; Gardella, J.A., Jr.; Salvati, L., Jr. "Studies of Surface Composition and Morphology in Polymers. 2. Bisphenol A Polycarbonate and Poly(dimethylsiloxane) Blends" *Macromolecules* **1986**, *19*, 648.

Shoichet, M.S.; McCarthy, T.J. "Convenient Synthesis of Carboxylic Acid Functionalized Fluoropolymer Surfaces" *Macromolecules* **1991**, *24*, 982.

Scholtens, B.J.R.; Bijsterbosch, B.H. "The Influence of Molecular Architecture on the Surface Activity ofVinyl Alcohol-Acetate Copolymers" *J. Coll. and Interf. Sci.* **1980**, *77*, 162.

Schonhorn, H. "Heterogeneous Nucleation of Polymer Melts on High-Energy Surfaces II" *Macromolecules* **1968**, *1*, 145.

Shull, K.R.; Kramer, E.J.; Hadziioanou, G.; Tang, W. "Segregation of Block Copolymers to Interfaces between Immiscible Homopolymers" *Macromolecules* **1990**, *23*, 4780.

Shull, K.R.; Winey, K.I.; Thomas, E.L.; Kramer, E.J. "Segregation of Block Copolymer Micelles to Surfaces and Interfaces" *Macromolecules* **1991**, *24*, 2748.

Shull, K.R.; Kramer, E.J.; Bates, F.S.; Rosedale, J.H. "Self-Diffusion of Symmetric Diblock Copolymer Melts near the Ordering Transition" *Macromolecules* **1991**, *24*, 1383.

Steiger, R.E. In *Organic Syntheses*; Blatt, A.H., John Wiley and Sons: New York, 1965, Coll. Vol. III, p. 66.

Swalen, J.D.; Allara, D.L.; Andrade, J.D.; Chandross, E.A.; Garoff, S.; Israelachvili, J.; McCarthy, T.J.; Murray, R.; Pease, R.F.; Rabolt, J.F.; Wynne, K.J.; Yu, H. "Molecular Monolayers and Films" *Langmuir* **1987**, *3*, 932.

Theodorou, D.N. "Lattice Models for Bulk Polymers at Interfaces" *Macromolecules* **1988**, *21*, 1391.

Theodorou, D.N. "Structure and Thermodynamics of Bulk Homopolymer/Solid Interfaces: A Site Lattice Model Approach" *Macromolecules* **1988**, *21*, 1400.

Theodorou, D.N. "Microscopic Structure and Thermodynamic Properties of Bulk Copolymers and Surface-Active Polymers at Interfaces. 1. Theory" *Macromolecules* **1988**, *21*, 1411.

Theodorou, D.N. "Microscopic Structure and Thermodynamic Properties of Bulk Copolymers and Surface-Active Polymers at Interfaces" *Macromolecules* **1988**, *21*, 1422.

Thomas, H.R.; O'Malley, J.J. "Surface Studies on Multicomponent Polymer Systems by X-ray Photoelectron Spectroscopy. Polystyrene/Poly-(ethylene oxide) Diblock Copolymers" *Macromolecules* **1979**, *12*, 323.

Thomas, H.R.; O'Malley, J. J. "Surface Studies on Multicomponent Polymer Systems by X-ray Photoelectron Spectroscopy: Polystyrene/Poly(ethylene oxide) Homopolymer Blends" *Macromolecules* **1981**, *14*, 1316.

Torstensson, M.; Ranby, B.; Hult, A. "Monomeric Surfactants for Surface Modification of Polymers" *Macromolecules* **1990**, *23*, 126.

Triolo, P.M.; Andrade, J.D. "Surface Modification and Evaluation of Some Commonly Used Catheter Materials. I. Surface Properties" *J. Biomed. Mater. Res.* **1983**, *17*, 129.

Trott, G.F. "Surface Modification of Polymer Structures by an Imido-Alkylene Substitution Reaction" *J. Appl. Polm. Sci.* **1974**, *18*, 1411.

Uchida, E.; Uyama, Y.; Ikada, Y. "Surface Graft Polymerization of Acrylamide onto Poly(ethylene terephthalate) Film by UV Irradiation" *J. Polym. Sci. Polym. Chem.* **1989**, *27*, 527.

Urban, M.W.; Salazar-Rojas, E.M. "Ultrasonic PTC Modification of Poly(vinylidene fluoride) Surfaces and Their Characterization" *Macromolecules* **1988**, *21*, 372.

Varma, D.S.; Nedungadi, C. "Modification of Poly(vinyl alcohol) Fibers by Hexamethylene Diisocyanate" *J. Appl. Polym. Sci.* **1976**, *20*, 681.

Ward, W.J; McCarthy, T.J. In *Encyclopedia of Polymer Science and Engineering*, 2nd ed.; Mark, H.F.; Bikales, N.M.; Overberger, C.G.; Menges, G.; Kroschwitz, J.I., eds.; John Wiley and Sons: New York, 1989; suppl. vol., p. 674.

Whitaker, R.B.; Attalla, A.; Sullenger, D.B.; Wang, P.S.; Dichiaro, J.V.; Kenyon, A.S. "Characterization and Adhesive Bonding of Poly(ether ether ketone) Resins and Composites" *16th National SAMPE Tech. Conference* **1984**, 361.

Wilfong, D.L. "Resistance of PEEK and PPS to Molten Caprolactam" *Polym. Prepr. (Am. Chem. Soc., Div. Polym. Chem.)* **1987**, *28(1)*, 61.

Williams, D.F.; McNamara, A.; Turner, R.M. "Potential of Poly(ether ether ketone) (PEEK) and Carbon-Fiber-Reinforced PEEK in Medical Applications" *J. Mater. Sci. Let.* **1987**, *6*, 188.

Yang, J.; Wegner, G. "Polymerization in Lyotropic Liquid Crystals" *Macromolecules* **1992,** *25*, 1791.

Yasuda, H.; Sharma, A.K.; Yasuda, T. "Effect of Orientation and Mobility of Polymer Molecules at Surfaces on Contact Angle and Its Hysteresis" *J. Polym. Sci., Polym. Phys. Ed.* **1981**, *19*, 1285.

Yasuda, T.; Okuno, T.; Yoshida, K.; Yasuda, H. "A Study of Surface Dynamics of Polymers. II. Investigation by Plasma Surface Implantation of Fluorine-Containing Moieties" *J. Polm. Sci., Polym. Phys*. **1988**, *26*, 1781.

Yoon, S.C.; Ratner, B.D. "Surface Structure of Segmented Poly(Ether Urethanes) and Poly(Ether Urethane Ureas) with Various Perfluoro Chain Extenders. An X-ray Photoelectron Spectroscopic Investigation" *Macromolecules* **1986**, *19*, 1068.

Zisman, W.A. "Relation of the Equilibrium Contact Angle to Liquid and Solid Constitution" *Adv. Chem. Ser.* **1964**, *43*, 1.